Molecular Mechanisms and Tumour Heterogeneity in Breast Cancer

A thesis submitted to the National University of Ireland as partial fulfilment of the requirements for the degree of

Doctor of Philosophy (PhD)

By

Sonja Khan

BSc, MSc

Under the supervision of
Dr. Roisin M Dwyer
and the direction of
Professor Michael J Kerin

Discipline of Surgery, School of Medicine, National University of Ireland, Galway

February 2014

TABLE OF CONTENTS

Chapter 2 Materials and Methods

ACKNOWLEDGEMENTS

I would like to thank Dr. Roisin Dwyer for all the support throughout my PhD. She is an excellent teacher who has always been available to listen and support me with any project related and personal issues. Thank you for your guidance, patience and for your never-ending motivation to research. I will be forever thankful for all the support and direction in preparing this thesis.

I would also like to thank Professor Michael Kerin, for giving me the opportunity to work in his laboratory and for all his help and support throughout my PhD.

I would like to acknowledge the contribution of:

- Ms. Catherine Curran and Ms. Emer Hennessey who were approachable for any experiment related issues and especially with the acquisition of the breast cancer database and specimens from the biobank.
- Dr. John Newell and Dr. Deirdre Wall for all their guidance in the statistical analysis of my data sets.
- All the past and present members of the lab. I would like to especially mention Dr. Marion Hartman and Dr. James Ryan and all the people I shared Room 108 with.
- Ms. Grace Clarke who has been a great support and who I now am honoured to have as a friend.
- Ms. Teresa Cremin for being there for me throughout the years. Thank you for all the baby-sitting.

I would like to thank my Mother who supported me from the beginning and without whom this all could never have happened. Thanks go to my sister Sarah Maria, she is a great listener and my best friend. My Son Cillian, who is my greatest achievement ever and I hope to make him proud. My work is dedicated to them.

I would like to also mention the National Breast Cancer Research Institute (NBCRI) and the Health Research Board (HRB) who funded this work.
Finally I would like to express my sincere appreciation to all the patients who participated in the on-going research at the NBCRI.

DEDICATION

This work is dedicated to my Son Cillian,

my Mum and my Sister Sarah Maria.

Thank you for all your love and support always.

LIST OF FIGURES

Chapter 1 Introduction

Chapter 2 Materials and Methods

Chapter 6 Characterisation of Primary Tumour Microenvironment

LIST OF TABLES

Chapter 1 Introduction

Chapter 2 Materials and Methods

Chapter 3 MicroRNA mediated Regulation of Sodium Iodide Symporter (NIS) and its regulators in Breast Cancer

No Tables

Chapter 4 miR-339-5p and miR-10a in Breast Cancer

Chapter 5 miR-379 in Breast Cancer

No Tables

Chapter 6 Characterisation of Primary Tumour Microenvironment

ABBREVIATIONS

ANOVA	analysis of variance
BCT	Breast Conserving Therapy
cDNA	complementary DNA
cm	centimetre
Ct	cycle threshold
DCIS	ductal carcinoma *in situ*
ddH_2O	ultra-pure water
DNA	deoxyribonucleic acid
dNTP	deoxyribonucleotide(s)
ds	double stranded
DTT	dithiotritol
EC	Endogenous control
EDTA	ethylenediaminetetraacetic acid
ER	oestrogen receptor
ERα	oestrogen receptor alpha
FBS	Fetal Bovine Serum
g	gram
HER2	Human Epidermal growth factor Receptor 2 (ErbB-2)
M	molar
min	minute
miRNA	microRNA
mRNA	messenger RNA
mg	milligram
mM	millimolar
MRPL19	mitochondrial ribosomal protein L19
MSC	Mesenchymal Stem Cell
NaOH	sodium hydroxide
NIS	Sodium Iodide Symporter
nm	nanometres
NPI	Nottingham Prognostic Index
PBS	phosphate buffered saline
PCR	polymerase chain reaction

PPIA	peptidylprolyl isomerise A
PR	progesterone receptor
RARα	Retinoic Acid receptor Alpha
RARβ	Retinoic Acid receptor Beta
RNA	ribonucleic acid
RPMI	Roswell Park Memorial Institute
RQ-PCR	relative quantitative PCR
RT	reverse transcription
RT-PCR	reverse transcriptase PCR
SAGE	Serial analysis of gene expression
Sec	second
SERM	Selective estrogen receptor modulator
TAN	tumour associated normal
TE	Tris-EDTA buffer
THRα	Thyroid Hormone Receptor Alpha
THRβ	Thyroid Hormone Receptor Beta
TNM	Tumour size, Nodal status, Metastasis
U	units(s)
°C	degrees centigrade
µg	microgram
µl	microliter
µM	micromolar

COMMUNICATIONS ARISING FROM THIS WORK

Published Papers

- **Khan, S.,** Brougham, C. L., Ryan, J., Sahrudin, A., O'Neill, G., Wall, D., Curran, C., Newell, J., Kerin, M.J., Dwyer, R. M. 2013. miR-379 acts as a Tumour Suppressor and Regulates Cyclin B1 in Breast Cancer. *PlosOne,* **8**(7): p. e68753.

- Glynn, C.L., **Khan, S.,** Kerin, M.J., Dwyer, R.M. 2012. Isolation of secreted microRNAs (miRNAs) from cell-conditioned media. *Bentham Science* [MIRNA-EPUB-20121116-1]

- Potter, S. M., Dwyer, R. M., Hartmann, M. C., **Khan, S.**, Boyle, M. P., Curran, C. E.,Kerin, M. J. 2011. Influence of stromal-epithelial interactions on breast cancer in vitro and in vivo. *Breast Cancer Res Treat*.

- Martin, F. T., Dwyer, R. M., Kelly, J., **Khan, S**., Murphy, J. M., Curran, C., Miller, N., Hennessy, E., Dockery, P., Barry, F. P., O'Brien, T., Kerin, M. J. 2010. Potential role of mesenchymal stem cells (MSCs) in the breast tumour microenvironment: stimulation of epithelial to mesenchymal transition (EMT). *Breast Cancer Res Treat*.

- Dwyer, R. M., **Khan, S.**, Barry, F. P., O'Brien, T., Kerin, M. J. 2010. Advances in mesenchymal stem cell-mediated gene therapy for cancer. *Stem Cell Res Ther*, 1, 25.

Published Abstracts

- **S. Khan,** C.L. Brougham, L. Howard, L. Lalor, P. Dockery, M. Murphy, T. O'Brien, M.J. Kerin, R.M. Dwyer (2014) "Investigation of Mesenchymal Stem Cell (MSC) presence amd mode of action within the primary breast tumour microenvironment" Irish Association for Cancer Research (IACR), 28th February 2014, Galway. *Poster Presentation*
- **S. Khan,** C.L. Brougham, D. Wall, J. Newell, M.J. Kerin and R.M. Dwyer (2013) "Analysis of mir-339-5p expression and function in breast cancer" European Cancer Congress: Reinforcing Multidisciplinary 17th ECCO – 38th ESMO – 32nd ESTRO. 27th – 1st Oct 2013. Amsterdam – The Netherlands. *Poster Presentation*
- **S. Khan,** C.L. Brougham, D. Wall, J. Newell, M.J. Kerin and R.M. Dwyer (2013) "miR-339-5p acts as a tumour suppressor in breast cancer, mediated at least in part through regulation of cell proliferation" Sir Peter Freyer Surgical Symposium 6-9th Sept 2013. Galway. *Plenary Prize Presentation*
- **S. Khan,** C.L. Brougham, A. Sahrudin, G. O'Neill, D. Wall, J. Newell, M.J. Kerin and R.M. Dwyer (2013) "Identification of a novel tumour suppressor microRNA which targets Cyclin B1" International Student Congress of Biomedical Science (ISCOMS) 4-7th June 2013, Groeningen, The Netherlands. *Poster Presentation*
- **S. Khan,** C.L. Brougham, D. Wall, J. Newell, M.J. Kerin and R.M. Dwyer (2013) "Identification of a tumour suppressor role for miR-339-5p in breast cancer, mediated at least in part through regulation of cell proliferation" College of Medicine, Nursing & Health Sciences Postgraduate Research Day 2013 28th May 2013. *Oral Presentation*
- **S. Khan**, C. L. Brougham, J. Ryan, A. Sahrudin, G. O'Neill, D. Wall, C. Curran, J. Newell, M. J. Kerin and R. M. Dwyer (2013) "miR-10a acts as a tumour suppressor miRNA in Breast Cancer" Irish Association for Cancer Research (IACR), 28-2 March 2013, Dublin. *Poster Presentation*
- **S. Khan,** C.L. Brougham, J. Ryan, D. Wall, J. Newell, M.J. Kerin and R.M. Dwyer (2012) "Relationship between a novel tumour suppressor microRNA and retinoic acid receptor beta (RARβ) in breast cancer" Sir Peter Freyer Surgical Symposium 2-4 Sept 2012. Galway. *Oral Presentation*

- **S. Khan,** C.L. Brougham, J. Ryan, D. Wall, J. Newell, M.J. Kerin and R.M. Dwyer (2012) "Identification of a tumour suppressor miRNA that correlates with RARβ expression in breast cancer" The European Association for Cancer Research, Barcelona, 7-10 July 2012. *Poster*
- **S. Khan,** C.L. Brougham, J. Ryan, D. Wall, J. Newell, M.J. Kerin and R.M. Dwyer (2012) "Expression Of Retinoic Acid Receptor Beta (RARβ) Correlates With A Novel Tumour Suppressor MicroRNA In Breast Cancer" Postgraduate Research Day 28th May 2012. Galway. *Oral Presentation*
- **S. Khan,** C.L. Brougham, J. Ryan, D. Wall, J. Newell, M.J. Kerin and R.M. Dwyer (2012) "MicroRNA Mediated Regulation Of Retinoic Acid Receptor Beta (RARβ) In Breast Cancer" RAMI Biomedical Science Section 14th June 2012.Galway. *Poster*
- **Khan, S**., Dwyer, R.M., Sweeney, K.J. and Kerin, M.J. (2011) "Mesenchymal Stem Cells in the Primary Breast Tumour Microenvironment" Sir Peter Freyer Surgical Symposium, Galway. *Oral Presentation*
- **Khan, S.,** Dwyer, R.M., Potter, S.M. and Kerin, M.J. (2010) "Breast Tumour Stromal-Epithelial Interactions Stimulate Increased VEGF Secretion And Angiogenesis In Vitro and In Vivo." 35th Freyer, Galway. *Oral Presentation*
- **Khan, S.,** Dwyer, R.M., Hartmann, M.C., and Kerin, M.J. (2010) "Potential Role of Primary Breast Cancer Stromal Cells in the Development of Endocrine Resistance" IACR, Galway, 3-5th March 2010. *Poster*

Awards

2009 National Breast Cancer Research Institute (NBCRI) scholarship

2013 Health Research Board (HRB) of Ireland: National Cancer Institute (NCI) Summer School in Molecular Prevention held in August 2013 in Washington, USA

ABSTRACT

MicroRNAs play a critical role in regulation of gene expression and are known to be dysregulated in breast cancer. The aim of this study was investigate four microRNAs miR-875-5p, miR-339-5p, miR-10a and miR-379 which were selected based on their predicted binding site on target mRNAs Sodium Iodide Symporter (NIS), Retinoic acid receptor alpha (RARα), RARβ, oestrogen receptor alpha (ERα) and Thyroid hormone receptor alpha (THRα) in breast cancer. The secondary aim was to investigate tumour heterogeneity through detection of Mesenchymal Stem Cells (MSCs) within the stroma of primary breast tumours.

The expression of both microRNAs and target mRNAs was investigated in patient breast tissues. Gene expression analysis revealed significant loss of both RARβ and THRα expression in breast cancer patients compared to healthy controls, highlighting their relevance in disease. While miR-875-5p and miR-339-5p were not found to be dysregulated in breast cancer or involved in regulation of the target genes analysed, miR-10a and miR-379 expression was found to be significantly decreased in breast cancer patients compared to healthy controls, suggesting a tumour suppressor role for these miRNAs. Further, miR-379 was linked with patient clinicopathological details and with increasing tumour stage the level of miR-379 decreased significantly. Subsequently Cyclin B1 was identified as a target gene for this miRNA. Decreased Cyclin B1 protein levels and associated inhibition of cellular proliferation was observed in the presence of a miR-379 mimic in vitro. In vivo studies revealed that cells engineered to stably express miR-379 had reduced tumour forming potential and reduced growth rate, confirming a tumour suppressor role for this miRNA in breast cancer.

Analysis and culture of primary stromal cells highlighted the heterogeneity of the tumour microenvironment. Along with activated myofibroblasts, a subpopulation of MSCs was identified within the tumour microenvironment. This subset of stromal cells had characteristic MSC morphology, cell surface antigens and the proven ability to differentiate into osteoblasts and chondrocytes.

This promising data revealed loss of miR-379 in the tumour setting and supports the potential for replacement strategies in the clinical setting.

Chapter 1

Introduction

1.1 Breast Cancer Overview

Breast cancer is the most commonly diagnosed cancer among women in Ireland, with an annual incidence of approximately 2767 new cases [1]. In 2010, 649 women died as a result of breast cancer, making it the second greatest cause of cancer related deaths of Irish women, following lung cancer [1]. Metastasis is the single greatest contributor to cancer related deaths. Men are also affected by breast cancer with an annual incidence of approximately 20 cases and with 10 reported deaths in 2010 [1]. Globally breast cancer is the second most common cancer worldwide accounting for over 1.4 million new cases of the disease in 2010, resulting in approximately 458,500 deaths [2]. It is predicted that by 2030 this number will have increased to 2.1 million [3]. Breast cancer is a complex heterogeneous disease, for which no one universally appropriate treatment strategy is available. It is vital to further enhance our knowledge of the disease to improve the lives of cancer patients globally.

The mammary gland is made up of glandular and adipose tissues which are held together by loose fibres referred to as Cooper's ligaments [4]. Each breast consists of approximately 15-30 functional ducto-lobular units which are arranged radially around the nipple (Figure 1.1) [5].

Figure 1.1 Anatomy of the Breast [5].

The majority of cancerous cells are of epithelial origin and display altered appearance and cellular behaviour [6, 7]. Breast cancer can exist as in situ disease, where the disease remains within the ducts or lobules of the breast and is classed as Ductal Carcinoma In Situ (DCIS), or Lobular Carcinoma In Situ (LCIS). In situ carcinomas accounted for 333 patients diagnosed in 2010 [1]. In situ carcinomas are characterised by their inability to invade through the epithelial basement membrane. Once invasion occurs, these carcinomas are referred to as invasive carcinomas. These are the more predominant forms of cancers. In 2010, invasive carcinomas accounted for the remaining 2434 breast cancers cases diagnosed [1]. Of the invasive carcinomas approximately 75-80% are invasive ductal carcinomas and 10-15% are classed as invasive lobular carcinomas, and the less common forms are mixed lobular, inflammatory, colloid, tubular, medullary and papillary breast cancers [8].

Metastasis occurs when the cells spread from the primary site out to local or distant sites of chest wall or skin, lymphatic infiltration to axillary nodes, or via haematogenous spread to organs of lung, liver, brain and bone [9].

1.1.1 Breast Cancer detection

Early breast cancer detection is vital to ensure positive patient outcome. The highest incidence of the disease occurs between the ages of 50 and 64 years [1]. The National Breast screening program is in place in Ireland, providing free screening to women of that age-band. The main reason for clinical assessment of the breast is the presence of a palpable lump. There are also a number of other factors that require investigation:

- Altered shape or size of the breast
- Changes in appearance of the nipple or skin
- Blood nipple discharge
- Axillary swelling or lump

Following presentation, patients undergo triple assessment [10, 11]. This includes identifying any family history of the disease or other risk factors such as age at presentation, menopausal status, HRT use, age at childbirth etc. This is followed by a physical examination of the breasts and axilla and a mammogram of the breasts. If a lump is present, a core biopsy is taken to assess the tissue. This is performed by needle (core), stereotactic, excision or wire localisation biopsy. Ultimately confirmation of the disease relies on the removal of tissue from the affected area. The pathologist determines the histological abnormality and estrogen receptor (ER), progesterone receptor (PR) and human epidermal growth factor 2/neu (HER2/neu) status of the cancer [10].

1.1.2 Breast tumour Classification

Classification of breast tumours allows for the characterisation of prognostic groups and further influences the decision of future treatment strategy for the patient. Clinicopathological details are collected which include tumour size, stage and grade of the tumour, presence or absence of lymph node metastases, and distant metastases.

Breast cancer staging is based on the Tumour Node Metastasis (TNM) system. This was defined by the American Joint Committee on Cancer [12]. This TNM system uses tumour (T) size (cm), extent of regional lymph node

(N) involvement and the presence or absence of metastases (M) beyond the regional lymph nodes [13].

The **T** category describes the original primary tumour size

- **TX** Primary tumour cannot be assessed
- **T0** No evidence of primary tumour
- **Tis** Carcinoma in situ (cancer that has not spread to neighbouring tissue)
- **T1-T4** Size and extent of the primary tumour
    - **T1** Tumour < 20mm in greatest dimensions
    - **T2** Tumour > 20mm but <50mm in greatest dimensions
    - **T3** Tumour > 50mm in greatest dimensions
    - **T4** Tumour of any size growing into the chest wall or skin

The **N** Category describes cancer spread to the nearby lymph nodes

- **NX** Regional lymph nodes cannot be assessed
- **N0** No regional lymph node involvement
- **N1-N3** Involvement of lymph nodes (number/extent of spread)
    - **N1** Metastasis in 1-3 ipsolateral level axillary lymph node(s)
    - **N2** Metastasis in 4-9 ipsolateral axillary lymph nodes or internal mammary nodes.
    - **N3** Metastasis in 10 or more axillary lymph node(s) or clinically internal mammary lymph node(s), infraclavicular lymph node(s) or combination of axillary lymph nodes with ipsilateral internal lymph nodes.

The **M** category details metastatic spread

- **M0** No distant metastasis
- **M1** Distant metastasis present

For the clinician staging is very useful as it aids accurate prognosis. There is a strong correlation between disease stage at diagnosis and patient survival. Relative 5-year survival rates are reported to be much higher when diagnosed at earlier stages (Stage I, 92%) compared to late stages (Stage IV, 26%, Table 1.1)[14].

Anatomic Stage/ Prognostic Groups				5-year Relative Survival [14]
Stage 0	Tis	N0	M0	
Stage IA	T1*	N0	M0	92%
Stage IB	T0	N1mi	M0	
	T1*	N1mi	M0	
Stage IIA	T0	N1**	M0	84%
	T1*	N1**	M0	
	T2	N0	M0	
Stage IIB	T2	N1	M0	
	T3	N0	M0	
Stage IIIA	T0	N2	M0	62%
	T1	N2	M0	
	T2	N2	M0	
	T3	N1	M0	
	T3	N2	M0	
Stage IIIB	T4	N0	M0	
	T4	N1	M0	
	T4	N2	M0	
Stage IIIC	Any T	N3	M0	
Stage IV	Any T	Any N	M1	26%

Table 1.1 TNM Breast Cancer Staging [12]. Relative 5-year survival data based on tumour stage in Ireland between 2004-2008 [14]. * T1 includes T1mi (Tumour <1mm in greatest dimensions). ** T0 and T1 tumours with nodal micro metastases are excluded from Stage IIA and are then classified as Stage IB. N1mi includes Micro metastases (greater than 0.2 mm and/or more than 200 cells, but no greater than 2.0 mm).

1.1.3 Breast Cancer Grading

Breast cancer grading is carried out by microscopic examination of cancer cells and tissue structures and comparing it to the structure and behaviour of normal cells. It is also an indicator of tumour growth and metastasis. Tumours are graded from 1-3 depending on the level of abnormality. Cells in the tumour that appear similar in morphology to normal cells are defined as "well-differentiated" and these tumours tend to grow and spread less than tumours that are defined as "undifferentiated" or "poorly differentiated" [15]. These types of tumours lack normal-like cell resemblance and behave differently. Categories for defining tumour grade are as follows:

GX: Grade cannot be assessed (undetermined grade)

G1: Well differentiated (low grade)

G2: Moderately differentiated (intermediate grade)

G3: Poorly differentiated (high grade)

Tumour grade is a means of histologically assessing the tumour based on tubule gland/ formation, nuclear features (pleomorphism), and mitotic counts. Each of these factors is then given a score (1-3) and then each score is added to give a final score of 3-9. The final value is then used to determine the grade of the tumour. Grade 1 tumours have a score of 3-5, Grade 2 tumours have a score of 6-7 and Grade 3 tumours have a score of 7-9. This was initially developed by pathologists from Nottingham and is known as the Nottingham Grading System (NGS) [16, 17]. Numerous factors affect the patient outcome in cancer and these include: the type of cancer, location, and stage of cancer. One of the key determinants of patient outcomes is the Nottingham Prognostic Index (NPI), a program aimed at identifying the correct patient prognosis following surgery [18]. This system is based on tumour size, lymph node stage, and histological grade. The NPI divides patients into separate treatment groups. It also allows for a reliable and sensitive means of assessing clinical aggressiveness of a tumour [19]. The NPI can classify patients into three defined subgroups based on the likelihood of dying from the disease. The limitations however, are that this

system fails to effectively predict treatment outcome of individual patients. It is also subject to operator variability which is a direct result of tumour heterogeneity. Classifications of tumours are based on molecular profiling. This offers immense potential in conjunction with histological grading.

1.1.4 Molecular Profiling – Epithelial Subtype

Over the past three decades, the complex heterogeneous nature of breast cancer has been characterised extensively, by applying genetic and biochemical markers. Recently technological advances have been made using microarray and Serial Analysis of Gene Expression (SAGE) technology [20]. The nature of breast cancer can be somewhat explained by the different epithelial subtypes identified in the disease. These sub-classes of breast cancer were initially identified by Sørlie et al [21]. Using microarray technology, this group investigated the gene expression patterns of 78 breast cancer tissues and 4 normal breast tissue samples. The gene expression profile revealed a distinct subdivision of tissues, and these were subsequently classified into five subtypes. Based on the gene expression profiles obtained, five subtypes were established: Luminal A, Luminal B, and Her2 over expressing, Basal and Normal-like breast [21, 22]. Tumour subtypes can be classified based on their expression of oestrogen, progesterone and HER2/neu receptors. The Luminal A subtype is characterised by positive expression of ER, PR and no amplification of HER2/neu. Luminal B subtypes are typically referred to as triple positive, while basal breast cancers are triple negative. Her2 cancers show amplification of HER2/neu receptor and lack expression of ER and PR.

These five subtypes differ in their expression of genes and response to treatment and patient outcome [23]. Overall the Luminal A subtype has been shown to have the most successful treatment outcome for patients, while those with triple negative or basal subtypes display poorer outcomes [21, 22]. Estrogen receptor alpha (ERα) is present on approximately 70-80% of breast cancers [24]. Blocking this ERα therefore has been shown to be a very successful treatment strategy for early breast cancers. Therapeutic agents typically used are Tamoxifen which is a Selective Estrogen Receptor

Modulator (SERM) and cooperatively blocks the ER. Aromatase Inhibitors (AI's) are also used and are drugs that are capable of blocking the synthesis of estrogen. While these agents successfully treat ER positive breast cancer, they are essentially ineffective in ER negative cancers. With the development of the HER2/neu targeting drug Trastuzumab, treatment of Luminal B cancers in combination with AIs has proven very successful [25, 26]. In the HER2 subtype Trastuzumab in conjunction with chemotherapy has proven to be effective [27]. Triple negative and basal-like breast cancers on the other hand have drawn a lot of attention due to their lack of expression of ER, PR and Her2 and therefore show no benefit with treatments such as anti-estrogen hormonal therapies or Trastuzumab [28]. 15% of all breast cancers are classified as basal-like and show poor relapse-free and overall survival in patients [29-31]. These cancers mainly affect women of a younger age and are characterised by a more aggressive type of tumour with high mitotic activity and high grade invasiveness [32, 33]. Treatment of basal-like cancers relies on aggressive chemotherapy regimens [32].

The tumour epithelial subtype offers immense potential to allow for individualised patient therapy. The Oncotype DX™ (ODX) breast cancer assay was developed by Genomic Health (Redwood City, CA) [34]. This test evaluates the expression of a panel of 21 genes present in a tumour, which have previous association with tumour proliferation, invasion and estrogen and HER2 signalling [35]. This assay applies computational algorithms to estimate the likelihood of breast cancer recurrence within 10 years of diagnosis and further assesses the probable benefit from chemotherapy [36-38]. It is very effective in identifying a subgroup of ER positive patients with an Oncotype score <18 who derive a benefit from chemotherapy.

1.1.5 Breast Cancer Treatment

In 1880 W.S. Halsted introduced radical mastectomy as a treatment option for breast cancer [39]. Since then, the prognosis for breast cancer patients has improved tremendously. Limited treatment options have evolved to

include a vast array of different alternatives with overall improved patient outcome observed. Treatment strategies available now include surgery, chemotherapy, radiation therapy, and previously mentioned biological therapies such as monoclonal antibodies, and hormonal (anti-estrogen) therapy.

- Surgery involves the removal of the tumour and subsequent analysis of tissue for staging of the disease. Nowadays sentinel node biopsy is commonly used for staging. Lumpectomy (breast sparing surgery) involves the removal of only the tumour tissue and some surrounding normal breast tissue to ensure all cancer and any abnormal tissues are removed. Mastectomy refers to the complete removal of the breast as an option to treat or prevent the disease. It is carried out when breast conservation is not possible due to large or multicentric tumours. Nowadays sentinel lymph node biopsies are carried out and are appropriate for staging. Other surgical procedures include axillary clearance confined to those with positive nodes to stage the disease.
- Chemotherapy is a chemical treatment aimed at killing all fast replicating cells in the body. This is the most commonly used treatment for cancer, as cancer cells grow and multiply at a much faster pace than normal cells. However, this therapy is not tumour targeted. There are major drawbacks with chemotherapy, as some normal cells possess high cell proliferation capacity and therefore become a target of chemotherapeutic agents that are intended for the cancer cells. These areas of high cellular proliferation include the gastrointestinal tract, bone marrow, testicles and ovaries. This results in severe side effects for the cancer patient, resulting in gastric side effects, reduced haematopoiesis and sterility.
- Targeted therapy offers improved sensitivity and aims at reducing common side effects observed with chemotherapy. This is done by improving sensitivity of the drug for cancer cells over normal cells. Trastuzumab (Herceptin) is a monoclonal antibody that aims at interrupting cellular proliferation and promoting anti-apoptotic

behaviour of HER2/neu. Another form is the inhibition of Vascular Endothelial Growth Factor A (VEGFA) which is responsible for tumour angiogenesis [40, 41].

- Hormone therapy targets breast cancers which are sensitive to certain hormones. Estrogen is a major component of tumour cell proliferation in ER positive cancers. The expression of ER in breast cancer is one of the key prognostic markers. It is used to identify patients who will benefit from anti-estrogen therapy such as Tamoxifen or more recently AIs such as Anastrozole. These drugs prevent the biosynthesis of estrogen [42, 43]. Tamoxifen which is a non-steroidal anti-estrogen drug, is the most widely used type of hormonal therapy for ER positive breast cancers [44]. It is classed as a SERM with both agonist and antagonist features. It prevents estrogen from binding. Tumour growth is also reduced by blocking the G1 phase of the cell cycle [42]. Another feature of Tamoxifen is its ability to induce apoptosis [45].
- Radiotherapy is a key part of treatment, usually in conjunction with breast conservation therapy (BCT) or following mastectomy in patients with an increased risk of recurrence [46]. This treatment uses controlled ionizing radiation to destroy the DNA of malignant cells. Radiation therapy in breast cancer include, external, internal (brachytherapy) and intraoperative radiotherapy [47, 48]. As with surgery, the location of the cancer is vital for successful treatment. Therefore it has shown limited efficacy in treating metastatic disease.

Overall, patient outcome has been improving over the last 20 years in Ireland. This is due to enhanced breast cancer screening, earlier diagnosis, more targeted and better therapies and increased awareness. This can be attributed to screening and greater uptake of treatment and earlier diagnosis. Despite improvements in screening and therapy, there are still > 600 patients that die from the disease each year in Ireland alone. Stage IV and particularly Basal-like breast cancers require an understanding of the

molecular mechanisms underlying the disease within the tumour microenvironment.

1.2 MicroRNA

MicroRNAs (miRNAs) are short non-coding RNA molecules of between 19-25 nucleotides in length. Initially these non-coding RNA molecules were regarded as "junk" RNA with no apparent function. However, over the past two decades miRNAs have become a vital part of research worldwide because of their gene regulatory roles. MicroRNAs were initially discovered in 1993. They have since been revealed to be part of the non-coding genome and play a vital role in controlling many important processes among a variety of species [49].

MicroRNAs are known to regulate cellular gene expression at a post-transcriptional level and mediate their effect through mRNA cleavage and mRNA decay. This induces degradation or translational inhibition through imperfect or complementary pairing with their target genes or translational repression through complementary binding [49]. Functional studies have shown that miRNAs play a crucial role in the regulation of almost every cellular process that has been analysed and that their altered expression correlates with many human malignancies [50].

At the time of writing, there have been 25,521 reported mature miRNA sequences identified in 206 species: miRBase version 20, updated June 2013. In the human genome alone, there are approximately 2555 miRNAs identified (last update June 2013). MiRNAs have been shown to regulate processes in diverse regulatory pathways, including development, differentiation, apoptosis, cell proliferation and organ development [49].

1.2.1 MicroRNA Biogenesis

The knowledge of miRNAs has evolved tremendously over the past decade, allowing a detailed understanding of the function and mechanism of action of miRNAs. MiRNAs are transcribed in the cell nucleus by RNA polymerase II, obtained from independent genes or from introns of protein

coding genes, to form large capped and polyadenylated primary miRNA transcripts (pri-miRNAs) (Figure 1.2) [50]. This transcription process occurs within distinct genomic locations. Often these are intergenic with independent promoters while others are clustered in polycistronic transcripts. Approximately 50% of pri-miRNAs are located in introns of host genes and this would suggest that transcriptional regulation may be influenced by host gene promoter control [49]. These pri-miRNAs (precursor molecules) then fold into hairpin structures containing imperfectly base-paired stems and are further processed in two steps by the RNase III type endonucleases Drosha (RN3) and Dicer. The resulting pre-miRNA, which is a 70-90 nucleotide precursor, consists of an imperfect stem-loop hairpin structure, containing 2-nucleotide 3' ends, similar to small interfering RNAs (siRNAs) which function in RNA interference (RNAi). The strand with the 5' end terminus is generally located at the thermodynamically less-stable end of the duplex and functions as a mature miRNA, while the other strand is degraded [51-54]. This pre-miRNA is created through Drosha cleavage and is then exported into the cytoplasm via the shuttle protein exportin-5. In the cytoplasm, the hairpin structure is further cleaved by another RNase III endonuclease, called Dicer, together with its binding partner the transactivator RNA-binding protein (TRBP). This further develops it into a small transient dsRNA duplex (miRNA/miRNA*).

Following this processing, the mature sequence is incorporated into the miRNA-induced silencing complex (miRISC) containing Argonaut 2 (AGO2) protein. There are 4 Ago proteins (AGO1-4) that are responsible for miRNA-mediated repression of gene expression in mammals.

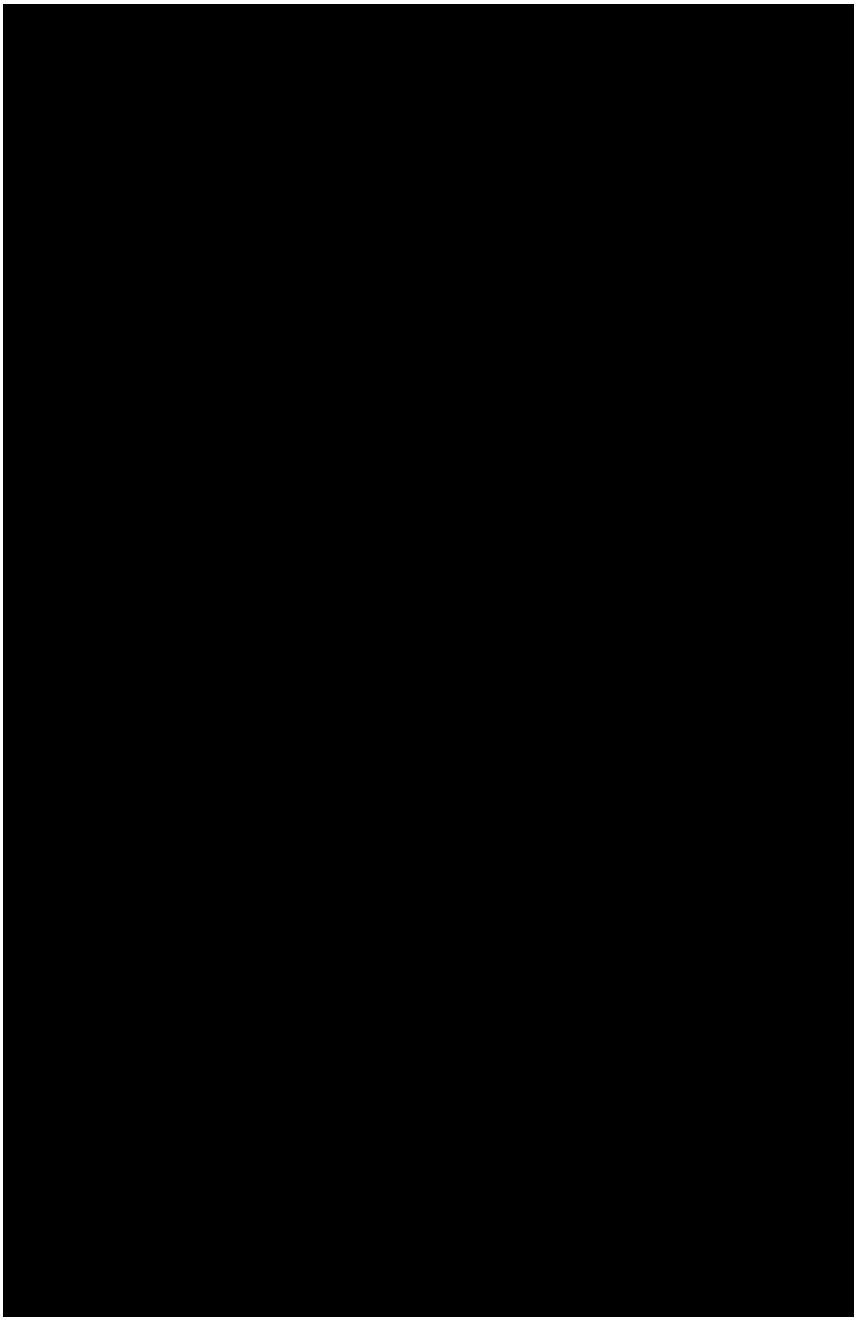

Figure 1.2 MiRNA Biogenesis and mechanism of action overview [50].

1.2.2 MicroRNA Function

MiRNAs apply their functional role via sequence-specific regulation of post-transcriptional gene expression and by targeting mRNAs through cleavage and translational repression. This targeting is carried out via binding to the 3' untranslated region (UTR) of mRNA targets. It has been reported that binding to the 5'UTR of mRNA targets also occurs [55, 56].

MicroRNAs then basepair with the target mRNAs and induce transcriptional repression or deadenylation and degradation (Figure 1.2) [57]. The ‘seed sequence’ is located on the 5’end of the mature miRNA (position 2-8). This is a critical region which allows for mRNA target recognition [49]. Complementarities of miRNA seed sequence with mRNA allows for the regulation of gene expression and protein translation. This occurs through one or two mechanisms:

- Binding of the miRNA to protein-coding mRNA with perfect base pairing homology results in RNA-mediated interference (RNAi). This leads to cleavage of the mRNA by the Argonaut in the RISC.
- The more commonly applied mechanism by which it targets genes is through imperfect binding to the partially complementary sequence in the 3’UTR of the downstream target mRNA. This results in repression of protein translation and therefore, reduces protein levels present [57-59].

This highlights that the exact role in translational repression is still somewhat unclear. It is thought that this process is related to P-bodies (GW182) which are cytoplasmic structures containing enzymes responsible for mRNA decay. These are known to be involved in the storage and degradation of translationally repressed mRNAs [60, 61].

Investigation of miRNA targets and further understanding their regulatory role has proven difficult, due to the nature of miRNAs and their relationship with mRNA targets. Research now includes the use of computational target prediction tools to identify putative miRNA targets. These predictive algorithms use the seed sequence of the miRNA to search for the complementary sequence in the 3’UTR of known genes. From research carried out using computational prediction, it is thought that each miRNA has the potential to bind to as many as 200 target genes. It is also estimated that they can regulate up to 30% of all human coding genes [62]. There are major draw backs with the use of predictive algorithms. The main reason is that not all miRNAs target the 3’UTR [55, 56]. Relevant targets are also being missed through ineffective search criterions that fail to take into

account variation in species for the target selection. It is therefore crucial to validate novel targets using functional experiments that allow for the investigation of the effect of a particular miRNA in vitro or in vivo on downstream gene or protein expression.

1.2.3 MicroRNA Nomenclature

Due to the rapid growth of the microRNA field, consistent naming of these miRNAs has been applied since their first large scale discovery [63-65]. Currently miRNA naming is regulated by the MicroRNA Registry [66] which allocates the names to newly identified microRNAs. Prior to submitting novel miRNAs to the Registry, these miRNA must be validated by cloning or showing experimental evidence of expression and processing [66]. MiRNAs are given sequential numerical identifiers. This usually consists of 3-4 letter prefixes to designate the origin of species, for example hsa-miR-101 states a human (homo sapiens, hsa) gene origin, whereas mmu-miR-101 refers to mouse (mus musculus, mmu) miRNA (Figure 1.3). Mature sequences of approximately 22- miRNA molecules are identified by 'miR' in the database and the ~70-nt precursor hairpins subsets are labelled 'mir' [67]. Paralogous mature miRNA sequences that only differ at one or two positions are given lettered suffixes such as hsa-miR-10a and hsa-miR-10b in humans [68]. In cases where the miRNA products are identical but are expressed on different loci, they are given numbered suffixes (e.g. hsa-miR-281-1 and hsa-miR-281-2) [63]. Cloning studies have also isolated two mature products, one from each arm of the double stranded miRNA hairpin. More often one of these is a by-product without any relevant function and is then referred to as the 'star' sequence. These miRNAs are labelled with a (*) at the end of the miRNA name [69]. When mature miRNA sequences are excised from opposite arms of the same hairpin precursor, they are identified by naming them in the form of hsa-miR-17-5p (5' arm) and hsa-miR-17-3p (3' arm) (Figure 1.3) [70]. Overall the microRNA registry provides for accurate naming of novel microRNA genes and contains a comprehensive database of published miRNA sequences.

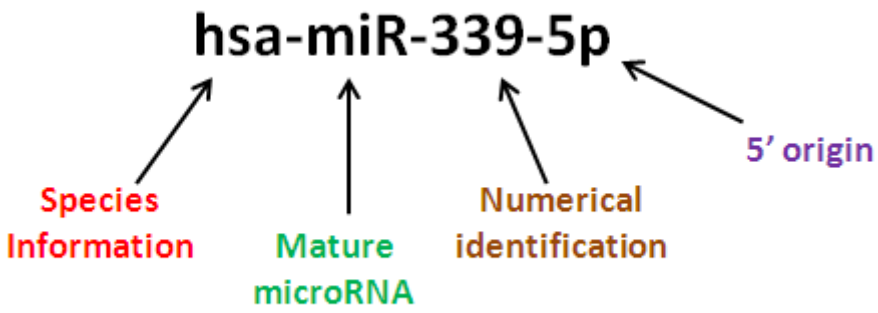

Figure 1.3 Explanation of microRNA nomenclature

1.2.4 MicroRNA Dysregulation in Cancer

The process of cell malignancy is defined by a number of key steps. These are defined as the Hallmarks of Cancer [71]: self-sufficiency in growth signals, loss of growth inhibition signals, evasion of programmed cell death (apoptosis), abnormal proliferation, increased angiogenesis and tissue invasion and metastasis [71] (Figure 1.4).

Figure 1.4 Revised Hallmarks of Cancer by Hanahan and Weinberg [72].

The first report of miRNA implication in human cancers originated in a chronic lymphocytic leukaemia (CLL) study. Both miR-15a and miR16-1 were found to be down-regulated in CLL patients [73]. This was the first study to hypothesise that miRNAs may play a role in the pathogenesis of human cancers. Following these findings it was necessary to establish the role of miRNAs by extensive profiling. Global expression analysis was carried out on different miRNAs in normal tissues and diseased tissues. This gave rise to the potentially important role for miRNAs as tools for tumour classification, diagnosis and prognosis [74]. MicroRNAs affect cellular transformation, carcinogenesis, and metastasis, acting as either oncomiRs or tumour suppressor miRs [75]. MiRNAs have been shown to target critical leukaemia suppressors and therefore act as proto-oncogenes in the hematopoietic compartments [74]. In colon cancer, miR-17-92 was shown to be up-regulated in microsatellite stability (MSS) compared to microsatellite instability (MSI-H). This paper suggested that this miRNA may play a role as an oncomir, as it is more prevalent in the aggressive MSS compared to the MSI-H colon cancers [76]. One of the most researched miRNAs in this area was miR-21 which has previously been shown to be up-regulated in various solid tumours [77-80]. This suggested that miR-21 may exert a role as an oncogene. However, much of the data implicating these miRNAs in cancers only show results in terms of profiling, and are limited to in vitro functional assays. MicroRNAs are more often identified as tumour suppressors. The miR-15 and miR-16 family have been shown to be down-regulated in a number of cancers, including malignant pleural mesothelioma (MPM) [81], and reintroduction of miR-16 into tumour bearing mice lead to reduced tumour growth. A recent study by Peng et al [82], investigated the potential role of miR-486 as a tumour suppressor in lung cancer. They showed decreased expression of miR-486 levels in malignant lung tissues compared to adjacent normal tissues. miR-486 expression was shown to be targeted by components of Insulin Growth Factor (IGF) signalling. This miRNA had previously been linked to a potential non-invasive biomarker for lung cancer by detection in sputum and

plasma [83, 84]. Peng et al [82] further identified a link between p53 and miR-486 suggesting miR-486 is partially dependent on p53 expression.

An important factor is the potential for predicting disease outcomes using miRNAs. This was first highlighted in the CLL study, where a miRNA signature was correlated with prognostic factors and disease progression [85]. In a lung cancer study, over-expression of miR-155 and down-regulation of let-7a were used to predict poor patient outcome [86], while other reports have shown great potential of miRNAs as prognostic biomarkers [87, 88]. Predicting the response to therapy is yet another area of evaluation for miRNAs. This would enable the accurate selection of specific patient treatment strategies. MicroRNAs display a huge potential as a diagnostic tools to discriminate between tumour and normal tissue and between different subgroups of tumours as well as predicting patient outcome and response to therapy.

Some of the innate properties of microRNAs make them ideal candidates as biomarkers of disease. MicroRNAs can be easily detected in small sample volumes using sensitive techniques such as RQ-PCR. They have been readily isolated from most body fluids, including whole bloods, serum, plasma, urine, saliva, breast milk, tears, and semen, allowing them to circulate freely in a relatively stable form [89, 90]. Altered miRNA expression profiles of cancer patients have been investigated in whole blood, plasma and/or serum [91].

In 2008, miRNAs were first identified to be stably expressed in the circulation [92-94]. Mitchell et al [92] described the stability of miRNAs in the circulation, despite the large amount of RNase present. The ability of miRNAs to differentiate between healthy and diseased bloods demonstrates huge diagnostic potential [94, 95].

1.2.5 MicroRNAs and Breast Cancer

As previously highlighted, miRNAs display regulatory functions in a broad range of tissues and tumours. Identification of direct mRNA targets and subsequent functional roles of miRNAs is a common route of investigation.

Functional assays are carried out to determine this effect by gene expression analysis of target mRNAs and on protein levels. To date a wide range of miRNAs have been found to be differentially expressed in breast cancer and have been further characterised in breast cancer cell lines, tumour tissues, serum and whole bloods.

The first report of miRNA dysregulation in breast cancer was carried out by Iorio et al [96]. This group performed a microRNA array study on a total of 86 RNA samples from 76 malignant breast tissues and 10 normal breast tissues. This study highlighted a range of miRNAs to be significantly dysregulated in breast cancer [96]. The results observed showed miRNAs were effectively capable of differentiation between normal and malignant breast tumour tissues [96]. It was established that miRNAs not only distinguish between normal and malignant tissues, but also distinguish between different subtypes of breast cancer, highlighted by differential expression in basal like breast cancers [97, 98]. MicroRNAs have also been associated with tumour grade, ER, PR and HER2/neu receptor status [96, 99, 100]. miR-125b, miR-145 and miR-10b were down-regulated in breast cancer suggesting a potential tumour suppressor role. miR-21 and miR-155 were found to be over-expressed in breast cancer and highlighted a role as an oncomiRs. This study reported correlation of miRNA expression levels with patient clinicopathological details such as hormonal subtype, tumour stage, vascular invasion and cell proliferation index [96]. Results observed indicated that miRNAs have the potential to differentiate between molecular and pathological profiles. Since then significant advances have been made. Some miRNA signatures are differentially expressed between luminal A and basal-type tumours [97, 99, 101]. MicroRNA expression in the circulation has been a focus especially for the use as potential non-invasive biomarkers of the disease. To date there are numerous studies on circulating miRNAs in breast cancer. miR-195 has been previously shown to be up-regulated in whole bloods of breast cancer patients and was further shown to return to baseline expression following excision of the primary tumour [102]. Differentially expressed miRNA levels in patients with DCIS were observed when comparing the expression of miR-125b, miR-182 and miR-183 to

invasive carcinomas [103]. Expression levels in serum revealed elevated expression of a range of miRNAs (miR-21, miR-106a, miR-155) in breast cancer patients compared to healthy controls [104]. A study by Waters et al [105] investigated a potential relationship between circulating and tissue microRNAs in an in vivo breast cancer study. This report assessed whether or not aberrantly expressed miRNAs in the circulation reflect the tissue expression. This study highlighted distinct roles for miRNAs in the circulation and in tissue.

1.2.6 Target microRNAs of interest

The miRNAs chosen for this study were identified based on predictive algorithms. These miRNAs all have a common binding site on the Sodium Iodide Symporter (NIS), Retinoic Acid Receptor alpha (RARα), Retinoic Acid Receptor beta (RARβ), Estrogen Receptor alpha (ERα) and Thyroid Hormone Receptor alpha (THRα).
The NIS gene is located on chromosome 19p13.11 and its 3' UTR is 2,928 bp in length. Computational algorithms (TargetScan and MiRanda software [106, 107]) predicted a binding site for the following miRNAs (Figure 1.5):

- miR-875-5p starting at position 982
- miR-10a starting at position 279 and 444
- miR-339-5p starting at position 227
- miR-379 starting at position 915

Figure 1.5 Target Prediction on NIS gene using miRanda software [107].

The RARα gene is located on chromosome 17q21 and its 3'UTR is 1417 bp in length and it has a predictive binding site on:

- miR-875-5p starting at position 470
- miR-339-5p starting at position 426/1232
- miR-379 starting at position 43

The RARβ gene is located on chromosome 3p24.2 and its 3'UTR is 1315 bp in length and it has a predictive binding site on:

- miR-10a starting at position 1142
- miR-379 starting at position 905/433

The ERα gene is located on chromosome 6q25 and its 3'UTR is 4307 bp in length and it has a predictive binding site on:

- miR-875-5p starting at position 2981
- miR-10a starting at position 635
- miR-339-5p starting at position 823/1135/1756
- miR-379 starting at position 175/2190/2254/2699

The THRα gene is located on chromosome 11D-E and its 3'UTR is 581 bp in length and it has a predictive binding site on:

- miR-339-5p starting at position 183-189

To date there have been no published reports of miR-875-5p expression in normal physiology or in any disease models.

miR-10a is located within the HOX gene clusters (HOXB and HOXD) [108]. It is expressed in T cells and is induced by retinoic acid (RA) and transforming growth beta (TGF-β) [109]. In relation to cancer, it has been found to directly target HOXA1 in leukaemia cell lines [110]. Inhibition of both miR-10a and miR-10b were found to promote metastasis in neuroblastoma cell lines [111, 112]. In the context of breast cancer, it is down-regulated in mammary mouse tumours [113]. miR-10a is over-expressed in MCF-7 and MDA-MB-231 cells compared to miR-10b

expression [108]. High expression of miR-10a in tumours is associated with longer relapse-free time in ER-positive breast cancers following Tamoxifen treatment [114].

So far there have been no published reports on the normal physiological role of miR-339-5p. It has however, been implicated in a number of different cancers. Altered expression of miR-339-5p was observed in gastric cancer, colorectal cancer, papillary thyroid carcinoma, lung cancer, cervical cancer and in neural cell lines [115-119]. There is currently only one study on miR-339-5p in relation to breast cancer [120]. Elevated expression was observed in benign breast disease compared to malignant tissues, confirmed by RQ-PCR in a small patient group of 25 breast cancer tissues and 9 benign tissues. This was further confirmed by In Situ Hybridisation (ISH) in 90 breast cancer tissues and 26 benign breast disease tissues. It is worth noting that this study did not include any normal breast tissues. Over-expression of miR-339-5p was found to inhibit cell migration and invasion in breast cancer cell lines [120].

Expression of miR-379 is somewhat unknown in the current literature. In relation to breast cancer, there is currently one paper which reported over-expression of miR-379 directly affected Interleukin-11 (IL-11) expression in the metastatic breast cancer cell line MDA-MB-231(SA) variant and its parental MDA-MB-231 breast cancer cell line, through the TGF-β pathway [121]. This study aimed at identifying miRNAs capable of mediating the metastatic process in breast cancer through the known TGF-β pathway. A global miRNA expression analysis was carried out to identify dysregulated miRNAs between the highly metastatic MDA-MB-231 (SA) and the parent MDA-MB-231 cell line. They identified 3 miRNAs that were potentially involved in regulation of TGF-β induced IL-11 production, miR-204, miR-211 and miR-379. miR-379 was shown to directly bind to the 3'UTR of IL-11 and also was reported to down-regulate IL-11 expression in breast cancer cell lines along with the expression of several genes involved in TGF-β signalling, including prostaglandin-endoperoxidase synthase 2 (PTGS2) [121].

1.3 Target genes of interest

The Sodium Iodide Symporter (NIS) is a transmembrane glycoprotein also known as solute carrier family 5, member 5 (SLC5A5). It is predominantly expressed in the basolateral membrane of the thyroid follicular cells. NIS folds into 13 transmembrane domains, containing a hydrophilic (extracellular) NH_2 terminus and a hydrophobic (intracellular) COOH terminus [122] (Figure 1.6). NIS functions in the active uptake of iodide from the bloodstream to the thyroid follicle, for the synthesis of thyroid hormones, Tri-iodothyronine (T_3) and Thyroxine (T_4) [122].

Figure 1.6 Diagram of NIS structure [123].

NIS drives the transport of iodide into the cells by using the extracellular: intracellular Na^+ cation concentration gradient. NIS requires 2 Na^+ cations to transports one I^-anion down the concentration gradient and across the membrane [124] (Figure 1.7). This allows for the natural build-up of I^- concentrations in the thyroid of approximately 20-40 higher concentrations than in the blood plasma [125].

Figure 1.7 Uptake of Iodine by the Thyroid [126].

The ability of NIS to accumulate iodide in the follicular cells has been harnessed for the treatment of thyroid cancer. The diagnostic use of radioiodide and NIS has been safely applied for more than 60 years. It is an essential part of therapy which has little or no side effects. In combination with low side effects and being a non-invasive treatment option, it also reports excellent patient prognosis since its first use in the 1950s [127]. NIS radioiodide accumulation is observed in cells expressing functional NIS. Radioiodide build up emits energy in the form of radioactive decay. Therefore, 90% of this decay is discharged as beta decay or radiation. This can be strong enough to penetrate cells up to 2 mm away from the initial source, depending on the amount of radiation accumulated during the process [128]. Beta radiation causes mutations and DNA disruption resulting in cell death. This has immense implications in a homogeneous tissue environment, where beta decay can efficiently kill cells which are located centrally at the site of iodide accumulation.

NIS expression in the thyroid has been also used for thyroid imaging. This occurs since 10 % of the energy released from decay of the radioiodide is released as gamma radiation. This type of gamma radiation is known to be visible through a certain amount of tissue. NIS expression can be visualised using gamma cameras, and sensitive software tools, therefore highlighting the source of iodide accumulation. This visualisation of the thyroid is made

possible through the use of non-toxic radioiodide. This makes it possible to image the thyroid tissue and subsequently determine suitable treatment strategies using cytotoxic radioiodide (Figure 1.8).

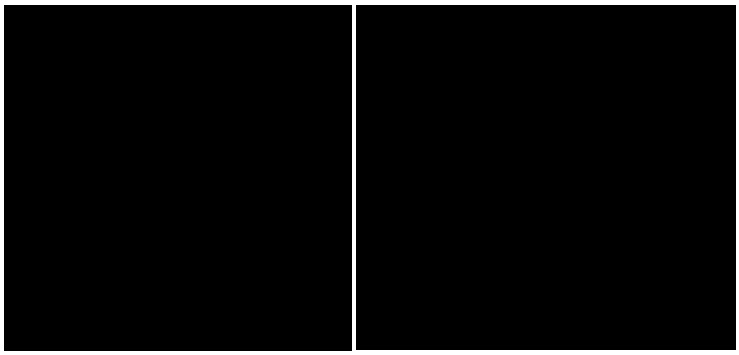

Figure 1.8 Thyroid Scan using NIS-based accumulation of radiolabelled iodide [129, 130].

1.2.7 NIS Expression in Breast Cancer

NIS is expressed in normal lactating mammary tissue to sustain iodide concentration into the breast milk for neonatal nutrition [131]. It is not normally expressed in the non-lactating breast. However, NIS has been reported in malignant breast tissues [132-136]. A study by Tazebay et al [131] revealed that approximately 80% of breast cancers show elevated levels of NIS. This was demonstrated by immunohistochemistry in 29 malignant samples and 9 normal breast tissues. NIS was also confirmed to be expressed in 88% of DCIS compared to 76% detection in invasive carcinomas. NIS expression was further confirmed by Upadhay et al [134], revealing expression present at mRNA and protein level throughout breast cancer samples. Functional NIS expression has been previously validated through scintigraphy [134, 137]. These studies suggested an exciting potential for exploitation of NIS expression in breast cancer for imaging and treatment of the disease. Moon et al [137] raised the issue of the lack of functional NIS protein. This study showed that only 16% of the NIS expression in tumours had functional NIS protein. A recent paper published from this laboratory, by Ryan et al [138] revealed significantly higher NIS expression in fibroadenoma tissue compared to breast tumours. This in turn

has highlighted the potential of NIS as a tumour suppressor in breast cancer. Loss of NIS expression in benign tissues may be an indicator of progression to malignancy [138]. Native expression of NIS in breast cancer is highly variable and its regulation is poorly understood.

1.2.8 Mammary NIS Regulation

Regulation of NIS expression in thyroid tissue is well established. However, the regulation of mammary NIS has yet to be elucidated. NIS regulation in the lactating mammary gland was shown to be optimal in the presence of estrogen, prolactin and oxytocin [131].

Estrogen receptor alpha (ERα) has been shown to activate mammary NIS transcription [139]. This study was carried out in ER positive breast cancer cell lines and supported the presence of an estrogen responsive element in the NIS gene promoter [139]. A quantitative IHC analysis was carried out on 100 breast tumours to identify differences in expression of NIS across patient subtype [140]. This study identified a positive relationship between NIS and ER expression in breast cancer. 70% of breast tumours were found to be positive for NIS expression, with the highest expression observed in the ER-positive, PR-positive and HER2-negative subpopulation [140]. ERα is a key regulator of NIS gene expression in ER-positive breast cancer cells [139]. A correlation was observed between Retinoic Acid (RA)-responsive NIS expression with functional ERα [139]. Therefore, all-trans RA (atRA)-induced NIS in breast cancers suggests a possibility as a marker for ERα-positivity. This could be used as a target for visualisation and therapy with radioiodide.

RA has previously been shown to induce NIS expression in MCF-7 and T47D cells in vitro [138, 141-143]. This was also confirmed in a transgenic breast cancer mouse model [144]. Many forms of RA including 9-cis RA as well as synthetic ligands of retinoic acid receptors (RAR) have a regulatory role in NIS in breast cancer [141, 142, 145]. Combination treatments of RA and Dexamethasone have also been shown to induce functional NIS expression in breast cancer xenograft models [146]. A study by Ryan et al [138] observed significant associations between NIS and RARα, RARβ, as

well as ERα expression in breast tissue samples. The greatest relationship was reported between NIS and RARβ [138].
Ryan et al [138] further highlighted a potential role for thyroid hormones in the regulation of NIS in breast cancer, as dimerization between RARs and THRs are known to occur [147, 148]. It is important to understand the regulation of NIS in breast cancer. This could be potentially mediated through miRNA regulation.

1.4 Breast Tumour Microenvironment

The tumour microenvironment has been recognised as a major contributor to breast cancer progression [149]. The solid tumour is composed of a network of cells including endothelial cells and their precursors, smooth muscle cells, pericytes, fibroblasts, carcinoma associated fibroblasts, myofibroblasts, neutrophils, basophiles, eosinophil, mast cells, T and B lymphocytes, natural killer cells and antigen presenting cells which include macrophages and dendritic cells [150] (Figure 1.9).

Figure 1.9 Tumour Microenvironment Overview [151]

The tumour microenvironment has been recognised as a regulator of carcinogenesis [72]. Due to its involvement in invasion and metastasis, there is an immense interest in developing novel treatment strategies aimed at targeting the microenvironment rather than just isolating cancer cells. Pathologists agree on the wound-like appearance of desmoplastic tumours, which is also observed in some breast carcinomas. Dvorak et al [152], defined tumours as wounds that never heal. This has been exploited to further elucidate the nature of the tumour microenvironment in relation to cancer progression [152]. Studies have revealed recruitment of inflammatory cells to the microenvironment by neoplastic epithelial cells. This recruitment occurs as a response to tumour hypoxia and necrosis, stimulated by the secretion of chemoattractive growth factors and cytokines [153]. This recruitment of inflammatory cells, allows the formation of a

microenvironment enabling tumour growth [154], created through a series of dynamic and reciprocal interactions between inflammatory cells and tumour cells [153]. It is emerging that metastatic traits are acquired through exposure of epithelial cancer cells to paracrine signals obtained from mesenchymal cell types within the tumour-associated stroma [155].

1.5 Carcinoma Associated Fibroblasts (CAFs)

Tumour promoting role of the stromal cells have been reported which is enhanced by vascular cells, immune cells, fibroblasts, myofibroblasts, adipocytes and bone marrow derived progenitors [156-159]. It is important to note that these stromal cells have been implicated in the failure of systemic drug delivery to tumours and further have aided development of resistance to therapy [160, 161]. Carcinoma associated fibroblasts (CAFs) are activated fibroblasts which were originally isolated from prostate cancer in 1999, and are the predominant cell type in the tumour microenvironment [162]. CAFs are known to play a role in carcinogenesis of breast cancer [163, 164]. They are present in almost all solid tumour tissues including colon, lung, liver, prostrate, pancreas and gastric cancer where they have an established role in tumour development through cell-cell interactions and cross-talk with tumour cells [162, 165-167]. However, the origin of CAFs is still unclear. It is thought that CAFs arise from activated resident fibroblasts, bone-marrow derived MSCs, or from cancer cells that have undergone epithelial-mesenchymal transition (EMT) [168-170], highlighting diverse origins. This ability to promote tumour neoangiogenesis and tumour growth are well established [163, 171]. However, recent reports have indicated that CAFs play a role in modulating cancer stem cell (CSC) traits and further promote metastasis [172, 173]. It is the interaction between CAFs and epithelial cancer cells that has been shown to facilitate the development of aggressive tumours during cancer progression. CAFs induce the transformation of otherwise resting tumour cells into highly malignant cells which are then capable of spreading to and infiltrating into distant sites

[174]. However, the molecular mechanisms surrounding this CAF-induced malignant conversion remains to be elucidated.

1.6 Mesenchymal Stem Cells (MSCs)

MSCs are non-hematopoietic adult derived multipotent stem cells. They are progenitor cells that contribute to the maintenance and regeneration of a variety of connective tissues [175]. Studies have shown that the bone-marrow derived MSCs are actively recruited to the microenvironment of developing tumours [155]. MSCs are characterised by their inherent ability to both self-renew and to differentiate into multiple lineages including, osteoblasts, chondrocytes and adipocytes [175]. These cells are isolated from the stromal compartment of the bone-marrow, along with a number of other sources which include adipose tissue, trabecular bone and skeletal muscle [176]. Currently there is not one single marker available to identify MSCs. However, a panel of specific antigens have been identified and these include the expression of CD105, CD73 and CD90 in >95% of the cells, and the absence of CD14, CD34, CD19, HLA-DR and CD45 [177]. Studies have shown that when systemically administered to healthy animals, MSCs migrate to the lung, liver and bone and were also found at low levels in other tissues. However, upon insult or injury, the migratory pathway is altered to allow migration to sites of injury [178]. This has been specifically shown to be due to endocrine signals released from the sites of inflammation or injury. These are then transmitted to the bone-marrow and subsequently lead to mobilization of multi-potent MSCs to sites of injury [179]. Their ability to be recruited to sites of injury, inflammation and tumours has suggested a potential role as anticancer agents for delivery of therapeutic drugs [180]. There are conflicting reports implicating MSCs in cancer progression due to their pro-angiogenic properties and immunosuppressive nature [181]. The process of MSC mobilization is thought to be similarly regulated to leukocyte migration which is facilitated through integrins, selectins and adhesion molecules [182].

Although many studies have been carried out using MSCs mixed with tumour cells in animal models of disease, there is little information available on the presence and number of native MSCs within the patient tumour tissue.

1.7 Aim of Study

The aim of this study was to investigate the role of four miRNAs and their potential target mRNAs in breast cancer. A secondary aim was to investigate tumour heterogeneity through analysis of MSCs within primary breast tumours.

Individual aims were:

- To characterise the level of expression of miR-875-5p, miR-339-5p, miR-10a and miR-379 in breast cancer patients and healthy controls.
- To quantify the expression of NIS, RARα, RARβ, and ERα and THRα in breast cancer.
- To determine any potential relationship between the miRNAs of interest with target genes.
- To assess any relationship between miRNA/ mRNA expression and patient clinicopathological details.
- To determine functional relevance of selected miRNAs in vitro.
- To assess the tumour suppressor potential of a specific miRNA in an in vivo model.
- Finally, to characterise primary stromal cells and indentify a subpopulation of MSCs within the tumour microenvironment.

Chapter 2

Materials and Methods

2.1 Cell Culture

2.1.1 Background

Cell culture is defined as a technique which allows the culture of cells in a strictly controlled environment in the study of cell biology. It involves the cultivation of cells isolated from tissue samples or organs. The cells are maintained by controlling various factors that influence cell growth. Environmental factors such as temperature, pH, nutritional factors such as sugars, amino acids, vitamins and salts can all be applied to maintain and control the cell type being cultured. In some cases further factors are applied such as serums which are vital for optimal cell growth. These contain growth factors that cannot be produced synthetically. However these serums have been found to introduce certain amounts of variability for cell behaviour and therefore must be carefully selected to ensure consistency [183]. The media were supplemented with antimicrobial agents such as penicillin or streptomycin which help prevent the onset of contamination [184, 185].

All cell manipulations were performed under strict aseptic technique to reduce the risk of contamination and cross infection within the laboratory environment. This involved the use of standard personal protective equipment (PPE) such as laboratory coats and gloves to ensure no exposed areas of skin pass into the laminar air flow (LAF) hoods (Haraeus, Germany) or the incubators. The use of 70% industrial methylated spirit (IMS) solution to clean LAF hoods and any containers, flasks or equipment passing between the LAF hood and incubators further served to reduce contamination. Cell line cultures were separated from primary cells at all times by the use of designated LAF hoods and incubators. Cell lines are essentially transformed cells, which are easily expandable and are well characterised. The disadvantages of cell lines are that they are susceptible to genetic drift. Primary cell culture were directly derived from the patient tissue itself post surgery. These cells are clinically relevant as they contain the cells from the tumour microenvironment. They are often difficult to obtain and frequently hard to culture. When handling cells, the use of aseptic technique and of laminar flow Biosafety cabinets is vital for cell line

integrity but also to protect the operator from transmissible disease. The cells were maintained in a controlled Stericycler CO_2 incubator –HEPA class 100 (Thermo Electron Corporation) at 37ºC and 5 % CO_2. A strict regimen of laboratory etiquette, maintenance and cleaning served to minimise the risk of contamination and infection and optimise efficiency in the cell culture laboratory.

2.1.2 Immortalised Breast Cancer Cell lines

This study used cell lines, representing genotypically different variants of breast cancers (Table 2.1).

Cell line	**Epithelial Subtype**	**Expression**	**Media Constituents**
T47D	Luminal A	ER+, PR+, Her2 low	RPMI 1640 w/L-glutamine + 10% FBS + Pen/Strep
MDA-MB-231	Basal	ER-, PR-, Her2 low	Leibovitz-15 w/L-glutamine +10% FBS + Pen/Strep
SK-Br-3	Her2 Over-expressing	ER-, PR-, Her2 high	McCoys 5A w/L-glutamine +10% FBS + Pen/Strep
ZR-75-1	Luminal A	ER+, PR+, Her2 low	RPMI 1640 w/L-glutamine + 10% FBS + Pen/Strep
BT-474	Luminal B	ER-, PR+, HER2+	RPMI 1640 w/L-glutamine + 10% FBS + Pen/Strep
MCF10-2A	Normal-like	N/A	1:1 mixture of Dulbecco's modified Eagle's medium and Ham's F12 medium, 20 ng/ml human epidermal growth factor, 100 ng/ml cholera toxin, 0.01 mg/ml bovine insulin, 500 ng/ml hydrocortisone and 5% horse serum

Table 2.1 Cell line Characteristics

All media were supplemented with 10% Fetal Bovine Serum (FBS) (Gibco), 100 IU/mL Penicillin/ 100µg/mL Streptomycin (Pen/Strep, Lonza) and 1% L-glutamine if not a constituent already. The cell lines were commercially available through the American Type Culture Collection (ATCC) and were

selected based on breast cancer epithelial subtypes and distinct differences in hormone receptor status.

The main cell lines used for this study were T47D and SK-Br-3 cells. The T47D (Human ductal breast epithelial cell line) were isolated in 1979 from a pleural effusion obtained from a 54 year old female patient with an infiltrating ductal carcinoma of the breast. These cells are luminal A subtype and display a "cobble-stone-like" morphology.
The MDA-MB-231 cell lines were initially isolated in 1973 from a pleural effusion obtained from a 51 year old female patient with an adenocarcinoma. MDA-MB-231 cells are referred to as "triple negative" breast cancer cell lines as they form from poorly differentiated adenocarcinomas.
The SK-Br-3 cells were isolated in 1970 from a pleural effusion obtained from a 43 year old female patient with an adenocarcinoma.

2.2 Primary Breast Cell Culture

2.2.1 Collection of Fresh Tissue specimens

Following ethical approval (Galway University Hospitals Research Ethical Committee) and informed patient consent (Appendix 1) fresh specimens of human breast tissues were obtained from patients undergoing surgery (Appendix 2).
In this study these cells were obtained from tumour (TUM) tissue samples and from tumour associated normal (TAN) tissue, which is essentially a tissue sample taken from the patient's breast but is located ≥2 cm away from the tumour. A normal (NORM) tissue sample was obtained from breast reduction mammoplasty. Fresh tissues were placed in 2 mL if Dulbecco's Modified Eagle's Medium (DMEM) supplemented with 200 IU/ml Pen/Strep and then transferred to the Tissue Culture Laboratory for further processing.

2.2.2 Primary Cell Culture Isolation Protocol

The tissue samples were received from theatre, and processed as soon as possible to ensure cell viability. Each tissue sample was rinsed twice in Phosphate Buffer Saline (PBS) lacking Calcium and Magnesium supplemented with 200 IU/ml Pen/Strep. The tissue sample was then placed in a 10 cm Petri-dish and finely minced using sterile scalpels with number 11 scalpel blades [186]. Tissues were minced down to pieces of tissues that were $\leq 1mm^3$ and therefore allowing a greater surface area for collagenase to digest. Each sample was then placed in three times the tissue volume of 0.1 % Collagenase Type III (BioChem Corp) and incubated at 37ºC, 5% CO_2 for 12-18 hours in DMEM supplemented with 10 % FBS. Collagenase acts by splitting collagen's triple helical conformation to yield uncoiled fibre fragments and thereby disassociate cells (Figure 2.1).

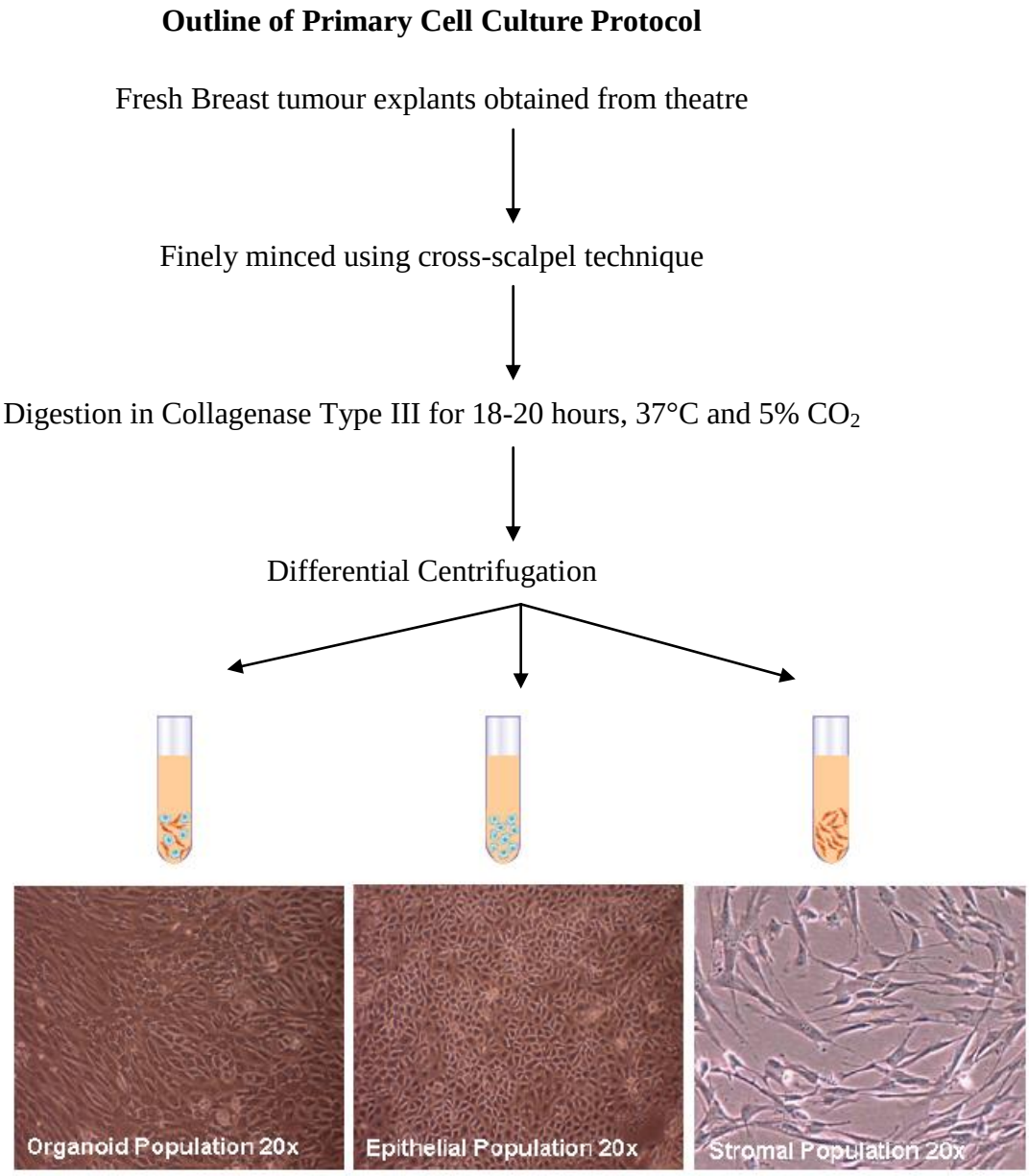

Figure 2.1 Overview of Primary Cell Culture protocol [186]

After incubation digested tissue suspension was shaken vigorously by hand to disaggregate any remaining large clumps. Three cell populations were isolated using differential centrifugation [186]. This process involved spinning the mixed cell population at different centrifugal speeds to separate the cells based on their density, (Table 2.2).

Cell Type	Centrifugation (rpm)	Time (min)
Organoid (crude) Fraction	400	1
Epithelial Fraction	700	2
Stromal Fraction	1,000	4

Table 2.2 Outline of Primary Cell Culture protocol [186]. The same protocol was applied to samples obtained from reduction mammoplasties.

The digested suspension was centrifuged at 400 rpm for 1 minute. The pellet contained mixed cell fragments and was therefore termed the organoid cell fraction. The supernatant was transferred to a fresh falcon and centrifuged at 700 rpm for 2 minutes. The resulting cell pellet contained the epithelial cells. The supernatant was transferred to a fresh falcon and centrifuged at 1000 rpm for 4 minutes. This pellet contained the stromal cell fraction. The three cell pellets were all resuspended in 2 ml stromal cell culture medium (DMEM + Glutamax with 10% Heat inactivated FBS (HI-FBS, i.e. FBS heated at 65°C for 30 minutes), 200 U/ml Pen/Strep). The cells were seeded onto T-25cm^2 tissue culture flasks (Sarstedt) and maintained at 37°C, 5% CO_2. To positively promote the growth of organoid and epithelial cells these cell fractions were cultured in 3:1 ratio of organoid medium (DMEM + Glutamax, 200 U/ml Penicillin and 200 µg/ml Streptomycin, 0.075 % Bovine Serum Albumin, 0.5 µg/ml Hydrocortisone, 5 µg/ml Insulin, 5 ng/ml Epidermal growth factor, 10ng/ml Cholera toxin): stromal medium solution for initial 24 hours post seeding. Following incubation, cells were maintained in organoid medium from then on. The lack of FBS in organoid medium prevents the growth of stromal cells and therefore keeps the epithelial cells free from stromal cell contamination. The stromal cells were

cultured in complete stromal medium, this allowed for positive selection of stromal cells. Medium change was performed three times a week and cells were passaged every 7 -10 days.

2.3 Feeding Cell Lines / Media Change

Cell media was replaced three times a week to ensure cells received adequate nutrients, to remove waste and then maintained in an antibiotic supplemented environment to prevent any onset of contamination. All media and its supplements were incubated in a water bath at 37°C for 15 minutes prior to feeding the cells. Cells were inspected using a light microscope before feeding, to monitor for contamination and cell density ratio. A class II Biosafety Cabinet was turned on, cleaned using 70% IMS and let run for 15 minutes prior to use. Using aseptic technique, spent media was decanted carefully into a waste container. Fresh, pre-heated media was then added down the base of the flask to prevent disruption of monolayer of cells. The flask was then returned to the incubator and stored at 37°C, 5% CO_2 until further use. 8 mL of media was used for a T-25 cm^2 flask, 12 mL was used for a T-75 cm^2 flask and 25 mL was used for a T-175 cm^2 flask.

2.4 Subculture of Cells

Once cells reached a cell density of approximately 80-90%, or when cells where used as part of an experiment, they were sub-cultured. Cells require subculturing at 80-90% confluency, in order to maintain cells in the log phase of growth and therefore prevent senescence. Briefly, media was pre-heated in a water bath at 37°C, along with PBS and 0.25% Trypsin/EDTA (T/E) (Sigma) for 10-15 minutes. Media was decanted and cells were rinsed with PBS (Calcium and Magnesium free) to remove any FBS present on the monolayer of cells, as this would prevent the action of T/E. Trypsin was added to the monolayer of cells for 1 minute, part of this trypsin was then discarded to leave enough to permeate monolayer. The flask was returned to the incubator at 37°C for 3-5 minutes to allow cell disassociation. The flask was gently tapped, to lift the cells from the flask and using a light microscope cell detachment was inspected. Once all cells had lifted, fresh pre-warmed media (including serum) was added to the cell suspension to

stop the action of T/E and to resuspend cells. Clumps of cells were disaggregated by pipetting up and down in the flask. The collected cell suspension was then counted and seeded at appropriate cell densities for either expansion or cell culture experiments, and incubated at 37°C until further use.

2.5 Cell Counting

Cells in a single cell suspension were counted using a NucleoCounter® (Chemometec). This automated procedure uses a fluorescent dye, Propidium Iodide (PI) to distinguish between viable and non-viable cells, by its ability to permeate the membrane of the cells. PI can only enter non-viable cells as their membrane is permeable. Once it enters it forms a complex with the DNA of the cell nucleus. Viable cells exclude PI. This allows for the quantification of concentration of viable cells, (Figure 2.2).

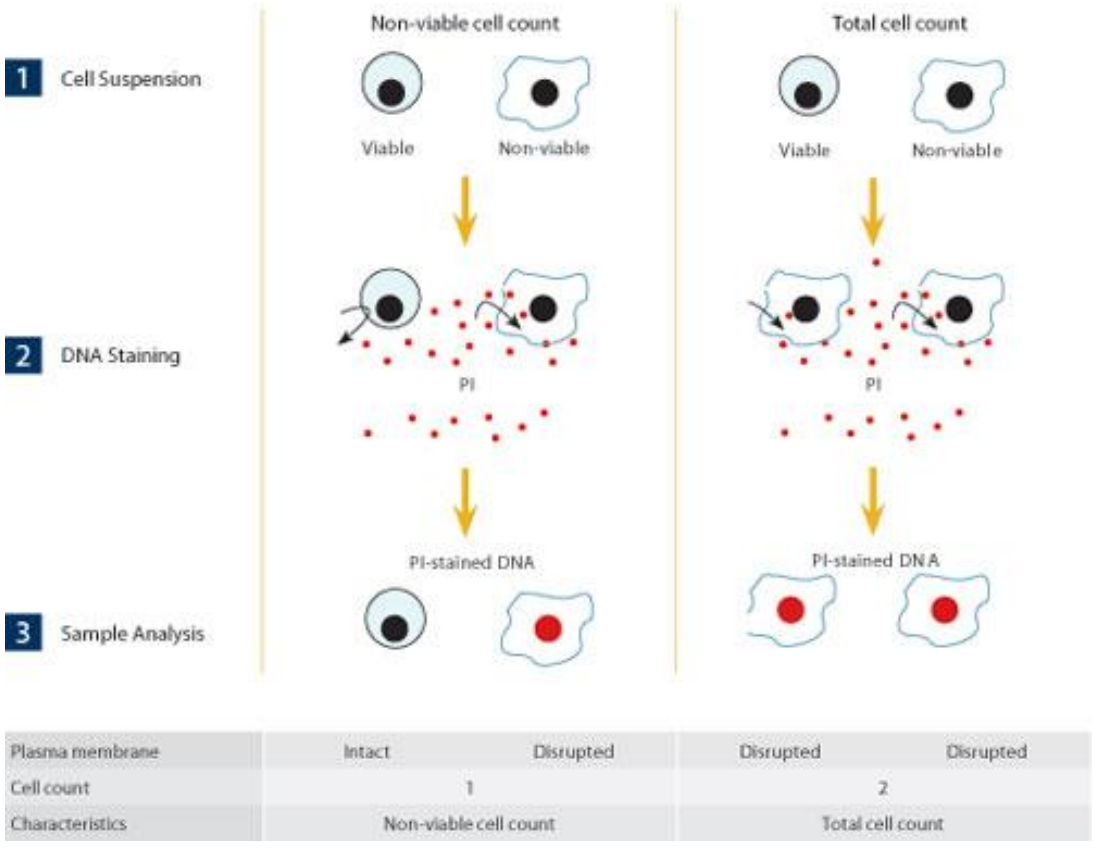

Figure 2.2 Principle of cell count.

Briefly, a volume of 100µl of trypsinised single cell suspension was added to two labelled eppendorfs. One eppendorf was used to determine the total cell count/mL and had 100µl of Reagent A100 (Lysis Buffer) and 100µl Reagent B (Stabilizing Buffer) added. The solution was vortexed between each addition. These reagents lyse the cell membranes of the viable cells. This suspension was then loaded onto a NucleoCassette containing the fluorescent dye PI (Figure 2.3).

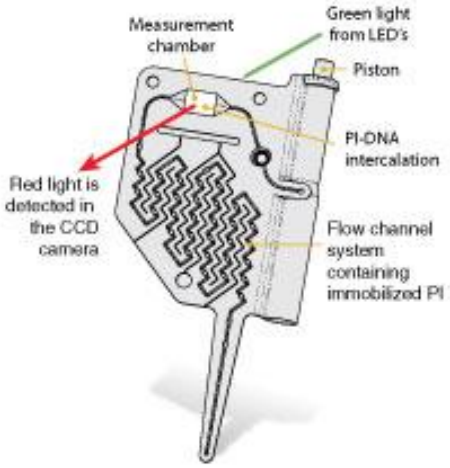

Figure 2.3 Image of a NucleoCasette.

The loaded cassette was then placed into the NucleoCounter®. A total cell count (viable and non-viable) was determined. This value was then multiplied by three to account for the dilution with ReagentA100 and Reagent B. The second eppendorf, containing 100µl of cell suspension was not exposed to any reagents and was loaded directly onto a fresh NucleoCassette and placed into the NucleoCounter®. The value estimated here reflected the amount of dead cells present in the cell suspension as only the cells with a permeable membrane stained for the PI. The non-viable cells were subtracted from the total cell count to give a value for the viable cell count per mL of suspension.

2.6 Cryopreservation of Cells

At the end of a cell culture experiment or if stocks of cells needed to be generated, cells were frozen using complete media supplemented with 5%

Dimethylated Sulphoxide (DMSO). Cells were trypsinised into a single cell suspension and counted as previously described. Cells were then frozen in the presence of 5% DMSO which prevents crystallisation and subsequent lysis of cells during this step. The cryovials used must be chilled on ice before adding the cell suspension, as DMSO is highly toxic at 37°C. The required number of cells were then added to the chilled cryovial containing 5% DMSO and then transferred and frozen in a "Mr Frosty" container at -80°C for 3 hours before transferring it for long-term storage in liquid Nitrogen (-196°C). The "Mr. Frosty" container is an isopropanol bath which allows for the slow freezing of cells at a rate of -1°C/ minute.

2.7 Recovering Cells

When using a frozen stock of cells, cells were recovered from liquid nitrogen. Cells need to be thawed quickly, to prevent cell lysis by action of the DMSO. Media was pre-warmed at 37°C for 10-15 minutes. Prior to removing the cells from long term storage, this pre-warmed media was added to a flask to ensure quick addition of cell suspension following thawing of cells. Cells were removed from liquid nitrogen and immediately immersed in the pre-heated water bath and gently swirled to support thawing of cells. Before the last bit of cell suspension had melted, the cryovial was aseptically transferred to the LAF hood. Cells were resuspended in the appropriate amount of media and incubated at 37°C until further use.

2.8 Mesenchymal Stem Cells

Mesenchymal stem cells (MSCs) are self-renewing multipotent precursors. They reside in the stromal adherent fraction of the bone marrow (BM). MSCs can be easily expanded in vitro to generate MSC cultures which under appropriate conditions can differentiate into different lineages including osteoblasts, chondrocytes and adipocytes, (Figure 2.4).

Figure 2.4 MSC Differentiation potential [187].

MSCs were supplied by the Regenerative Medicine Institute (REMEDI) at National University of Ireland, Galway (NUIG). Following informed patient consent and ethical approval, bone marrow was aspirated from the iliac crest of healthy donors following a defined clinical protocol [188]. MSCs were isolated from the marrow aspirates by direct plating method and consequently cultured for 12-15 days to diminish the non-hematopoietic cell fraction present. MSCs were cultured in Alpha Minimum Essential Medium (α-MEM – Sigma) containing 1,000 mg/L glucose and L-glutamine and was supplemented with pre-selected FBS (10%) (Hyclone Ltd.) and 100 IU/mL Penicillin/ 100 µg/mL Streptomycin (Lonza). At present no specific individual marker for MSCs has been identified. Therefore characterisation of MSCs was carried out by analysis of cell surface receptors targeting surface markers CD105, CD73, CD90 (positive) and CD34 and CD45 (negative). MSC isolation was performed by REMEDI at NUIG who subsequently supplied the cells used in experiments described here.

2.9 Determine Differentiation potential of primary stromal cells

2.9.1 Osteogenesis Assay

MSCs are multipotent adult stem cells which are capable of differentiation into multiple lineages of mesenchymal tissues, including bone, fat and

cartilage. The osteogenesis assay was used to determine differentiation potential of human MSCs and identify a subpopulation of stromal cells within the tumour capable of differentiating or with MSC-like characteristics. Cells were trypsinised into a single cell suspension and seeded at a density 2 x 10^4 cells/cm^2 in complete hMSC media. Cells were incubated at 37 °C and 5 % CO_2 overnight. Positive cell cultures received differentiation inducing media composed of α-MEM + Glutamax supplemented with 10% pre-selected FBS, 10 mM β-glycerophosphate, 50 µM Ascorbic acid2-Phosphate, 100 nM Dexamethasone, 100 U/mL penicillin and 100 µg/mL Streptomycin. The low dose of glucocorticoid in this case hydrocortisone and dexamethasone committed the cells towards the osteogenic path and potential maturation into osteoblasts. The control cells received complete hMSC medium. Media was replaced twice a week and cells were harvested between day 10 and day 17, or before cells lifted from the wells.

Calcium deposition was determined using Von Kossa Staining [189]. This method was used to validate the presence of mature osteoblast formation following 10-17 days of culture in differentiation inducing conditions. Cells were fixed in 4% paraformaldehyde for 15 minutes. The cells were washed three times using PBS. Fixed cells were then stained in 3 % silver nitrate for 15 minutes under UV light, which ensured calcium was reduced from the phosphate complexes. Following silver nitrate exposure, cells were washed three times in PBS and incubated in 5 % sodium thiosulphate for a further 5 minutes, thus removing any trace of non-reduced calcium. Repeated wash step and then counter-stained with haematoxylin for 3 minutes, rinsed cells in distilled water and examined for the presence of calcium deposits.

Nodules containing calcium mineral stained black. Depending on the amount of calcium present the colour intensity changes. Less developed nodules present, stained in a lighter shade ranging from yellow to brown following the differentiation process. The negative controls which received hMSCs medium, showed a typical blue colour of haematoxylin staining of the cell nucleus. Cells images were taken to prove confirmation of

differentiation in test cells and absence in control wells cultured in standard medium, using inverted microscope containing a digital camera (Olympus CK2).

2.9.2 Adipogenenic Differentiation

Cells were trypsinised and counted. The cells were seeded at a density of 2 x 10^4 cells/cm^2, in a 24-well plate. Four control wells and four positive wells were set up for each cell type. Cells were incubated at 37°C, 5% CO_2 and let grow until they reached confluency (approximately 2-3 days). Once confluent, adipogenic induction media (containing α-MEM media supplemented with 1 mM Dexamethasone, 1 mg/ml Insulin, 100 mM Indomethacin, 500 nM MIX (3-Isobutyl-1-Methyl-Xanthine), 100 U/mL penicillin and 100 µg/mL Streptomycin and 10% FBS) was added to the positive wells. The control wells received maintenance medium (containing α-MEM media supplemented with 1 mg/ml Insulin, 100 U/mL penicillin and 100 µg/mL Streptomycin and 10% FBS). After three days the media was changed, maintenance media was added to both test and control wells and incubated for one day. This cycle was repeated three times. For the final media change, cells were incubated in maintenance medium for 5-7 days. Cells were fixed in and prepared for Oil Red O staining.

Briefly, cells were washed and fixed in 10% Neutral buffered Formalin for 15-20 minutes at room temperature. Formalin was removed and cells were rinsed with distilled water. Working solution of Oil Red O (mixed 6 parts of Oil Red O with 4 parts of distilled water) was added to cover the cell surface layer for 5 minutes. Cells were washed using 60% Isopropanol, and then rinsed with tap water. Cells were stained for 1 minute using a 10% Haematoxylin. Finally, cells were rinsed in warm tap water, and then proceeded to take pictures of cells.

2.10 Flow Cytometry

Flow Cytometry is a method that allows for the investigation of individual cells in suspension on the basis of size, complexity, viability and protein markers. This is achieved by passing a cell suspension through a focused stream therefore allowing one cell at a time to pass through the beam of light, creating a light deflection which is then quantifiable (Figure 2.5).

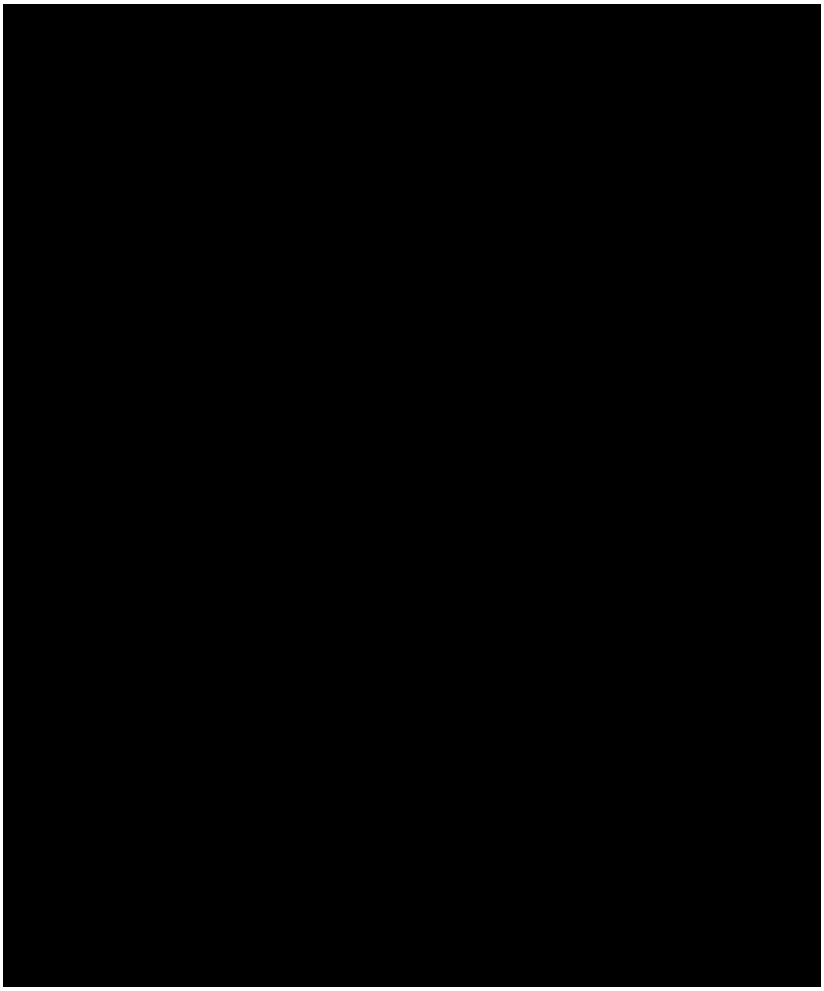

Figure 2.5 Hydrodynamic focusing of Cells [190].

Light detectors can be aligned perpendicular (side scatter) and in line with laser light (forward scatter) to measure amount of deflection created by each individual cell passing [191]. Factors governing this include, a light source, fluid lines that control the liquid stream carrying the particles, an electronic network for detection and a computer to record and analyse the data. In order to visualise these cells, monoclonal antibodies conjugated to different

fluorescent markers were used investigate the presence of surface markers on cells by formation of antibody-antigen complexes (Figure 2.6).

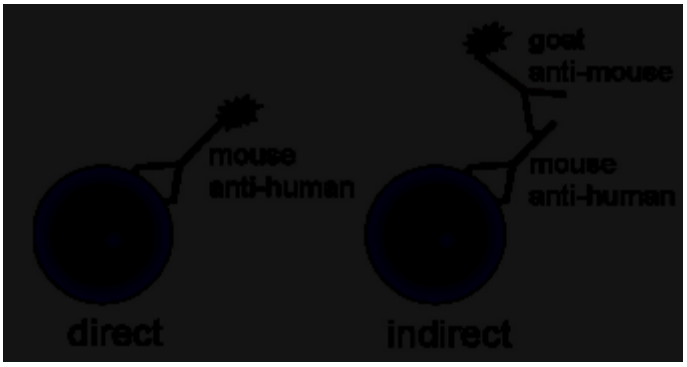

Figure 2.6 Fluorescently conjugated antibody [192].

Correct use of antibodies is very important in flow cytometry. Preferably, monoclonal antibodies were used which have previously been validated for flow cytometry. If possible they were directly conjugated to a fluorophore which prevents the need for a secondary conjugated antibody. Isotype controls were also used to determine the level of non-specific background signal caused by primary antibodies. The use of an isotype control permits the correction of this non-specific fluorescent signal and reveals the fluorescence of the antibody (Figure 2.7). Isotype controls were selected for each antibody type and fluorochrome used e.g. Mouse IgG1 κ antibody conjugated to Allophycyanin (APC) requires Mouse IgG1 κ Isotype Control conjugated to APC.

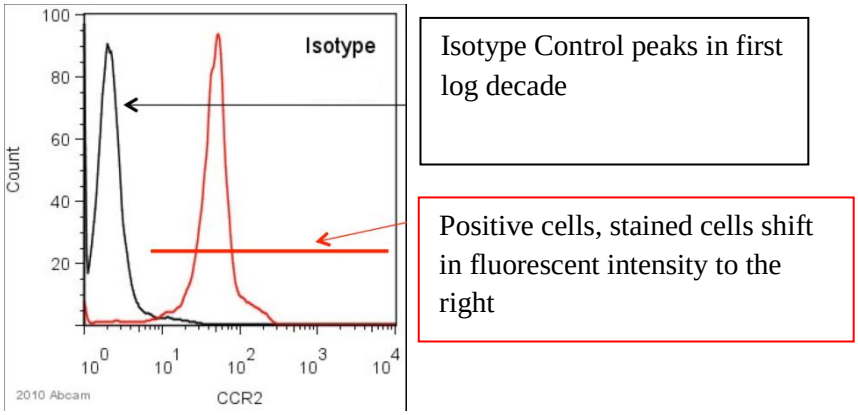

Figure 2.7 Isotype control accounts for non-specific binding

All the analysis was carried out on a Guava® EasyCyte 8HT™ Flow Cytometry system (Millipore). The Guava® EasyCyte 8HT™ flow cytometer is a compact bench top instrument which can be used for traditional flow cytometry analysis of cell suspensions. This bench top flow cytometry system however eliminates the need for sheath fluid which is normally needed to create a hydro dynamically focused stream of cells, Figure 2.5. This allows for cheaper analysis and reduces the amount of cells needed and waste generated. It has eight detection parameters including: forward and side scatter, and detection of 6 fluorescent colours from excitation of red and blue lasers.

2.11 Maintenance Steps

There are a number of critical steps that needed to be adhered to before commencing analysis on the Guava® EasyCyte 8HT™ flow cytometry system. Thorough cleaning of the instrument and flow cells is important as this ensures no obstruction in the microfluidics and repeated calibration guarantees consistency of results. The first step for each protocol is to sign in the log sheet (Table 2.3), and then to clean the instrument before each assay. Correct reporting of cleaning and usage of the flow cytometer were critical in ensuring accurate results.

Date	Time	3x Quick cleans (Y/N)	Comments (What program was used, any problems encountered etc.)	Bead check (Y/N)	Cleaning (Y/N)	Capillary Shutdown (Y/N)	Shutdown Laptop	Turn off Guava	Initials

Table 2.3 Flow Cytometry maintenance Log Sheet

2.12 Start-up Protocol

The guava software offers three cleaning cycles, **Quick Clean**, **Clean & Rinse** and **Guava Clean 8.1**. Quick Clean can be run as often as needed throughout an assay it cleans the fluid system. Run Clean & Rinse to thoroughly clean the system after an assay or before running an assay when instrument sensitivity is critical. Guava Clean 8.1 was run at the end of each day before shutting down the instrument to thoroughly clean the fluid system.

2.13 Calibration using EasyCheck Kit

Calibration of the instrument is performed at the start of each day of use. This ensured Guava easyCyte HT System is performing correctly. The Guava easyCheck Kit (Cat. no.:4500-0025, Millipore) was used to verify performance, assessing counting accuracy and fluorescence detection, using a standardised fluorescent bead reagent. The kit contains Guava easyCheck Bead Reagent and Guava Check Diluent. The bead reagent was provided as a concentrated fluorescent bead suspension of known concentration. EasyCheck averages the results from three acquisitions of Guava easyCheck bead sample to determine if the results are within the desired range. Particle counts that are outside the expected range are displayed in red.

To perform an easyCheck procedure a 1:20 dilution of the concentrated bead reagent was performed with the bead diluents. The results were acquired on the Guava® EasyCyte 8HT™ using the easyCheck programme in the guavaSoft 2.1 software. The particle counts were compared with the known concentration of bead reagent and the Coefficient of Variation (CV) calculated. This particle result must fall within 10% of the standard concentration of the beads and with a 5% CV between replicates before proceeding to experimental work.

2.14 Antibodies

Antibodies employed were chosen based on antigens present on different cell types. It is vital to use a range of antibodies to characterise the stromal cell populations [177](Table 2.4).

Mesenchymal Stem Cells (MSCs)	**Positive for:** CD105, CD73, CD90 **Negative for:** CD31, CD45, CD34
Tumour stromal Markers	**Positive for:** CD90, αSMA, Prolyl-4-hydroxylase FSA and Vimentin **Negative for:** CD68 CD31, CD45 and cytokeratin (MNF116)
Epithelial cells	**Positive for:** MUC1 **Negative for:**CD90

Table 2.4 Cell Surface Markers used to characterise Primary stromal cells

2.15 Preparation of Cell suspension for Flow Cytometry

Cells were trypsinised into a single cell suspension as previously described in section 2.4. Cells were centrifuged at 1000 rpm for 4 minutes. The supernatant was discarded and the cells were resuspended in PBS. Cells were counted and the suspension was diluted to a required concentration of 2.5×10^5 cells/ml. 500µl of this cell suspension was stained with a fluorochrome conjugated antibody and for each specific conjugated antibody a representative staining was carried out for the appropriate isotype control. The cells were stained as specified by the antibody manufacturer (Table 2.5). The cells were then washed twice using PBS. This removed any unbound antibody present. Cells were subsequently maintained on ice and away from light until used for analysis.

Protein	Protein Description	Ab type	Fluorochrome	Colour	Supplier
CD105	Endoglin is a type I membrane glycoprotein located on the cell surface	IgG1 x	PerCP-Cy™ 5.5	Red1	BD Pharmingen ™, 560819
CD90	Thy-1 is a glycosylated conserved cell surface protein	IgG1 x	PE-Cy™ 5	Red1	BD Pharmingen ™, 555597
CD73	5'nucleotidase is an enzyme that catalyses 5'-mononulceotides to nucleosides	IgG1 x	APC	Red2	BD Pharmingen ™, 560847
α-SMA	Alpha Smooth Muscle Actin is an important muscle contraction marker of myofibroblasts	IgG1 x	Required 2° Ab	N/A	ABD Serotec, MCA1906
2° Ab	Goat pAB to Ms IgG	IgG1 x	APC	Red2	AbCAM, ab72553-100
CD10	Membrane metallo-endopeptidase is a zinc-dependent metalloprotease enzyme	IgG1 x	FITC	Green	ABD Serotec, SFL1556F
CD31	PECAM-1 plays a key role in removing aged neutrophoils from the body	IgG1 x	FITC	Green	BD Pharmingen ™, 555445
CD34	Cell surface glycoprotein functions as a cell-cell adhesion factor	IgG1 x	PE	Yellow	BD Pharmingen ™, 555822
CD45	PTPRC is a member of the tyrosine phosphatase family – hematopoietic stem cell marker	IgG2 a	RPE	Yellow	ABD Serotec, MCA87PET
MUC1/ CD227	Mucin penetrates cell membranes, binds to pathogens and prevents infection – epithelial cell marker	IgG1 x	FITC	Green	BD Pharmingen ™, 559774
CD24	Heat stable antigen CD24 is a cell adhesion molecule – lymphocyte marker	IgG1 x	FITC	Green	ABD Serotec, MCA1379FT
CD14	Glycosylphophatidylinositol (GPI)-linked membrane glycoprotein also known as a LPS receptor – monocytes and macrophages	IgG1	PE	Yellow	BioLegend, 325605
HLA-DR	Cross-reacts with the human class ii antigen of the major histocompatibility complex (MHC).	IgG2 a	PerCP-Cy™ 5.5	Red1	BD Pharmingen ™, 552764

Table 2.5 Details of Antibodies used.

2.16 Flow Cytometry Analysis of stained cell suspension

Before analysis the Guava® EasyCyte 8HT™ was prepared for use by performing a Guava Clean 8.1 (as previously described) and ensuring optimum performance by running the EasyCheck bead reagent.

A detailed worklist was created in the InCyte program which allocated the sample locations, detailed the cleaning steps during analysis, and specified number of events to be counted (Figure 2.8).

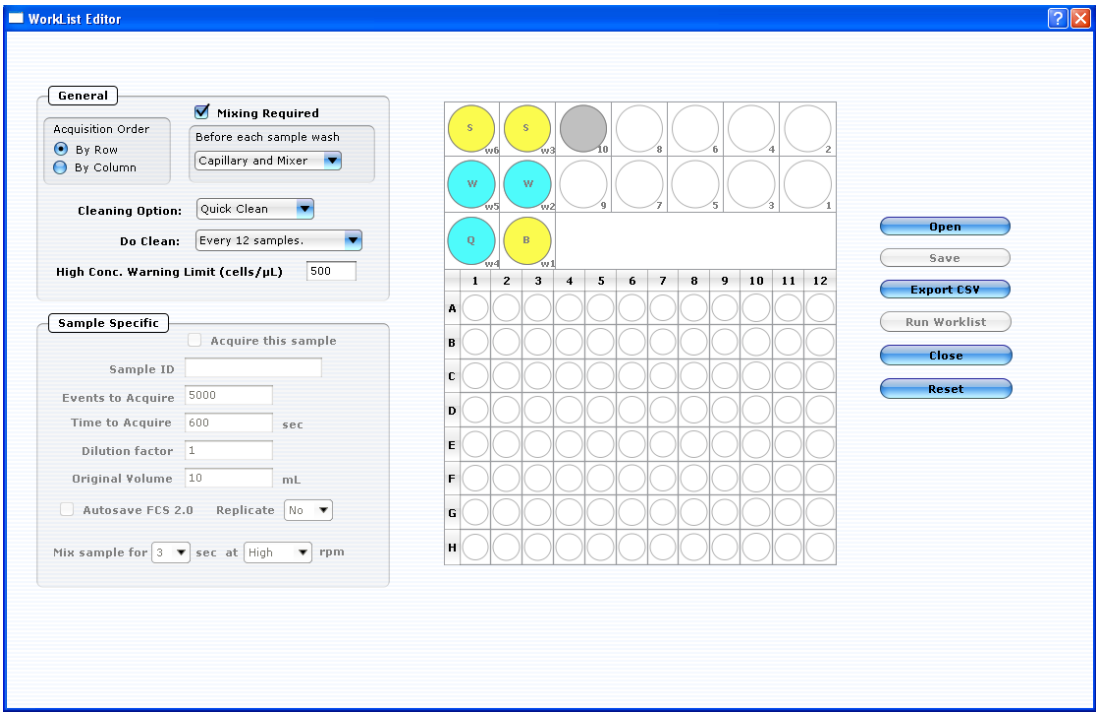

Figure 2.8 Guava InCyte Worklist Editor.

The cells were then loaded in duplicate into wells of a 96-well plate. One well of each sample was used to adjust the settings to ensure optical acquisition. This included adjusting the voltages for amplifying forward and side scatter and fluorescent signals. The gates were set to include only viable cells in the analysis. Adjustments were made to account for isotype control non-specific binding.

2.17 Data Analysis

The analysis of raw data obtained was also carried out in the InCyte software, by importing the results into a "Heat map-pie" chart. Cells were gated to include viable cells only. This was based on the side/forward scatter dot-plot using an elliptical

region. The cells within this region were the representative sample on which all subsequent analysis was then performed. Histograms were also generated which allowed for visualisation of positive or negative expression of samples of the markers of interest (Figure 2.9).

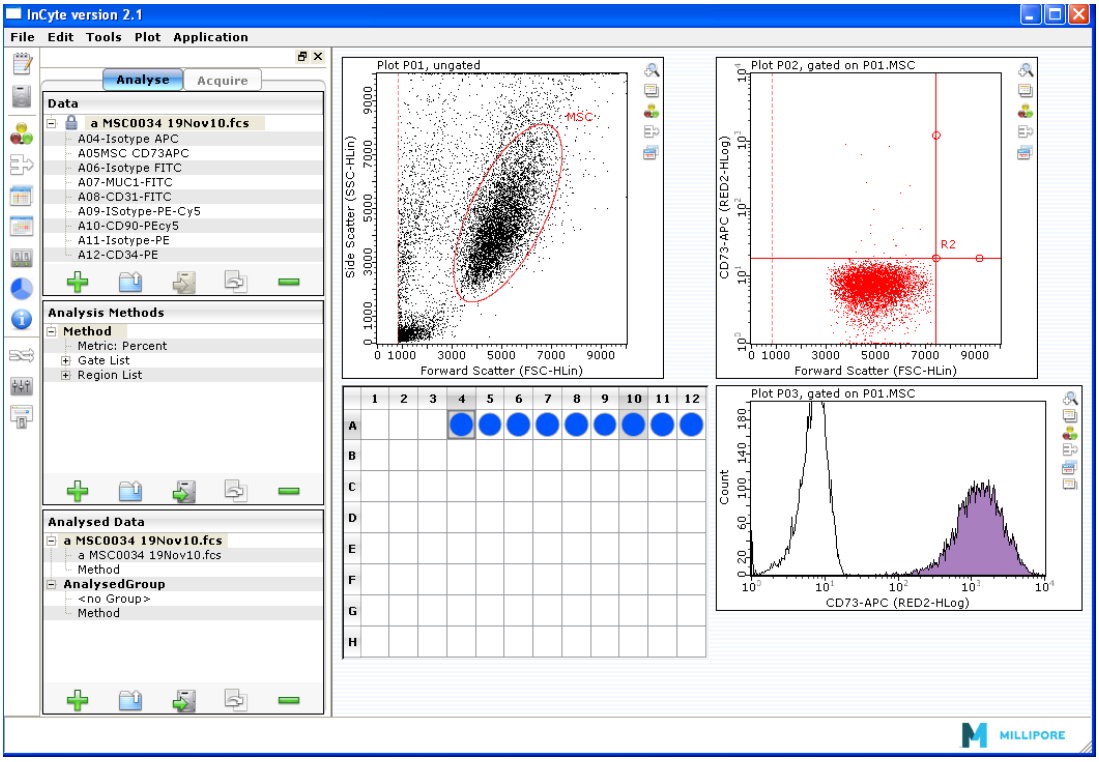

Figure 2.9 Example of Flow Cytometry data analysis

The percentage positivity was determined using ‘current run stats’ window, on the gated population. If the isotype region overlapped with the positive region on the histogram, this was subtracted from the total percent positive cell population. Overall this percentage represents the number of cells expressing a particular surface marker which was corrected for by non-specific binding of the antibody and its background fluorescence.

2.18 Cell Transfection using Lipofectamine™ 2000

To assess the effect of a particular microRNA on breast cancer epithelial cells, cells were transfected with a microRNA mimic and appropriate controls. Breast cancer cell lines (T47D and SK-BR-3) were seeded into 6-well plates at a density of $2.5x10^5$ cells/ well in complete antibiotic-free media. Cells were cultured to approximately 80-95% confluence at the time of transfection. The microRNA mimics were used at a concentration of 50 nM, containing miR-379 (MIM0367), miR-10a (MIM0028) and the non-target control mimic (NTC-mimic) which acts as a scramble mimic (MIMcontrol). All mimics were obtained from SwithgearGenomics, USA. The transfection reagent used was Lipofectamine™ 2000 (Invitrogen, USA). This was diluted in Opti-MEM® I Medium, and incubated for 5 minutes at room temperature. The miRNA mimics and controls were also diluted in Opti-MEM® I Medium (Life Technologies). Following incubation the diluted complexes were combined and incubated at room temperature for 20 minutes. The combined solutions were then added to the appropriate wells containing the cells in antibiotic-free media. The plates were incubated at 37°C in 5% CO_2 for 24-48 hours, (Figure 2.10).

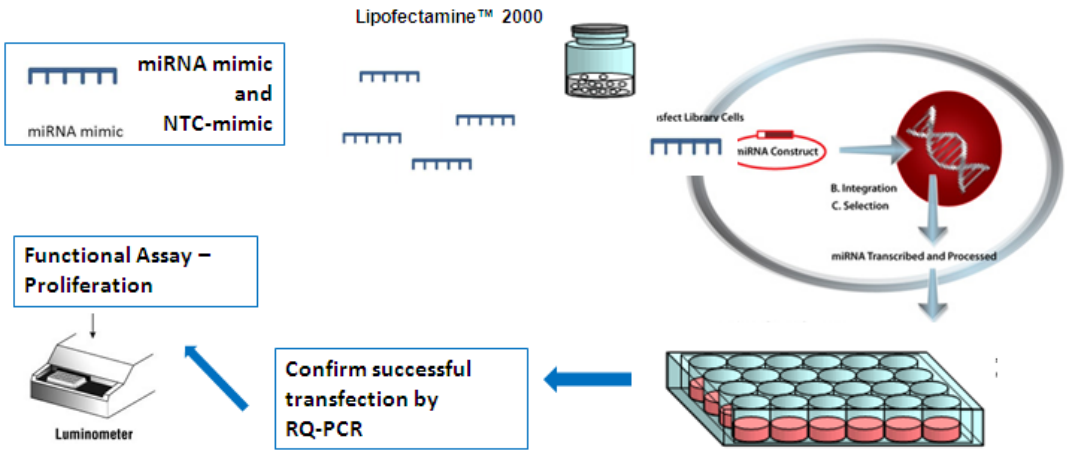

Figure 2.10 Transfection Protocol Outline

2.19 Cell Proliferation – MTS assay

Cells were seeded into a 96 well plate at a seeding density of 6 x10^4 cells/ well in complete antibiotic-free medium. Cells were then transfected using Lipofectamine™ as previously described. Following 48 hour incubation, cell proliferation was assessed using the MTS assay (Promega). Briefly, 20µl of MTS reagents were added to the cells and then incubated for 3 hours at 37°C. Proliferation was measured using the plate reader at 490 nm.

2.20 Immunohistochemistry (IHC) of Transfected cells

Cells were seeded onto chamber slides (Millipore), at a density of 5 x 10^4 cells/ well on 4-well slides. T47D cells were transfected with a miR-379 mimic a NTC-control mimic.

Following incubation, cells were fixed for IHC staining as follows:

1. Chamber slides were placed on ice for 15 minutes.
2. Media was aspirated and cells were washed with ice-cold Methanol (1-2mL per slide).
3. A further 1 mL of ice-cold methanol was added to each chamber slide and incubated at -20°C for 15 minutes.
4. Each well was washed with 1X PBS and the chamber wall was removed at this stage.
5. Slides were stored in 1X PBS, protected from light at 4°C until required for IHC, they can be stored for up to a week before continuing on to IHC.

Slides were exposed to 10% Normal Goat serum (NGS) diluted in PBS - 0.05% Tween-20 (PBS-T) for 30 minutes. This step was used as a blocking agent. This step enabled binding to all non-specific sites and further prevented background staining. Chamber slides were blotted dry to remove excess NGS. The slides were then exposed to the primary antibody, Cyclin B1 (rabbit polyclonal AB – ab48574, 1:50 dilution). 500µl of primary antibody dilution was added to each experimental slide and incubated for 1 hour. This was followed by two wash steps with PBS-T. The secondary antibody conjugated with HRP was added to each appropriate slide and

incubated for 20 minutes. This was followed by two repeat wash steps with PBS-T. Finally slides were washed in running tap water for 1 minute.

The detection step was performed using the DAB Kit (Vektor Laboratories, Cat. No. 4100) as per manufacturer's instructions. The slides were incubated with the working reagent solution at room temperature for 2-10 minutes or until a stain developed. The slides were washed in warm tap water for 5 minutes, and counterstained in Haematoxylin for 3 minutes and rinsed in warm tap water for 5 minutes. Once this step was completed slides were dehydrated in serial alcohol immersions and mounted on DPX mounting medium. Slides were allowed to dry overnight before proceeding on to imaging. IHC slides were imaged with an Olympus BX60 light microscope and analySIS software.

2.21 Identifying targets of microRNAs with the LightSwitch Luciferase Assay

Studies have shown that most miRNA regulatory binding sites are on the 3'UTR [193, 194]. It is vital to reliably identify endogenous miRNA targets. While computational algorithms like miRBase, TargetScan and PicTar [69, 195, 196] offer effective means of identifying a list of putative mRNA targets for any miRNA, this alone will not be sufficient. Evidence-based research is necessary to correctly recognize targets de novo or to validate predicted targets. Simply measuring the mRNA or protein level of a predicted target gene following addition of a miRNA will not distinguish between direct effects of a miRNA or down-stream signalling effects. Thus, 3'UTR-reporter assays were applied to provide functional evidence of a miRNA's direct binding to a particular 3'UTR. Together with computational target prediction or expression, this can provide evidence that a particular 3'UTR is directly regulated by the miRNA of interest.

In a 3'UTR-reporter assay, the 3'UTR from a gene of interest is fused to the end of a luciferase reporter gene (Figure 2.11).

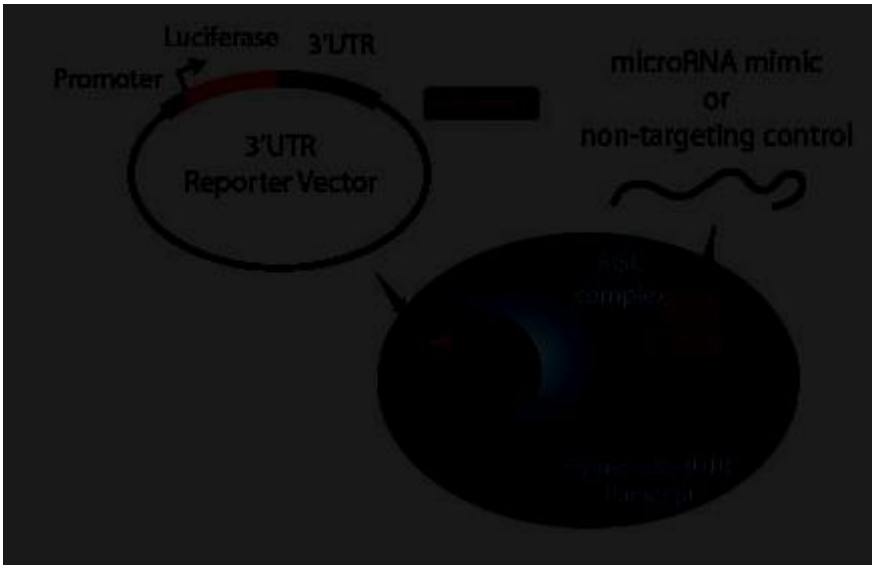

Figure 2.11 Luciferase-reporter constructs [197].

The LightSwitch Luciferase assay system is a fully optimised reporter system that includes GoClone constructs utilizing the RenSP luciferase gene and LightSwitch luciferase assay reagents (SwitchGear Genomics Ltd.). This protocol is optimised for use with a 50nM miRNA mimic in a 96-well plate. All steps were performed in a LAF hood using sterile aseptic technique.

2.21.1 Cell Culture and Seeding into 96-well plate

For this assay, T47D cells were used as these cells expressed relatively low endogenous levels of miR-10a, miR-339-5p and miR-379.

The cells were trypsinised and counted as previously described. T47D cells were seeded at $1x10^4$cells/ well in 100µL complete media in a 96-well white walled tissue culture plate. This yielded approximately 80% confluence at time of transfection. Cells were incubated at 37°C with 5% CO_2 overnight.

Following overnight incubation, the 3'UTR constructs and microRNA mimics (SwitchGear Genomics) were thawed at room temperature (Table 2.5).

Random 3'UTR	30ng/µL	S890001
B-Act 3'UTR	30ng/µL	S804753
NIS 3'UTR(SLC5A5)	30ng/µL	S800697
RARβ 3'UTR	30ng/µL	S808633
miRNA-379 mimic	5nmol	MIM0367
miRNA-10a mimic	5nmol	MIM0328
miRNA-339-5p mimic	5nmol	MIM0028
non-target_1 (NTC) mimic	5nmol	MIMcontrol

Table 2.6 List of 3'UTR constructs and microRNA mimics.

The 3'UTR constructs and the miRNA mimic were all centrifuged prior to use to remove condensation from the caps. The master-mix was prepared as shown in Table 2.6. All experiments were performed in triplicate for each treatment 3'UTR combination.

	3'UTR	**3'UTR+miR379**	**3'UTR+10a**	**3'UTR+NTC**
3'UTR	11.75 µL	11.75 µL	11.75 µL	11.75 µL
2 µM miRNA mimic/ NTC	0	8.75 µL*	8.75 µL*	8.75 µL*
Serum-free media:	23.33	14.58 µL	14.58 µL	14.58 µL
Total µL	35 µL	35 µL	35 µL	35 µL

Table 2.7 Example of 3'UTR construct set up, this included controls (3'UTR alone and with a non-target control)

For this study 50nM of each microRNA mimic was used (Table 2.7).

Mixture 2	1x
DharmaFECT Duo	0.2 *µL
Serum-free media	9.8 µL
Total	10 µL

Table 2.8 Mastermix 2 DharmaFECT Duo reagent [198].

2.21.2 Cell Transfection using DharmaFECT

The DharmaFECT Duo mixture was incubated for 5 minutes at room temperature. 35 µL of Mastermix 2 DharmaFECT Duo was added to each prepared tube containing 35 µL 3'UTR construct and /or miRNA mimic (Mastermix 1). The mixture was then incubated for 20 minutes at room temperature. 280 µL of pre-warmed antibiotic-free media was added to each tube.
The samples were mixed gently by pipetting up and down several times. The 96-well plate was removed from the incubator. Prior to analysis, cell seeding density was verified to be at least at 80% confluent. The media was removed from each well. 100µL of the appropriate transfection reagent mixture was added to each well. The cells were then placed in the incubator overnight. The luciferase signals were measured within 24 hours, as the level of repression may show greater well-well variability at later time-points.

2.21.3 LightSwitch Luciferase Measurement

The 96-well plate was taken out of incubator, wrapped in tinfoil and frozen at -80°C overnight. Freezing generally increases cell lysis and luciferase signal to give enhanced results. Following overnight freeze, cells were thawed at room temperature.

The luciferase activity was measured using LightSwitch Assay reagents as follows:

1. Removed the plate from the freezer and let thaw at room temperature.
2. Prepared LightSwitch Assay reagents (SwitchGear Genomics Ltd., LS100).

i. Reconstitute 100X Substrate by adding 1mL of substrate solvent to tube of lyophilised assay substrate. Protected this reagent from light and minimised the time at room temperature. Used freshly prepared 100X substrate for best results.
ii. Prepared assay solution. Thawed 100mL Assay Buffer at room temperature and added this to the 1X substrate mix prior to use.
iii. Added Assay Solution to appropriate wells. Used a multichannel pipette to add 100µL Assay Solution (buffer+ substrate) directly to each well (100µL cells + media).
iv. Wrapped plate in tinfoil and incubated for 30 minutes at room temperature.
v. Plates were read for 2 seconds in a plate reader (LuminoSkan Ascent DLR Reader (Thermo)).
vi. Calculated the knock-down from the luciferase signal ratio for each construct for the specific miRNA over the NTC. Used the data from the housekeeping and random 3'UTR to account for non-specific effects.

2.22 Western Blot Analysis

2.22.1 Whole Cell Lysate preparation

Cells were cultured in T75cm^2 flasks and transfected according to previous experimental protocol as described in section 2.18. Cells were placed on ice for 5 minutes, the media was then discarded and the surface of monolayer was washed with ice-cold PBS. Cells were lysed in 3-4 ml/ T75cm^2 flask of ice-cold lysis buffer (1% Triton X-100 in 20mM Hepes, 2 mM EDTA, 150mM NaCl, 10mM Sodium fluoride, 100X anti-protease inhibitor cocktail III, 2 mM sodium orthovanadate). Cells were then scraped, and clumps were dispersed, transferred to an eppendorf and stored at -20°C overnight. Once cells were thawed, they were centrifuged at 500 x g @ 8°C for 15 minutes to remove cellular debris. The supernatant was retained. Samples were concentrated at this stage, to a volume of approximately 500µl. An

aliquot was set aside for the quantification of the protein content using the Pierce MicroBCA protein assay Kit. The remainder of the sample was stored at -80°C.

2.22.2 Protein Quantification

Protein was quantified using Pierce MicroBCA™ protein kit. Bovine serum albumin (BSA) standard (0.5µg/mL -200µg/mL) was diluted in lysis buffer. 150µl of standard or sample was added in duplicate to wells of a 96-well plate followed by the addition of 75 µl of reagent A, 72 µl reagent B and 3 µl of reagent C. The samples were mixed for 30 seconds on an orbital shaker before incubating at 37°C for 2 hours in the dark. Absorbances were read at 560nm and protein quantity was determined through interpolation of the standard curve.

2.22.3 SDS Polyacrylamide Gel Electrophoresis and Protein transfer

Electrophoresis was performed on samples using BioRad MINI-PROTEAN II Electrophoresis Module as per manufacturer's instructions.

Samples (40µg) were prepared as outlined in Table 2.8, and then placed in the thermal cycler PCR Sprint machine and denatured at 70°C for 10 minutes.

Protein sample + dH_2O	6.5 µl (40µg Protein)
4X sample buffer (blue)	2.5 µl
10X reducing agent*	1 µl
Total volume	10 µl

Table 2.9 Sample preparation *Added reducing agent last

Samples were loaded onto a 15% BioRad gel (BioRad Mini-Protean® TGX™ Gels, Cat. No. 456-1083) and electrophoresed at 200V in 1 X NuPAGE® MOPS SDS Running Buffer (Invitrogen) for 30 minutes. A protein ladder (MagicMark XP Western Protein Standard 20-220 kDa, Invitrogen) was also added to the first and last well of the gel, to facilitate confirmation of the sizes of proteins being investigated. Following electrophoresis, proteins were transferred to a nitrocellulose membrane using a wet transfer system (Figure 2.12), (BioRad) in 1X transfer buffer

(20X stock transfer buffer: 20% Methanol, 2.5mM Tris-base, and 19.2 mM glycine). The transfer process was set up for 30 minutes at 100 V.

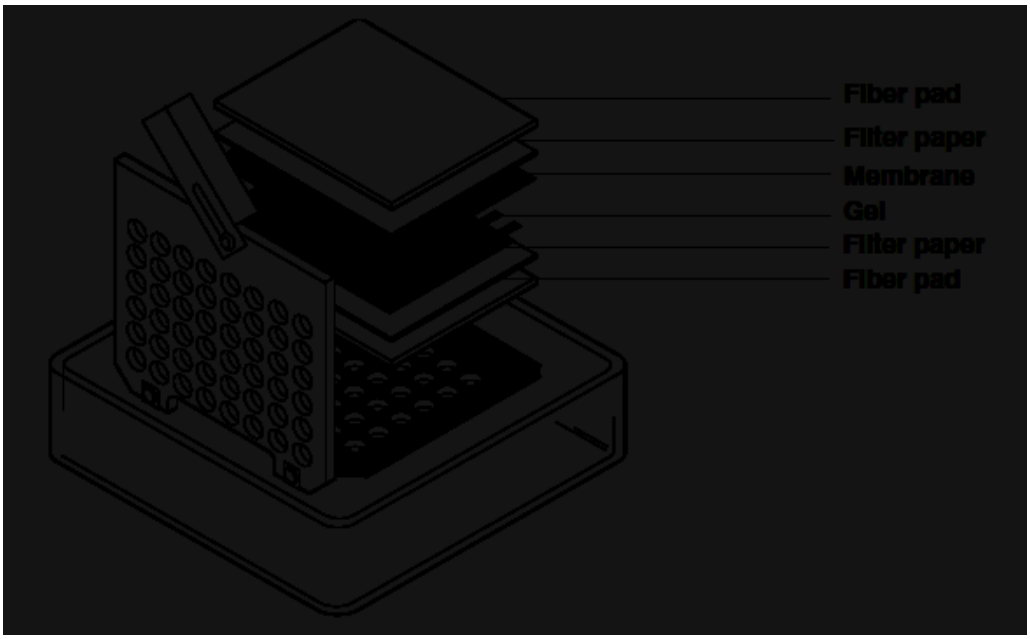

Figure 2.12 Gel sandwich set-up to allow for protein transfer onto nitrocellulose membrane.

2.22.4 Immunoblotting

Following protein transfer, the nitrocellulose membrane was blocked with 5 % milk powder in TBS (0.5 M Tris-base, 1.5 M NaCl) supplemented with 0.05 % Tween-20 (TBS-T) for 1 hour with gentle shaking. Membranes were washed 3 times (1x 15 min, 2x 5 minutes) in TBS-T and then incubated with a specific antibody (Cyclin B1 antibody ab32053, 1:5000 dilution) overnight at 4°C. A loading control was also added using β-Actin (anti-beta Actin antibody, ab8227, 1:5000) to account for loading variability. The wash step was repeated. This was followed by incubation with a HRP conjugated antibody (goat anti-rabbit, 1:3000 dilution) in 0.1% milk then incubated for 1.5 hours. The wash step was repeated this time to include 1 x 15 min followed by 4 x 5 min in TBS-T. The membranes were exposed to SuperSignal West Pico Chemiluminescent Substrate for 5 minutes at room temperature. Images were captured using Syngene G- Box and GeneSnap Software.

2.23 Gene and MicroRNA Analysis

2.23.1 Ethics and Written informed consent

Prior written, informed consent was obtained from each participant in this breast cancer cohort (breast tumour tissue cohort and breast cancer blood specimen cohort). All the studies were approved by the ethics review board of Galway University Hospital.

2.23.2 Sample Preparation

Extraction techniques were specific for each sample type investigated. Co-purification for large (mRNA) and small RNA (miRNA) was performed using RNeasy® Mini Kit (74106, Quiagen).

Cells were trypsinised and centrifuged at 1000 rpm for 4 minutes. Supernatant was discarded and the cell pellet was immediately transferred to -80°C until further use.

Tissue specimens were obtained from theatre and collected in RNAlater® solution (Ambion, USA). This stabilises the RNA before they were stored at -80°C until further use. In this study the breast tissues specimens consisted of malignant, normal tissue which was obtained from reduction mammoplasty and fibroadenoma tissue that are benign breast disease tissues. Approximately 100 mg of tissue was homogenised in 1mL of Trizol® (Qiagen) using a bench-top homogeniser (Kinematica AG).

2.23.3 RNase Contamination

In order to maintain the stability of RNA and prevent subsequent degradation, certain procedures were put in place to ensure the quality of RNA. This included:

- All RNA extraction procedures were performed in a dedicated Class II Safety Cabinet (ECSCO®). Appropriate PPE was used, such as lab coats and gloves.
- All samples were handled with Gilson pipettes and contained pipette tips.
- Samples were kept on ice at all times.
- RNA was extracted using RNeasy® Minikit (Quiagen) according to manufacturer's instruction.

2.23.4 Tissue RNA Extraction Procedure

Tissue homogenates were removed from the -80°C freezer and let thaw on ice. Once thawed, samples were transferred to a 1.5ml eppendorf. Cell pellets were gently dispersed in 1 ml of Trizol®. 200µl/ml of homogenate received chloroform, followed by vigorous vortexing for 15 seconds. Samples were let stand for 5-10 minutes at room temperature. An initial centrifugation at 12,000 rpm for 15 minutes at 4°C was carried out to remove insoluble material. RNA migrated to the upper, clear aqueous phase. This clear phase was carefully transferred to a 15 ml falcon and 3.5 times the volume of 100% of ethanol was added to the solution and gently mixed. 700µl of this solution was put onto the RNeasy column for RNA extraction and centrifuged at 14,000 rpm for 21 seconds at 4°C. This step was repeated until all the solution had passed through the column. This process allowed capture of RNA onto the membrane. The same centrifugation speed and time was used for the subsequent washes using 350µl of RW1. To ensure the highest quality of RNA, a DNase treatment was performed as follows: 80µl of DNase mix was prepared by adding reagents from an RNase-free DNase set (Quiagen), this was applied to the membrane for 15 minutes at room temperature. Repeat wash steps using RW1 were performed, followed by two wash steps using 500µl of RPE. The final addition of RPE was carried out at a longer centrifugation time of 2 minutes, to dry the membrane. The last step was elution of total RNA using 30-35 µl of chilled nuclease-free water (NFW) which was added directly to the membrane. The sample was centrifuged at 14,000 rpm for 1 minute at 4°C. The collected RNA was then transferred to labelled screw-capped tube, 1.2 µl was set aside to assess the quality and quantity of the RNA by NanoDrop 1000 spectrophotometry (NanoDrop Technologies). The remaining RNA was stored at -80°C until further use.

2.23.5 Whole Blood RNA Extraction

Total RNA was extracted from 1 ml of whole blood using a modification of the TRI Reagent BD co-purification technique (Molecular Research Centre, Inc.,). The whole bloods assessed were not from the same cohort as the tissues analysed. The extraction procedure was as follows: 1 ml of whole blood was extracted using the phase separation technique. Briefly, 3 ml Trizol and 200 µl of 1-bromo-4-methoxybenzene (BAN) were added directly to the whole blood. This enhanced the

RNA phase separation. The solution was then incubated at room temperature for 5 minutes before centrifugation at 12,000 x g for 15 minutes at 4 °C. The clear aqueous upper phase was then transferred to a fresh collection tube. The RNA was then precipitated using 1 ml isopropanol, before being centrifuged at 12,000 x g for 8 minutes at 18 °C. The supernatant was discarded and the pellet if visible was resuspended in 1 ml of 75% Ethanol. An additional step was included to wash the pellet, this allowed for the improvement of the overall purity of the sample. The pellets were then air-dried at room temperature for 5 minutes, before resuspending the pellet in 30 µl of ultra-pure distilled water (Figure 2.12). The RNA concentration was assessed and the remaining RNA sample was stored at -80°C until further required.

2.23.6 RNA Analysis - concentration and integrity

Total Large and miRNA concentration and purity were assessed using the Nanodrop 1000® Spectrophotometer (NanoDrop Technologies). For the analysis of total RNA, 'RNA-40' was selected as the sample type. The extinction coefficient was set as 40. When quantifying microRNA levels, 'Other' was selected as the sample type, and an extinction coefficient of '33' was manually entered. A 1.2 µl aliquot of RNA was added onto the apparatus pedestal. The sample arm was used to apply pressure to the sample by surface tension. Spectral measurements were made with a special path length of 0.1 cm. RNA concentrations were automatically calculated using the following equation:

RNA concentration (ng/µL) = (A_{260} x e)/b

A_{260} = Absorbance at 260nm, e= excitation coefficient (ng-cm/mL), b= path length (cm)

An absorbance ratio was deemed appropriate when falling between 1.8 and 2.2 at 260 and 280 nm (A260/A280) measurements (Figure 2.13).

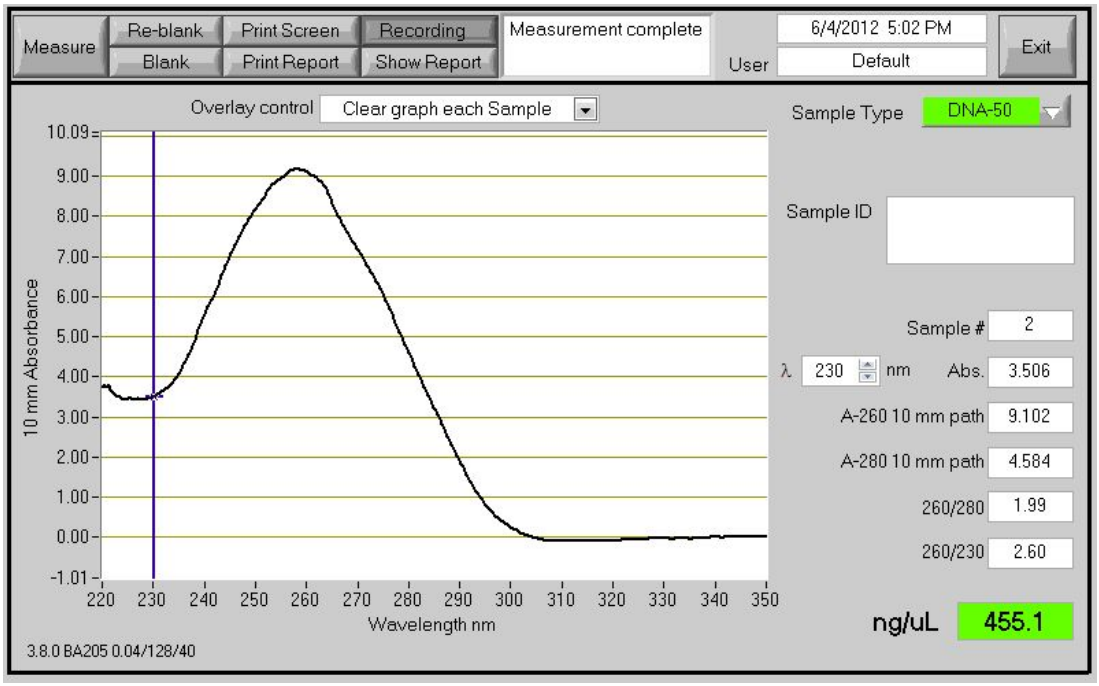

Figure 2.13 Nanodrop quantification using spectrophotometer

The presence of protein or phenol was indicated by a high absorption at 280 nm, producing a lower A260/A280 ratio. Ratios below this were an indication of carry-over of guanidium salts.

2.23.7 Reverse transcription of mRNA to cDNA

This process makes use of random hexamers to prime to the RNA and M-MLV reverse transcriptase which converts single stranded RNA into a double stranded RNA / cDNA hybrid.

1 µg total RNA was reverse transcribed using the SuperScript™ III Reverse Transcriptase enzyme (200U/µl, Invitrogen, Carlsbad, USA). The mRNA was reverse transcribed as follows (Table 2.9):

Total RNA (1µg)	11.67 µl
dNTP mix (10 mM)	1 µl
Random Primer (9*N; 3 µg/µl)	0.33 µl

Table 2.10 Mastermix I: denatures the RNA

The denaturation reaction was performed using a GeneAmp® thermal cycler (9700, Applied Biosystems, USA). Samples were incubated at 65°C for 5 minutes. An RT-negative control was included in each batch of reactions. After the initial denaturation step, the following mastermix II was added to the samples (Table 2.10).

Total RNA	13 µl
5X RT Buffer (250mM Tris-HC(pH8.3), 375mM KCL, 15Mm $MgCl_2$)	4 µl
DTT (0.1 M)	1 µl
RNaseOut (40U/µl, Quiagen Ltd, Crawley, UK)	1 µl
SuperScript™ III (200U/µl, Invitrogen)	1 µl

Table 2.11 Mastermix II

Samples were incubated at 25°C for 5 minutes, 50°C for 60 minutes and finally 70°C for 15 minutes to denature any double-stranded duplexes present. 30 µl of nuclease free water was added to each sample after reverse transcription, this brought the total volume of cDNA generated to 50 µl. The cDNA was then stored at -20°C until further use.

2.23.8 Reverse transcription of miRNA to cDNA

MicroRNA (100ng) was reverse-transcribed using MultiScribe Reverse Transcriptase (Applied Biosystems, USA). Each reaction was primed using a miRNA-specific stem-loop primer. Where sequences were accessible, primers were obtained from MWG Biotechnology. Otherwise, assays containing the RT stem-loop

primer and the PCR primers and probes were used (Applied Biosystems). MiRNAs was reverse transcribed as follows (Table 2.11):

Small RNA (20ng/µl)	5.0 µl
dNTPs (100 nM)	0.17 µl
10X RT Buffer	1.65 µl
Nuclease-free water	4.57 µl
RNase Inhibitor (20U/µl)	0.21 µl
Stem-loop primer (50 nM)	3.1 µl
MultiScribe RT (50U/µl)	1.1 µl

Table 2.12 Reverse transcription mastermix

The reaction was performed using a GeneAmp® thermal cycler (9700, Applied Biosystems, USA). Samples were incubated at 16°C for 30 minutes, 42°C for 30 minutes and finally 85°C for 5 minutes to denature any double-stranded duplexes present. An RT-negative control was included in each batch of reactions.

2.23.9 Real-time Quantitative Polymerase Chain Reaction (RQ-PCR)

RQ-PCR is a very sensitive technique capable of amplification and quantification of a specific nucleic acid sequence with detection of the PCR product in real time. Detection is made possible by incorporating a specific DNA-binding dye or fluorescently labelled probe.

The PCR reaction consists of an exponential phase. At this stage the product being amplified has doubled during each cycle of denaturation. The next phase is primer annealing and template extension followed by a non-exponential or plateau phase. This plateau occurs as a result of reduced reagents present in the reaction. The threshold cycle or Ct is the time point at which enough amplified product has been generated to produce a detectable fluorescent signal. The greater the amount of starting product present in the reaction, the smaller the Ct value (Figure 2.14).

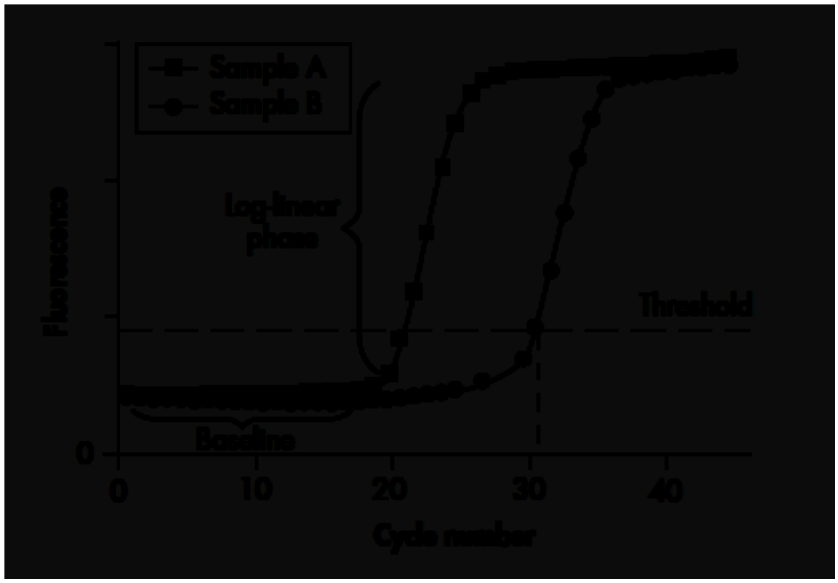

Figure 2.14 Outline of three phases during RQ-PCR

2.23.10 RQ-PCR Terminology

Amplicon	Short sequence generated during RQ-PCR
Ct	Threshold Cycle (Ct). The Ct value is defined as the cycle number at which the fluorescence generated within the reaction crosses the threshold line.
EC	Endogenous control (EC).This is a gene sequence that is present in the sample and should not differ significantly between samples. Endogenous controls are also used to control for loading differences. Two endogenous control genes used for gene expression analysis in breast cancer are Mitochondrial Ribosomal Protein L19 (MRPL19) and Peptidylprolyl Isomerase A (PPIA). These two genes were previously validated [199] and are known to be stably expressed across breast tissue specimens. For miRNA analysis, let-7a was used [200].
NTC	No Template Controls (NTC). This is a control, which contains all PCR components but no cDNA template. This

	sample should not yield a signal, this is used as an indicator that the RT or PCR reagents were contaminated with DNA.
Target	A sequence or gene of interest.
TaqMan Probes	TaqMan probes are oligonucleotides that have a fluorescent reporter dyes attached to the 5' end and a quencher moiety coupled to the 3' end. These are capable of hybridising internally on the PCR product. In its free unhybridised state the distance between the Fluor and quench molecules prevents the detection of fluorescent signal from the probe. During PCR, when the polymerase replicates a template on which the TaqMan probe is bound, this cleaves the probe. This results in the decoupling of the Fluor and quench followed by Fluorescence Resonance Energy Transfer (FRET) no occurring. Therefore the fluorescence signal intensity increases in each cycle, proportional to the amount of probe cleavage.

2.23.11 Accuracy of RQ-PCR Results

- In order to assess the accuracy of the RQ-PCR run, results were analysed by comparing the Ct of triplicate samples. The run was questioned and repeated if triplicate samples failed to achieve a Ct standard deviation of <0.3
- All PCR work was carried out in designated Class II Safety Cabinets (Captair® bio, Erlab).
- Accurate pipetting was a key to successful PCR results. Pipettes were calibrated regularly and low volume pipetting (<1µl) was avoided, dilutions were prepared when necessary. All plates and tubes were spun at low speed prior to use. Samples for PCR were handled only with Gilson pipettes. Barrier pipette tips were also used.

2.23.12 RQ-PCR of mRNA

The PCR reactions were carried out in a final volume of 10µl using an ABI Prism 7900 Sequence Detection System (Applied Biosystems, Warrington, UK). Reactions consisted of 1µl cDNA, 9µl 2X TaqMan® Universal Fast Mastermix (No

AmpErase*UNG) and 1µl Nuclease-Free water. The PCR plates were set up as outlined on a plate plan shown in Figure 2.15.

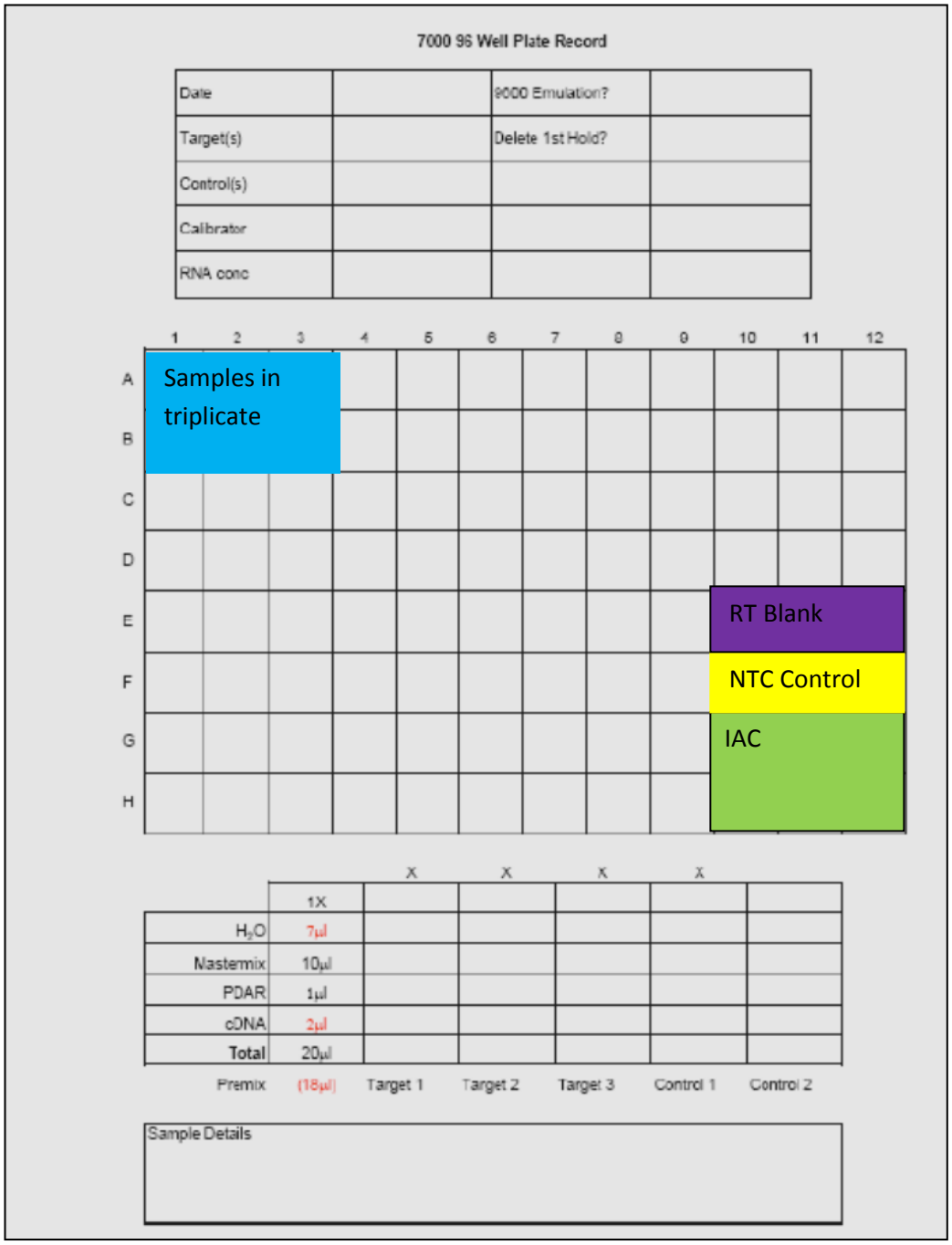

Figure 2.15 Example of mRNA PCR Plate plan, designed in the Discipline of Surgery, NUI, Galway. Reverse transcription (RT) Blank and Inter Assay Control (IAC).

The reaction consisted of 10 minute incubation at 95°C and 60°C for 60 seconds. TaqMan® Gene Expression Assays designed for the target genes, (Table 2.12). MRPL19 and PPIA were used as endogenous RNA reference genes.

Gene	Description	Gene Locus	Assay ID	Amplicon Length
NIS	Solute carrier family 5 (sodium iodide symporter), member 5	19p13.11	Hs00166567_m1	78
RARα	Retinoic Acid Receptor Alpha	17q21	Hs00940446_m1	68
RARβ	Retinoic Acid Receptor Beta	3p24.2	Hs00977140_m1	61
THRα	Thyroid Hormone Receptor Alpha	17q11.2	Hs00268470_m1	89
CCNB1	Cyclin B1	14q11.2	Hs01565448_g1	79
MRPL19	Mitochondrial Receptor Protein L-19	2p11.1-q11.2	Hs00608519_m1	72
PPIA	Peptidylprolyl Isomerase A	7p13	Hs04194521_s1	97

Table 2.13 Details of TaqMan® Gene Expression Assays used in experimental protocols.

MicroRNA expression analysis was carried out targeting the following miRNAs of interest (Table 2.13).

miRNA	Gene Locus	Assay ID	Amplicon Length
hsa-miR-10a	17q21.32	000387	UACCCUGUAGAUCCGAAUUUGUG
hsa-miR-339-5p	7p22.3	002257	UCCCUGUCCUCCAGGAGCUCACG
hsa-miR-875-5p	8	002203	UAUACCUCAGUUUUAUCAGGUG
hsa-miR-379	14q.31.1	001138	UGGUAGACUAUGGAACGUAGG
Let-7a	9	000377	UGAGGUAGUAGGUUGUAUAGUU
miR-16	13q14.2	000391	UAGCAGCACGUAAAUAUUGGCG

Table 2.14 Details of TaqMan® miRNA assays used in experimental protocols.

2.23.13 RQ-PCR of miRNA cDNA

RQ-PCR reactions were carried out in a final volume of 10 µl using AB7900HT. Reactions consisted of the following, (Table 2.14).

First strand miRNA-specific cDNA	0.7 µl
TaqMan Fast Mastermix (2X)	5.0 µl
TaqMan Probe (0.2 µM)	0.5 µl
Nuclease-free water	1.68 µl
Forward Primer (1.5 µM)	1.5 µl
Reverse Primer (0.7 µM)	0.7 µl

Table 2.15 Mastermix for reverse transcription

Uniform 'Fast' thermal cycling conditions were applied. This comprised 40 cycles at 95°C for 15 minutes and 60°C for 60 seconds. cDNA synthesised from a T47D breast cancer cell line was used as an Inter-assay control (IAC), which was included on each 96-well plate. This served as a control and a calibrator of the experiment. All reactions were carried out in triplicate to allow the determination of assay variation. The threshold standard deviation for intra-assay replicates was 0.3.

2.24 Generation of a stably Transduced T47D Cell line with miR-379 (T47D^{379})

Viruses are capable of delivering their genomic material into the cells that they infect. This process is referred to as transduction. The purpose of this study was to create a cell line with stable, long-term over-expression of miR-379.

2.24.1 Lentiviral Transduction

Lentiviral vectors are a subtype of the Retroviridae family. They display a broad tropism and allowing for stable, long-term integration of genomic material into cells. They are effective in delivery of genomic material into both dividing and non-dividing cells and are therefore one of the most competent transduction tools available. Lentiviruses are derived from HIV. The lentivirus used in this study was pre-made from SmartChoice (ThermoScientific Ltd.). These particles have been modulated to be replication deficient and therefore contain less than 30% of the wild type HIV1-genome. A further safety aspect is that these vectors are self-inactivating which also reduces the possibility of the production of recombinant particles [187] (Figure 2.16).

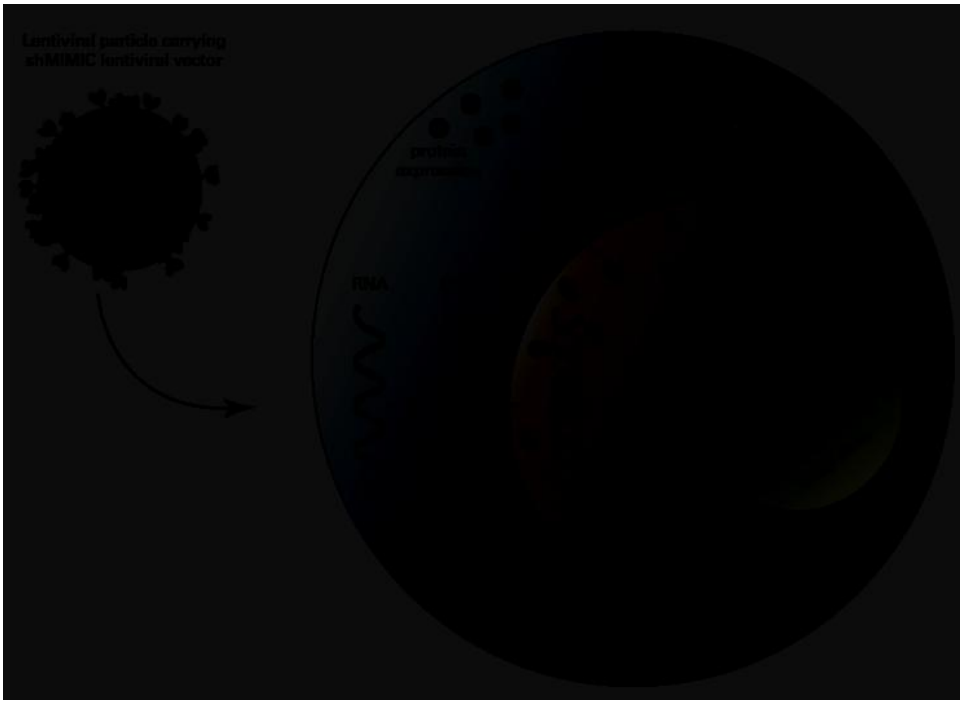

Figure 2.16 Overview of Lentiviral packaging into the cell [187].

The lentivirus used for the current study displayed some key features making it a very effective transduction tool for the delivery of miRNAs into the host cells (Figure 2.17). Examples include a universal SmartChoice scaffold which holds the miRNA of interest and allows for integration into the cells' RNA machinery. The lentivirus was constructed with a turbo RFP (red fluorescent protein) promoter allowed for the optimisation of the transduction process by facilitating visualisation of the miRNA expressed in the cells. An additional feature of this vector includes the Puromycin resistance gene ($Puro^R$). This blocks the ability of the antibiotic Puromycin to inhibit protein synthesis. This feature allows for antibiotic drug selection of positively transduced cells only, eradicating any non-transduced cells present. For this study a human CMV (Cytomegalovirus) promoter was chosen as this was previously shown to be efficient in this particular cell line.

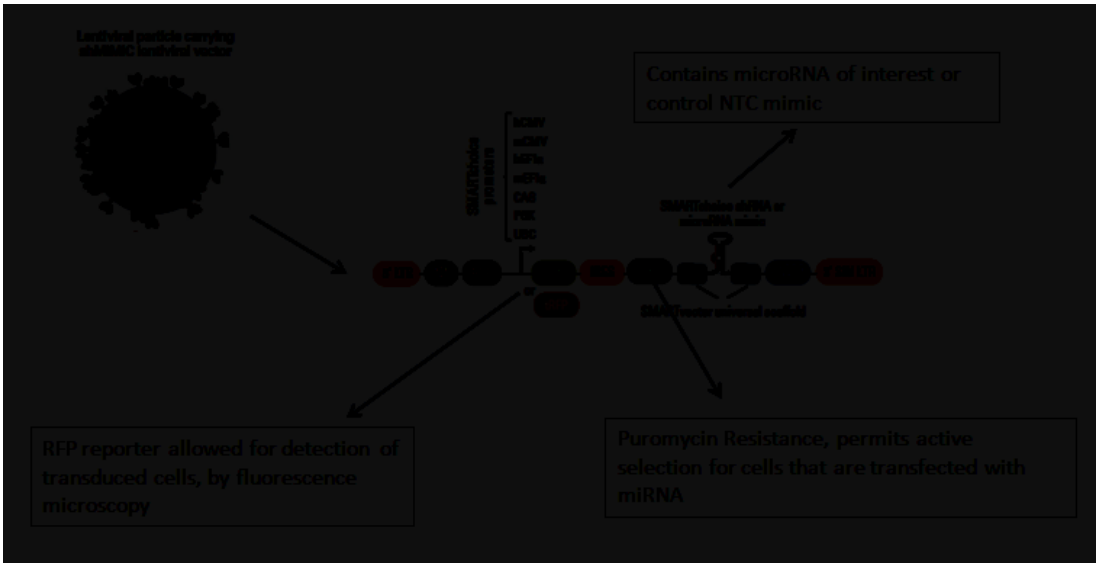

Figure 2.17 Features of the Lentiviral construct [187].

The control used in this study was the non-targeting control (NTC) mimic. This lentivirus shares many features of the miR-379 lentivirus construct, such as the RFP promoter and the Puromycin resistance gene. In place of the miR-379 mimic however, is a scramble mimic. Transduction of the cells was carried out at a low Multiplicity of Infection (MOI). This is the ratio of lentiviral transduction units to cells. A low MOI prevents multiple insertions of the virus into the same cell. Efficient transduction was aided by the addition of Polybrene (Hexadimethrine

bromide) which has been shown to enhance transduction of cells by 2 -10 fold [187]. This is done by binding to the cell surface and neutralizing the surface charge.

2.24.2 Determination of correct Cell density and Transduction efficiency

Successful transduction of the cells is dependent on a range of factors: cell type, cell density, passage number, MOI during transduction and purity of lentiviral preparation. Polybrene (Hexadimetrine bromide, Sigma) is a reagent used to aid successful transduction [201]. This is however toxic to certain cells. Cells were transduced with lentiviral particles at approximately 40% confluence. Cells were seeded at three different seeding densities ($5x10^3$, $7.5x10^3$ and $10x10^3$ cells/ well) in a 96 well plate to identify correct seeding density. Polybrene was added at increasing concentrations (0-10µg/ml) to the cells in the wells (Figure 2.18). The effect of Polybrene was investigated in the absence of serum. Serum inhibits the transduction and Polybrene was added during transduction, so it was therefore necessary to optimise Polybrene concentration in the absence of serum. Next the optimal Puromycin dihydrochloride concentration (P9620-10mL, Sigma) was determined in the presence of serum, as this was added following transduction and during selection of transduced cells. This is an antibiotic selection agent and was used to select for successfully transduced cells only. It is toxic to any non-transduced cells. The optimal concentration to efficiently kill non-transduced cells is different for each cell type. Cells were seeded into a 96-well plate at increasing concentrations of Puromycin (0-10µg/ml, Figure 2.18).

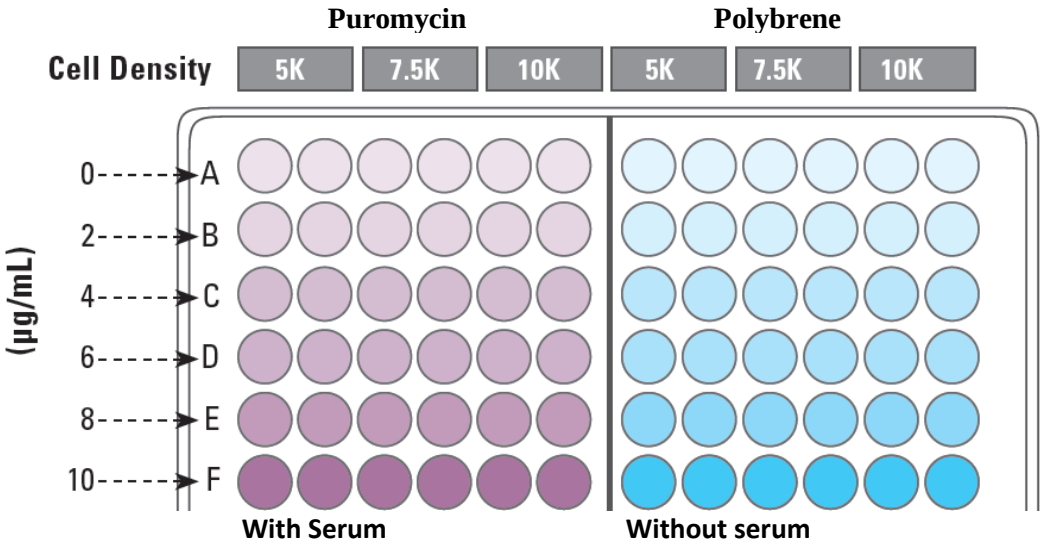

Figure 2.18 Plate plan for the optimisation of puromycin, polybrene and cell seeding density, in the presence (left) or absence (right) of serum, performed in a 96-well plate.

Cells were incubated at 37°C, 5% and CO_2 for 72 hours and were inspected daily. Cell proliferation was measured using the Promega MTS Assay to assess the viability of the cells following addition of Polybrene and Puromycin.

2.24.3 Cell Culture and Transduction

Prior to Lentivirus transduction, an Environmental Protection Agency (EPA) Licence was obtained. T47D breast cancer cells were used for this study. Culture and maintenance of these cells was described in section 2.3. The miR-379 mimic and the NTC mimic were stably transduced into T47D cells using a lentiviral construct (SMARTchoice shMIMIC, Thermo Scientific Ltd.). Lentiviruses are capable of long-term delivery of miRNAs into actively dividing cells. Any handling with the SMARTchoice vector was performed in a Class II biosafety cabinet. Surfaces coming in contact with the lentiviral particle, including pipette tips and culture flasks were sanitised in bleach and autoclaved before disposal. Liquid waste was collected in a labelled beaker containing bleach. Once optimal transduction conditions for the cells (correct cell density, Polybrene and Puromycin concentrations) were determined, lentiviral transduction was performed on T47D cells.

2.24.3 Cell Transduction using Lentiviral particles

T47D cells were transduced in the presence of Polybrene with either a miR-379 mimic or a NTC mimic in serum-free media and incubated at 37°C, 5% CO_2 for 6 hours. Following incubation, the media was changed to include complete media and cells were incubated at 37°C, 5% CO_2 for 48 hours. The appropriate concentration of Puromycin was then added to the cells and fresh media containing Puromycin was replenished every 48 hours for 6 days. This ensured selection of only transduced cells and further allowed for the creation of a stably transduced cell line.

2.25 Confirmation of Successful Lentiviral Transduction

2.25.1 Fluorescent microscopy

The lentiviral vector constructs contained a turbo RFP reporter which allowed for visual tracking of the transduced cells. Cells cultured on slides were fixed and counterstained using DAPI (4', 6-diamidino-2-phenylindole).

2.25.2 Cell Fixation for Fluorescent Staining

1. The slides were washed with 1 X PBS.
2. Cells were fixed in 4% paraformaldehyde for 20 minutes at room temperature.
3. The chamber walls were removed and the slides were washed 3 times for 5 minutes in 1 X PBS.
4. The fixed cells were removed from 1 X PBS and immersed in 1µg/ml DAPI solution for 5 minutes at room temperature and protected from light.
5. The wash step was repeated as described in step 3.
6. The slides were dehydrated in a series of alcohol washes.
7. A layer of DPX (Distyrene, Dibutyl phthalate and Xylene) Mounting Medium was added along the base of the slides and covered with a cover slip.
8. The slides were wrapped in tinfoil and left to dry overnight in the fume hood before viewing.
9. Cells were examined using an Olympus IX81-ZDC fluorescent microscope.

10. The excitation/emission wavelengths for turbo RFP promoter were 553nm/574nm and 345nm/455 for DAPI. Appropriate filters were used to capture individual single channel images, followed by merging images to create composites.

2.25.3 RQ-PCR

Following transduction and 1 week selection, cells were cultured and expression of miR-379 was quantified by RQ-PCR. Cells were trypsinised as previously described in section 2.5. The cell pellets were extracted using RNeasy® Mini Kit. MiRNA was reverse transcribed and amplified for mir-379 and the endogenous controls used were let-7a and miR-16. The results were compared to the cells that received the NTC-mimic.

2.26 Study of the Impact of miR-379 Over-expression on Tumour initiation and growth

The effect of a miR-379 mimic on tumour establishment, growth and metastasis was determined using an in vivo model. T47D cells were stably transduced with a miR-379 mimic or a NTC mimic as described previously. For this study, athymic nude mice were used, as this allowed for the accurate analysis of miRNA expression in tumours and circulation without the interference of a host immune response. The animal experiments were performed following NUI Galway Ethical Committee approval. An animal licence under the Cruelty to Animals Act 1876 by the Department of Health and Children was also obtained. An individual certification (LAST- Certificate) was obtained to perform experiments (Appendix 3).

2.26.1 Animal Facility

In vivo experiments were carried out in the animal research facility of the National Centre for Biomedical Engineering Science (NCBES), NUI Galway. The animals were housed in individually ventilated cages, with 3-4 animals per cage. A Named Day to Day Care Person was responsible for maintaining animal husbandry. Throughout the experimental process, bedding was changed twice weekly. All materials used were autoclaved prior to use in the facility. Any manipulations

performed were carried out in Class II laminar flow hoods, to minimise the risk of infection of immunocompromised animals. Appropriate personal protective equipment (PPE) was worn at all times and this comprised of appropriate gowns, hairnet, mask and gloves.

2.26.2 Tumour Induction protocol

Inbred female athymic nude mice (Harlan Sprague-Dawley, Indianapolis, IN) aged 6-8 weeks were used for this study. These mice express very low endogenous levels of circulating oestrogen and therefore required supplementation with an oestrogen pellet. To support growth of the oestrogen receptor positive T47D cells, female athymic nude mice (n=10) were implanted with a 60-day Slow Release17-β-estradiol pellets (Innovative Research of America, Sarasota, FL). The animals received subcutaneously implanted pellets, 3mm in diameter, containing 0.18 mg 17 β-estradiol. A 0.5 cm incision was made in the loose skin of the mouse's neck and a small pocket was bluntly dissected caudolaterally, in which the pellet was then inserted using tweezers. The incision was closed using dermal glue. During the implantation strict aseptic technique was applied to ensure hygiene was maintained and any risk of infection was minimized. This procedure was carried out under anaesthesia with intramuscular Ketamine (80-100mg/kg) and Xylazine (10mg/kg) injection. Mice were also tagged on the right ear lobe and weights were taken. Post procedure, all mice were monitored until fully awake, capable of moving freely and able to access food and water. Approximately 14 days following implantation, mice were divided into two groups:

- Group 1: Right flank subcutaneous injection of T47D transduced with a NTC mimic ($2.5x10^5$ cells, n=5)
- Group 2: Right flank subcutaneous injection of T47D transduced with a miR-379 mimic ($2.5x10^5$ cells, n=5)

Cells were resuspended in 150µl RPMI-1640 and administered subcutaneously using a 1mL syringe and a 24 gauge needle. Baseline bloods were also collected from individual mice prior to tumour induction (n=4, Figure 2.19).

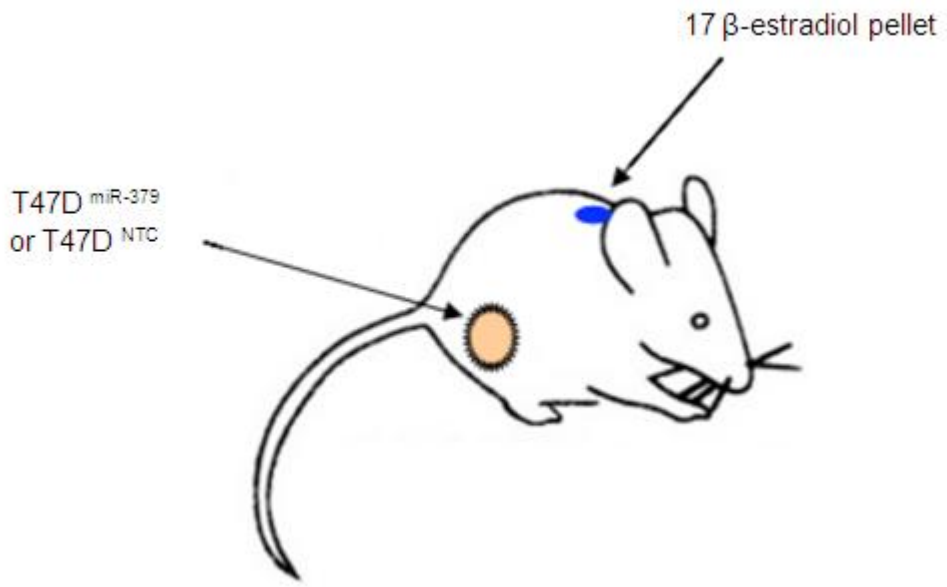

Figure 2.19 Mouse model showing 17 β-estradiol implantation (blue circle). Right flank subcutaneous injection of transduced T47D cells (orange circle).

2.26.3 Confirmation of miR-379 over-expression at Tumour Induction Day

An aliquot of the stably transduced T47D cells was set aside after tumour induction for analysis of miR-379 expression. $T47D^{379}$ were further maintained in culture to quantify miR-379 expression at day 3 and day 7 post tumour induction, in parallel with tumour growth in vivo.

2.27 Specimen Collection Protocol

At week 9 following tumour induction, all mice were sacrificed by CO_2 inhalation. Any tumours present were harvested and immediately snap frozen in liquid nitrogen at -80°C until required. A terminal cardiac bleed was performed on all mice for analysis of circulating miR-379 by RQ-PCR. The blood was stored at 4°C in 2 mL EDTA tubes until required. Mice were weighed at weekly intervals. This was another form of monitoring the health of the animal.

2.28 RNA Extraction

Tissue homogenisation and subsequent RNA extraction was performed as previously detailed in section 2.14.3.

Total RNA was extracted from 100µl of murine blood rather than 1mL as previously described in section 2.23.5. Due to the small volumes of blood present, reagents used for the blood extraction protocol were scaled down to adjust to 100µl blood analysed (Table 2.15).

Blood (µl)	100	1000
Tri Reagent (µl)	300	3000
BAN (µl)	20	200
Isopropanol (µl)	100	1000
75% Ethanol (µl)	100	1000
Water to dissolve pellet (µl)	30	30

Table 2.16 Downscaling of RNA extraction protocol for human blood (100 µl).

2.29 Statistical Analysis

Data is presented as Mean±SEM. Data was analysed using Minitab 16 for Windows. Results with a $p<0.05$ were considered statistically significant. All tests were two-tailed.

Chapter 3

MicroRNA-mediated Regulation of Sodium Iodide Symporter (NIS) and its Regulators in Breast Cancer

3.1 Introduction

The Sodium Iodide Symporter (NIS) is a glycoprotein which facilitates the active uptake of iodide into thyroid follicular cells from the circulation, for the synthesis of triiodothyronine (T_3) and thyroxin (T_4) hormones [122]. This ability of NIS to accumulate iodide has been exploited therapeutically for many years in the treatment of hyperthyroidism in Graves' disease [202] and also thyroid cancer [203]. NIS expression is detectable at relatively low levels in the salivary and lacrimal glands, stomach, kidneys, intestines and interestingly the mammary gland [204, 205]. In the normal breast NIS is expressed only during lactation, to contribute to neonatal nutrition [131]. During lactation NIS expression is optimal through the release of prolactin, oestrogen and oxytocin [131]. NIS expression has been confirmed in some breast cancers but not in normal non-lactating breast tissues [206-208]. Reports revealed elevated NIS expression in benign breast disease compared to malignant tissues [138], which highlights a potential role for NIS as a tumour suppressor in breast cancer. The therapeutic potential of NIS in thyroid cancer is well established. However the potential application in breast cancer is currently sought after. Due to variability of endogenous expression of NIS in breast cancer tissues and poor understanding of its regulation, therapeutic application of radiolabelled iodide has not yet been established for breast cancer patients. Loss of NIS in dedifferentiated thyroid cancers is also an important target, as these tumours cannot concentrate sufficient radioiodide for effective treatment [209]. Understanding of its regulation in breast cancer would potentially support systemic radioiodide treatment of the disease.

Up-regulation of native NIS in breast cancer has been a focus of much research [144, 210, 211]. The microRNAs of interest for this study were chosen based on predicted binding sites on NIS and its regulators RARα, RARβ, and ERα. The chosen microRNAs are miR-875-5p, miR-10a, miR-339-5p and miR-379.

There are currently no published reports on miR-875-5p function or expression in the normal physiology or disease setting. In the miR-10 family, particularly miR-10a and miR-10b, previous reports have highlighted a role in developmental as well as pathological pathways including cancer [212]. Inhibition of both miR-10a and miR-10b was reported to enhance metastasis in neuroblastoma cell lines [111, 112]. In the

context of breast cancer, miR-10a expression has only been analysed in breast cancer cell lines [213, 214], where it was shown to inhibit Hoxd4 expression in vitro [108].

Recent studies have shown altered expression of miR-339-5p in several cancers [115-117, 119]. There is currently one paper which investigated the role of miR-339-5p in breast cancer [120]. This study reported decreased expression of miR-339-5p in aggressive breast cancer cell lines compared to non-invasive cells. Elevated expression of miR-339-5p in the benign samples compared to the malignant cohort was revealed [120]. Reduced migration and invasion was also observed following transfection with a miR-339-5p mimic in vitro [120].

To date, very little is known about the role of miR-379 in normal physiology or disease. In the context of breast cancer, there is currently one report implicating miR-379 in direct negative regulation of interleukin-11 (IL-11) production in metastatic breast cancer cell lines through stimulation of TFG-β [121]. This has implications in regulation of the key pathogenic process in breast cancer through inhibition of IL-11 production [121].

3.2 Aim

To determine the level of expression of miR-875-5p, miR-10a, miR-339-5p and miR-379 in breast tissues and to investigate any relationship between these miRNAs of interest and potential target genes NIS, RARα, RARβ, and ERα in breast cancer.

3.3 Materials and Methods

A panel of breast tissues had previously been analysed to quantify the level of NIS expression. RNA was analysed from a group selected from a large cohort of samples. RNA samples were selected based on samples with the highest (n=10) and lowest (n=10) detectable level of NIS expression. The level of expression of chosen miRNAs, with predicted binding sites on the 3'UTR of NIS, RARα, RARβ, and ERα were then determined in the same RNA samples. Any inverse relationship seen between expression of the miRNAs and the target gene could potentially indicate miRNA binding and regulation of the gene. Luciferase reporter constructs containing the 3'UTR of NIS and RARβ were also employed to determine whether the chosen miRNAs played a direct role in regulation of NIS and RARβ 3'UTR.

3.4 MicroRNA Expression

The following miRNAs were included in this study: miR-875-5p, miR-10a, miR-339-5p and miR-379. The results observed showed when NIS gene expression was low in the breast tissues, expression of miR-875-5p, miR-10a and miR-379 were also relatively low. Higher NIS expression correlated with increased miR-875-5p expression (2.31(0.33) Log_{10} RQ, Figure 3.1) compared to miR-875-5p expression in the low NIS group (0.46(0.14) Log_{10} RQ, $p<0.001$). miR-10a was also significantly increased in the high NIS group (2.39(0.28) Log_{10} RQ) compared with miR-10a expression in the low NIS group (0.87(0.21) Log_{10} RQ, $p<0.002$). The same was true for miR-379 expression in the high NIS group (1.86(0.39) Log_{10} RQ) compared with miR-379 expression in the low NIS group (0.46(0.24) Log_{10} RQ, $p<0.01$,). The levels of miR-339-5p did not change between high NIS (1.43(0.21) Log_{10} RQ) and low NIS group (1.51(0.07) Log_{10} RQ, $p=0.71$, Figure 3.1).

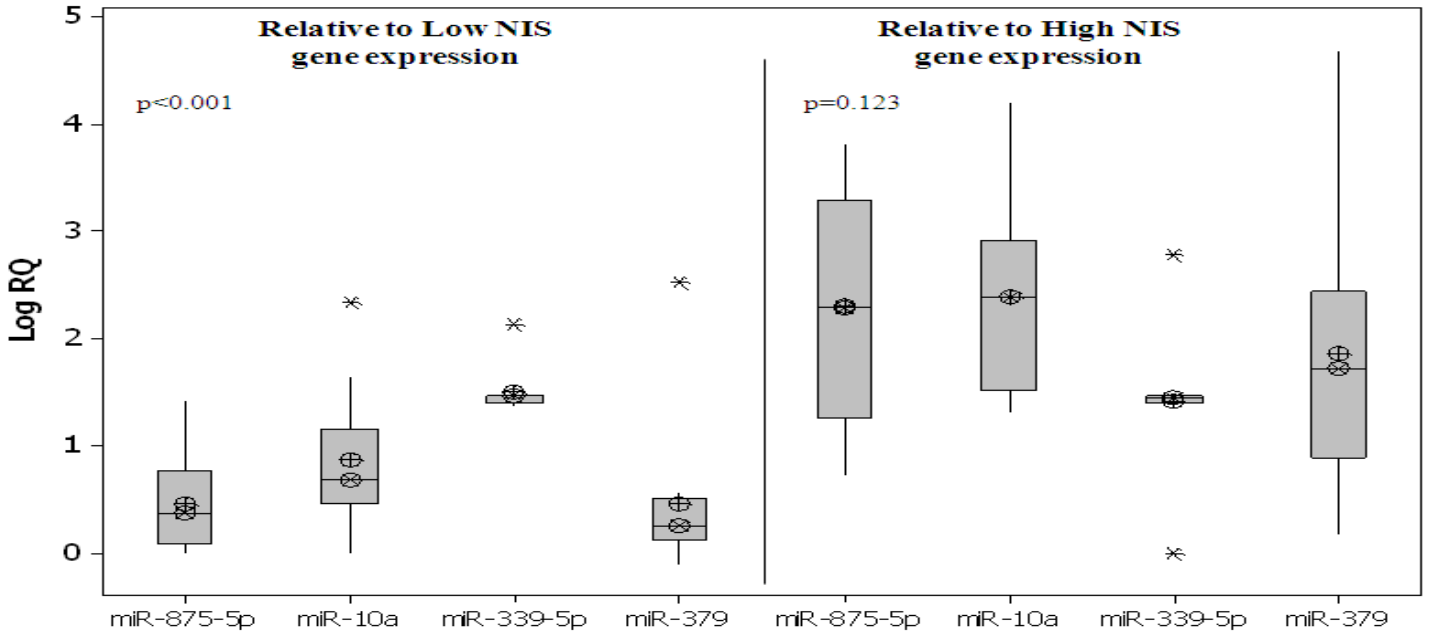

Figure 3.1 MicroRNA Expressions across Breast Tissue Samples. The results were expressed relative to samples with low NIS expression on the left. The tissues with high NIS expression on the right, revealed a different miRNA expression profile. * Represents outliers.

3.5 Expression of miR-875-5p

Since expression of miR-875-5p changed significantly with increasing NIS gene expression, any potential relationship between miR-875-5p and NIS, RARα, RARβ and ERα was investigated. A correlation analysis was performed across the pilot samples. miR-875-5p expression correlated positively with NIS gene expression (r=0.818, p<0.001, Figure 3.3) and with RARβ gene expression (r=0.710, p<0.001, Figure 3.2). No significant correlations were observed between miR-875-5p and RARα (r=0.29, p=0.2) or ERα (r=0.31, p=0.17, results not shown).

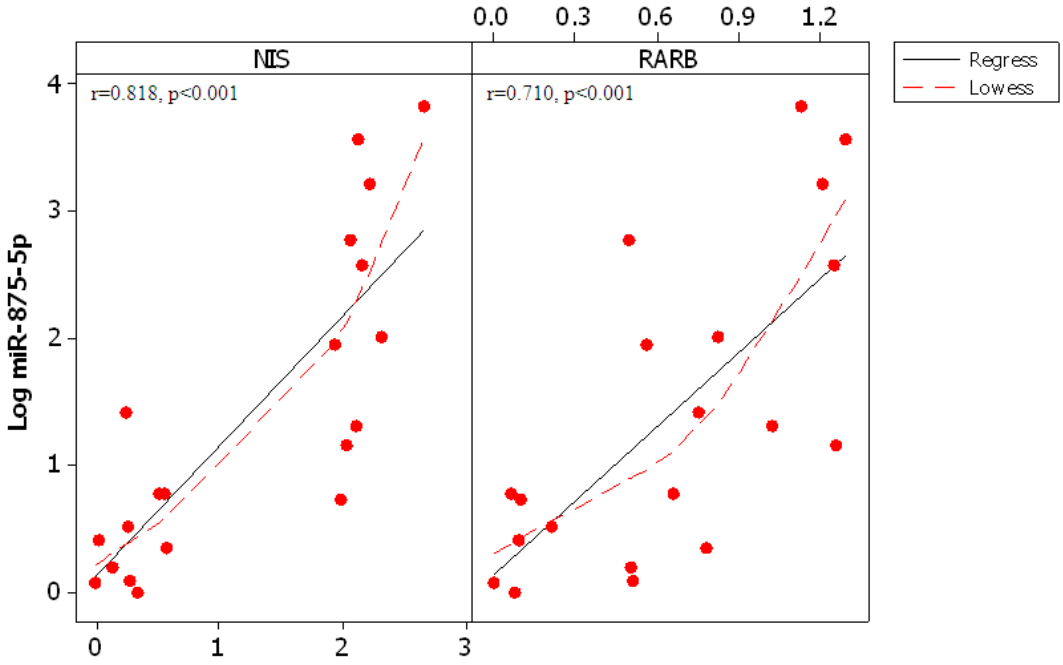

Figure 3.2 Investigate a correlation between miR-875-5p and NIS and RARβ.

Expression of miR-875-5p was then further investigated across a larger cohort of breast cancer tissues, including malignant n=43 and normal breast tissues n=16. The results revealed no significant difference across breast cancer tissues (1.45(0.09) Log_{10}RQ) compared to normal tissues (1.79(0.09) Log_{10} RQ, p=0.092, Figure 3.3).

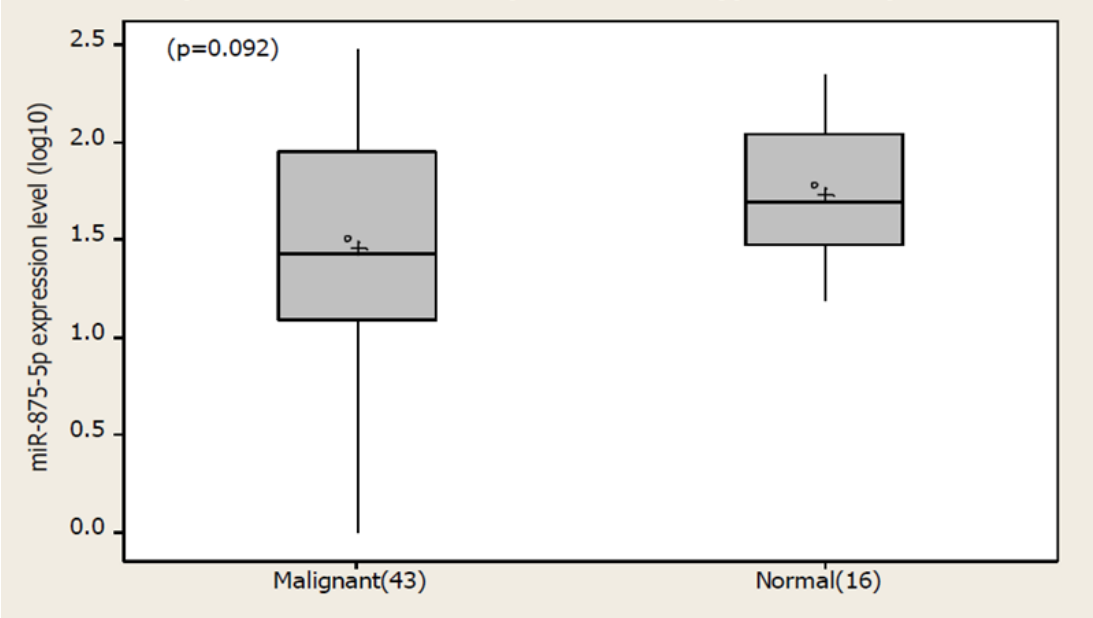

Figure 3.3 Expression of miR-875-5p across breast cancer patients and healthy controls.

3.6 Expression of miR-10a

Any relationship between miR-10a and NIS, RARα, RARβ and ERα was investigated. miR-10a expression revealed a robust positive correlation with NIS gene expression ($r=0.738$, $p<0.001$, Figure 3.6) and with RARβ ($r=0.643$, $p<0.001$, Figure 3.4).

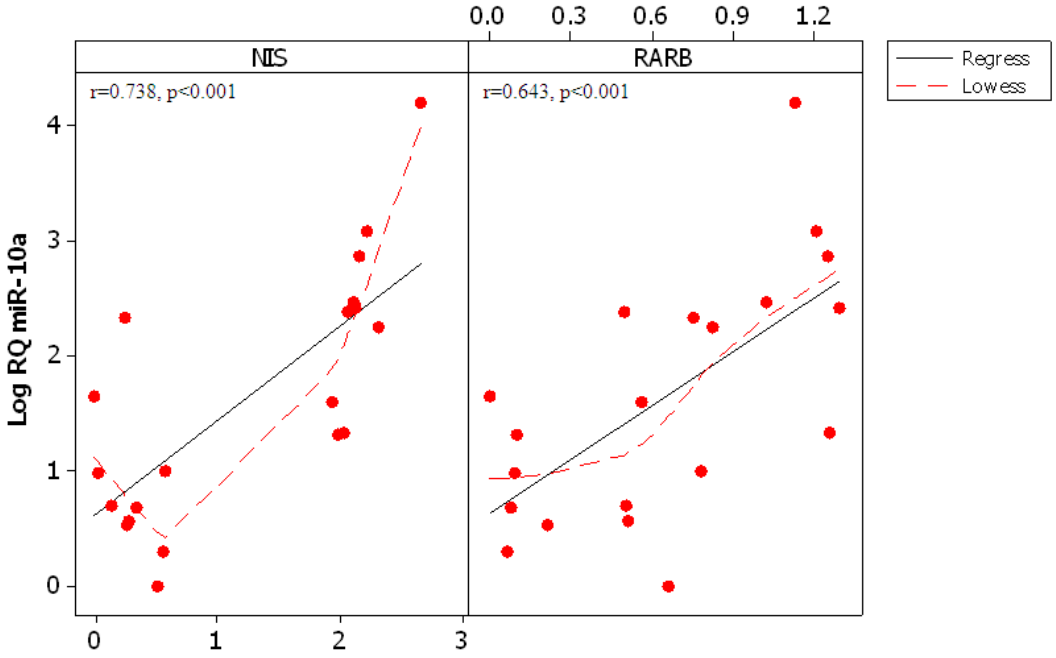

Figure 3.4 Investigate a correlation between miR-10a and NIS and RARβ.

No significant correlation was observed between miR-10a and RARα (r=0.28, p=0.23) or ERα (r=0.27, p=0.25, results not shown).

3.6.1 Investigation of Direct Binding of miR-10a with NIS or RARβ 3'UTR

Since miRNAs can exert their effect without altering the level of target mRNA present, potential direct binding of miR-10a with NIS or RARβ was investigated using a 3'UTR reporter construct. The effect on 3'UTR-luciferase reporter activity by a miR-10a mimic was measured in T47D cells by co-transfecting 50ng of each reporter construct with 50nM miR-10a or a NTC mimic, and incubating it for 24 hours. β-Actin 3'UTR is a housekeeping control reporter and was used as a reference gene for normalisation of the assay. The Random 3'UTR is a control used to accurately separate sequence-specific vs. non-specific effects. The cells luminescent reporter signal was read using LightSwitch Luciferase Assay reagents on a luminometer (Figure 3.5). miR-10a has a predicted binding site on NIS and RARβ 3'UTR. Signals from human 3'UTR reporters of NIS and RARβ were not significantly knocked-down in the presence of a miR-10a microRNA mimic (Figure 3.5).

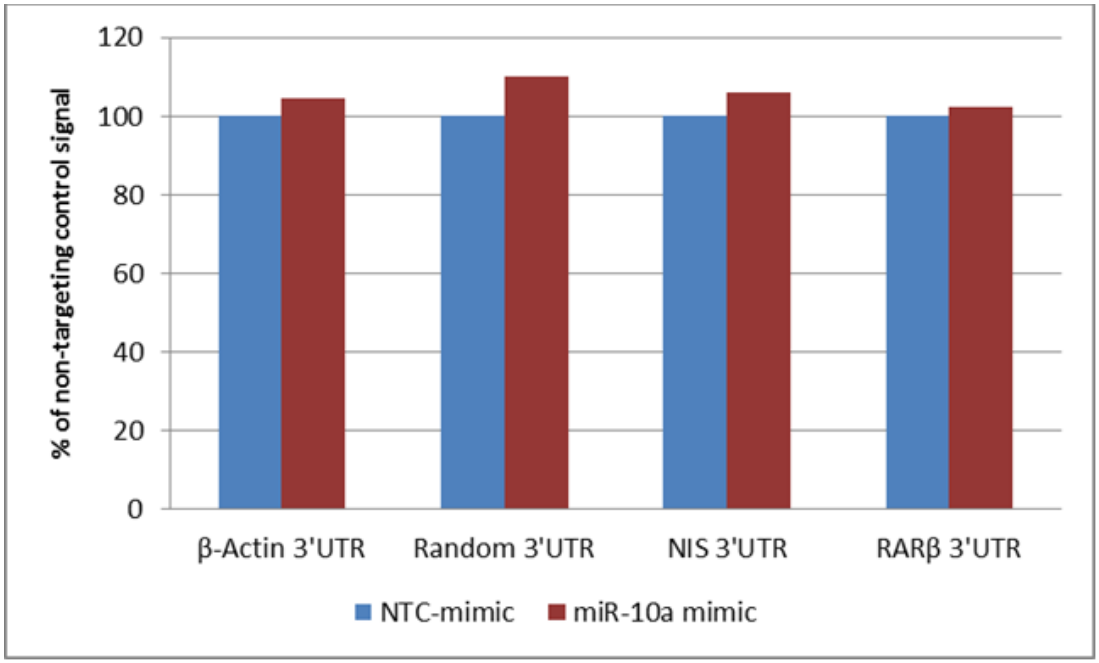

Figure 3.5 Luciferase Assay for the detection of miR-10a binding to NIS or RARβ 3'UTR.

A more detailed investigation was performed on a larger cohort on the expression of miR-10a in breast cancer patients overall compared to healthy controls in Chapter 4.

3.7 Expression of miR-339-5p

Expression of miR-339-5p was not found to change with increasing NIS gene expression. However, miR-339-5p expression showed a trend toward negative correlations with NIS, RARα and ERα, although the correlations observed did not reach significance (results not shown). Further, expression of miR-339-5p showed no relationship with levels of RARβ ($r=0.133$, $p=0.57$, results not shown).

3.7.1 Investigation of Direct Binding of miR-339-5p with NIS or RARβ 3'UTR

miR-339-5p has a predicted binding site on NIS. Signals from human 3'UTR reporters from NIS and RARβ were not significantly knocked-down in the presence of miR-339-5p microRNA mimic (Figure 3.6).

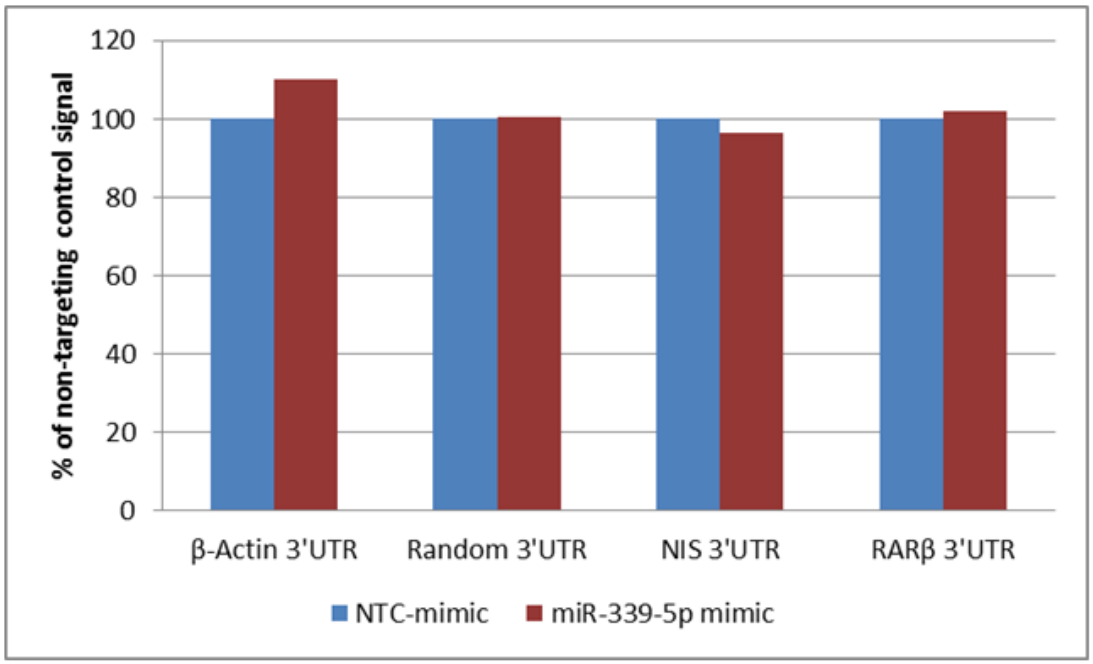

Figure 3.6 Luciferase Assay for the detection of miR-339-5p binding to NIS and RARβ 3'UTR.

Although direct regulation of NIS and RARβ was ruled out here, in order to investigate the potential role in cancer, this study was expanded to include analysis of n=168 breast tissues. The findings are detailed in Chapter 4.

3.8 Expression of miR-379

Finally, miR-379 expression was investigated. Any potential relationship with NIS, RARα, RARβ and ERα was determined. miR-379 expression showed a robust positive correlation with NIS gene expression ($r=0.661$, $p<0.01$, Figure 3.9) and RARβ gene expression ($r=0.649$, $p<0.02$, Figure 3.7).

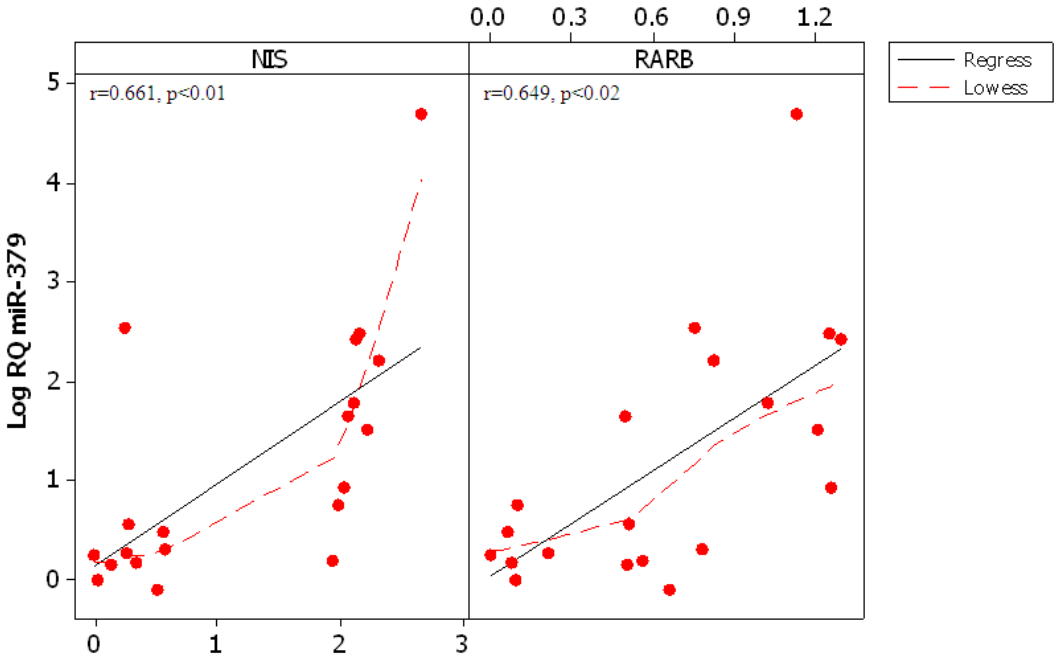

Figure 3.7 Investigate a correlation between miR-379 and NIS and RARβ.

No significant relationship between miR-379 and RARα (r=0.354, p=0.12) or ERα (r=0.307, p=0.19, results not shown) were detected.

3.8.1 *Investigation of Direct binding between miR-379 and NIS or RARβ 3'UTR*

miR-379 has a predicted binding site on NIS and RARβ 3'UTR. Signals from human 3'UTR reporters from NIS and RARβ were not significantly knocked-down in the presence of miR-379 microRNA mimic (Figure 3.8).

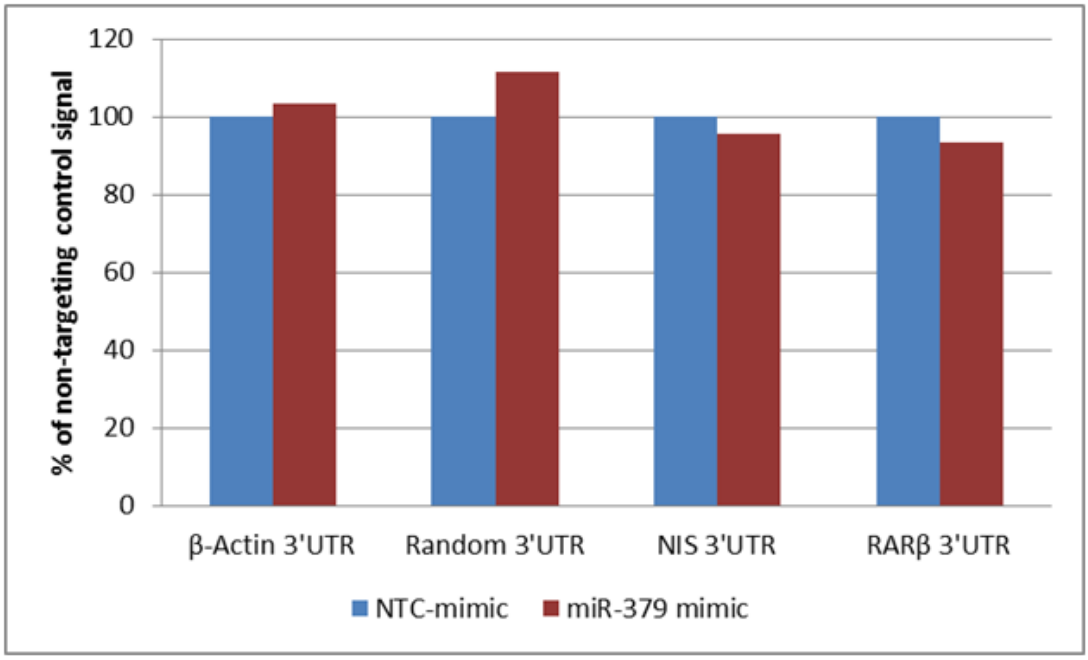

Figure 3.8 Luciferase Assay for the detection of miR-379 binding to NIS or RARβ 3'UTR.

Due to the interesting positive correlations between NIS and RARβ observed in this pilot study, a detailed investigation of miR-379 performed in a total of 168 breast tissues to investigate their potential tumour suppressor role in breast cancer. The results of this analysis are detailed in Chapter 5.

3.9 Discussion

This study aimed at identifying potential relationships between miR-875-5p, miR-10a, miR-339-5p and miR-379 expression with target genes NIS, RARα, RARβ and ERα.

If the miRNA was targeting the particular gene, an inverse correlation between miRNA and gene expression may be observed. However, microRNAs can exert their effects through binding to the target mRNA and preventing translation without degradation of the mRNA. Therefore, constructs containing the 3'UTR of the gene of interest tagged with a luciferase reporter are useful to detect direct binding of a miRNA mimic which is observed by consequent quenching of luciferase signal. It

would be worth noting that the luciferase assay did not include a successful positive control which resulted in signal quenching and therefore further future analysis should aim to include this.

Increasing NIS expression was shown to correlate with the expression of miR-875-5p, miR-10a and miR-379. Most miRNAs revealed elevated expression in samples with high NIS gene expression when comparing it to samples with low NIS gene expression. miR-339-5p levels were not changed between samples with high NIS and low NIS expression.

A positive correlation was observed between miR-875-5p expression and NIS and RARβ gene expression. This suggests that miR-875-5p does not have a regulatory role for NIS or RARβ. Since RARβ has a well-established role as a tumour suppressor in breast cancer [215], its positive correlation with miR-875-5p in the initial pilot study potentially suggested miR-875-5p could behave similar to RARβ in breast cancer. Expression of miR-875-5p was then further analysed by RQ-PCR in a larger cohort of breast cancer patients and healthy controls. Currently, there are no published reports on the expression of miR-875-5p. In this study, miR-875-5p expression was not significantly altered across malignant and normal breast tissues. Based on these findings, miR-875-5p expression was not further investigated as part of this study.

miR-10a expression was shown to have a positive correlation with NIS, RARβ and ERα. Combined with the luciferase reporter assay results, it suggested no direct regulatory role for miR-10a with NIS or RARβ. The positive correlation observed however, was in agreement with previously published work revealing RA-mediated stimulation of miR-10a. A RA-antagonist effectively blocks expression of miR-10a and subsequently inhibits metastasis in pancreatic cancer cells [216]. A study by Meseguer et al [111], revealed both miR-10a and miR-10b were essential mediators of RA-induced neuroblastoma cell differentiation. The most recent paper focused on RA-mediated induction of miR-10a in regulating the plasticity of helper T cells [109]. In relation to the positive correlation observed between miR-10a and RARβ in this study, it would also support the idea of RA-mediated stimulation of miR-10a in breast cancer. Thus, further investigation was warranted relating to miR-10a expression in breast cancer which is detailed in Chapter 4.

miR-339-5p was the only miRNA analysed to show a trend towards negative

correlation with NIS, RARα and ERα, however these finding were not significant. Further direct binding of miR-339-5p to the target 3'UTR of NIS and RARβ was ruled out using the luciferase reporter assay. Due to the small sample number analysed and a trend towards an inverse correlation with a range of target genes, a thorough investigation of miR-339-5p expression was carried out in Chapter 4. Finally expression of miR-379 was shown to have a significant positive correlation with NIS and RARβ. Currently there is only one paper investigating miR-379 in relation to breast cancer [121]. This paper by Pollari et al [121], profiled miRNA expression in metastatic breast cancer cell lines. The use of predictive algorithms allowed for the selection of key miRNAs involved in potential regulation of TGF-β induced IL-11 production which is a key process of breast cancer metastasis [121]. In the current study, no direct binding could be confirmed between miR-379 and NIS or RARβ 3'UTR, based on luciferase reporter results. The positive correlation observed between miR-379 with NIS and the tumour suppressor RARβ in breast cancer warrants further investigation, this was elucidated in Chapter 5.

Analysis of this pilot study revealed interesting correlations between miR-10a, miR-339-5p and miR-379 with expression of NIS and RARβ in breast cancer. This study has ruled out any direct binding and therefore no miRNA-mediated regulatory role on the target mRNAs. However, the positive correlations observed with the target genes which have all previously been implicated in breast cancer progression, suggested that these miRNAs may play a role in breast tumourigenesis. Therefore further investigation on miR-339-5p, miR-10a and miR-379 was warranted and is presented in greater detail in the subsequent results chapters.

Chapter 4

miR-339-5p and miR-10a Expression in Breast Cancer

4.1 Introduction

Although initially chosen based on potential regulation of NIS, RARα, RARβ and ERα expression in breast cancer, the focus now moves to relative expression of miR-339-5p and miR-10a in breast cancer patients compared to healthy controls. As previously mentioned, miR-339-5p has currently only been investigated in one paper in relation to breast cancer, where it was reported to be elevated in benign breast disease tissues compared to malignant breast tissues and was further found to affect breast cancer migration and invasion in aggressive breast cancer cell lines [120]. In the previous chapter levels of miR-339-5p was quantified in a small cohort and revealed a trend towards inverse correlations with NIS, RARα and ERα. This would suggest a potential regulatory role for miR-339-5p with NIS, RARα, and ERα. Ki-67 is a key proliferation marker in breast cancer [217] and predictive algorithms revealed a binding site for miR-339-5p on position 1176-1182 of Ki-67 3'UTR [218].

Expression of miR-10a has only been investigated in breast cancer cell lines [213, 214] with no reports on levels in clinical specimens. The results from Chapter 3 reported positive correlations with the tumour suppressor RARβ. This finding combined with previously published work, suggested RA-mediated stimulation of miR-10a.

Expression of miRNAs miR-339-5p and miR-10a as well as NIS, RARβ and THRα were further investigated in a larger cohort, due to a possible role in breast cancer progression.

4.2 Aim

- Quantify NIS gene expression along with RARβ and THRα in breast tissues. Investigate any potential relationship with patient clinicopathological details.
- Determine the level of miR-339-5p and miR-10a in breast tissues and investigate any relationship with patient clinicopathological details.
- Investigate any correlation between NIS, RARβ and THRα gene expression and expression of miR-339-5p and miR-10a.
- Examine the effect of miR-339-5p and miR-10a over-expression on breast cancer cell proliferation in vitro.

- Determine circulating miR-339-5p and miR-10a levels in breast cancer patients and healthy controls.

4.3 Materials and Methods

Breast tissue specimens (n=168) analysed consisted of 103 malignant tissue biopsies, 30 normal mammary tissue biopsies, and 35 fibroadenoma tissues. Full patient demographics and clinicopathological details were collected and maintained prospectively (Table 4.1). Gene expression analysis for NIS, THRα and RARβ were carried out on all patient samples and any relationship with patient clinicopathological details was investigated. The results were expressed relative to the average endogenous controls MRPL19 and PPIA. Levels of miR-339-5p and miR-10a were quantified in the same patient breast tissue cohort, relative to Let-7a. Native expression of miR-339-5p and miR-10a were also determined across a range of breast cancer cell lines. T47D and SK-BR-3 cells were transfected with a miR-339-5p mimic (mature sequence: UCCCUGUCCUCCAGGAGCUCACG; 50nM), a miR-10a mimic (mature sequence: UACCCUGUAGAUCCGAAUUUGUG; 50nM) or a NTC mimic. Transfections were performed using Lipofectamine™ 2000 according to manufacturer's instructions. Cell proliferation was assessed 48 hours following transfection using the Promega MTS Assay. Whole blood samples were also collected from 51 breast cancer patients pre-operatively and 37 healthy controls with no family history of the disease (Table 4.3). Circulating levels of miR-339-5p and miR-10a were quantified by RQ-PCR.

Patient Clinicopathological details	**Cancer**	**Fibroadenoma**	**Normal**
Number of patients	103	35	30
Median Patient Age yrs	56 (35-90)	44 (17-62)	46.5 (24-58)
Menopausal Status			
Post	72		
Pre	31		
Histological Subtype			
Invasive Ductal	78		
Invasive Lobular	11		
Other	*14*		
Intrinsic Subtype			
Luminal A (ER/PR+, HER2/neu-)	42		
Luminal B (ER/PR+, HER2/neu+)	18		
HER2 Over expressing (ER-, PR-, HER2/neu+)	16		
Triple-Negative (ER-, PR-, HER2/neu-)	16		
Unknown	*11*		
Tumour Grade			
1	5		
2	32		
3	56		
Tumour size			
T1	19		
T2	39		
T3	10		
UICC Stage			
Stage 1	23		
Stage 2	36		
Stage 3	21		
Stage 4	10		

Table 4.1 Patient Clinicopathological details.

4.4 Gene Expression analysis of mRNA targets

Analysis of mRNA targets included: NIS, RARβ and THRα. These targets were quantified by RQ-PCR in 168 breast tissues specimens. The results were expressed as Log_{10} relative quantity (RQ).

NIS gene expression was detectable in 84 out of 102 breast cancer samples (Figure 4.1). As for the normal breast cohort, NIS expression was positive in only 9 out of 30 samples analysed. The wide range in NIS expression and subsequent lack of normally distributed box plot for normal samples can be explained by low sample numbers expressing NIS.

In the benign cohort, 15 out of 35 tissues showed positive NIS gene expression. The greatest incidence of NIS expression was observed in the malignant cohort. However, the highest level of NIS expression was observed in the benign group. NIS gene expression was significantly lower in breast cancer tissues (n=84, 1.53(0.07) Log_{10} RQ) compared to fibroadenoma (n=15, Mean (SEM) 2.31(0.24) Log_{10} Relative Quantity (RQ), $p<0.005$). NIS expression was not differentially expressed between normal breast tissues (n=9, 1.95(0.55) Log_{10} RQ) and malignant samples (Figure 4.1), which could be explained by the low sample number in the normal cohort.

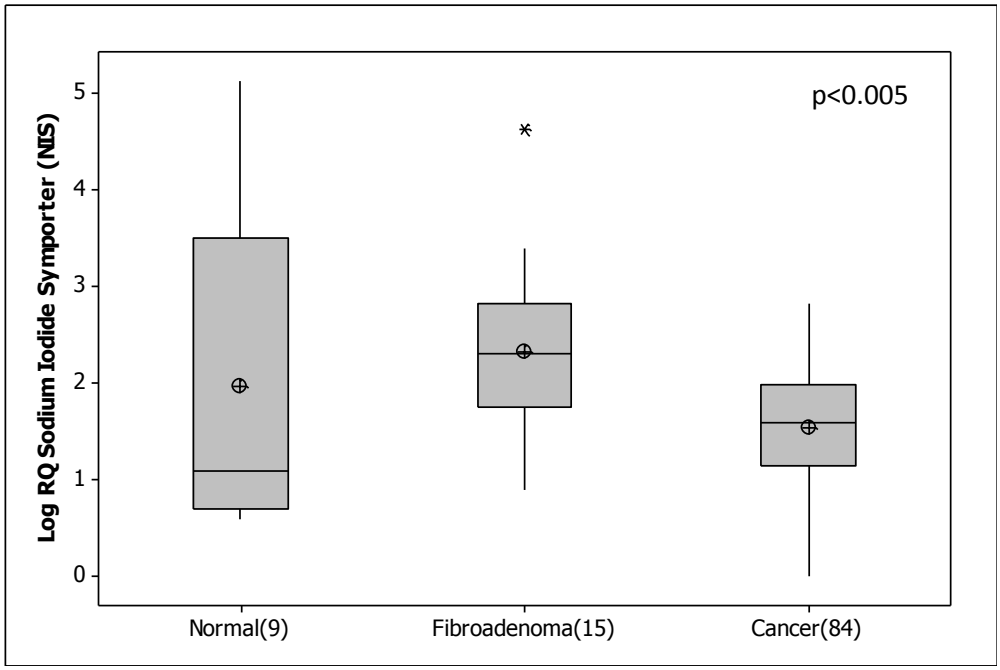

Figure 4.1 NIS gene expression across breast tissue specimens. * Represents outliers.

NIS gene expression within the tumour group was also further stratified based on patient clinicopathological details. No significant deregulation of NIS expression was observed across epithelial subtype (p=0.136, Figure 4.2).

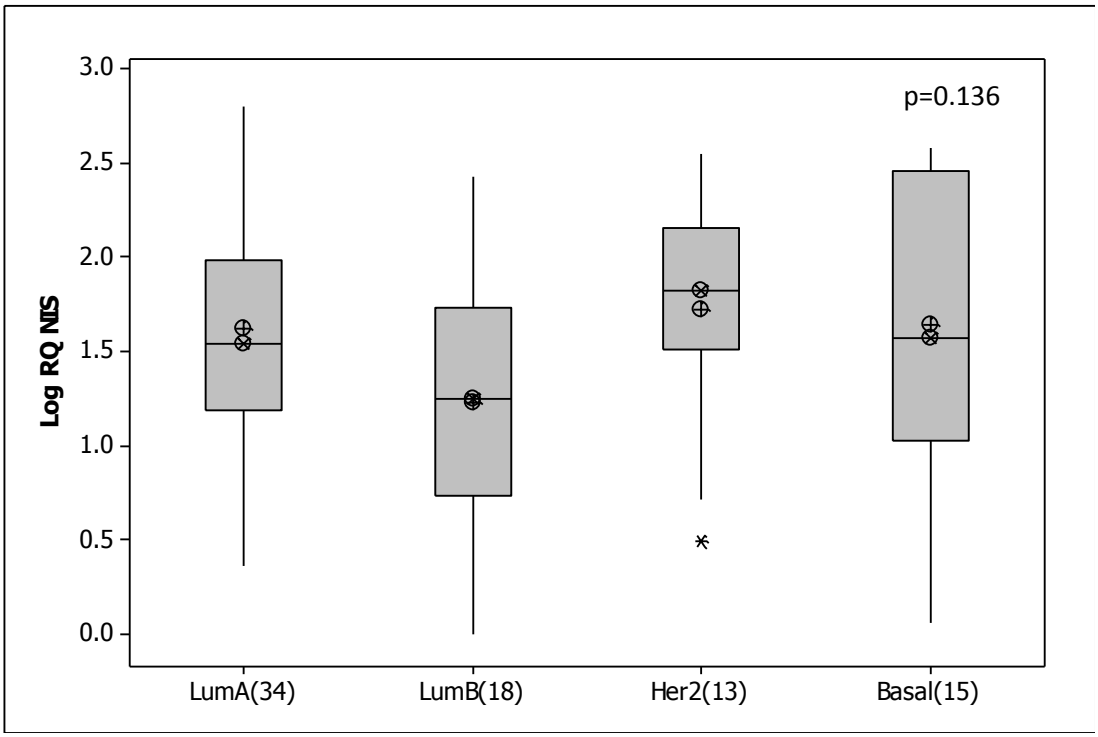

Figure 4.2 NIS gene expression across epithelial subtype. * Represents outliers.

Further, no significant association with other clinicopathological characteristics was observed, including tumour grade (p=0.515), tumour stage (p=0.686) and menopausal status (p=0.566, results not shown).

RARβ gene expression was detectable in all 101/101 malignant samples, 27/30 normal tissues and in 32 out of 35 benign samples. RARβ gene expression was found to be significantly down-regulated in breast cancer (n=101, 0.83(0.04) Log_{10} RQ) compared to both normal (n=27, 1.35(0.09) Log_{10} RQ, p<0.001) and fibroadenoma tissue (n=32, 1.49(0.07) Log_{10} RQ, p<0.001, Figure 4.3).

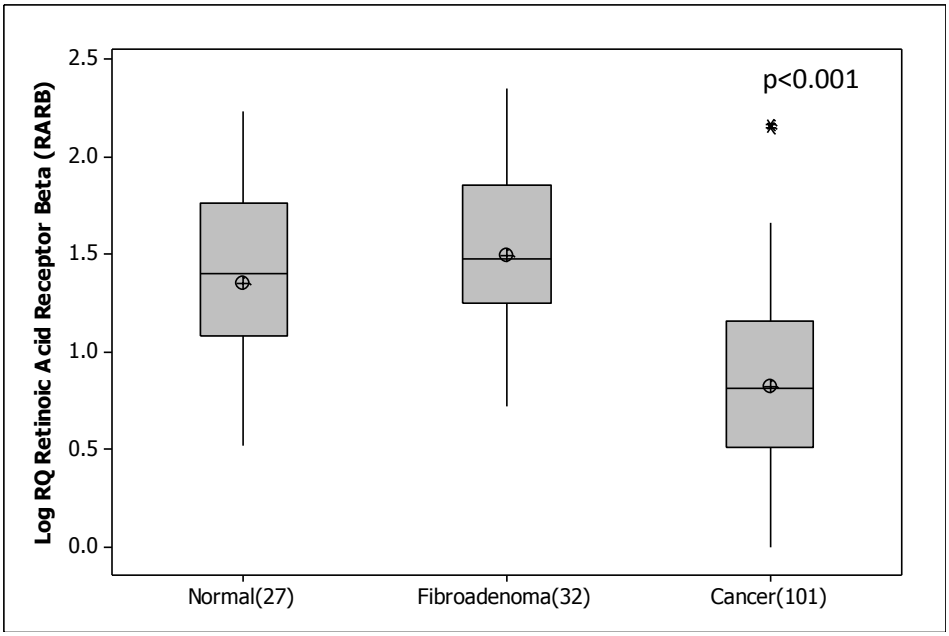

Figure 4.3 RARβ gene expression across all breast tissues. * Represents outliers.

RARβ gene expression was also investigated across the breast cancer cohort. No significant association was observed with epithelial subtype (p=0.122, Figure 4.4).

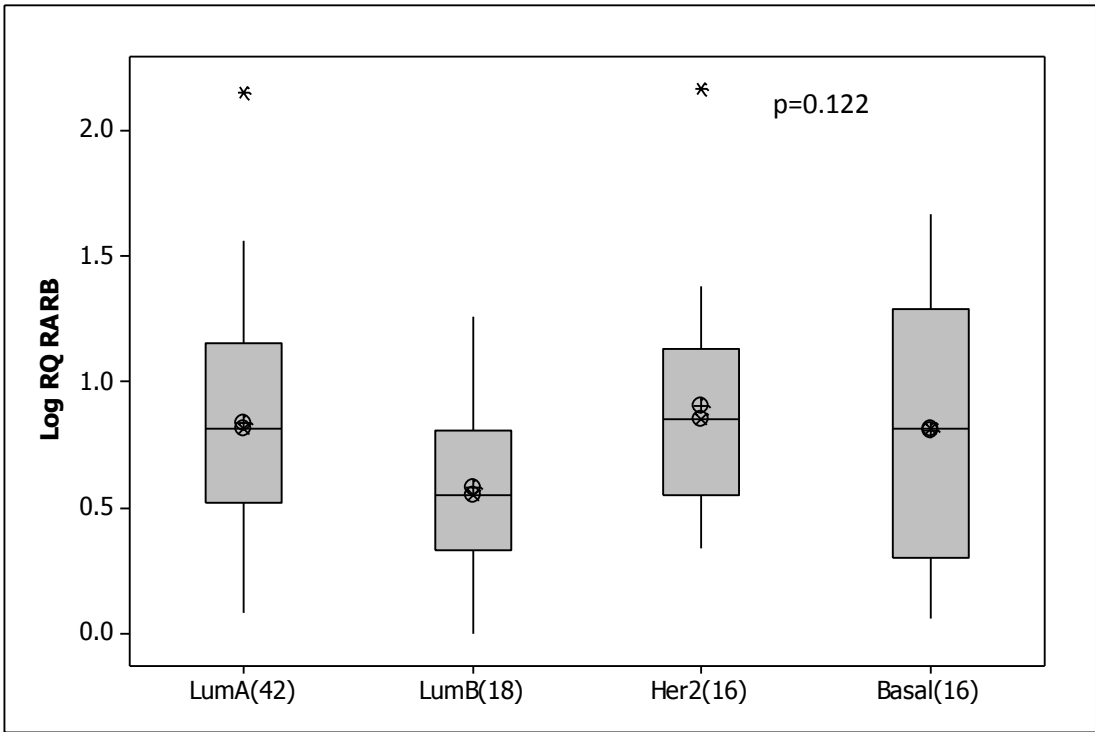

Figure 4.4 RARβ gene expression across epithelial subtype. * Represents outliers.

No significant relationships were observed between RARβ and tumour grade (p=0.363), tumour stage (p=0.614) or menopausal status (p=0.635, results not shown).

Finally, THRα gene expression was detectable in all breast tissue samples. Levels were found to be significantly decreased in breast cancer (n=101, 0.90(0.03) Log_{10} RQ) compared to both normal (n=27, 1.50(0.06) Log_{10} RQ, p<0.001) and fibroadenoma tissues (n=32, 1.28(0.07), p<0.001, Figure 4.5).

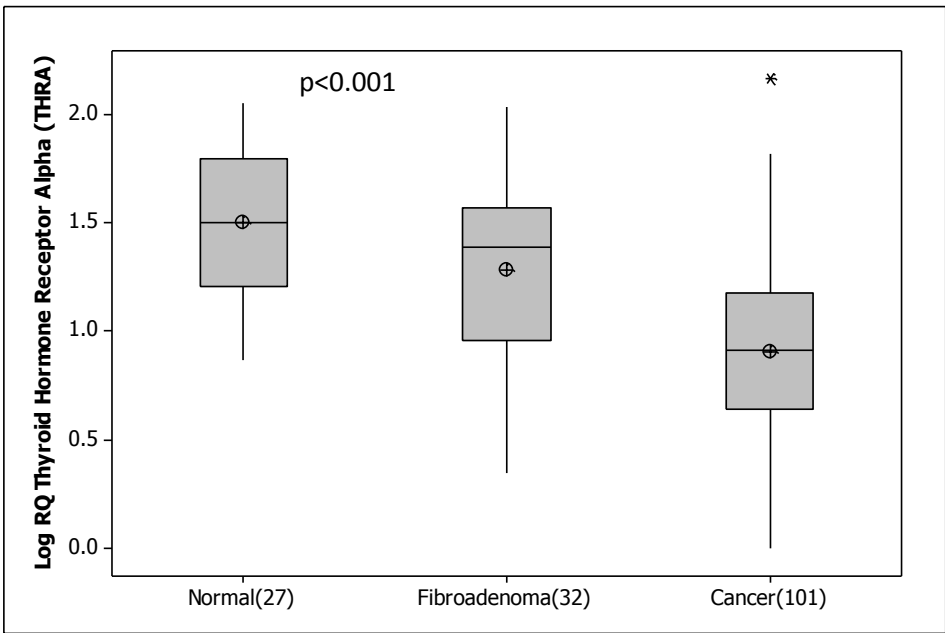

Figure 4.5 THRα gene expression across breast tissues. * Represents outliers.

THRα gene expression was not significantly deregulated across epithelial subtype (p=0.116, Figure 4.6).

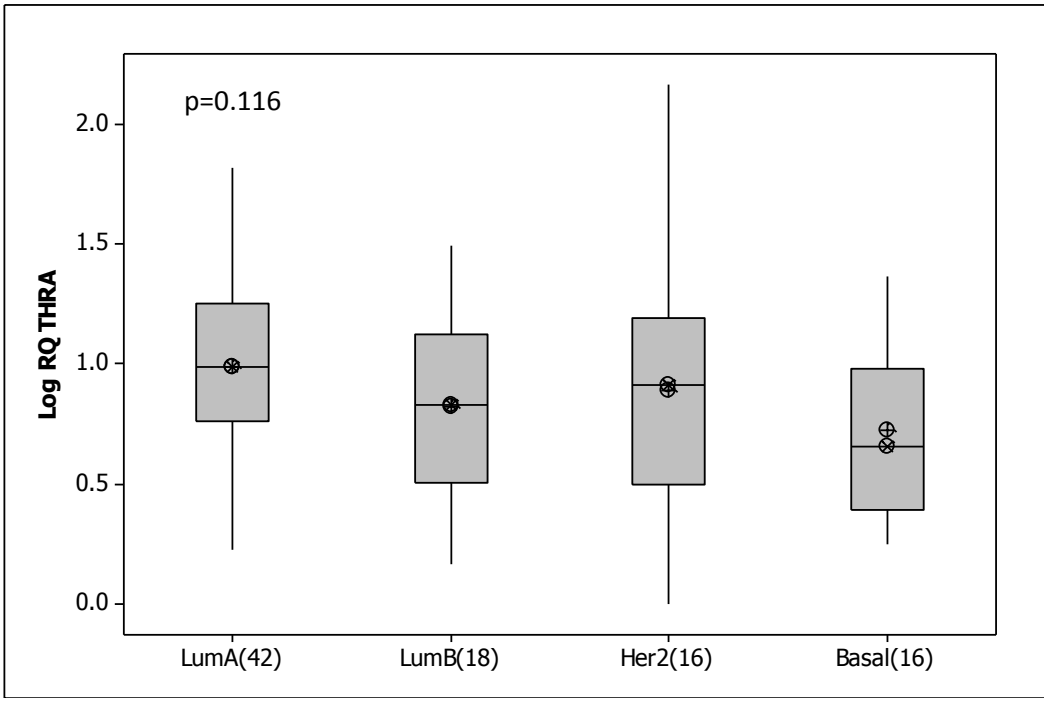

Figure 4.6 THRα gene expression across epithelial subtype.

Any potential relationship between THRα gene expression and patient clinicopathological details was investigated. THRα gene expression was observed to be differentially expressed across tumour grade ($p<0.005$). THRα gene expression was elevated in grade 2 (n=32, 1.09(0.06) Log_{10} RQ) compared to both grade 1 (n=5, 0.78(0.14) Log_{10} RQ, $p< 0.001$) and grade 3 (n=56, 0.82(0.05) Log_{10} RQ, $p<0.002$, Figure 4.7).

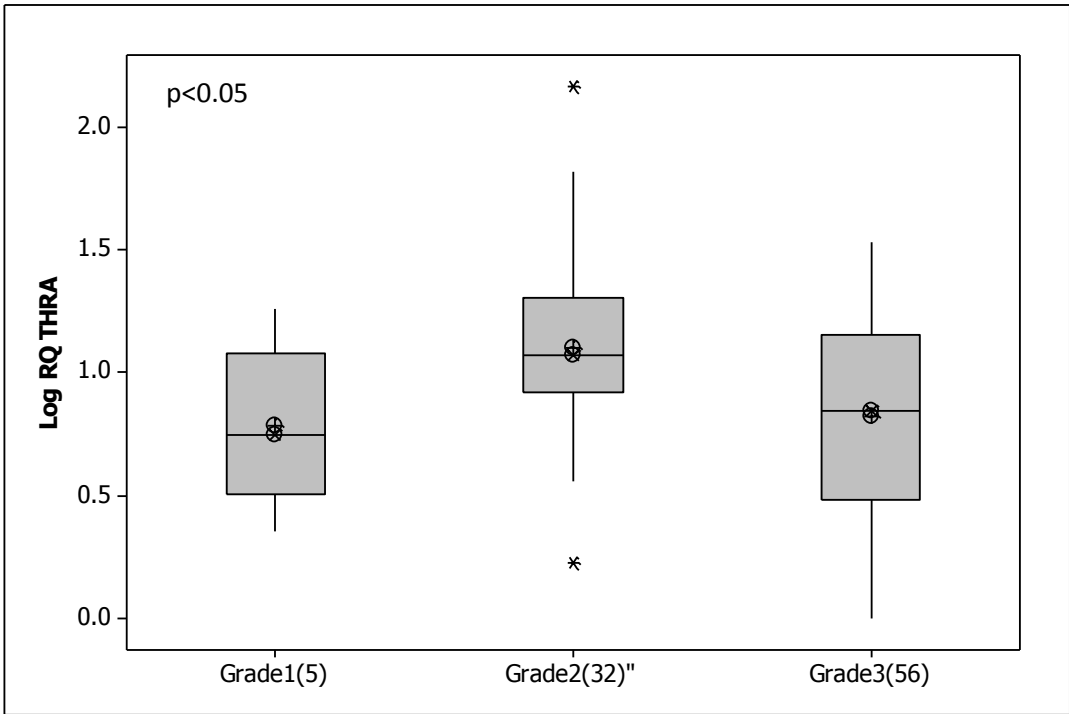

Figure 4.7 THRα gene expression across tumour grade (p<0.005). * Represents outliers.

THRα gene expression across the remainder of clinicopathological characteristics investigated, revealed no significant dysregulation relating to tumour stage (p=0.859) or menopausal status (p=0.679, results not shown).

4.5 Expression of miR-339-5p

The same RNA samples extracted from malignant (n=103), normal (n=30) and fibroadenoma (n=35) breast tissue biopsies were also analysed by RQ-PCR targeting miR-339-5p and miR-10a.

miR-339-5p was detectable in 102/103 malignant tissues, 34/35 fibroadenoma tissues and in all normal breast tissues. RQ-PCR of miR-339-5p revealed significantly greater expression in fibroadenoma tissues (n=34, 3.14(0.12) Log_{10} RQ) compared to normal breast tissue (n=30, 2.5(0.23) Log_{10} RQ, p<0.01). miR-339-5p expression was not significantly dysregulated in malignant breast tissues (n=102, 2.9(0.06) Log_{10} RQ, Figure 4.8) compared to healthy controls.

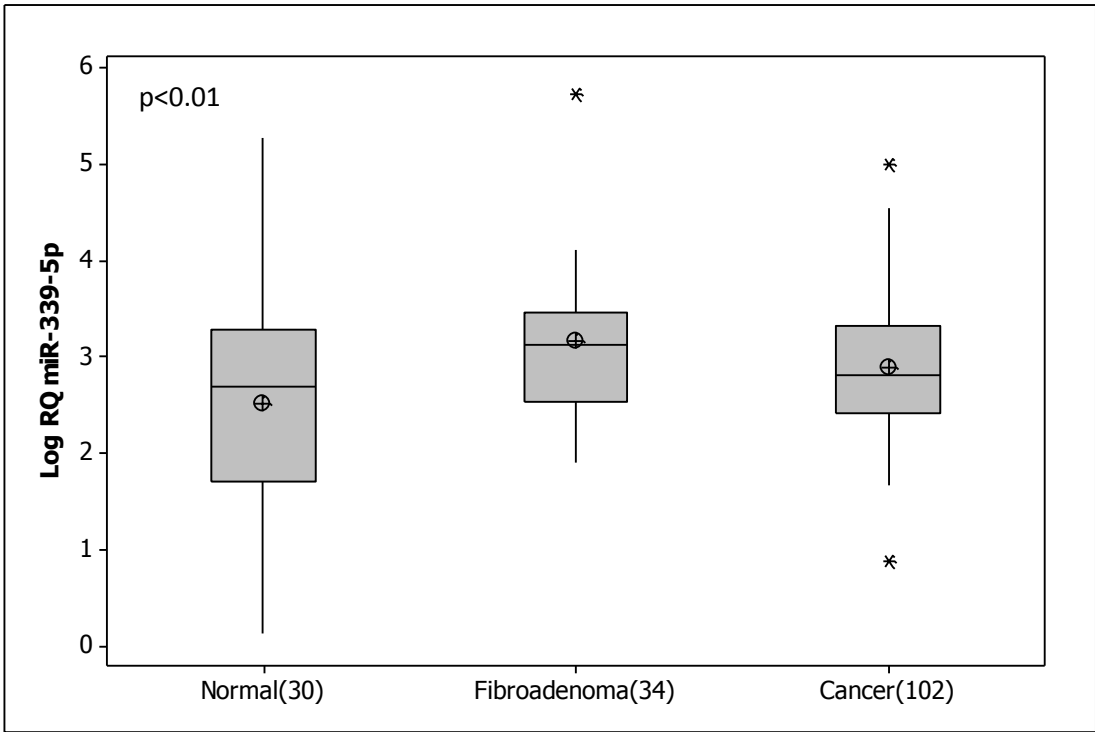

Figure 4.8 miR-339-5p expression across all breast tissue specimens. * Represents outliers.

Samples were then stratified based on patient clinicopathological details. miR-339-5p was stably expressed across tumour epithelial subtype (p=0.350, Figure 4.9).

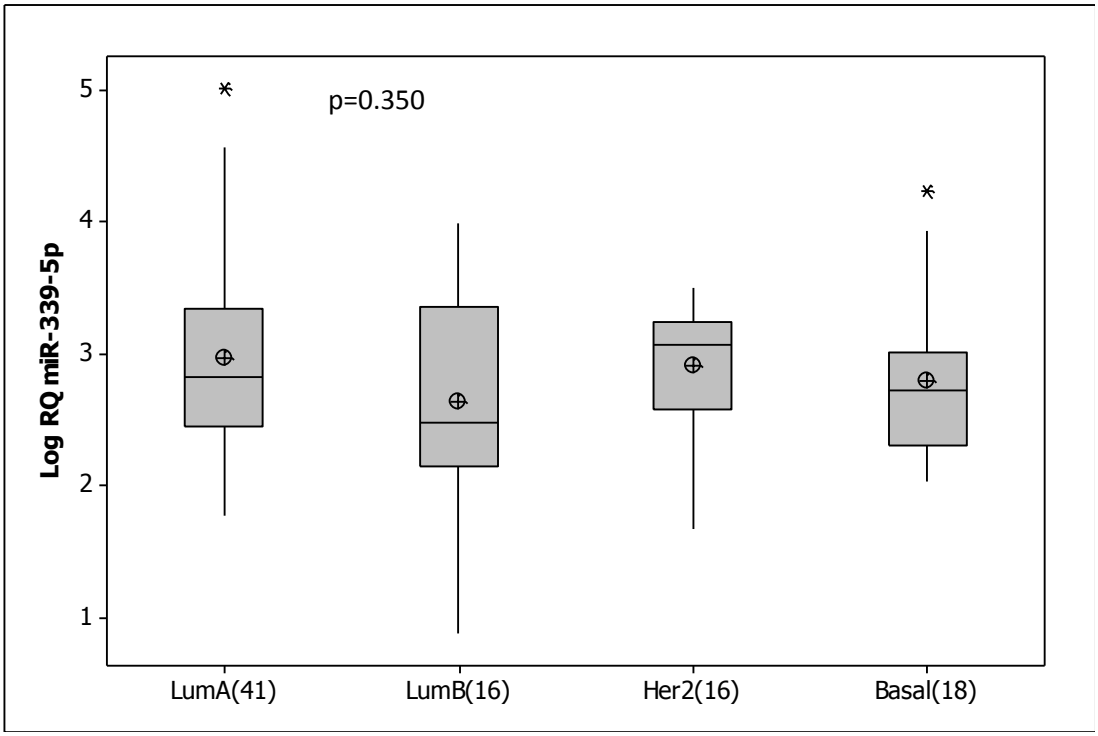

Figure 4.9 miR-339-5p Expression across Epithelial subtype. * Represents outliers.

miR-339-5p expression displayed no significant dysregulation across any of the patient clinicopathological details investigated, including tumour grade (p=0.971), tumour stage (p=0.399) and menopausal status (p=0.085, results not shown).

4.5.1 Investigation of relationship between miR-339-5p and NIS, RARβ and THRα

Investigate correlation of miR-339-5p with the RQ-PCR results obtained from NIS, RARβ and THRα gene expression. No significant relationship was observed between miR-339-5p and any of the potential target genes analysed (Table 4.2).

	miR-339-5p
NIS	r=0.08, p=0.427
RARβ	r=0.03, p=0.707
THRα	r=0.04,p=0.633

Table 4.2 Investigation of correlation between miR-339-5p and NIS, RARβ and THRα.

4.5.2 Endogenous levels of miR-339-5p in Breast Cancer Cell Lines

Expression of miR-339-5p was quantified in a range of breast cancer cell lines by RQ-PCR, relative to average endogenous controls miR-16 and Let-7a. This was carried out to determine the cell line with the lowest expression of miR-339-5p for cell transfections. Native miR-339-5p expression was detectable in all breast cancer cell lines. The lowest expression was observed in the non-tumourigenic MCF-10-2A cell line (Figure 4.10).

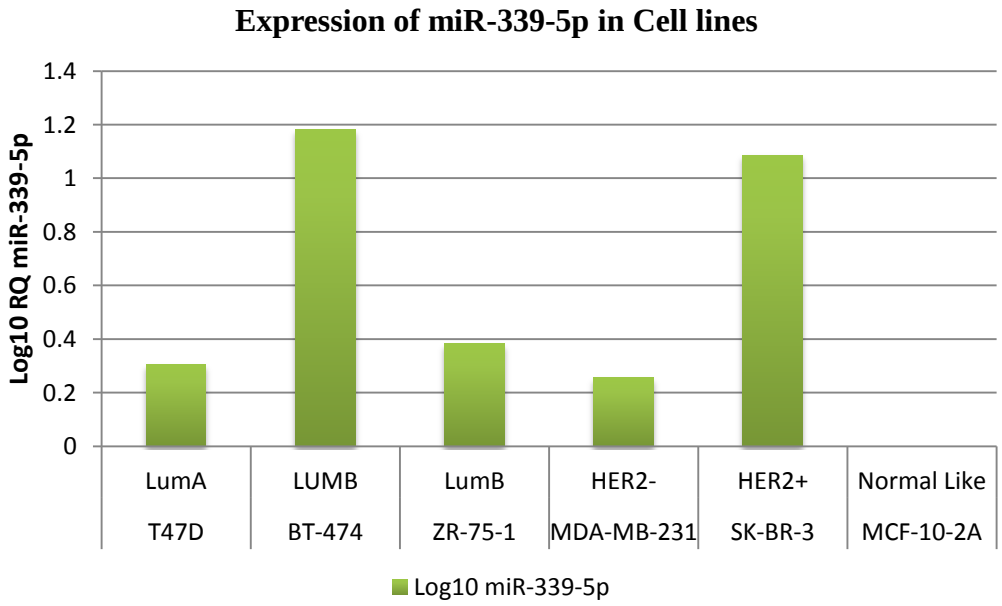

Figure 4.10 miR-339-5p expression across a range of breast cancer cell lines.

4.5.3 Effect of a miR-339-5p mimic on breast cancer cell proliferation

Prior to analysis of the effect of a miR-339-5p mimic on breast cancer cell proliferation, over-expression following transfection was confirmed by RQ-PCR. Increased expression was observed in the cells transfected with miR-339-5p mimic compared to those transfected with an NTC-mimic. This was observed in both T47D (+4 $\log_{10}$ RQ) and SK-BR-3 cells (+4.8 $\log_{10}$ RQ) (Figure 4.11).

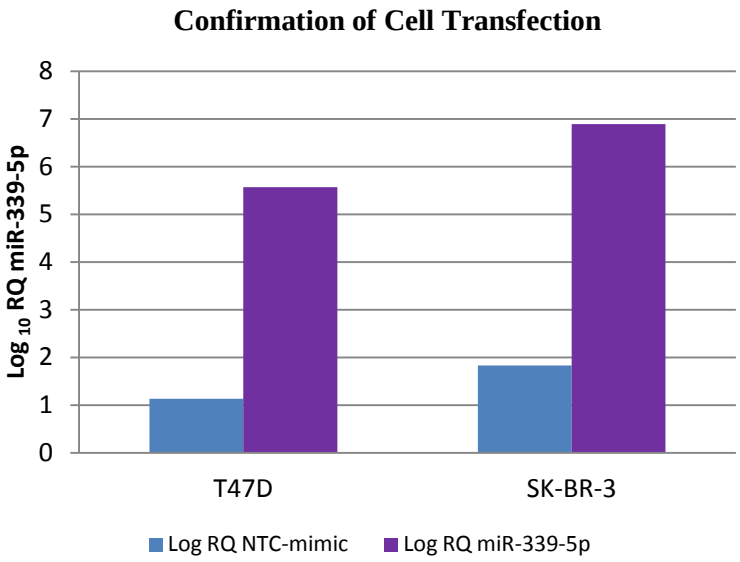

Figure 4.11 Confirmation of miR-339-5p over-expression in both T47D and SK-BR-3 cell lines following transfection.

The CellTiter 96® AQ_{ueous} Non-Radioactive Cell proliferation Assay (Promega) was used to determine cell proliferation 48 hours following transfection of T47D and SK-BR-3 cells. An inhibition of cellular proliferation was observed (-17% for T47D and -26 % inhibition for SK-BR-3 cells) in cells over-expressing miR-339-5p mimic compared to those transfected with a NTC mimic ($p<0.05$ Figure 4.12).

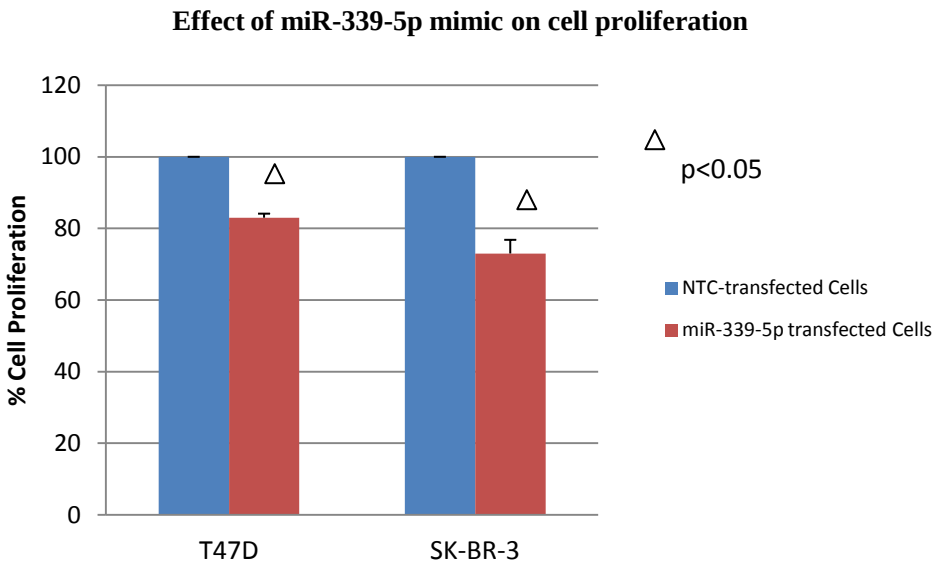

Figure 4.12 Proliferation Assay following transfection of breast cancer cell lines with a miR-339-5p-mimic or NTC controls.

4.5.4 Circulating miR-339-5p

The circulating level of miR-339-5p was quantified in microRNA extracted from whole blood of 51 breast cancer patients and 37 healthy controls (Table 4.3).

Patient Clinicopathological details	**Cancer**	**Controls**
Number of patients	51	37
Median Patient Age yrs	57.8	50.4
Menopausal Status		
Post	29	
Pre	22	
Histological Subtype		
Invasive Ductal	39	
Invasive Lobular	5	
Other	*7*	
Intrinsic Subtype		
Luminal A (ER/PR+, HER2/neu-)	18	
Luminal B (ER/PR+, HER2/neu+)	4	
HER2 Over expressing (ER-, PR-, HER2/neu+)	3	
Triple-Negative (ER-, PR-, HER2/neu-)	26	
Tumour Grade		
1	2	
2	21	
3	8	
Tumour size		
T1	19	
T2	20	
T3	3	
UICC Stage		
Stage 1	27	
Stage 2	21	
Stage 3	3	
Stage 4	0	

Table 4.3 Patient Clinicopathological details of patients from whom whole bloods were collected.

Expression of miR-339-5p was detectable in the circulation of all breast cancer patients and healthy controls. However, no significant difference was observed between circulating miR-339-5p in breast cancer patients (n=51, 1.49(0.06) Log_{10} RQ) and healthy controls (n=37, 1.59(0.07) Log_{10} RQ, p=0.41, Figure 4.13).

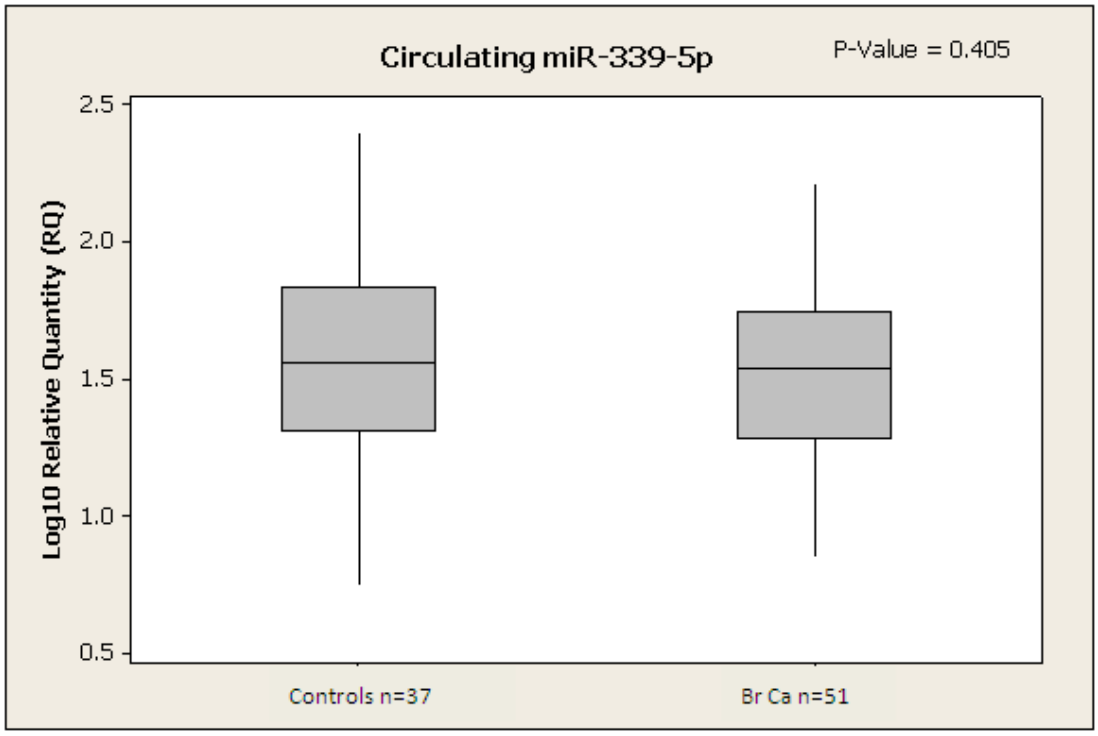

Figure 4.13 Circulating miR-339-5p expression in breast cancer patients and healthy controls.

4.6 Expression of miR-10a

MicroRNA extracted from malignant (n=103), normal (n=30) and fibroadenoma (n=35) breast tissue biopsies was analysed by RQ-PCR (Table 6.1). miR-10a expression was detectable in all breast tissue samples. With levels significantly decreased in breast cancer tissues (n=102, 2.3(0.08) Log_{10} RQ) compared to both normal (n=30, 3.1(0.17) Log_{10} RQ, $p<0.001$) and fibroadenoma tissue (n=35, 2.9(0.15) Log_{10} RQ, $p<0.001$, Figure 4.14).

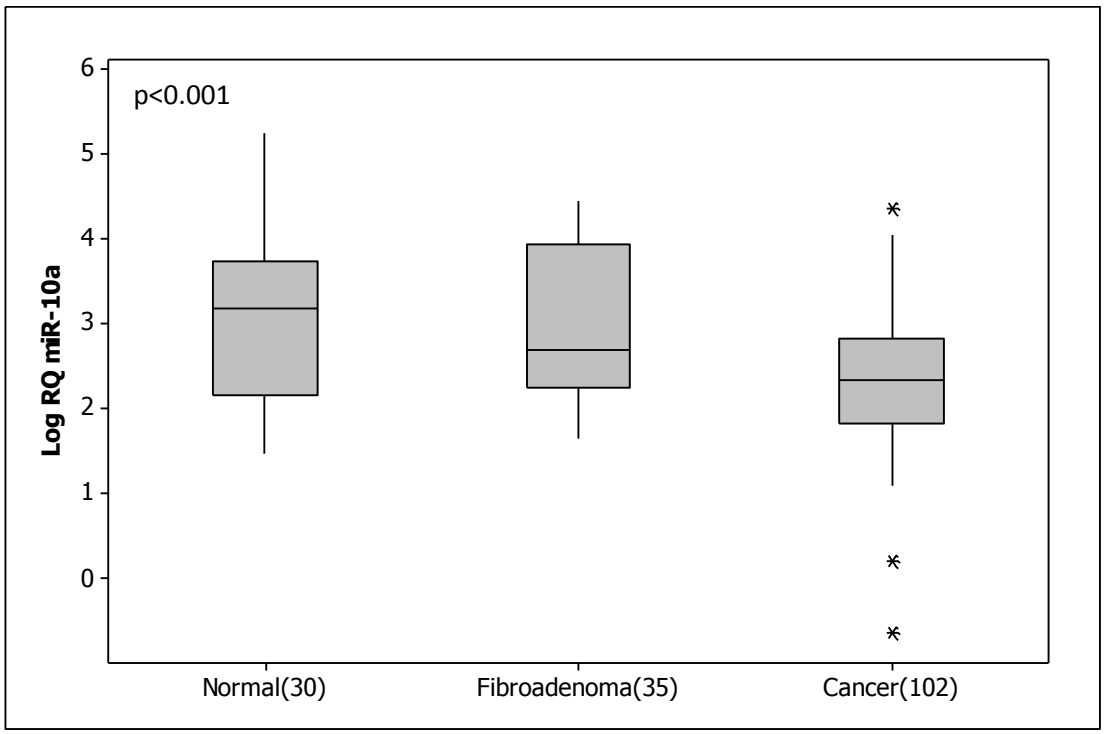

Figure 4.14 miR-10a expression across all breast tissue types. * Represents outliers.

miR-10a expression was further stratified based on patient clinicopathological details. Expression of miR-10a was not dysregulated across epithelial subtype (p=0.168, Figure 4.15).

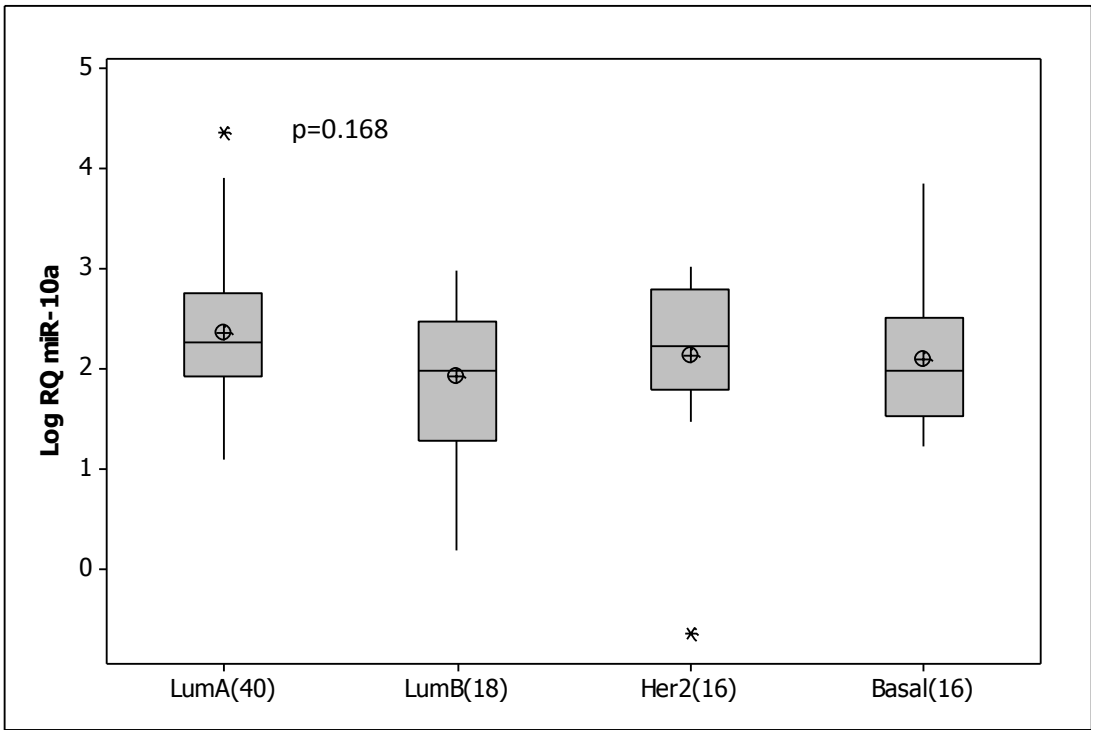

Figure 4.15 miR-10a expression across epithelial subtype. * Represents outliers.

Further analysis of the clinicopathological details revealed no significant deregulation across tumour grade (p=0.299), tumour stage (p=0.340) and menopausal status (p=0.126, results not shown).

4.6.2 Investigation of relationship between miR-10a and NIS, RARβ and THRα gene expression

Investigation of potential correlation of miR-10a with results obtained from target gene expression. miR-10a expression showed no significant relationship with NIS gene expression (r=0.14, p=0.15, results not shown). However a significant positive correlation with RARβ gene expression was observed (r=0.31, p<0.001, Figure 4.16).

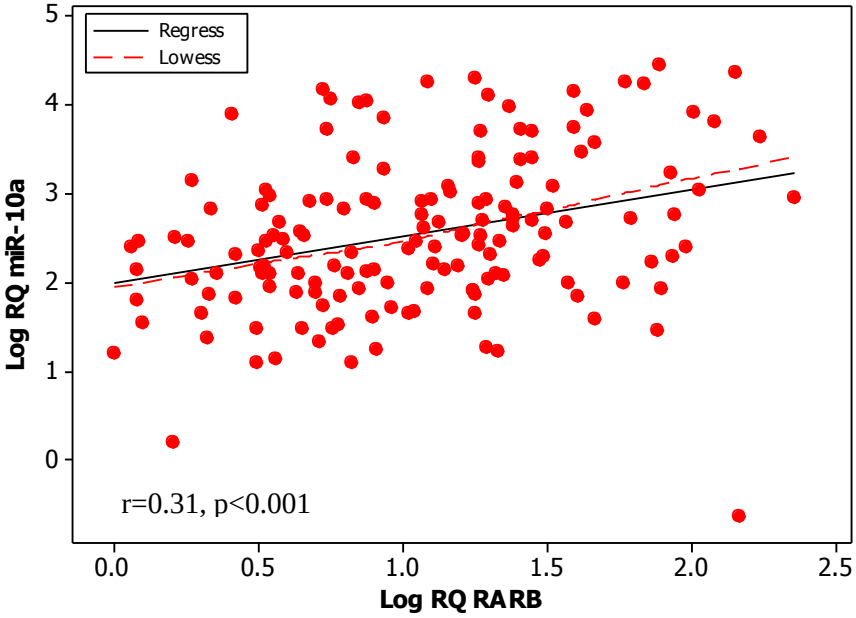

Figure 4.16 Investigation of a correlation between miR-10a and RARβ gene expression.

miR-10a expression also revealed a robust positive correlation with THRα gene expression (r=0.32, p<0.001, Figure 4.17).

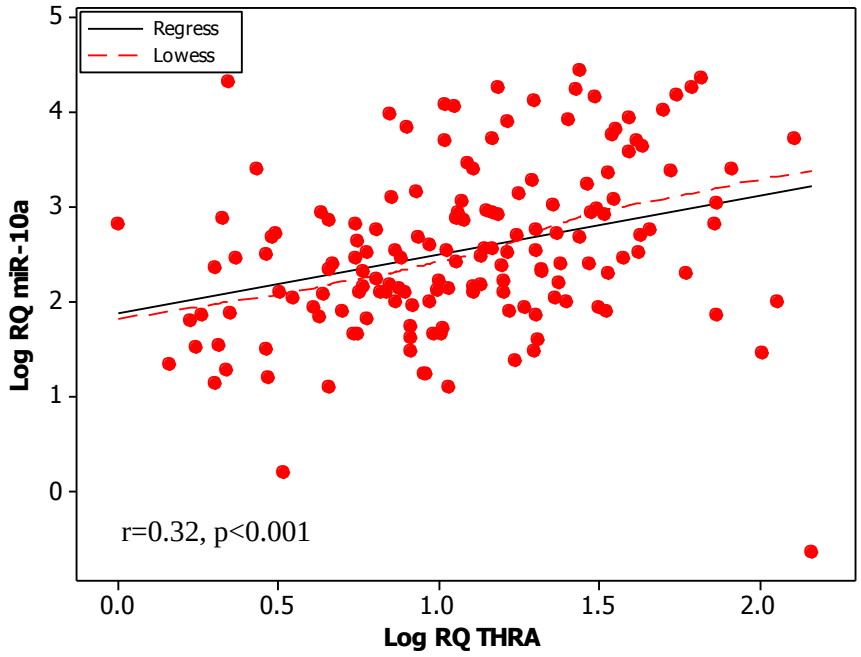

Figure 4.17 Investigation of a correlation between miR-10a expression and THRα gene expression.

4.6.2 Endogenous expression levels of miR-10a in Breast Cancer cell lines

Expression of miR-10a was detectable in a range of breast cancer cell lines by RQ-PCR relative to average endogenous controls miR-16 and Let-7a. Lowest expression was observed in the ZR-75-1 cells (Figure 4.18).

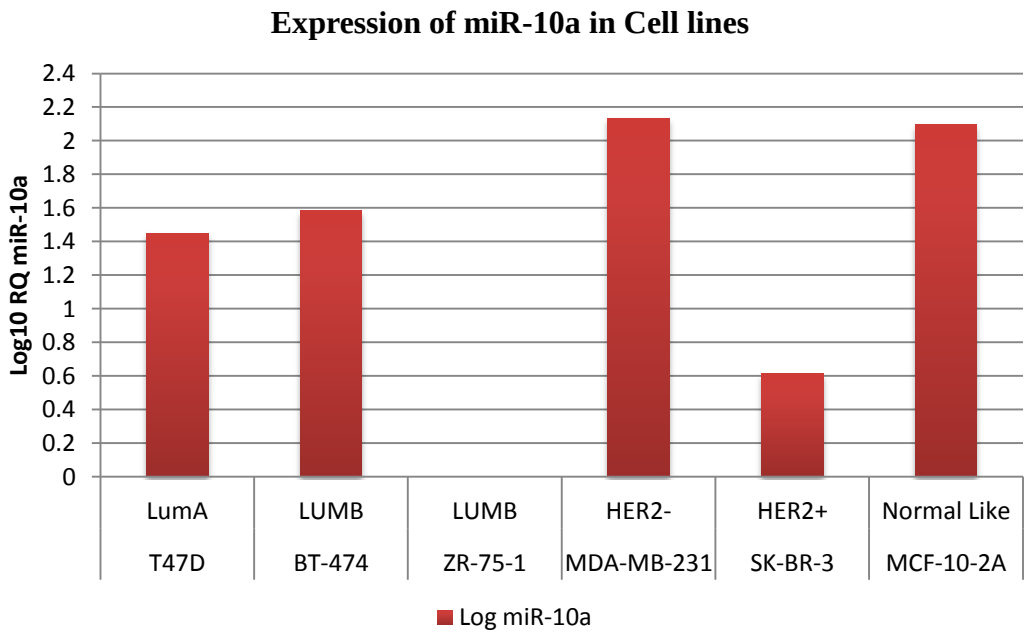

Figure 4.18 miR-10a expression in breast cancer cell lines.

4.6.3 Effect of a miR-10a mimic on breast cancer cell proliferation

T47D and SK-BR-3 cells were transfected with a miR-10a mimic or a NTC-mimic. Increased miR-10a expression was confirmed in both T47D (+4.5 $\log_{10}$ RQ) and SK-BR-3 cells (+4.0 $\log_{10}$ RQ), relative to cells transfected with an NTC mimic (Figure 4.19).

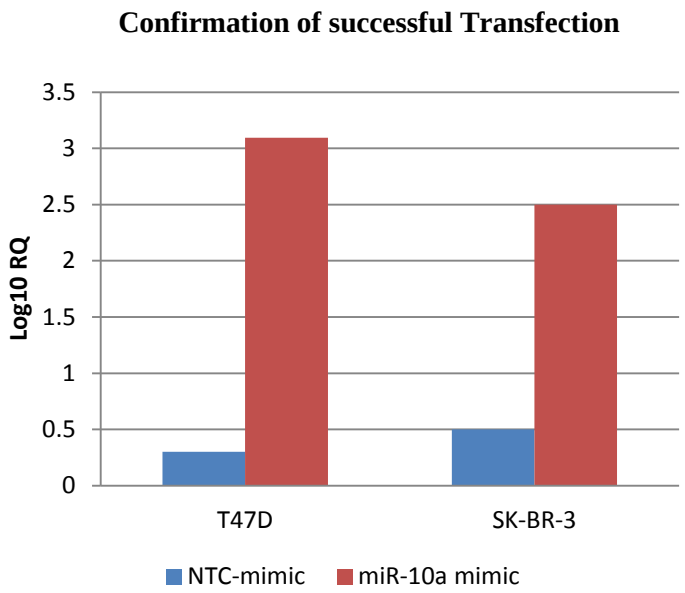

Figure 4.19 Elevated miR-10a expression following transfection of T47D and SK-BR-3 cells.

Investigation of the effect on cellular proliferation revealed no significant change in proliferation in both T47D and SK-BR-3 cells after transfection (results not shown).

4.6.4 Circulating miR-10a

The circulating level of miR-10a was quantified in whole blood of 51 breast cancer patients and 37 healthy controls, with full clinicopathological details collected (Table 4.3). miR-10a expression was detectable in the circulation of all patients. No significant difference was observed for miR-10a expression between breast cancer patients (n=51, 1.7(0.05) Log_{10} RQ) and healthy controls (n=37, 1.81(0.05) Log_{10} RQ, p=0.34, Figure 4.20)

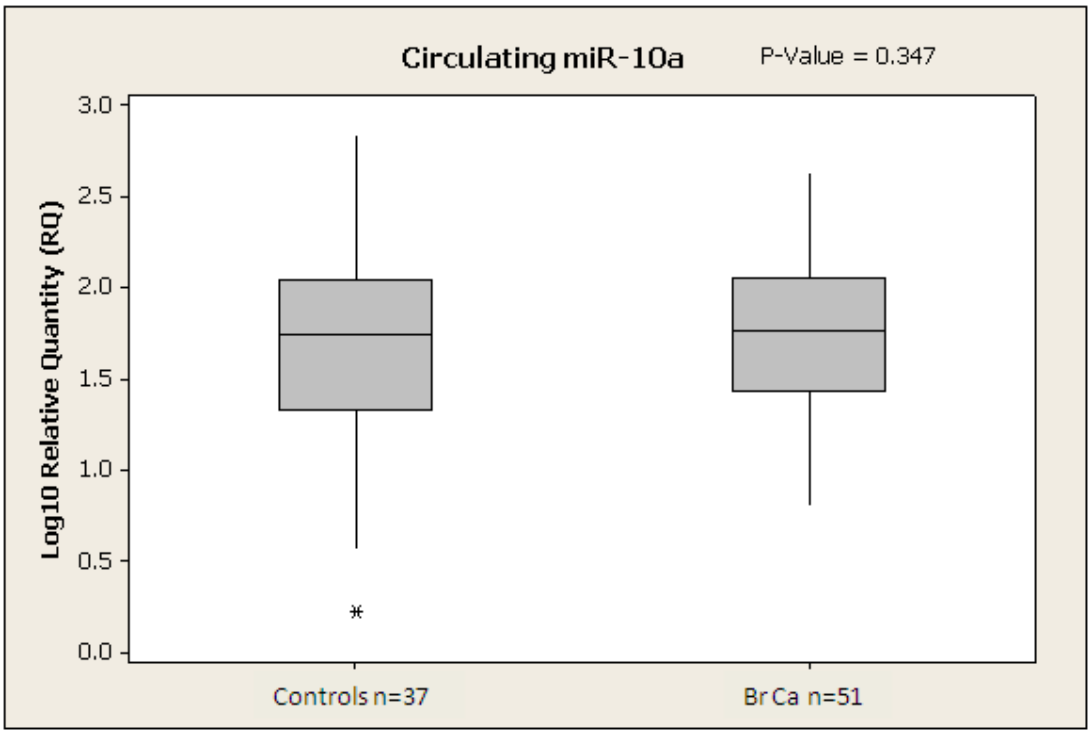

Figure 4.20 miR-10a expression in the circulation. * Represents outliers.

4.7 Discussion

In the present study NIS gene expression was quantified by RQ-PCR in patient breast tissues and was found to be expressed in 80% [82/102] of the tumour samples analysed. This is in agreement with previous reports [131, 206-208]. Tazebay et al [131] used immunohistochemistry to detect NIS expression in malignant breast tissues (n=29) compared to normal breast tissues (n=8). 80% of breast cancer samples expressed NIS while no expression was observed in the normal tissues. In the present study, the highest level of expression was observed in the fibroadenoma tissues (n=35) compared to both normal (n=30) and malignant samples (n=103). This increased expression of the NIS gene in fibroadenoma tissues has previously been published [136, 138, 219]. The first report of elevated NIS levels in fibroadenoma tissues was reported by Berger et al [219], this study reported radioiodine accumulation in a lesion of the right breast of a patient with papillary thyroid carcinoma. This lesion was subsequently identified as a fibroadenoma. Ryan et al [138] quantified NIS gene expression by RQ-PCR in 10 fibroadenoma tissues and found the highest levels of NIS in fibroadenoma tissues compared to 75 malignant tissues and 15 normal breast tissues. Expression of NIS in breast cancer is therefore not a suitable marker of malignancy. The NIS gene in the normal cohort was detectable in only 9 out 30 tissues analysed. Some isolated normal tissues displayed increased NIS gene expression. NIS gene expression is widely known to be absent in non-lactating normal breast tissue.

RA is a known regulator of NIS in breast cancer [142]. The effect of RA and its receptors has previously been investigated in breast cancer cell lines, animal models and in breast tissue cohorts [138, 139, 220, 221]. These study revealed increased induction of NIS in breast cancer cells following exposure to RA in vitro and in vivo. A receptor of RA, RARβ has been shown to positively correlate with NIS expression in patient clinical specimens [138]. Kogai et al [222] revealed both RA receptors RARβ and RXR to induce NIS expression in MCF7 cells.
RARβ was quantified in the present study and was found to have decreased expression in breast cancer tissues compared to normal and fibroadenoma tissues further highlighting a tumour suppressor role in breast cancer. This reduced expression was previously observed in neoplastic malignancies including non-small

cell lung cancer, squamous cell carcinoma of the head and neck and in breast cancer [215, 223-225].

THRα in combination with THRβ have previously been linked to breast cancer as putative regulators of NIS gene expression [138]. Loss of THRα has been previously revealed by a study using semi-quantitative analysis of THRα and THRβ in 70 breast cancer tissues [226]. In the present study, THRα gene expression was down-regulated in breast cancer compared to healthy controls and was found to have an association with tumour grade. This loss of THRα in breast cancer suggests a tumour suppressor role in breast cancer. The observed positive correlation between miR-10a and THRα gene expression strengthens the hypothesis of miR-10a as a tumour suppressor in breast cancer.

Expression of miR-339-5p was investigated by Wu et al [120], it was quantified by RQ-PCR in 25 malignant breast tissues compared to 9 benign breast disease tissues. This report revealed elevated expression in the benign tissues compared to the malignant breast tissues. In the current study, elevated expression of miR-339-5p was also reported in the benign cohort (n=35) compared to the malignant samples (n=103) and normal tissues (n=30). The paper by Wu et al [120] also investigated the native miR-339-5p expression in three cell lines, it reported decreased expression in MDA-MB-231 and MDA-MB-468 cells compared to MCF-7 cells [120]. In the current study, endogenous expression of miR-339-5p was investigated across a range of breast cancer cell lines. The overall expression observed of miR-339-5p was relatively low in all cell lines, with the lowest expression observed in the non-tumourigenic MCF-10-2A cell line. Wu et al [120] did not to include any normal-like cell lines in their analysis. It is necessary to note that in the present study, miR-339-5p expression was determined in one representative normal-like cell line, therefore additional analysis should be carried out on a wider range of breast and normal-like cell lines in order to make a definitive statement regarding the endogenous miR-339-5p expression in vitro.

Over-expression of miR-339-5p in both T47D and SK-BR-3 cells resulted in reduced cellular proliferation. This could be attributed to the fact that miR-339-5p has a putative binding site on the key proliferation marker Ki-67, it would be worth to further assess this potential binding in future studies.

Circulatory miR-339-5p levels were analysed in whole bloods collected from breast

cancer patients and healthy controls, no significant difference was observed between the two groups.

miR-10a together with its family member miR-10b belongs to a conserved group of miRNAs that differ by one nucleotide in the centre and are situated within the HOXD gene clusters [108]. miR-10a has been previously shown to be down-regulated in metastatic mouse mammary tissue [113]. There is still very little known about its role in breast cancer. Most recently, elevated expression of miR-10a in conjunction with miR-126 were identified to predict prolonged relapse-free time of primary oestrogen receptor-positive breast cancer following Tamoxifen treatment [114]. In the present study miR-10a was found to have reduced expression in breast cancer, suggesting a tumour suppressor role. No associations with patient clinicopathological details were observed. Correlation analysis with the target genes analysed revealed a significant positive correlation between miR-10a and RARβ and THRα. This positive correlation rules out any direct regulatory function of miR-10a for RARβ or THRα. However it further strengthens the hypothesis of miR-10a's role as a tumour suppressor in breast cancer. This positive correlation with both RARβ and THRα is potentially very interesting in terms of a stimulatory effect on miR-10a, as RA has previously been shown to stimulate miR-10a expression [216]. This is further validated by the fact that dimerization between RARβ and THRα is known to occur [147, 148]. Circulating levels of miR-10a were detectable in all samples analysed, however no significant deregulation was observed between breast cancer patients and healthy controls.

Overall miR-10a was highlighted in this study to have a potential role as a tumour suppressor in breast cancer and this may be stimulated by gene expression of both RARβ and THRα in breast cancer.

Chapter 5
MicroRNA-379 regulates Cyclin B1 expression and is decreased in Breast Cancer

5.1 Introduction

The miRNA of interest in this study, miR-379, is located on chromosome 14q32.31 and to date, very little is known about its role in normal physiology. In the context of breast cancer, there is currently one report implicating miR-379 in the regulation of interleukin-11 (IL-11) production in metastatic breast cancer cell lines [121]. miR-379 has a predicted binding site on a key gene associated with breast cancer, Cyclin B1, which is known to be up-regulated and associated with poor patient outcome [227-230]. The Cyclin B1 3' UTR region is 612bp in length, with computational algorithms predicting a binding site for miR-379 starting at position 404 [62, 195, 231].

Cyclin B1 is a key initiator of mitosis. It has a crucial role in regulating Cyclin-dependent kinase 1 (Cdk1), which initiates the progression from G2 phase to mitosis [232]. Over-expression of Cyclin B1 is associated with a number of different cancers including breast cancer [227, 230, 233], oesophageal squamous cell cancer [234, 235], non-small cell lung cancer [236, 237] and renal cancer [238]. Further, over-expression of Cyclin B1 is associated with poor patient survival and increased resistance to radiotherapy in head and neck squamous cell carcinoma [239, 240]. Researchers are investigating the potential of depleting Cyclin B1 expression in tumours as a therapeutic strategy, by initiating anti-proliferative and apoptosis-inducing properties [241, 242]. Understanding miRNA mediated regulation of Cyclin B1 is therefore an exciting avenue of investigation.

5.2 Aim

- Relative quantification of miR-379 expression in clinical samples which included tissues from breast cancer patients (n=103), healthy controls (n=30) and patients with benign breast disease (n=35).
- Investigation of any relationship with patient clinicopathological details.
- Quantify Cyclin B1 gene expression in a subset of samples and any association with miR-379 expression examined.
- Investigations of the effect of a miR-379 mimic on Cyclin B1 protein expression and function in vitro.
- Determine Relative levels of circulating miR-379 in patients with breast cancer (n=40) and healthy controls (n=34).

- Investigate the impact of miR-379 in terms of tumour establishment, growth and metastasis in an in vivo model.

5.3 Materials and Methods

Breast tissue specimens (n=168), comprised of 103 malignant tissue biopsies, 30 normal mammary tissue biopsies, and 35 fibroadenoma tissues. Full patient demographics and clinicopathological details were collected and maintained prospectively (Table 4.1). Whole blood samples (n=88) were also collected from 51 breast cancer patients pre-operatively and 37 healthy controls with no family history of the disease (Table 4.2).

miR-379 expression was quantified in all breast tissues and whole bloods collected. Gene expression analysis for Cyclin B1 was carried out on a subset of breast tissues n=84.

T47D cells were transfected with a miR-379-5p mimic (mature sequence: UGGUAGACUAUGGAACGUAGG; 50nM) or a non-specific control miRNA (non-target control (NTC)) mimic. Transfections were performed using Lipofectamine™ 2000 according to manufacturer's instructions. Cell proliferation was assessed 48 hours following transfection with a miR-379 mimic and a NTC-mimic.

Cell proliferation was measured using CellTiter 96® AQ_{ueous} Non-Radioactive Cell proliferation Assay. Western blot analysis and Immunohistochemistry of Cyclin B1 protein expression were also carried out following transfection.

An in vivo mouse model was established using (n=10) athymic nude mice. The mice were supplemented with a 17 β-estradiol pellet to support the tumour growth of T47D cells. T47D cells were stably transfected with miR-379 and a NTC control using lentiviral transduction. Two groups were set up with n=5 in each group. Group 1 received $T47^{379\ mimic}$ and group 2 received $T47D^{NTC\ mimic}$. Nine weeks following tumour induction animals were sacrificed and blood and tumours were collected. The samples were then analysed by RQ-PCR for expression of miR-379.

5.4 miR-379 expression in human breast tissues

miR-379 was detected in 100 out of 103 breast tumours samples, and was detectable in both normal and fibroadenoma tissue. Results were expressed as Log_{10} Relative Quantity (RQ). RQ-PCR of mature miR-379 in these samples revealed a significant decrease in expression in breast tumour samples (Mean(SEM) 1.9(0.09)Log_{10} Relative Quantity) compared to normal tissue n=30 (2.6(0.16) Log_{10} RQ, $p<0.01$, Figure 5.1).

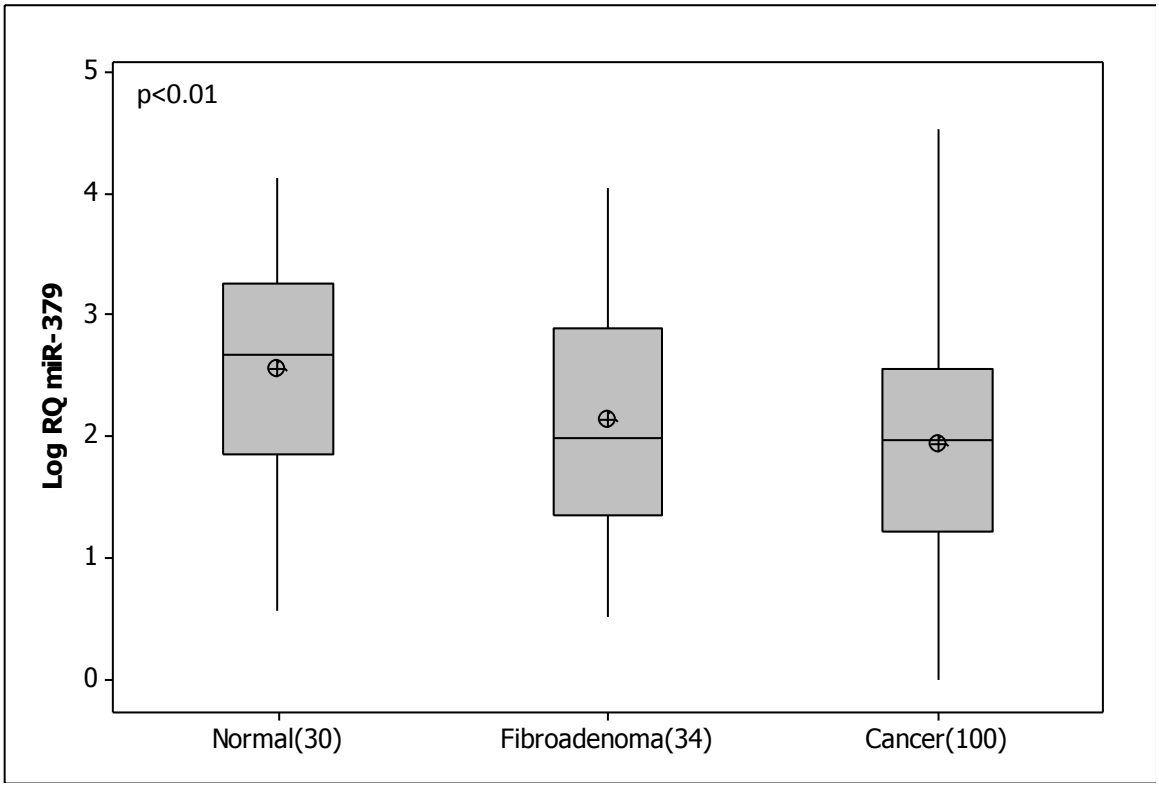

Figure 5.1 miR-379 expression in normal, fibroadenoma and malignant breast tissues.

Samples were then stratified based on patient clinicopathological details (Table 5.1). miR-379 expression was found to show a relationship with tumour stage, with increasing tumour stage (from Stage 1 to Stage 3), the level of miR-379 decreased significantly ($p<0.05$, Figure 5.2A). A similar trend was observed for tumour grade however this did not reach significance (Figure 5.2B). There was no association between miR-379 with other clinicopathological parameters, including histological

subtype (p=0.329), tumour size (p=0.243), menstrual status (p=0.486) or epithelial subtype (p=0.965, results not shown).

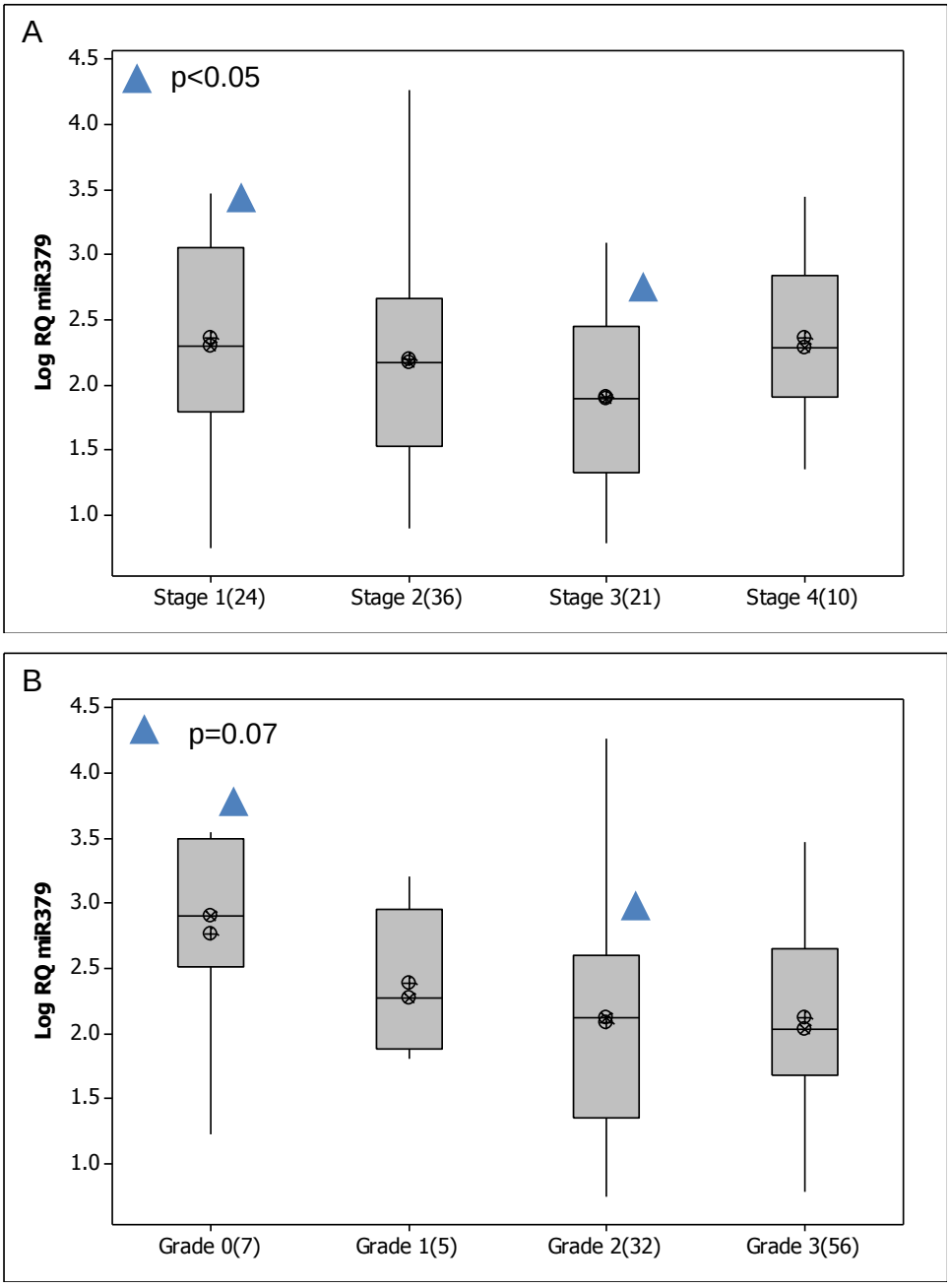

Figure 5.2 miR-379 expression across tumour stage and grade. (A) miR-379 expression across tumour stage. (B) Level of miR-379 across tumour grade.

5.5 Cyclin B1 expression in human breast tissues

Cyclin B1 expression was also quantified across a subset of 84 breast tissue specimens, selected based on tissue RNA availability. Expression levels of Cyclin

B1 were significantly elevated in breast cancer (n=40, 2.52(0.10) Log_{10} RQ) compared to fibroadenoma (n=23, 2.15(0.11) Log_{10} RQ, $p<0.05$) and normal breast tissue (n=21, 1.78(0.10) Log_{10} RQ, $p<0.001$, Figure 5.3).

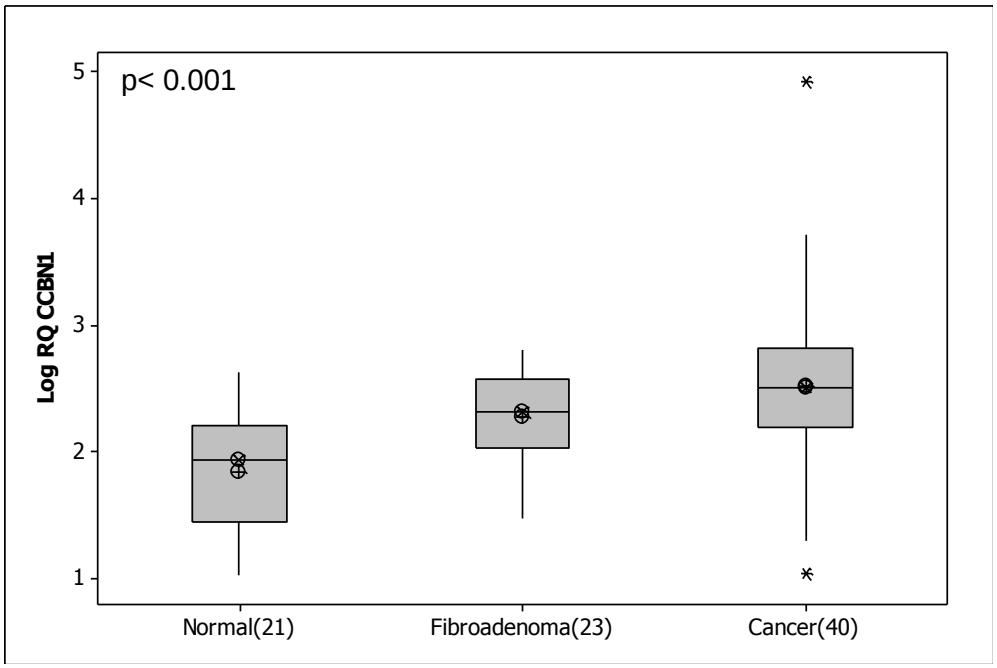

Figure 5.3 Cyclin B1 expression in normal, fibroadenoma and malignant breast tissues.

Any relationship between Cyclin B1 and miR-379 was then investigated. A significant negative correlation was observed between Cyclin B1 and miR-379 ($r= -0.31$, $p<0.002$, Figure 5.4).

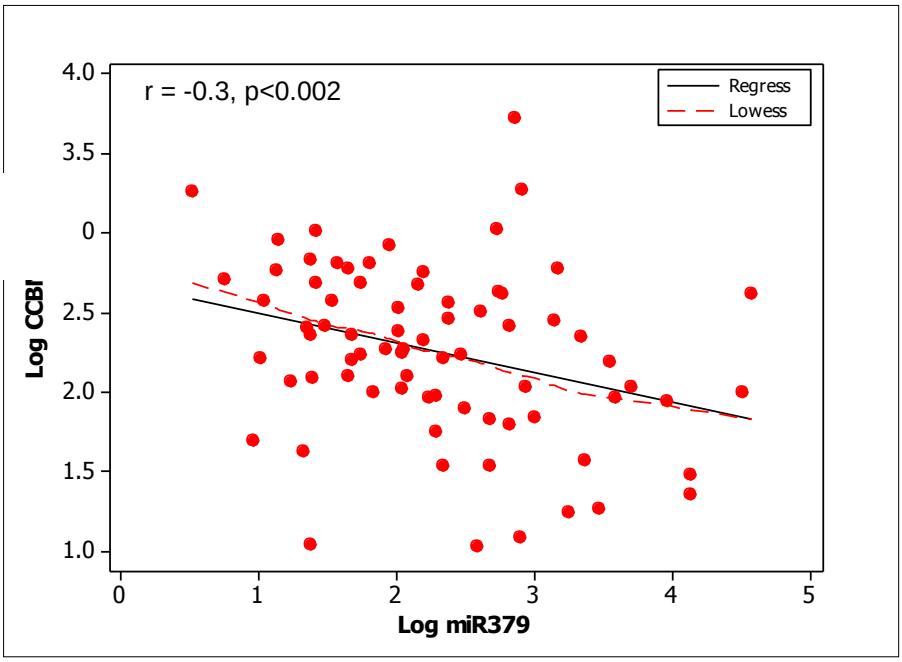

Figure 5.4 Investigate correlation of miR-379 with Cyclin B1.

5.6 miR-379 Effect on Cell Proliferation

T47D cells were transfected with miR-379 and NTC- mimic as described, and the change in miR-379 expression quantified by RQ-PCR (Figure 5.5). A significant elevation in miR-379 (5.76 $\log_{10}$ RQ relative to T47D cells transfected with NTC mimic) was confirmed (Figure 5.5A) prior to analysis of cell proliferation or Cyclin B1 protein expression. The CellTiter 96® AQ_{ueous} Non-Radioactive Cell proliferation Assay (Promega) was used to determine cell proliferation 48hrs following transfection with miR-379 in T47D cells. An inhibition of cell proliferation was observed (7-24 % inhibition, $p<0.05$, Figure 5.5B) in cells transfected with miR-379 compared to those transfected with NTC-mimic.

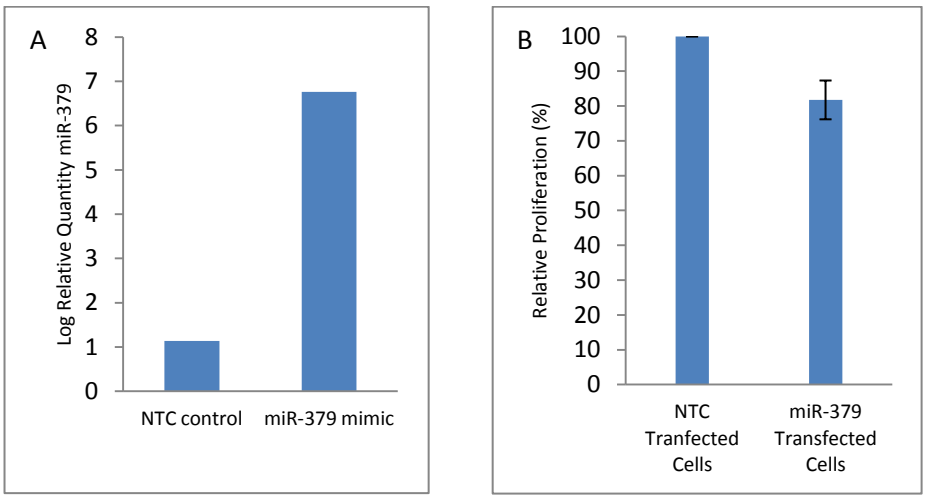

Figure 5.5 Transfection of T47D cells with miR-379 or a NTC mimic. (A) Confirmation of elevated miR-379 expression 48 hours following transfection with miR-379 mimic. (B) Quantify cell proliferation following transfection.

5.7 Cyclin B1 protein expression in cells transfected with miR-379

To confirm the effect of miR-379 on Cyclin B1 expression in T47D cells, cells were transfected with a miR-379 or an NTC mimic. Cells were fixed and protein was extracted for analysis by immunohistochemistry (IHC) (Figure 5.6A) and western blot (Figure 5.6 B). The negative control wells which did not receive an antibody, showed no staining (Figure 5.6 A(i),(ii)). Robust native Cyclin B1 expression was detected in cells that had been transfected with a NTC-mimic (Figure 5.6 A(iii),(iv)). A significant reduction in Cyclin B1 staining was observed in cells transfected with a miR-379 mimic (Figure 5.6 A(v),(vi)).

This change in Cyclin B1 expression was confirmed by western blot. Cyclin B1 was detected at the expected size of ~58kDa, with β-actin (loading control) detected at ~47kDa (Figure 5.6B). The level of immunoreactivity detected in miR-379 transfected cells was weaker than that observed when cells were transfected with the NTC mimic, with relative densitometry analysis revealing a >40% decrease in Cyclin B1 protein.

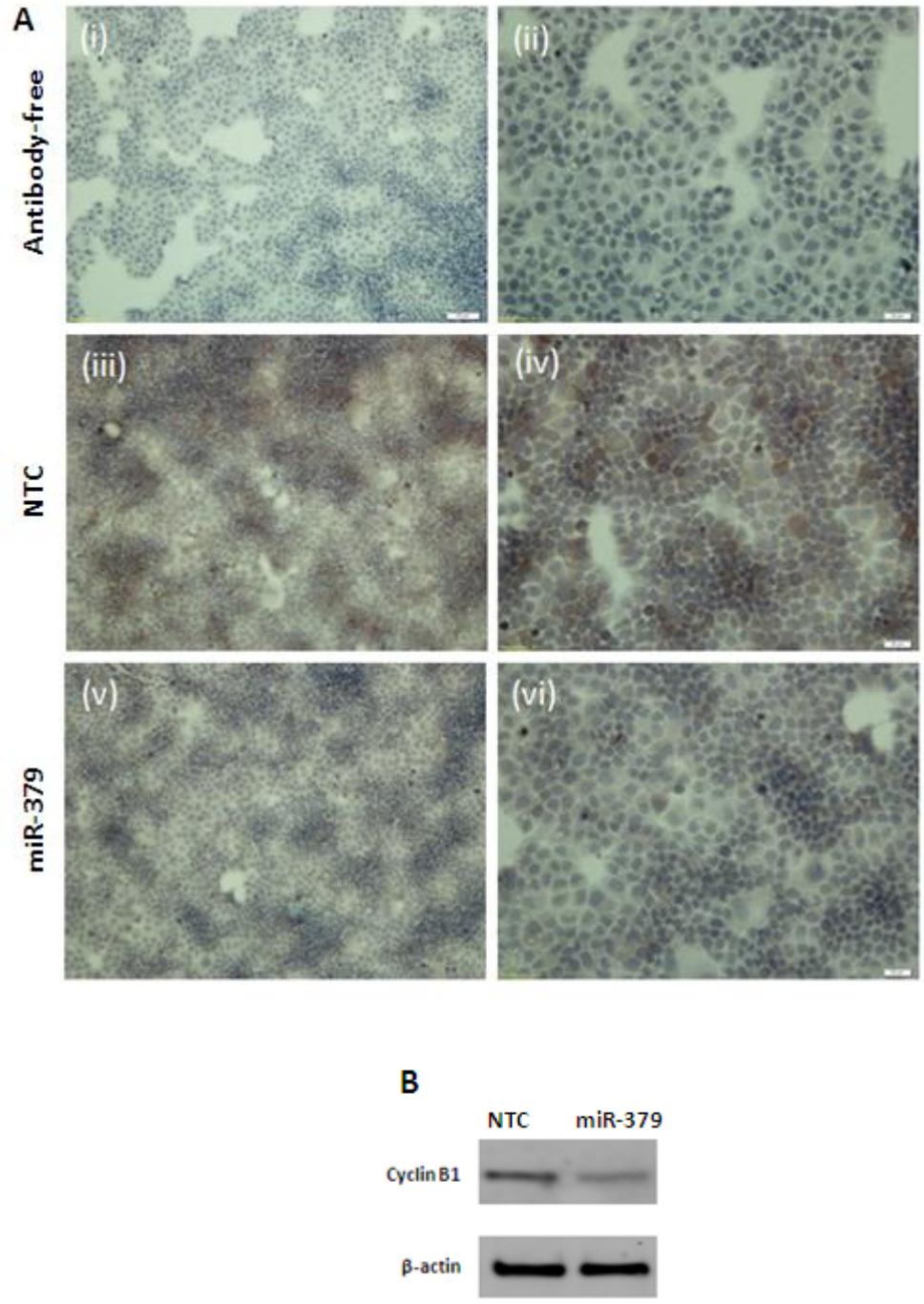

Figure 5.6 Analysis of Cyclin B1 protein expression following transfection of T47D cells with miR-379 by (A) IHC and (B) Western blot. (A) (i,ii) antibody-free, (iii,iv) Cells transfected with NTC mimic, (v,vi) Cells transfected with miR-379 and (B) Western blot analysis of Cyclin B1 relative to β-Actin.

5.8 Circulating miR-379

The circulating level of miR-379 was quantified in whole blood of 51 breast cancer patients and 37 healthy controls. No significant difference was observed between circulating miR-379 in breast cancer patients (0.95(0.07) Log_{10} RQ) and healthy controls (1.03(0.05) Log_{10} RQ, p=0.42, Figure 5.7).

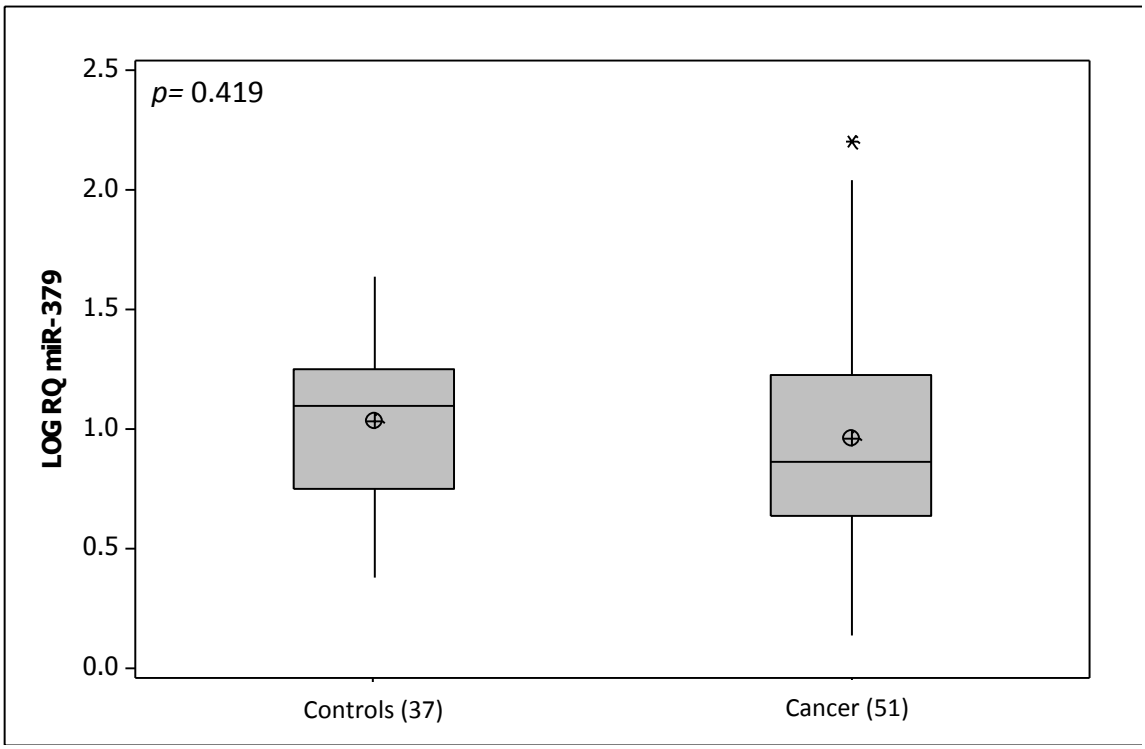

Figure 5.7 Circulating miR-379 expression across breast cancer patients and controls.

5.9 Generation of a stably transduced T47D cell line

5.9.1 Optimisation of Cell seeding density and transduction conditions

The T47D cells were seeded at three different seeding densities ($5x10^3$, $7.5x10^3$ and $10x10^3$ cells/ well) in a 96-well plate. The optimal seeding density was $7.5x10^3$ cells/ well as it provided approximately 40% confluence on the day of transduction. The optimal Polybrene concentration which was used to aid transduction efficiency was determined at 2µg/ml, as increasing the concentration any further caused significant loss in cell viability (Figure 5.8).

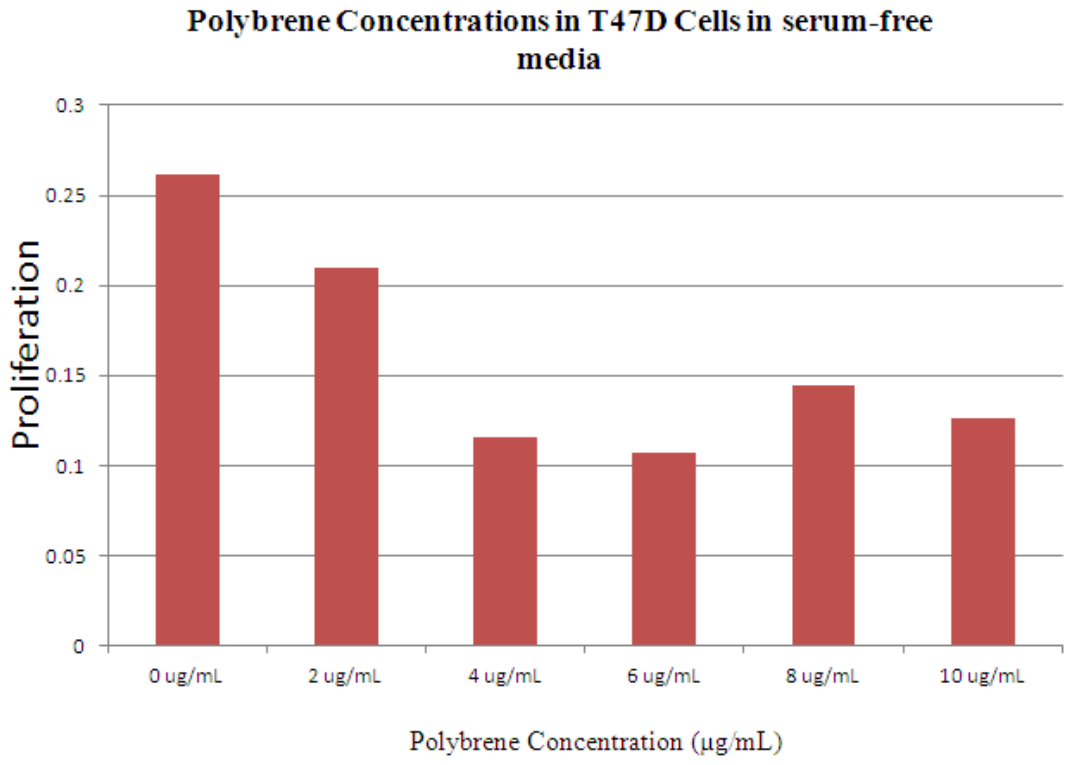

Figure 5.8 Optimisation of Polybrene concentration in T47D Cells.

For optimisation of the Puromycin concentration, the aim was to find the lowest concentration suitable to efficiently eradicate non-transduced T47D cells. The ideal Puromycin concentration determined was 4µg/ml (Figure 5.9). At this concentration viability of non-transfected cells was lost by approximately 70 % within 48 hours.

No benefit was gained by increasing Puromycin concentration above that level (Figure 5.9).

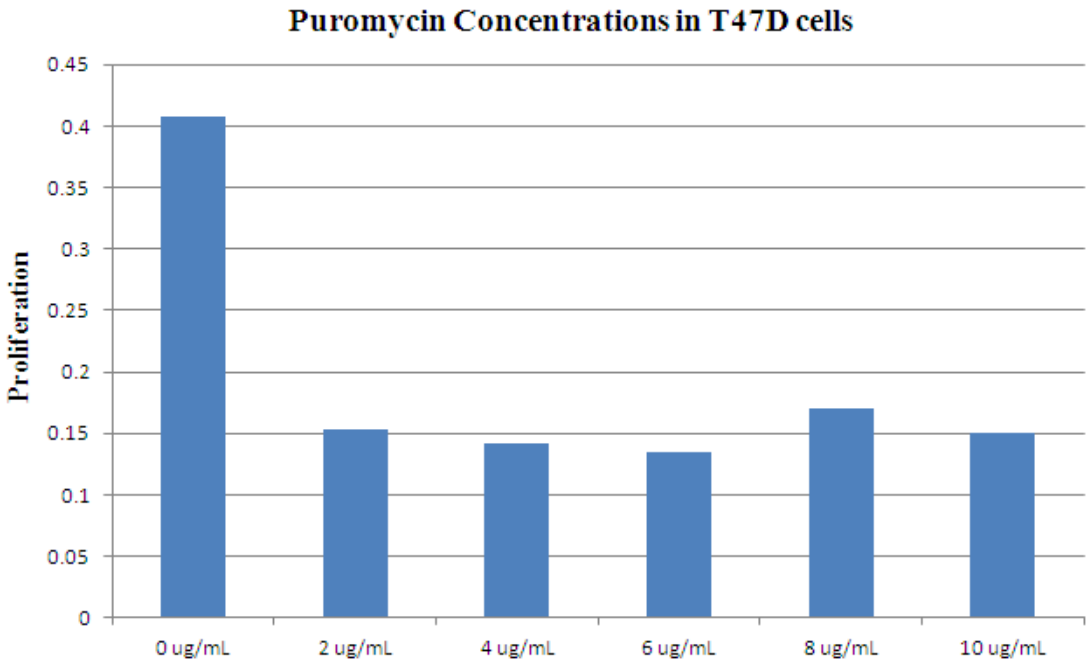

Figure 5.9 Optimisation of Puromycin concentration in T47D cells.

5.9.2 Confirmation of successful miR-379 over-expression

Following lentiviral transduction of T47D cells with a miR-379 mimic or a NTC mimic, successful over-expression of miR-379 was confirmed by RQ-PCR. Cells showed significantly increased expression of miR-379 in $T47D^{379}$ cells (5.34 $\log_{10}$ RQ) compared to $T47D^{NTC}$ cells (0.70 $\log_{10}$ RQ, Figure 5.10A). Further, since the lentivirus constructs used contained a red fluorescence protein, cells were visualised by fluorescent microscopy following transduction. DAPI stained nuclei were visualised in blue, while transduced cells were visualised in red (Figure 5.10B).

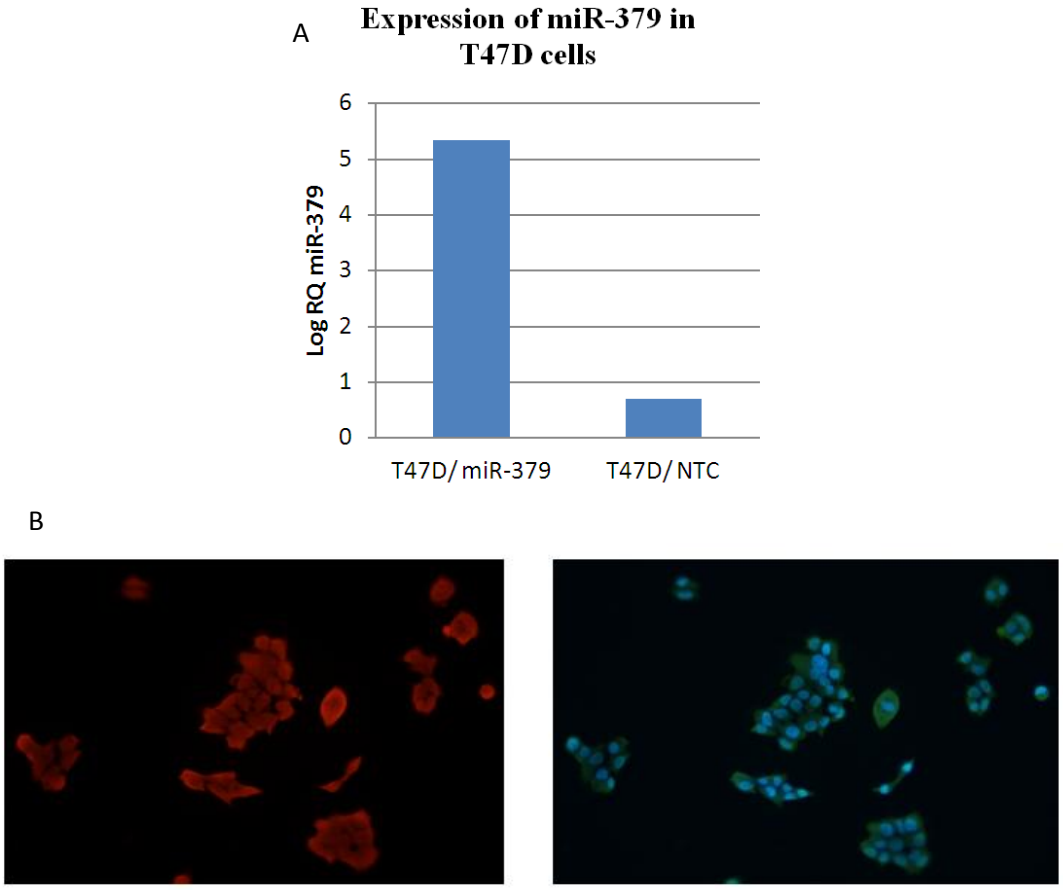

Figure 5.10 Confirmation of successful transduction. (A) RQ-PCR of miR-379 expression (B) slides were counterstained with DAPI (blue) to visualise cell nuclei and the transduced cells were visualised in red.

5.10 Study of the Impact of miR-379 over-expression on tumour initiation and progression.

On the day of tumour induction, an aliquot of transduced cells was set aside for confirmation of transduction and quantitative analysis of miR-379 expression. Cells were cultured and subsequently harvested for confirmation of continued over-expression of miR-379 at day 3 following tumour induction and again at day 7 following tumour induction. Cells harvested on induction day showed increased expression of miR-379 (4.07 $\log_{10}$ RQ) and again at day 3 post induction (4.23 $\log_{10}$ RQ), and finally at day 7 (4.56 $\log_{10}$ RQ) compared to average low expression observed in the NTC transduced cells (0.70 $\log_{10}$ RQ, Figure 5.11).

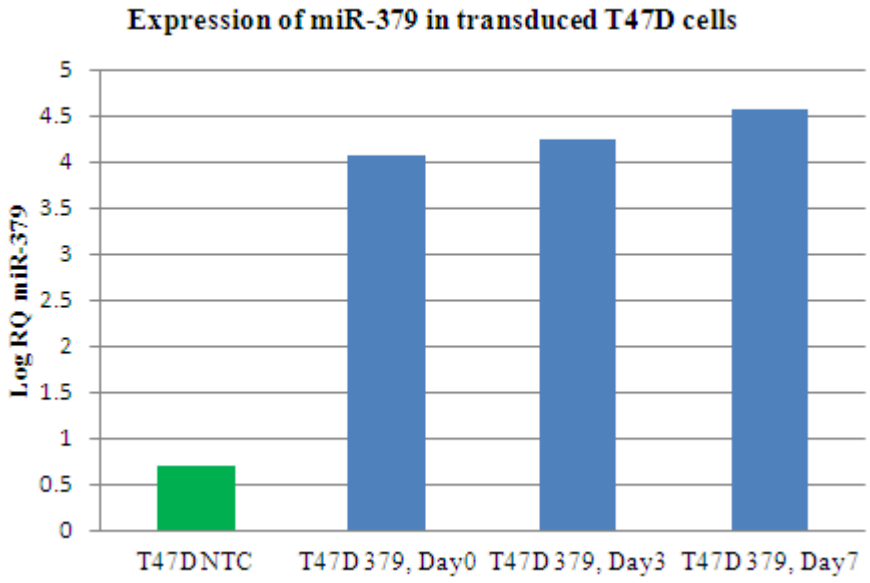

Figure 5.11 Long-term over expression of miR-379 investigated at Induction Day, day 3 post induction and day 7 post induction.

The T47D cells, with confirmed elevated expression of miR-379 were inoculated subcutaneously into the right flank of athymic nude mice. Cells stably transduced with a NTC were also inoculated into the control group of animals. Nine weeks following tumour induction, animals were sacrificed by CO_2 inhalation. Once all animals were sacrificed, whole bloods and tumours if present were collected. In the control group of animals with NTC mimic transduced T47D cells, tumours developed in all animals (n=5). In the group with tumours growing from T47D cells transduced with a miR-379-mimic, tumours developed in only 2 out of 5 animals. These tumours were excised, weighed and photographed (Figure 5.12). Along with increased tumour incidence, average weights for the NTC tumours were greater (n=5, Mean(SEM)60.9(50.0)mg) compared to tumours in the miR-379 group (n=2, 6.05(3.0)mg, p=0.38, results not shown). Images of tumours were also taken, showing tumours from control NTC groups were on average larger than tumours from the miR-379 transduced groups (Figure 5.12).

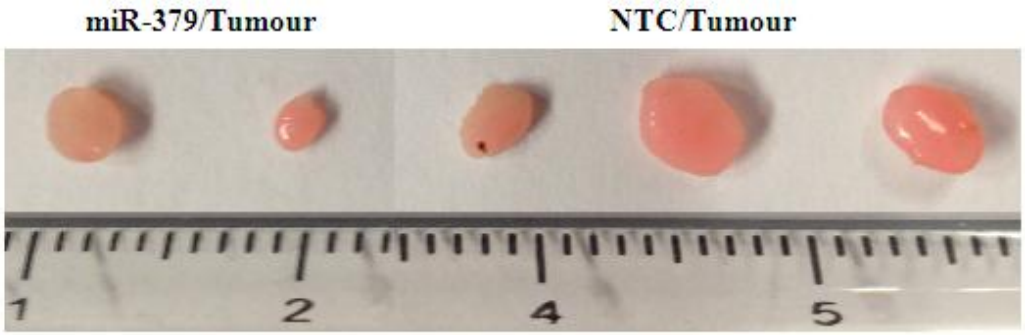

Figure 5.12 In Vivo assessment of tumour growth and development.

5.10.1 Murine Blood Analysis

Terminal cardiac bleeds were performed on animals bearing miR-379 tumours or NTC tumours to determine whether this had any effect on the circulating levels of miR-379. MiRNA extraction from blood was carried out as previously described. miR-379 expression was detectable in all bloods analysed. No significant difference was observed between circulating levels in animals with NTC transduced tumours (n=5, Mean(SEM)0.79(0.24)Log_{10} RQ) and in miR-379 transduced tumours (n=2, 0.61(0.17) Log_{10} RQ, p=0.538 , Figure 5.13)

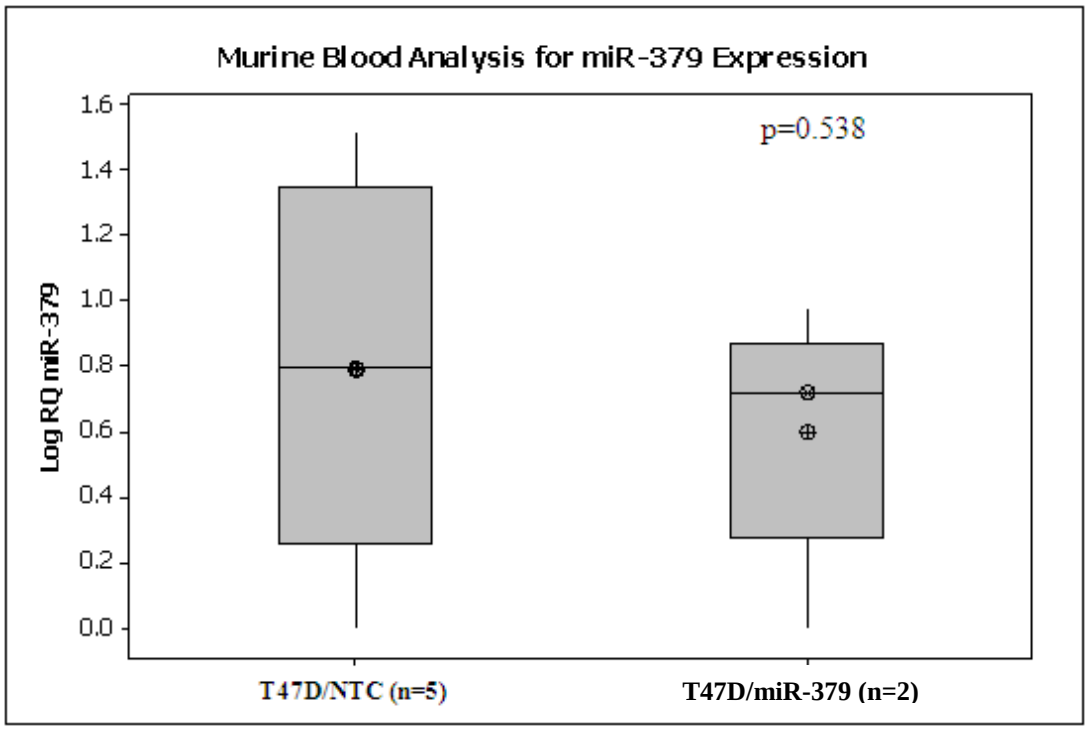

Figure 5.13 miR-379 Expression in murine bloods collected at harvest day.

5.11 Discussion

There is no doubt that miRNAs play an important role in breast cancer, but the mode of action of many microRNAs has yet to be elucidated. Located on chromosome 14q32.31, miR-379-410 is defined as a large cluster of brain-specific miRNAs and has been implicated in neuroblastoma as a potential biomarker [243]. While miR-379 has been shown to regulate IL-11 production in breast cancer cell lines, there have been no previous reports regarding expression levels in breast tissues. In the present study, expression of miR-379 was examined in breast tissue specimens, and was

detectable in 100 out of 103 samples, and all control tissues. The level of miR-379 was significantly decreased in breast cancer compared to normal breast tissue. Due to the decreased levels of miR-379, its expression was also investigated in the breast cancer cohort for any potential relationships with patient clinicopathological details. miR-379 expression showed a significant relationship with tumour stage. With increasing tumour stage the level of miR-379 decreased significantly. A similar trend was observed with tumour grade ($p=0.077$). It would be worth noting that increased numbers in the Grade 1 and 2 groups may have given more significance to this aspect of the study.

miR-379 has a putative binding site on Cyclin B1 which is a key initiator of mitosis and has previously shown a relationship with tumour stage and grade in breast cancer [230]. An immunohistochemistry-based analysis of specimens from over 1,300 invasive breast cancer patients also revealed a significant association with advanced tumour stage, grade, size, oestrogen and progesterone receptor status [230]. High Cyclin B1 expression is associated with poor patient prognosis [230]. Cyclin B1 expression was investigated in a subset of breast tissue specimens ($n=84$), with expression levels found to be up-regulated in breast cancer compared to normal and benign breast tissue. This is in agreement with previously published work [227, 230, 233]. Kawamoto et al [227] showed Cyclin B1 expression increases from benign into malignant stages of breast disease. The present study also showed a significant increase from benign to malignant breast tissues. Further, a significant increase in expression of Cyclin B1 was detected in benign compared to normal tissues. Following this investigation, a scatter plot with linear regression lines was used to assess the relationship between miR-379 and Cyclin B1, with a strong negative correlation observed, indicating a potential negative regulation of Cyclin B1. Previous studies showed knock-down of Cyclin B1 in cancer cell lines resulted in reduced cell proliferation [241, 242].Therefore potential introduction of miR-379 could be used as a therapeutic intervention to regulate the expression of Cyclin B1 and further control tumour cell proliferation. Transfection of a breast cancer cell line with a miR-379 mimic resulted in reduced Cyclin B1 protein expression and inhibition of proliferation, supporting a role for miR-379 in direct regulation of Cyclin B1. Future analysis should include the investigation of direct binding of miR-379 to the 3'UTR of Cyclin B1 using a luciferase assay. Circulating miRNAs have the potential as biomarkers for many diseases [244]. Levels of miR-379 were

investigated in whole bloods collected from cancer patients and healthy controls. While detectable in all samples, no significant difference was observed between breast cancer patients and controls.

The T47D cell line was stably transduced with a miR-379 mimic ($T47D^{379}$) and subsequently administered into nude mice. The control group received T47D cells stably transducede with a NTC ($T47D^{NTC}$). Nine weeks following tumour induction, animals were sacrificed. Results revealed miR-379 transduced tumours were only present in 2 out of 5 animals, compared to the control group which had a tumour present in all animals. This strengthens the hypothesis of miR-379 as a tumour suppressor in breast cancer.

Further, the effect on tumour growth was determined. Tumours in the miR-379 group were on average smaller in size and weighed less than the tumours from the NTC group. This revealed a significant effect of miR-379 over-expression on tumour growth.

Analysis of circulating miR-379 levels revealed no significant deregulation in animals bearing $T47D^{379}$ tumours compared to animals bearing $T47D^{NTC}$ tumours. This is in agreement with the findings from the analysis on circulating miR-379 levels in the patient breast cancer cohort. This confirms the hypothesis that miR-379 is not a suitable biomarker of the disease, however, has a potentially important role in the primary breast tumour microenvironment.

Based on the data presented in this study, which included analysis carried out on in vitro cell lines, clinical patient samples and in vivo models, it would appear that miR-379 has an important role in the primary tumour microenvironment as a tumour suppressor in breast cancer. This effect is mediated at least in part through regulation of Cyclin B1. This could have potential therapeutic applications as re-introduction of miR-379 into tumours could inhibit tumour progression.

Chapter 6

Characterisation of the Primary Breast Tumour Microenvironment

6.1 Introduction

Breast cancer arises as a result of mutations within cancerous epithelial cells and therefore have since been a focus of much research to date [245]. However, the tumour microenvironment has also been shown to play a role in tumour initiation and progression [149, 245, 246]. The tumour contains various different cell types, including macrophages, dendritic cells, endothelial cells, pericytes and fibroblasts. Breast tumour stromal cells act as modifiers of breast cancer initiation and progression [150, 174]. During tumour development and progression, malignant cells interact with this tumour microenvironment through a bidirectional relationship which supports tumour growth and spread [247-250]. It is hypothesised that these metastatic traits are acquired through exposure of epithelial cancer cells to paracrine signals received from mesenchymal cell types in the surrounding tumour-associated stroma [174, 245]. Fibroblasts are mesenchymal-derived cell types which maintain the architecture of tissues. They play a role in wound healing during which they become activated. Cancer associated fibroblasts (CAFs) are modifiers of cancer progression and are thought to act as critical promoters of tumour growth and angiogenesis [171, 251]. During tumour progression precursor CAFs are recruited to the tumour microenvironment and upon interaction with the carcinoma they undergo trans-differentiation. In breast carcinomas, approximately 80% of stromal fibroblasts are thought to be CAFs [252]. They can be identified through expression of alpha-smooth muscle actin (α-SMA) and Vimentin and originate from resident fibroblasts and other mesenchymal cell types including pericytes and bone-marrow derived cells [169, 253-258].

Mesenchymal Stem Cells (MSCs) are a subset of non-hematopoietic multipotent stromal cells found primarily within the bone marrow. MSCs are capable of self-renewal and can differentiate into multiple lineages including osteoblasts, chondrocytes and adipocytes [188]. They play an important role in wound healing and tissue regeneration through differentiation and release of pro-angiogenic factors [259]. MSCs are thought to be an important component of the tumour microenvironment and are actively recruited in large numbers to the stroma of developing tumours [175]. They interact with breast cancer cells via direct contact or paracrine mechanisms [260]. It is evident that the primary tumour microenvironment is not an innocent bystander in tumour progression, but plays an active role in

facilitating the recruitment of specialised cells to tumours to facilitate tumourigenesis. Although many studies support a role for MSCs in the tumour setting, there has only been one study to date where native MSCs were successfully identified in patient breast tumour tissues [260]. The current aim was to characterise the stromal population and to further identify a subpopulation of native MSCs present.

6.2 Aim

- Culture of primary breast stromal cells from tumours, tumour associated normal (TAN) and normal tissues.
- Characterisation of primary breast stromal cells based on cell surface antigen profile.
- Investigate the presence of native MSCs within the breast tumour microenvironment.
- Determine the multilineage differentiation potential of primary stromal cells derived from tumours and TAN tissues.

6.3 Materials and Methods

Following ethical approval and informed patient consent, breast tissue specimens were obtained following surgery and were digested in mild collagenase. Cells were isolated by differential centrifugation. Stromal cells were cultured from tumours, TAN and normal tissues. Stromal cells were then characterised by flow cytometry (Figure 6.1), using standard stromal cell markers as well as markers commonly used to characterise MSCs. Control MSCs were provided by the Regenerative Medicine Institute (REMEDI) at NUIG, and were obtained from the iliac crest of healthy volunteers. Primary stromal cells derived from tumour and TAN tissues and MSCs were cultured under conditions that allowed for the differentiation into osteoblasts and adipocytes.

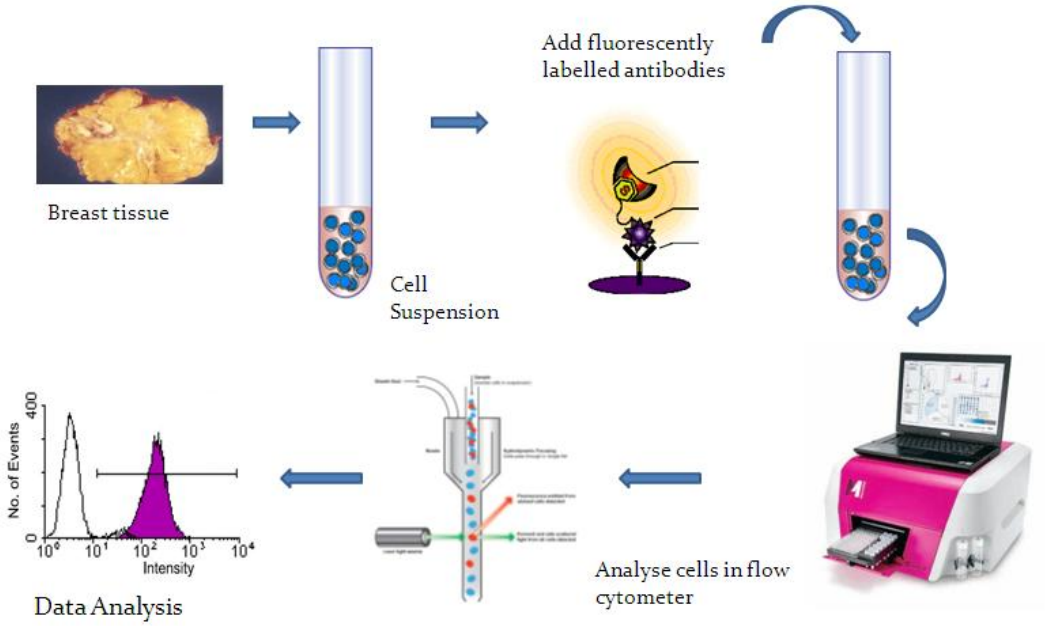

Figure 6.1 Overview of Analysis of Primary Stromal cells

6.4 Culture and Characterisation of Primary Breast Stromal Cells

Tissue specimens were digested in mild collagenase overnight before carrying out differential centrifugation on disrupted cells. Differential centrifugation allowed for the isolation of three distinct cell populations. An example of successful culture of organoid, epithelial and stromal cells was shown in Figure 6.2, [186]. The organoid cell fraction contained a mixed cell population including a range of different cell types and some partially undigested clumps. Both epithelial and organoid cells were cultured successfully from patient tissues. The main focus of this study was the stromal cell fraction (Figure 6.2).

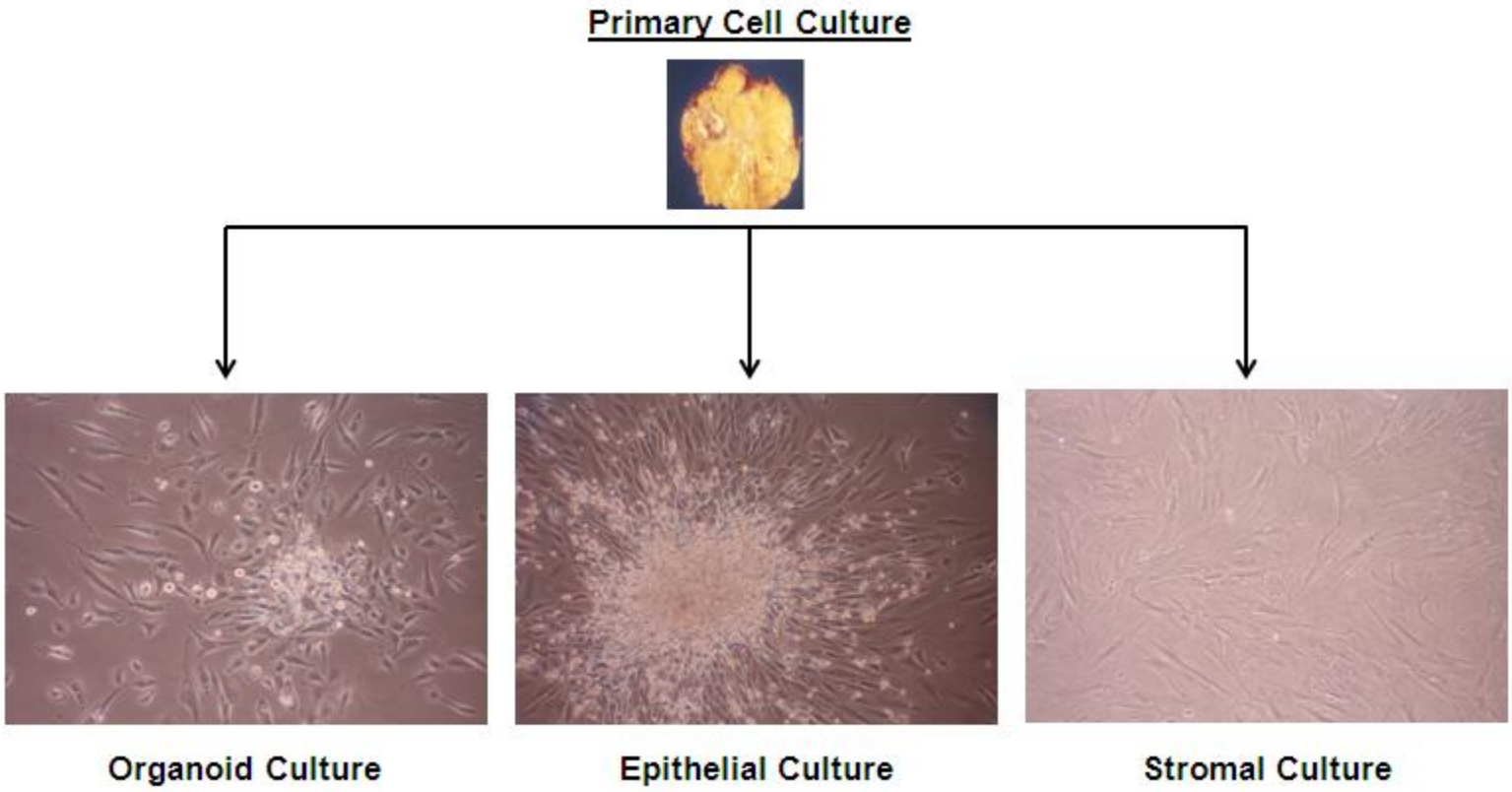

Figure 6.2 Overview of cultured organoid, epithelial and stromal cells following differential centrifugation [186].

6.4.1 Flow Cytometry of primary tumour, TAN and normal stromal cells

The stromal cells isolated from tumours (n=4), TAN (n=5) and normal tissues (n=5) were analysed using Flow cytometry (Figure 6.3). Tumour stromal cells showed expression of >50% for α-SMA. The surface molecules commonly used to characterise epithelial, endothelial and hematopoietic cell fractions included MUC1, CD31, CD10 and CD24. CD14 expression was also investigated in the stromal cells, this surface antigen is present on macrophages/monocytes. The tumour stromal cells showed < 5% expression for these markers thereby highlighting the absence of epithelial, endothelial and hematopoietic cells (Figure 6.3). TAN stromal cells were observed to have > 20% expression for α-SMA. TAN stromal cells were shown to have < 5% expression for MUC1, CD24, CD14 and CD31. Normal stromal cells revealed >30% expression for α-SMA and >15% expression for CD10. Normal stromal cell analysis revealed < 5% expression for epithelial, endothelial and hematopoietic surface antigens (Figure 6.3).

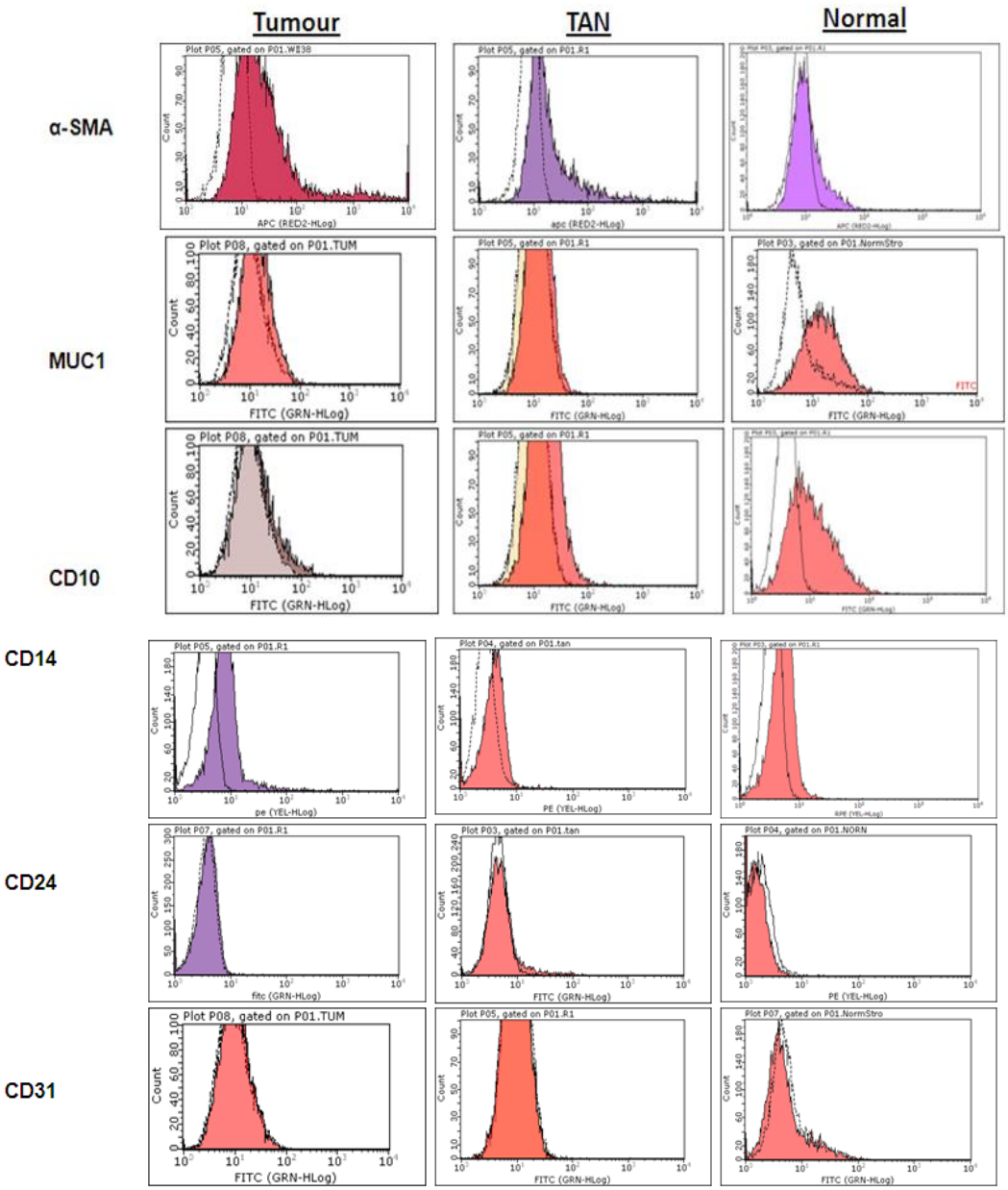

Figure 6.3 Characterisation of stromal cells derived from tumour, TAN and normal tissue. An *Open profile* represented an isotype control for background fluorescence and the *Coloured profile* showed the positive signal.

Cells were further analysed based on the Minimal Criteria for Defining MSCs [177]. MSCs are commonly characterised by the expression of a range of cell surface markers (Table 6.1). MSCs must also have the capacity to differentiate into multiple lineages including osteoblasts, adipocytes and chondrocytes [177].

MSC Positive Surface Markers	MSC Negative Surface Markers
CD105	CD45
CD90	CD34
CD73	CD14 or CD11b
	CD79 alpha or CD19
	HLA-DR

Table 6.1 List of cell surface markers that associated with MSC phenotype [177].

The stromal cells cultured from tumours, TAN and normal tissues all revealed > 95% positivity for mesenchymal lineage markers CD90, CD105 and CD73. These three cell types also revealed <5% expression for CD45, CD34 and HLA-DR (Figure 6.4).

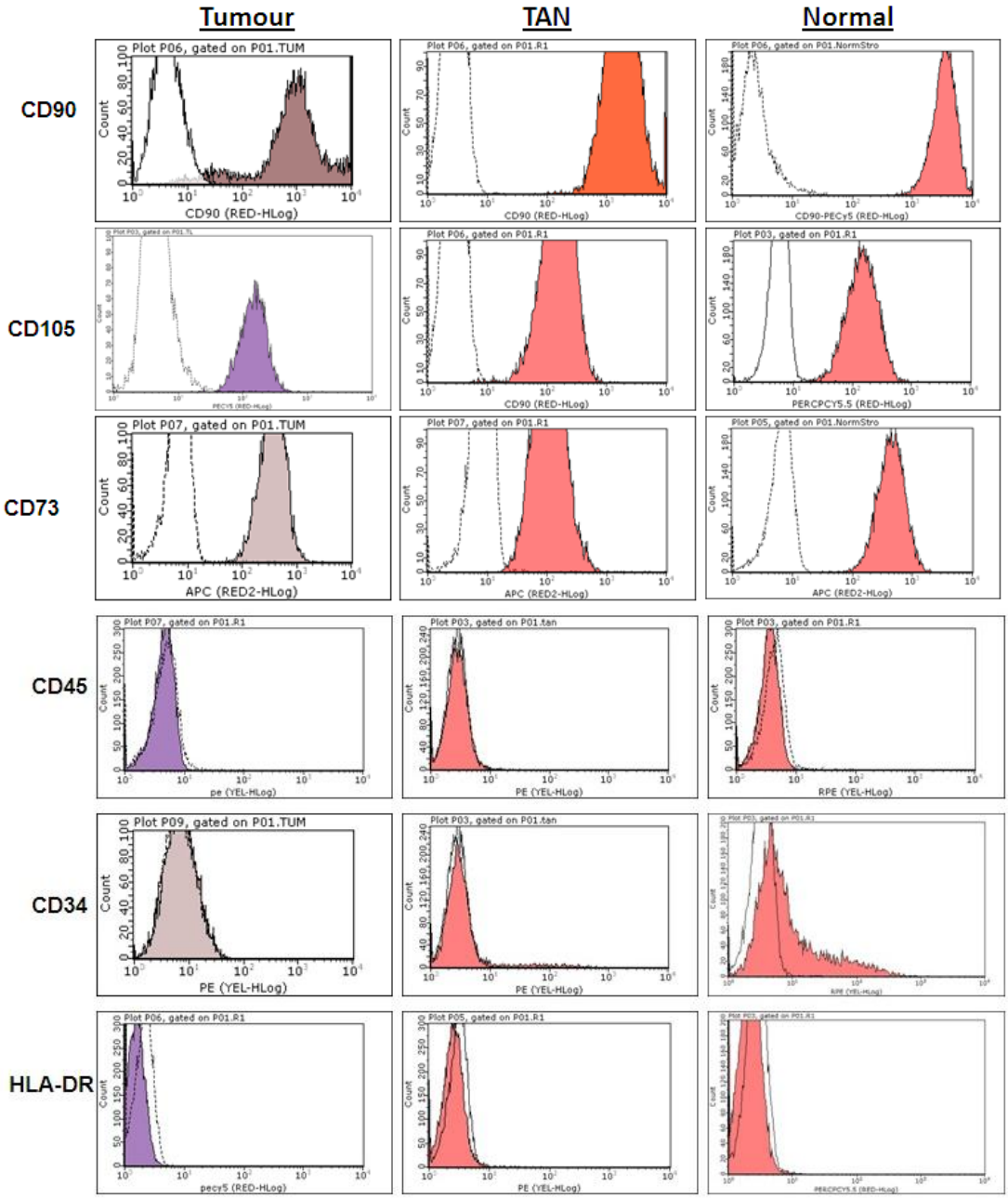

Figure 6.4 Characterisation of primary stromal cells using surface antigens commonly used to define MSCs. An *Open profile* represented an isotype control for background fluorescence and the *Coloured profile* showed the positive signal.

The overall expression of surface antigens analysed on tumour, TAN and normal stromal cells was summarised in Table 6.2.

Protein	**(+) Tumour stromal cells**	**(+) TAN stromal cells**	**(+) Normal stromal cells**
	n=4	**n=5**	**n=5**
	Mean(SEM)	Mean(SEM)	Mean(SEM)
CD90	100(0.00)	99.8(0.102)	99.34(0.26)
CD73	99.89(0.05)	99.93 (0.023)	95.99 (3.76)
CD105	99.88 (0.09)	99.66 (0.05)	99.69 (0.17)
α-SMA	55.9	41.2(12.5)	33.54(1.11)
CD14	15.2	5.55(4.15)	14.9(13.9)
CD10	2.72	1.41(1.85)	16.58(4.27)
CD31	0.12	0.48 (0.233)	098(0.51)
MUC1 (CD227)	0.08	1.26 (0.667)	1.09(0.28)
CD24	0.1	4.32	1.16(0.47)
CD45	0.01	0.06(0.44)	0.86(0.57)
CD34	0.09	4.34(2.5)	2.47(1.16)
HLA-DR	0.1	0.25	0.90(0.55)

Table 6.2 Summary of expression of markers for primary stromal cells from tumours, TAN and normal tissues.

6.5 Mesenchymal Stem Cell Culture and Characterisation

MSCs (Figure 6.5A (i)) were cultured alongside stromal cells (Figure 6.5A (ii)). MSCs in culture displayed homogenous morphology, sharing similar fibroblast-like morphology. In the present study, MSCs were characterised by flow cytometry for a panel of defined MSC markers. This analysis revealed MSCs were > 95% positive for CD90, CD73, CD105, and < 5% positive for the markers of endothelial and hematopoietic markers including CD31, CD45, MUC1, CD34 and CD24 (Figure 6.5B).

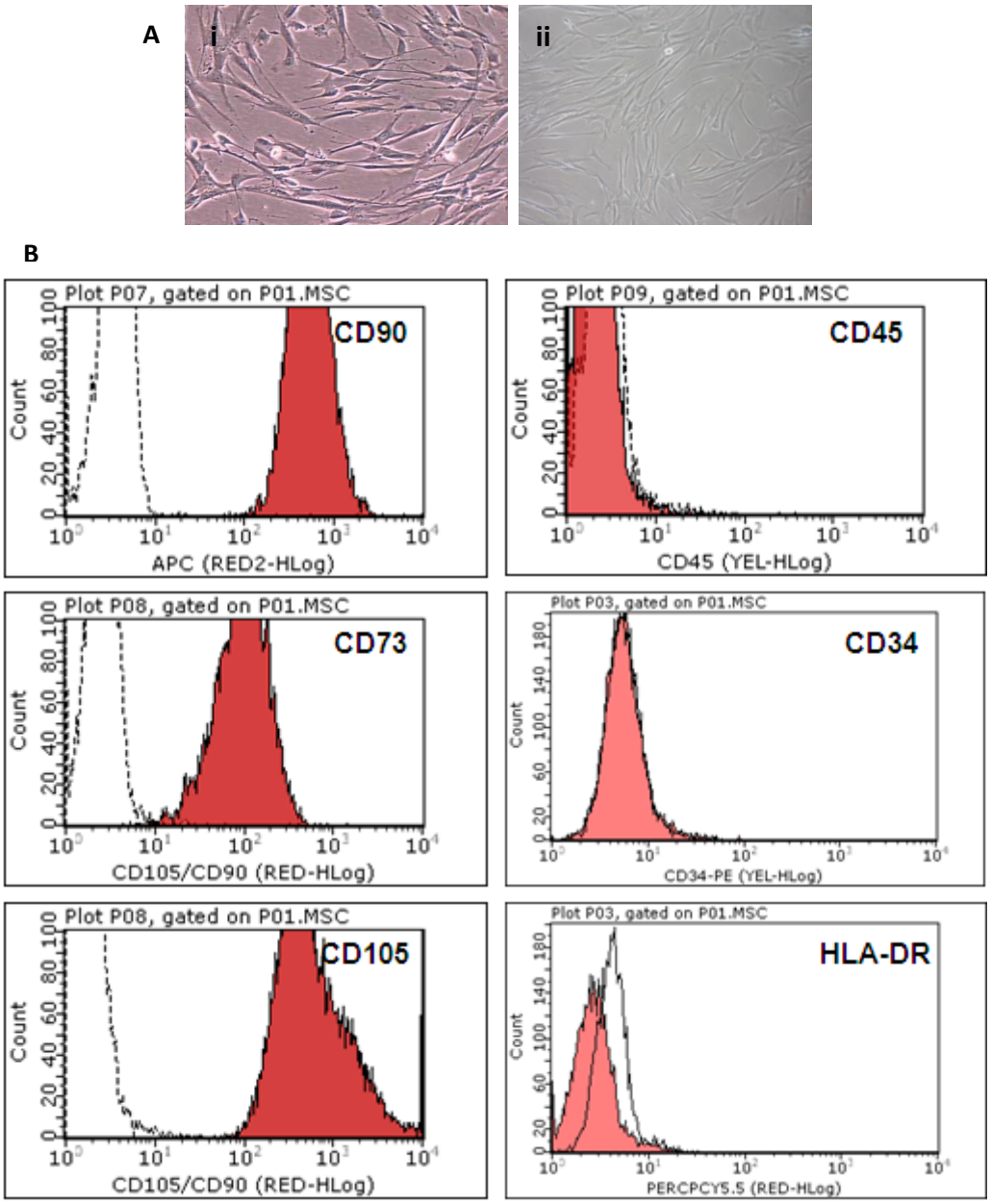

Figure 6.5 Characteristics of MSCs from bone-marrow. (A) Representative morphology of primary tumour stromal cells (i) and MSCs (ii) at 40X. (B) Immunophenotypic characteristics of MSCs. Flow Cytometry analysis showed that MSCs were homogenous. An *Open profile* represented an isotype control for background fluorescence and the *Coloured profile* showed the positive signal

In order to further characterise MSCs and potentially identify a marker to distinguish between MSCs and stromal cells, MSCs were analysed using the same range of cell surface antigens used to previously characterise stromal cells including, MUC1, α-SMA, CD31, CD14, CD24 and C10. Overall, the MSC population showed < 5% expression for MUC1, CD31, CD24 and CD10. The MSC population was shown to have 25% expression for α-SMA and 80% expression for CD14 (Figure 6.6).

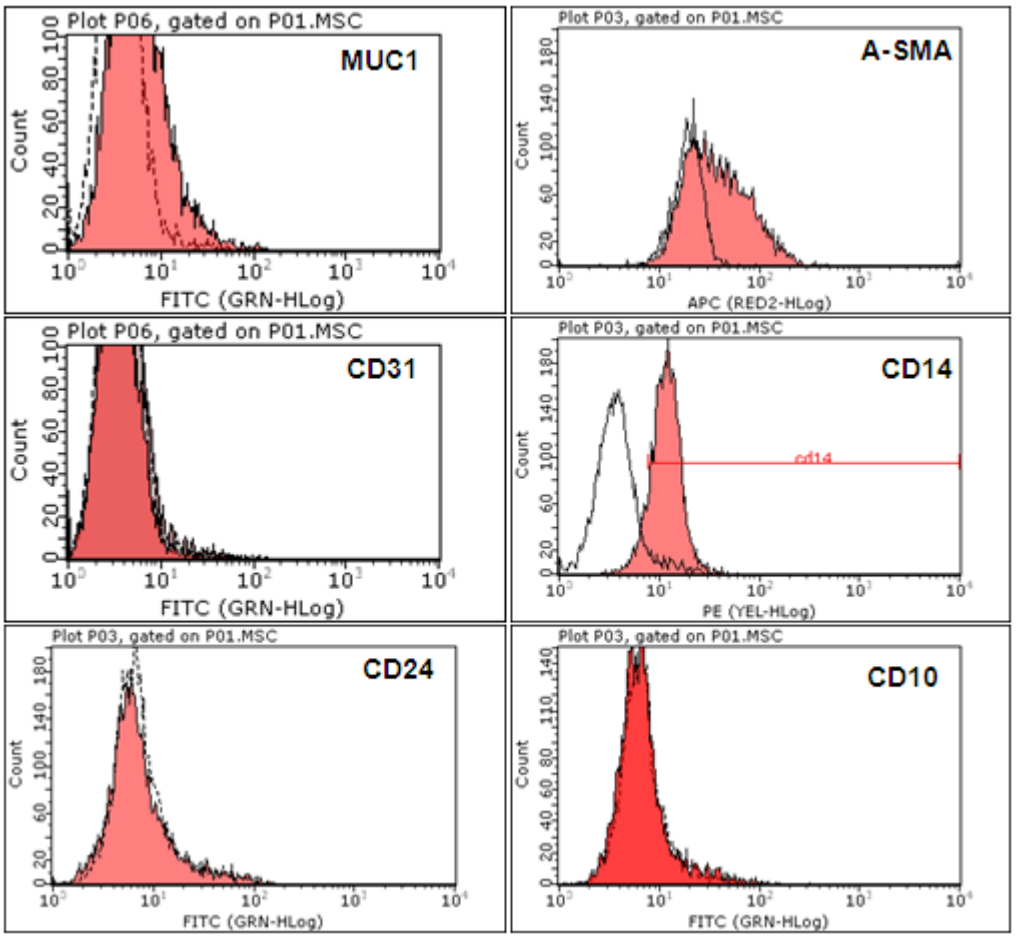

Figure 6.6 Immunophenotypic characteristics of MSCs based on stromal cell markers. An *Open profile* represented an isotype control for background fluorescence and the *Coloured profile* showed the positive signal.

6.6 Multilineage differentiation potential of Primary breast stromal cells

6.6.1 Osteoblast differentiation assay

In vitro multilineage differentiation potential is a functional standard to define MSCs in culture. The cells were cultured in osteogenic differentiation medium for 3 weeks. The morphology of breast stromal cells changed from spindle shape to cuboidal shape throughout the differentiation experiment. Calcium mineralisation was examined using Von Kossa staining after 3 weeks (Figure 6.7). The results revealed the ability of a subset of breast tumour stromal cells to undergo osteogenic differentiation. This was confirmed by black staining. Calcium deposition was observed, as seen in the 4x magnification for tumour stromal cells and MSCs (Figure 6.7).

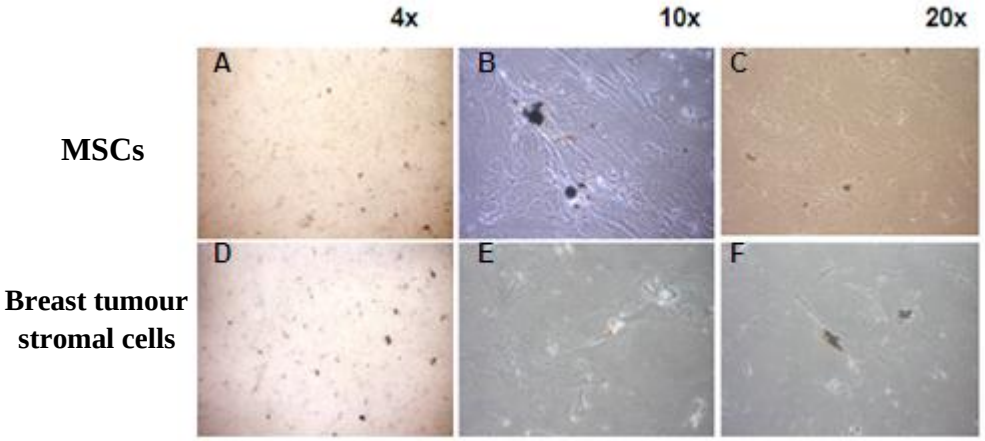

Figure 6.7 Differentiation potential of stromal cells derived from bone marrow (A-C) and breast tumours (D-F). MSCs calcium deposition (black staining). 4x (A,D), 10x (B,E) and 20x (C,F)

TAN stromal cells were also investigated for their osteogenic differentiation potential. A second stromal cell population derived from a breast tumour was also included. The results showed osteogenic differentiation of the MSCs when compared to cells receiving regular MSC maintenance medium in the first column (Figure 6.9). The TAN stromal cells revealed a greater

capacity for osteogenic differentiation than the tumour stromal cells. There was some isolated staining visible in both tumour stromal cell populations, however to a lesser degree than observed in the MSCs and TAN stromal cells (Figure 6.8). This highlights the differences between cancer patients.

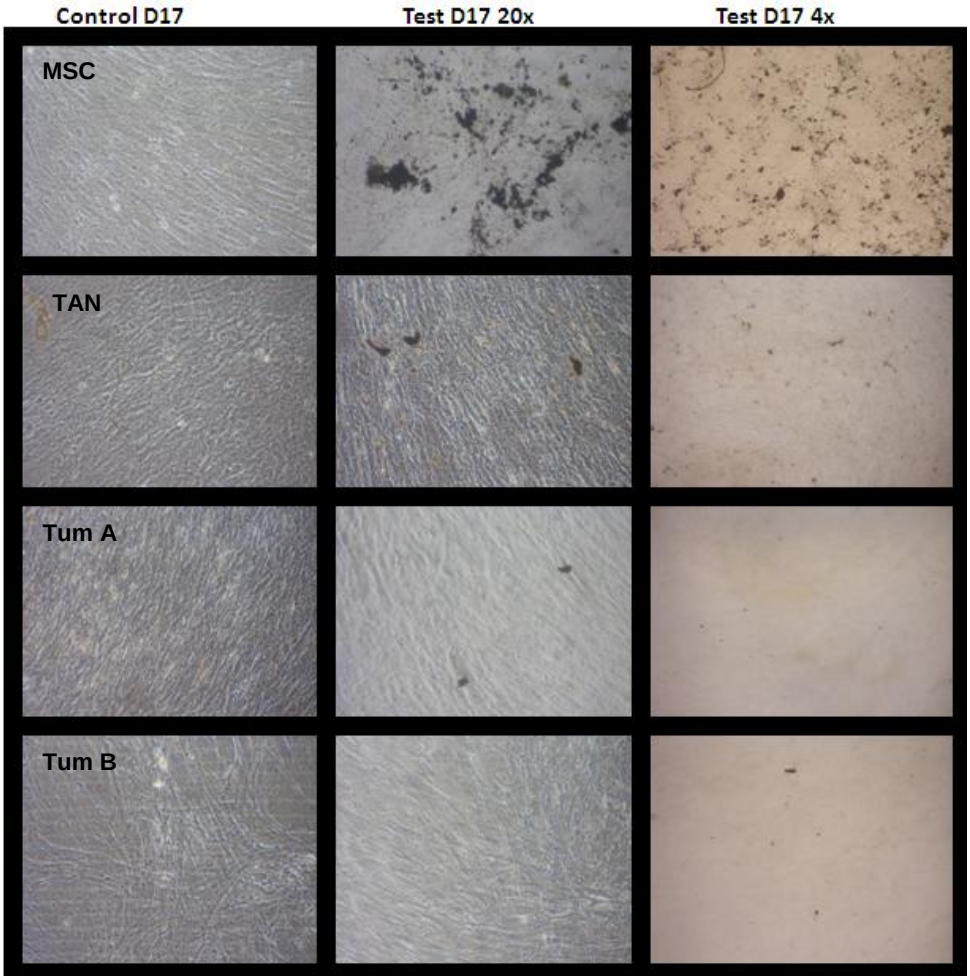

Figure 6.8 Differentiation potential of primary stromal cells and MSCs.

6.5.2 Adipogenic differentiation

The adipogenic differentiation potential of primary breast stromal cells was also investigated by intracellular lipid vesicle detection under phase-contrast light microscopy and by Oil-red O staining (Figure 6.10). The cells were cultured for up to 21 days in adipogenic induction media as previously described. Control cells received regular maintenance MSC medium. The MSCs receiving the induction media showed positive red staining which indicated adipogenic differentiation compared to the control MSCs (Figure

6.10). Adipose formation was also observed for a subset of both tumour and TAN stromal cells following adipogenic induction (Figure 6.10).

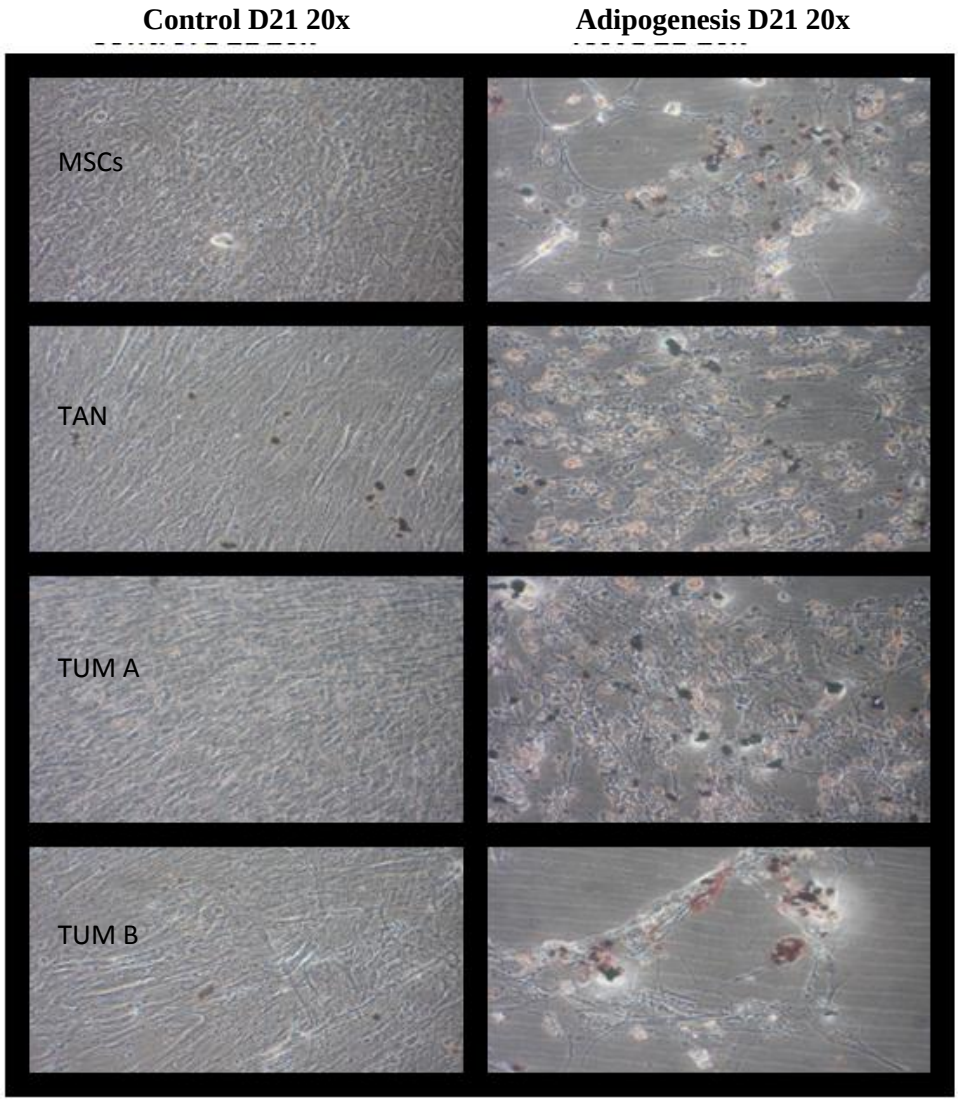

Figure 6.9 Adipogenic differentiation of primary stromal cells and MSCs.

6.7 Discussion

Breast tumour progression occurs through reciprocal interactions between epithelial cancer cells and the surrounding microenvironment. Fresh tumour tissues were obtained following surgery for primary culture of stromal cells. The stromal cell morphology was of bipolar spindle shape, which is a typical characteristic of fibroblast cells during in vitro culture [261]. Stromal cells were characterised by flow cytometry by applying markers commonly

used to define stromal cells, such as CD90 which confirms the presence of activated stromal cells or "myofibroblasts" [262, 263]. CAFs express markers specific to the myofibroblast lineage which include α-SMA, vimentin and fibroblast specific protein 1 (FSP1) [169]. A study by Quante et al [264] reported that approximately 20% of all CAFs analysed in a gastric cancer model were derived from the bone marrow. In the present study, the majority of the stromal cells expressed α-SMA and lacked expression of markers commonly used to characterise epithelial, endothelial and hematopoietic cells. Primary stromal cells were also successfully cultured from TAN and normal breast tissues and were then characterised using the same panel of stromal cell markers. The results highlighted the heterogeneity of the tumour microenvironment containing a variety of different cell types including myofibroblasts and MSCs. Cultured MSCs were shown to express a panel of surface antigens commonly used to identify MSCs. In order to elucidate the presence of native MSCs within the tumour, stromal cells derived from tumour and TAN tissue were further characterised using associated with MSCs. The results revealed similar expression profiles compared to cultured MSCs.

Investigation of MSCs differentiation into multiple lineages was carried out using the ostegenic and adipogenic assay [177]. A previous paper by Yan et al [260] revealed isolation of breast cancer-derived MSCs (BC-MSCs) with tri-lineage differentiation potential from malignant breast tumours. This analysis was carried out in stromal cells isolated from breast tumours (n=14) and these BC-MSCs were found to support tumour progression in an in vivo model [260]. The cultured stromal cells derived from tumour and TAN tissues in the present study were exposed to conditions that support differentiation into osteoblasts and adipoctytes. A subset of the stromal population was shown to possess the ability to differentiate into osteoblast, revealing a small proportion of MSCs present capable of differentiation. The same was observed during the adipogenic differentiation assay. Taken together primary stromal cells were successfully isolated and identified, further highlighting the presence of an MSC subpopulation within the tumour microenvironment was demonstrated. It is important to note that the cell surface antigens and differentiation assays are designed to detect

undifferentiated MSCs. It is likely that there are significantly more MSCs present within the tumour, at varying stages of differentiation in response to factors secreted in the primary tumour microenvironment. Reliable determination of the number and prevalence and role of these cells in the tumour will be dependent upon identification of one specific MSC marker that is retained regardless of differentiation status. This is a major task that has eluded interest to date, but would potentially represent a novel therapeutic target in the breast cancer setting.

Final Discussion and Conclusion

There is still not one universally appropriate treatment strategy available for breast cancer. This disease kills over 600 women in Ireland and over 450,000 women worldwide each year [1, 2]. Identifying prognostic targets and understanding the molecular mechanisms underlying the disease is challenging.

This study aimed to firstly investigate a potential regulatory role of four miRNAs, miR-875-5p, miR-339-5p, miR-10a and miR-379 with target genes NIS, RARα, RARβ, ERα and THRα which are involved in breast cancer progression. The secondary aim was to investigate tumour heterogeneity through detection of a subpopulation of MSCs within the stroma of primary breast tumours.
Investigation of miRNA-mediated regulation of key genes implicated in breast cancer progression is an exciting avenue of investigation. Gene expression analysis revealed significantly reduced expression of RARβ and THRα in breast cancer patients compared to healthy controls, suggesting a potential tumour suppressor role in breast cancer. RARβ was previously found to be lost in a number of different cancers including breast cancer [215, 225].

Expression of miR-875-5p and miR-339-5p showed no significant dysregulation across malignancy and was therefore not pursued any further. Due to the small sample number analysed in the pilot study and positive correlation observed between miR-10a and miR-379 with target genes RARβ and THRα, further investigation was warranted on the expression of these miRNAs in breast cancer.
Both miR-10a and miR-379 were found to decrease significantly in malignancy versus healthy controls. Further, miR-10a expression was shown to positively correlate with RARβ and THRα genes, making a role in regulation unlikely. It is thought that miR-10a is induced by RARβ expression. RA has previously been shown to induce miR-10a expression in T helper cells and in pancreatic cancer cells [109, 216]. Any relationship with patient clinicopathological details was also investigated. miR-10a expression did not alter across any clinicopathological details investigated, however miR-379 expression showed a trend towards decreasing expression with increasing tumour Stage and Grade. Functional assays were applied to investigate the effect of both miR-10a and miR-379 on breast cancer cell proliferation. Over-expression of miR-10a did not reveal any significant knock-down in proliferation. miR-379 however, did result in significant inhibition of cellular proliferation in vitro. The relationship of miR-379 with tumour stage and grade

altered the initial focus to investigate further genes associated with tumour Stage. Cyclin B1 was identified as having a predictive binding site on miR-379. Cyclin B1 expression is implicated in mitosis and it also demonstrates a robust relationship with tumour Stage and Grade in breast cancer [265]. Cyclin B1 expression was quantified in a subset of breast tissues and a negative correlation between Cyclin B1 and miR-379 was observed, suggesting a potential regulatory role for miR-379. MicroRNA-mediated regulation of Cyclin B1 in breast cancer would be very interesting as this could have a therapeutic potential in reducing cellular proliferation. To confirm this regulatory potential, a miR-379 mimic was over-expressed in T47D cells and the effect on Cyclin B1 protein expression was investigated using IHC and western blot. Over-expression of miR-379 resulted in decreased expression of Cyclin B1 protein levels. In order to validate miR-379 as a tumour suppressor in breast cancer, in vivo experiments were warranted to determine whether miR-379 directly impacts tumour establishment and growth. Tumour establishment and growth was successfully abrogated in vivo through up-regulation of miR-379, confirming the tumour suppressor status of miR-379. Previous reports have highlighted a role for miRNA replacement which could represent a viable and efficacious strategy for miRNAs that are down-regulated in tumours [266, 267]. Re-expression of even a single miRNA in tumour cells could have major implications and provide significant therapeutic benefits [268]. Viral delivery of a let-7a miRNA reported reduced tumour growth in a lung adenocarcinoma model [269]. Overall, this study highlighted that single miR-379 microRNA has the capacity to slow down tumour development. Tumours that developed were on average much smaller in size. This confirms the tumour suppressive nature of miR-379 in breast cancer.

A secondary aim of this study was to isolate and characterise stromal cells derived from primary breast tissues. This study investigated the cellular components of the primary breast tumour microenvironment with a specific focus on the MSC subpopulation. The breast tumour microenvironment is home to numerous cells with stromal cells being the predominant cell type. These cells were characterised by flow cytometry. Along with activated myofibroblasts, a subpopulation of MSCs was identified within the tumour microenvironment. Overall the stromal cells derived from tumours and TANs shared similar cell surface expression profile and morphology with the MSCs. One previous study by Yan et al [260] revealed the

presence of MSCs in the breast tumour microenvironment by confirming multilineage differentiation potential of these cells. This was also confirmed in the present study. Differentiation potential of tumour and TAN stromal cells was determined using adipogenic and osteogenic differentiation assays. The results observed highlighted a subpopulation of MSCs with multilineage capacity within in the primary tumour microenvironment.

In conclusion, this study identified a novel and potent tumour suppressor role for miR-379, demonstrated in patient samples and using both in vitro and in vivo models. This miRNA was demonstrated to exert its effects at least in part through binding to Cyclin B1. Further, miR-10a was highlighted as a potential tumour suppressor miRNA that warrants further investigation. The primary tumour microenvironment presents significant challenges to our understanding of breast cancer development and progression. This study demonstrated the presence of a subpopulation of multipotent MSCs within the primary tumour stroma. Understanding the molecular mechanisms underlying breast cancer, and the role of individual cell populations in these pathways, will be fundamental to the development of novel therapeutic strategies.

Chapter 7

References

1. Ireland, N.C.R., *Cancer in Ireland 2013: Annual report* 2013.
2. Center, M.M.S., R., Jemal, A., *Global Cancer Facts & Figures 2nd Edition.* American Cancer Society, 2011.
3. GLOBOCAN. *Breast Cancer statistics*. 2013; Available from: http://www.wcrf.org/cancer_statistics/cancer_facts/women-breast-cancer.php.
4. Gray, H.W., P.H., Bannister, L., *Gray's Anatomy*. 38 ed. 1995: Edinburgh : Churchill Livingstone.
5. My Breast Cancer Guide. *Anatomy of the breast*. 2013; Available from: http://www.my-breast-cancer-guide.com/what-is-breast-cancer.html.
6. Langley, R.R. and I.J. Fidler, *The seed and soil hypothesis revisited--the role of tumor-stroma interactions in metastasis to different organs.* Int J Cancer, 2011. **128**(11): p. 2527-35.
7. Sleeman, J.P. and N. Cremers, *New concepts in breast cancer metastasis: tumor initiating cells and the microenvironment.* Clin Exp Metastasis, 2007. **24**(8): p. 707-15.
8. Biglia, N., et al., *Increased incidence of lobular breast cancer in women treated with hormone replacement therapy: implications for diagnosis, surgical and medical treatment.* Endocr Relat Cancer, 2007. **14**(3): p. 549-67.
9. Hayes, D.F., I.C. Henderson, and C.L. Shapiro, *Treatment of metastatic breast cancer: present and future prospects.* Semin Oncol, 1995. **22**(2 Suppl 5): p. 5-19; discussion 19-21.
10. Jan, M., et al., *Triple assessment in the diagnosis of breast cancer in Kashmir.* Indian J Surg, 2010. **72**(2): p. 97-103.
11. Drew, P.J., et al., *Prospective comparison of standard triple assessment and dynamic magnetic resonance imaging of the breast for the evaluation of symptomatic breast lesions.* Ann Surg, 1999. **230**(5): p. 680-5.
12. Edge, S.B. and C.C. Compton, *The American Joint Committee on Cancer: the 7th edition of the AJCC cancer staging manual and the future of TNM.* Ann Surg Oncol, 2010. **17**(6): p. 1471-4.
13. Singletary, S.E. and J.L. Connolly, *Breast cancer staging: working with the sixth edition of the AJCC Cancer Staging Manual.* CA Cancer J Clin, 2006. **56**(1): p. 37-47; quiz 50-1.
14. Ireland, N.C.R., *Breast Cancer Incidence, Mortality, Treatment and Survival in Ireland: 1994-2009.* 2012.
15. National Cancer Institiute. *Tumour Grade*. 2013; Available from: http://www.cancer.gov/cancertopics/factsheet/detection/tumor-grade.
16. Bloom, H.J. and W.W. Richardson, *Histological grading and prognosis in breast cancer; a study of 1409 cases of which 359 have been followed for 15 years.* Br J Cancer, 1957. **11**(3): p. 359-77.
17. Elston, C.W. and I.O. Ellis, *Pathological prognostic factors in breast cancer. I. The value of histological grade in breast cancer: experience from a large study with long-term follow-up.* Histopathology, 1991. **19**(5): p. 403-10.
18. Galea, M.H., et al., *The Nottingham Prognostic Index in primary breast cancer.* Breast Cancer Res Treat, 1992. **22**(3): p. 207-19.
19. Miller, D.V., et al., *Utilizing Nottingham Prognostic Index in microarray gene expression profiling of breast carcinomas.* Mod Pathol, 2004. **17**(7): p. 756-64.
20. Velculescu, V.E., et al., *Serial analysis of gene expression.* Science, 1995. **270**(5235): p. 484-7.
21. Sorlie, T., et al., *Gene expression patterns of breast carcinomas distinguish tumor subclasses with clinical implications.* Proc Natl Acad Sci U S A, 2001. **98**(19): p. 10869-74.

22. Perou, C.M., et al., *Molecular portraits of human breast tumours.* Nature, 2000. **406**(6797): p. 747-52.
23. Rouzier, R., et al., *Breast cancer molecular subtypes respond differently to preoperative chemotherapy.* Clin Cancer Res, 2005. **11**(16): p. 5678-85.
24. Spears, M. and J. Bartlett, *The potential role of estrogen receptors and the SRC family as targets for the treatment of breast cancer.* Expert Opin Ther Targets, 2009. **13**(6): p. 665-74.
25. Kaufman, B., et al., *Trastuzumab plus anastrozole versus anastrozole alone for the treatment of postmenopausal women with human epidermal growth factor receptor 2-positive, hormone receptor-positive metastatic breast cancer: results from the randomized phase III TAnDEM study.* J Clin Oncol, 2009. **27**(33): p. 5529-37.
26. Johnston, S., et al., *Lapatinib combined with letrozole versus letrozole and placebo as first-line therapy for postmenopausal hormone receptor-positive metastatic breast cancer.* J Clin Oncol, 2009. **27**(33): p. 5538-46.
27. Pirollo, K.F., et al., *Oncogene- transformed NIH 3T3 cells display radiation resistance levels indicative of a signal transduction pathway leading to the radiation-resistant phenotype.* Radiat Res, 1993. **135**(2): p. 234-43.
28. Slamon, D.J., et al., *Use of chemotherapy plus a monoclonal antibody against HER2 for metastatic breast cancer that overexpresses HER2.* N Engl J Med, 2001. **344**(11): p. 783-92.
29. Nielsen, T.O., et al., *Immunohistochemical and clinical characterization of the basal-like subtype of invasive breast carcinoma.* Clin Cancer Res, 2004. **10**(16): p. 5367-74.
30. Carey, L.A., et al., *Race, breast cancer subtypes, and survival in the Carolina Breast Cancer Study.* JAMA, 2006. **295**(21): p. 2492-502.
31. Abd El-Rehim, D.M., et al., *Expression of luminal and basal cytokeratins in human breast carcinoma.* J Pathol, 2004. **203**(2): p. 661-71.
32. Livasy, C.A., et al., *Phenotypic evaluation of the basal-like subtype of invasive breast carcinoma.* Mod Pathol, 2006. **19**(2): p. 264-71.
33. Rodriguez-Pinilla, S.M., et al., *Prognostic significance of basal-like phenotype and fascin expression in node-negative invasive breast carcinomas.* Clin Cancer Res, 2006. **12**(5): p. 1533-9.
34. Genomic Health. *Genomic Health. Oncotype Dx Information*. 2013; Available from: http://www.genomichealth.com/en-US/Breast/PatientsCaregiversInvasive.
35. Sparano, J.A. and S. Paik, *Development of the 21-gene assay and its application in clinical practice and clinical trials.* J Clin Oncol, 2008. **26**(5): p. 721-8.
36. Paik, S., et al., *Gene expression and benefit of chemotherapy in women with node-negative, estrogen receptor-positive breast cancer.* J Clin Oncol, 2006. **24**(23): p. 3726-34.
37. Mamounas, E.P., et al., *Association between the 21-gene recurrence score assay and risk of locoregional recurrence in node-negative, estrogen receptor-positive breast cancer: results from NSABP B-14 and NSABP B-20.* J Clin Oncol, 2010. **28**(10): p. 1677-83.
38. Tang, G., et al., *Comparison of the prognostic and predictive utilities of the 21-gene Recurrence Score assay and Adjuvant! for women with node-negative, ER-positive breast cancer: results from NSABP B-14 and NSABP B-20.* Breast Cancer Res Treat, 2011. **127**(1): p. 133-42.
39. Bland, C.S., *The Halsted mastectomy: present illness and past history.* West J Med, 1981. **134**(6): p. 549-55.

40. Geyer, C.E., et al., *Lapatinib plus capecitabine for HER2-positive advanced breast cancer.* N Engl J Med, 2006. **355**(26): p. 2733-43.
41. Hudis, C.A., *Trastuzumab--mechanism of action and use in clinical practice.* N Engl J Med, 2007. **357**(1): p. 39-51.
42. Osborne, C.K., *Tamoxifen in the treatment of breast cancer.* N Engl J Med, 1998. **339**(22): p. 1609-18.
43. Baum, M., *Current status of aromatase inhibitors in the management of breast cancer and critique of the NCIC MA-17 trial.* Cancer Control, 2004. **11**(4): p. 217-21.
44. The Lancet, *Tamoxifen for early breast cancer: an overview of the randomised trials. Early Breast Cancer Trialists' Collaborative Group.* Lancet, 1998. **351**(9114): p. 1451-67.
45. Ellis, P.A., et al., *Induction of apoptosis by tamoxifen and ICI 182780 in primary breast cancer.* Int J Cancer, 1997. **72**(4): p. 608-13.
46. Poggi, M.M., et al., *Eighteen-year results in the treatment of early breast carcinoma with mastectomy versus breast conservation therapy: the National Cancer Institute Randomized Trial.* Cancer, 2003. **98**(4): p. 697-702.
47. Kirova, Y.M., *Recent advances in breast cancer radiotherapy: Evolution or revolution, or how to decrease cardiac toxicity?* World J Radiol, 2010. **2**(3): p. 103-8.
48. Vaidya, J.S., et al., *The novel technique of delivering targeted intraoperative radiotherapy (Targit) for early breast cancer.* Eur J Surg Oncol, 2002. **28**(4): p. 447-54.
49. Bartel, D.P., *MicroRNAs: genomics, biogenesis, mechanism, and function.* Cell, 2004. **116**(2): p. 281-97.
50. Iorio, M.V. and C.M. Croce, *MicroRNA dysregulation in cancer: diagnostics, monitoring and therapeutics. A comprehensive review.* EMBO Mol Med, 2012. **4**(3): p. 143-59.
51. Rana, T.M., *Illuminating the silence: understanding the structure and function of small RNAs.* Nat Rev Mol Cell Biol, 2007. **8**(1): p. 23-36.
52. Sontheimer, E.J., *Assembly and function of RNA silencing complexes.* Nat Rev Mol Cell Biol, 2005. **6**(2): p. 127-38.
53. Du, T. and P.D. Zamore, *microPrimer: the biogenesis and function of microRNA.* Development, 2005. **132**(21): p. 4645-52.
54. Filipowicz, W., et al., *Post-transcriptional gene silencing by siRNAs and miRNAs.* Curr Opin Struct Biol, 2005. **15**(3): p. 331-41.
55. Kloosterman, W.P., et al., *Substrate requirements for let-7 function in the developing zebrafish embryo.* Nucleic Acids Res, 2004. **32**(21): p. 6284-91.
56. Lytle, J.R., T.A. Yario, and J.A. Steitz, *Target mRNAs are repressed as efficiently by microRNA-binding sites in the 5' UTR as in the 3' UTR.* Proc Natl Acad Sci U S A, 2007. **104**(23): p. 9667-72.
57. Jackson, R.J. and N. Standart, *How do microRNAs regulate gene expression?* Sci STKE, 2007. **2007**(367): p. re1.
58. Brodersen, P., et al., *Widespread translational inhibition by plant miRNAs and siRNAs.* Science, 2008. **320**(5880): p. 1185-90.
59. Lanet, E., et al., *Biochemical evidence for translational repression by Arabidopsis microRNAs.* Plant Cell, 2009. **21**(6): p. 1762-8.
60. Parker, R. and U. Sheth, *P bodies and the control of mRNA translation and degradation.* Mol Cell, 2007. **25**(5): p. 635-46.
61. Eulalio, A., I. Behm-Ansmant, and E. Izaurralde, *P bodies: at the crossroads of post-transcriptional pathways.* Nat Rev Mol Cell Biol, 2007. **8**(1): p. 9-22.

62. Lewis, B.P., C.B. Burge, and D.P. Bartel, *Conserved seed pairing, often flanked by adenosines, indicates that thousands of human genes are microRNA targets.* Cell, 2005. **120**(1): p. 15-20.
63. Lagos-Quintana, M., et al., *Identification of novel genes coding for small expressed RNAs.* Science, 2001. **294**(5543): p. 853-8.
64. Lau, N.C., et al., *An abundant class of tiny RNAs with probable regulatory roles in Caenorhabditis elegans.* Science, 2001. **294**(5543): p. 858-62.
65. Lee, R.C. and V. Ambros, *An extensive class of small RNAs in Caenorhabditis elegans.* Science, 2001. **294**(5543): p. 862-4.
66. Griffiths-Jones, S., *The microRNA Registry.* Nucleic Acids Res, 2004. **32**(Database issue): p. D109-11.
67. Griffiths-Jones, S., *miRBase: microRNA sequences and annotation.* Curr Protoc Bioinformatics, 2010. **Chapter 12**: p. Unit 12 9 1-10.
68. Lim, L.P., et al., *Vertebrate microRNA genes.* Science, 2003. **299**(5612): p. 1540.
69. Griffiths-Jones, S., et al., *miRBase: microRNA sequences, targets and gene nomenclature.* Nucleic Acids Res, 2006. **34**(Database issue): p. D140-4.
70. Lagos-Quintana, M., et al., *Identification of tissue-specific microRNAs from mouse.* Curr Biol, 2002. **12**(9): p. 735-9.
71. Hanahan, D. and R.A. Weinberg, *The hallmarks of cancer.* Cell, 2000. **100**(1): p. 57-70.
72. Hanahan, D. and R.A. Weinberg, *Hallmarks of cancer: the next generation.* Cell, 2011. **144**(5): p. 646-74.
73. Calin, G.A., et al., *Frequent deletions and down-regulation of micro- RNA genes miR15 and miR16 at 13q14 in chronic lymphocytic leukemia.* Proc Natl Acad Sci U S A, 2002. **99**(24): p. 15524-9.
74. Calin, G.A. and C.M. Croce, *MicroRNA signatures in human cancers.* Nat Rev Cancer, 2006. **6**(11): p. 857-66.
75. Liang, Z., et al., *Blockade of invasion and metastasis of breast cancer cells via targeting CXCR4 with an artificial microRNA.* Biochem Biophys Res Commun, 2007. **363**(3): p. 542-6.
76. Lanza, G., et al., *mRNA/microRNA gene expression profile in microsatellite unstable colorectal cancer.* Mol Cancer, 2007. **6**: p. 54.
77. Moore, L.M. and W. Zhang, *Targeting miR-21 in glioma: a small RNA with big potential.* Expert Opin Ther Targets, 2010. **14**(11): p. 1247-57.
78. Selcuklu, S.D., M.T. Donoghue, and C. Spillane, *miR-21 as a key regulator of oncogenic processes.* Biochem Soc Trans, 2009. **37**(Pt 4): p. 918-25.
79. Krichevsky, A.M. and G. Gabriely, *miR-21: a small multi-faceted RNA.* J Cell Mol Med, 2009. **13**(1): p. 39-53.
80. Rossi, S., et al., *microRNA fingerprinting of CLL patients with chromosome 17p deletion identify a miR-21 score that stratifies early survival.* Blood, 2010. **116**(6): p. 945-52.
81. Reid, G., et al., *Restoring expression of miR-16: a novel approach to therapy for malignant pleural mesothelioma.* Ann Oncol, 2013.
82. Peng, Y., et al., *Insulin growth factor signaling is regulated by microRNA-486, an underexpressed microRNA in lung cancer.* Proc Natl Acad Sci U S A, 2013. **110**(37): p. 15043-8.
83. Yu, L., et al., *Early detection of lung adenocarcinoma in sputum by a panel of microRNA markers.* Int J Cancer, 2010. **127**(12): p. 2870-8.
84. Hu, Z., et al., *Serum microRNA signatures identified in a genome-wide serum microRNA expression profiling predict survival of non-small-cell lung cancer.* J Clin Oncol, 2010. **28**(10): p. 1721-6.

85. Calin, G.A., et al., *A MicroRNA signature associated with prognosis and progression in chronic lymphocytic leukemia.* N Engl J Med, 2005. **353**(17): p. 1793-801.
86. Yanaihara, N., et al., *Unique microRNA molecular profiles in lung cancer diagnosis and prognosis.* Cancer Cell, 2006. **9**(3): p. 189-98.
87. Li, X., et al., *Survival prediction of gastric cancer by a seven-microRNA signature.* Gut, 2010. **59**(5): p. 579-85.
88. Caramuta, S., et al., *MicroRNA expression profiles associated with mutational status and survival in malignant melanoma.* J Invest Dermatol, 2010. **130**(8): p. 2062-70.
89. Cortez, M.A., et al., *MicroRNAs in body fluids--the mix of hormones and biomarkers.* Nat Rev Clin Oncol, 2011. **8**(8): p. 467-77.
90. Kosaka, N., H. Iguchi, and T. Ochiya, *Circulating microRNA in body fluid: a new potential biomarker for cancer diagnosis and prognosis.* Cancer Sci, 2010. **101**(10): p. 2087-92.
91. Taylor, D.D. and C. Gercel-Taylor, *MicroRNA signatures of tumor-derived exosomes as diagnostic biomarkers of ovarian cancer.* Gynecol Oncol, 2008. **110**(1): p. 13-21.
92. Mitchell, P.S., et al., *Circulating microRNAs as stable blood-based markers for cancer detection.* Proc Natl Acad Sci U S A, 2008. **105**(30): p. 10513-8.
93. Lawrie, C.H., et al., *Detection of elevated levels of tumour-associated microRNAs in serum of patients with diffuse large B-cell lymphoma.* Br J Haematol, 2008. **141**(5): p. 672-5.
94. Chen, X., et al., *Characterization of microRNAs in serum: a novel class of biomarkers for diagnosis of cancer and other diseases.* Cell Res, 2008. **18**(10): p. 997-1006.
95. Gilad, S., et al., *Serum microRNAs are promising novel biomarkers.* PLoS One, 2008. **3**(9): p. e3148.
96. Iorio, M.V., et al., *MicroRNA gene expression deregulation in human breast cancer.* Cancer Res, 2005. **65**(16): p. 7065-70.
97. Blenkiron, C., et al., *MicroRNA expression profiling of human breast cancer identifies new markers of tumor subtype.* Genome Biol, 2007. **8**(10): p. R214.
98. Sempere, L.F., et al., *Altered MicroRNA expression confined to specific epithelial cell subpopulations in breast cancer.* Cancer Res, 2007. **67**(24): p. 11612-20.
99. Mattie, M.D., et al., *Optimized high-throughput microRNA expression profiling provides novel biomarker assessment of clinical prostate and breast cancer biopsies.* Mol Cancer, 2006. **5**: p. 24.
100. Lowery, A.J., et al., *MicroRNA signatures predict oestrogen receptor, progesterone receptor and HER2/neu receptor status in breast cancer.* Breast Cancer Res, 2009. **11**(3): p. R27.
101. Lowery, A. and Z. Han, *Assessment of tumor response to tyrosine kinase inhibitors.* Front Biosci, 2012. **17**: p. 1996-2007.
102. Heneghan, H.M., et al., *Systemic miRNA-195 differentiates breast cancer from other malignancies and is a potential biomarker for detecting noninvasive and early stage disease.* Oncologist, 2010. **15**(7): p. 673-82.
103. Hannafon, B.N., et al., *Expression of microRNA and their gene targets are dysregulated in preinvasive breast cancer.* Breast Cancer Res, 2011. **13**(2): p. R24.
104. Wang, F., et al., *Correlation and quantitation of microRNA aberrant expression in tissues and sera from patients with breast tumor.* Gynecol Oncol, 2010. **119**(3): p. 586-93.
105. Waters, P.S., et al., *Relationship between circulating and tissue microRNAs in a murine model of breast cancer.* PLoS One, 2012. **7**(11): p. e50459.
106. Jan, C.H., et al., *Formation, regulation and evolution of Caenorhabditis elegans 3'UTRs.* Nature, 2011. **469**(7328): p. 97-101.

107. Betel, D., et al., *The microRNA.org resource: targets and expression.* Nucleic Acids Res, 2008. **36**(Database issue): p. D149-53.
108. Tan, Y., et al., *Transcriptional inhibiton of Hoxd4 expression by miRNA-10a in human breast cancer cells.* BMC Mol Biol, 2009. **10**: p. 12.
109. Takahashi, H., et al., *TGF-beta and retinoic acid induce the microRNA miR-10a, which targets Bcl-6 and constrains the plasticity of helper T cells.* Nat Immunol, 2012. **13**(6): p. 587-95.
110. Garzon, R., et al., *MicroRNA signatures associated with cytogenetics and prognosis in acute myeloid leukemia.* Blood, 2008. **111**(6): p. 3183-9.
111. Meseguer, S., et al., *MicroRNAs-10a and -10b contribute to retinoic acid-induced differentiation of neuroblastoma cells and target the alternative splicing regulatory factor SFRS1 (SF2/ASF).* J Biol Chem, 2011. **286**(6): p. 4150-64.
112. Foley, N.H., et al., *MicroRNAs 10a and 10b are potent inducers of neuroblastoma cell differentiation through targeting of nuclear receptor corepressor 2.* Cell Death Differ, 2011. **18**(7): p. 1089-98.
113. Ma, L., et al., *Therapeutic silencing of miR-10b inhibits metastasis in a mouse mammary tumor model.* Nat Biotechnol, 2010. **28**(4): p. 341-7.
114. Hoppe, R., et al., *Increased expression of miR-126 and miR-10a predict prolonged relapse-free time of primary oestrogen receptor-positive breast cancer following tamoxifen treatment.* European Journal of Cancer, 2013(0).
115. Tie, J., et al., *MiR-218 inhibits invasion and metastasis of gastric cancer by targeting the Robo1 receptor.* PLoS Genet, 2010. **6**(3): p. e1000879.
116. Lee, J.W., et al., *Altered MicroRNA expression in cervical carcinomas.* Clin Cancer Res, 2008. **14**(9): p. 2535-42.
117. Keller, A., et al., *miRNAs in lung cancer - studying complex fingerprints in patient's blood cells by microarray experiments.* BMC Cancer, 2009. **9**: p. 353.
118. Liu, D.Z., et al., *Integrated analysis of mRNA and microRNA expression in mature neurons, neural progenitor cells and neuroblastoma cells.* Gene, 2012. **495**(2): p. 120-7.
119. Buda, I., et al., *Differential expression of microRNAs between aggressive and non-aggressive papillary thyroid carcinoma.* Head Neck Oncol, 2012. **4**(2): p. 52.
120. Wu, Z.S., et al., *MiR-339-5p inhibits breast cancer cell migration and invasion in vitro and may be a potential biomarker for breast cancer prognosis.* BMC Cancer, 2010. **10**: p. 542.
121. Pollari, S., et al., *Identification of microRNAs inhibiting TGF-beta-induced IL-11 production in bone metastatic breast cancer cells.* PLoS One, 2012. **7**(5): p. e37361.
122. De La Vieja, A., et al., *Molecular analysis of the sodium/iodide symporter: impact on thyroid and extrathyroid pathophysiology.* Physiol Rev, 2000. **80**(3): p. 1083-105.
123. Flow Cytometry. *NIS Stucture*. 2013; Available from: http://www.dflock.co.uk/portfolio/diagrams/images/Sodium%20Iodide%20Symporter.png.
124. Dohan, O., et al., *The sodium/iodide Symporter (NIS): characterization, regulation, and medical significance.* Endocr Rev, 2003. **24**(1): p. 48-77.
125. Dohan, O. and N. Carrasco, *Advances in Na(+)/I(-) symporter (NIS) research in the thyroid and beyond.* Mol Cell Endocrinol, 2003. **213**(1): p. 59-70.
126. Douglas, R.S. *Radioiodine Therapy for Hyperthyroidism*. N Engl J Med 2011; Available from: http://2.bp.blogspot.com/-XcjRvW2JhWQ/TVPqyaZVZ6I/AAAAAAAAAX0/ahqsAEQgOQc/s1600/1.jpg.
127. Gilliland, F.D., et al., *Prognostic factors for thyroid carcinoma. A population-based study of 15,698 cases from the Surveillance, Epidemiology and End Results (SEER) program 1973-1991.* Cancer, 1997. **79**(3): p. 564-73.

128. Skugor, J.B.W., *Thyroid Disorders: A Cleveland Clinic Guide*. 2006: Cleveland Clinic Press.
129. NIS Thyroid. *NIS accumulation in the Thyroid*. 2013; Available from: http://2012books.lardbucket.org/books/introduction-to-chemistry-general-organic-and-biological/section_14/b924b2d45c985679ce15660b8478f343.jpg.
130. Institiute, N.C., *What you need to know about Thyroid Cancer*. 2012.
131. Tazebay, U.H., et al., *The mammary gland iodide transporter is expressed during lactation and in breast cancer.* Nat Med, 2000. **6**(8): p. 871-8.
132. Renier, C., et al., *Endogenous NIS expression in triple-negative breast cancers.* Ann Surg Oncol, 2009. **16**(4): p. 962-8.
133. Rudnicka, L., et al., *Expression of the Na(+)/I(-) symporter in invasive ductal breast cancer.* Folia Histochem Cytobiol, 2003. **41**(1): p. 37-40.
134. Upadhyay, G., et al., *Functional expression of sodium iodide symporter (NIS) in human breast cancer tissue.* Breast Cancer Res Treat, 2003. **77**(2): p. 157-65.
135. Wapnir, I.L., et al., *Immunohistochemical profile of the sodium/iodide symporter in thyroid, breast, and other carcinomas using high density tissue microarrays and conventional sections.* J Clin Endocrinol Metab, 2003. **88**(4): p. 1880-8.
136. Kilbane, M.T., et al., *Tissue iodine content and serum-mediated 125I uptake-blocking activity in breast cancer.* J Clin Endocrinol Metab, 2000. **85**(3): p. 1245-50.
137. Moon, D., et al., *Correlation between 99mTc-pertechnetate uptakes and expressions of human sodium iodide symporter gene in breast tumor tissues.* Nucl Med Biol, 2001. **28**(7): p. 829-34.
138. Ryan, J., et al., *The sodium iodide symporter (NIS) and potential regulators in normal, benign and malignant human breast tissue.* PLoS One, 2011. **6**(1): p. e16023.
139. Alotaibi, H., et al., *Unliganded estrogen receptor-alpha activates transcription of the mammary gland Na+/I- symporter gene.* Biochem Biophys Res Commun, 2006. **345**(4): p. 1487-96.
140. Chatterjee, S., et al., *Quantitative immunohistochemical analysis reveals association between sodium iodide symporter and estrogen receptor expression in breast cancer.* PLoS One, 2013. **8**(1): p. e54055.
141. Kogai, T., et al., *Differential regulation of sodium/iodide symporter gene expression by nuclear receptor ligands in MCF-7 breast cancer cells.* Endocrinology, 2005. **146**(7): p. 3059-69.
142. Kogai, T., et al., *Retinoic acid induces sodium/iodide symporter gene expression and radioiodide uptake in the MCF-7 breast cancer cell line.* Proc Natl Acad Sci U S A, 2000. **97**(15): p. 8519-24.
143. Sponziello, M., et al., *Regulation of sodium/iodide symporter and lactoperoxidase expression in four human breast cancer cell lines.* J Endocrinol Invest, 2010. **33**(1): p. 2-6.
144. Kogai, T., et al., *Systemic retinoic acid treatment induces sodium/iodide symporter expression and radioiodide uptake in mouse breast cancer models.* Cancer Res, 2004. **64**(1): p. 415-22.
145. Tanosaki, S., et al., *Effect of ligands of nuclear hormone receptors on sodium/iodide symporter expression and activity in breast cancer cells.* Breast Cancer Res Treat, 2003. **79**(3): p. 335-45.
146. Willhauck, M.J., et al., *Functional sodium iodide symporter expression in breast cancer xenografts in vivo after systemic treatment with retinoic acid and dexamethasone.* Breast Cancer Res Treat, 2008. **109**(2): p. 263-72.

147. Lee, S. and M. Privalsky, *Heterodimers of retinoic acid receptors and thyroid hormone receptors display unique combinatorial regulatory properties.* Mol Endocrinol, 2005. **19**(4): p. 863-78.
148. Barton, K.N., et al., *Phase I study of noninvasive imaging of adenovirus-mediated gene expression in the human prostate.* Mol Ther, 2008. **16**(10): p. 1761-9.
149. Lorusso, G. and C. Ruegg, *The tumor microenvironment and its contribution to tumor evolution toward metastasis.* Histochem Cell Biol, 2008. **130**(6): p. 1091-103.
150. Coussens, L.M. and Z. Werb, *Inflammation and cancer.* Nature, 2002. **420**(6917): p. 860-7.
151. Junttila, M.R. and F.J. de Sauvage, *Influence of tumour micro-environment heterogeneity on therapeutic response.* Nature, 2013. **501**(7467): p. 346-54.
152. Dvorak, H.F., *Tumors: wounds that do not heal. Similarities between tumor stroma generation and wound healing.* N Engl J Med, 1986. **315**(26): p. 1650-9.
153. Robinson, S.C. and L.M. Coussens, *Soluble mediators of inflammation during tumor development.* Adv Cancer Res, 2005. **93**: p. 159-87.
154. Bhowmick, N.A., E.G. Neilson, and H.L. Moses, *Stromal fibroblasts in cancer initiation and progression.* Nature, 2004. **432**(7015): p. 332-7.
155. Hall, B., M. Andreeff, and F. Marini, *The participation of mesenchymal stem cells in tumor stroma formation and their application as targeted-gene delivery vehicles.* Handb Exp Pharmacol, 2007(180): p. 263-83.
156. Nieman, K.M., et al., *Adipocytes promote ovarian cancer metastasis and provide energy for rapid tumor growth.* Nat Med, 2011. **17**(11): p. 1498-503.
157. Joyce, J.A. and J.W. Pollard, *Microenvironmental regulation of metastasis.* Nat Rev Cancer, 2009. **9**(4): p. 239-52.
158. Hanahan, D. and L.M. Coussens, *Accessories to the crime: functions of cells recruited to the tumor microenvironment.* Cancer Cell, 2012. **21**(3): p. 309-22.
159. Gupta, G.P. and J. Massague, *Cancer metastasis: building a framework.* Cell, 2006. **127**(4): p. 679-95.
160. Meads, M.B., R.A. Gatenby, and W.S. Dalton, *Environment-mediated drug resistance: a major contributor to minimal residual disease.* Nat Rev Cancer, 2009. **9**(9): p. 665-74.
161. Olive, K.P., et al., *Inhibition of Hedgehog signaling enhances delivery of chemotherapy in a mouse model of pancreatic cancer.* Science, 2009. **324**(5933): p. 1457-61.
162. Lin, J., et al., *Carcinoma-associated fibroblasts promotes the proliferation of a lingual carcinoma cell line by secreting keratinocyte growth factor.* Tumour Biol, 2011. **32**(3): p. 597-602.
163. Orimo, A., et al., *Stromal fibroblasts present in invasive human breast carcinomas promote tumor growth and angiogenesis through elevated SDF-1/CXCL12 secretion.* Cell, 2005. **121**(3): p. 335-48.
164. Polyak, K. and W.C. Hahn, *Roots and stems: stem cells in cancer.* Nat Med, 2006. **12**(3): p. 296-300.
165. Korkaya, H., S. Liu, and M.S. Wicha, *Breast cancer stem cells, cytokine networks, and the tumor microenvironment.* The Journal of clinical investigation, 2011. **121**(10): p. 3804-9.
166. Fuyuhiro, Y., et al., *Cancer-associated orthotopic myofibroblasts stimulates the motility of gastric carcinoma cells.* Cancer Sci, 2012. **103**(4): p. 797-805.
167. Nakagawa, H., et al., *Role of cancer-associated stromal fibroblasts in metastatic colon cancer to the liver and their expression profiles.* Oncogene, 2004. **23**(44): p. 7366-77.

168. Petersen, O.W., et al., *Epithelial to mesenchymal transition in human breast cancer can provide a nonmalignant stroma.* Am J Pathol, 2003. **162**(2): p. 391-402.
169. Direkze, N.C., et al., *Bone marrow contribution to tumor-associated myofibroblasts and fibroblasts.* Cancer Res, 2004. **64**(23): p. 8492-5.
170. Jotzu, C., et al., *Adipose tissue-derived stem cells differentiate into carcinoma-associated fibroblast-like cells under the influence of tumor-derived factors.* Anal Cell Pathol (Amst), 2010. **33**(2): p. 61-79.
171. Mueller, M.M. and N.E. Fusenig, *Friends or foes - bipolar effects of the tumour stroma in cancer.* Nat Rev Cancer, 2004. **4**(11): p. 839-49.
172. Medema, J.P. and L. Vermeulen, *Microenvironmental regulation of stem cells in intestinal homeostasis and cancer.* Nature, 2011. **474**(7351): p. 318-26.
173. Strell, C., H. Rundqvist, and A. Ostman, *Fibroblasts--a key host cell type in tumor initiation, progression, and metastasis.* Ups J Med Sci, 2012. **117**(2): p. 187-95.
174. Kalluri, R. and M. Zeisberg, *Fibroblasts in cancer.* Nat Rev Cancer, 2006. **6**(5): p. 392-401.
175. Pittenger, M.F., et al., *Multilineage potential of adult human mesenchymal stem cells.* Science, 1999. **284**(5411): p. 143-7.
176. Barry, F. and J. Murphy, *Mesenchymal stem cells: clinical applications and biological characterization.* Int J Biochem Cell Biol, 2004. **36**(4): p. 568-84.
177. Dominici, M., et al., *Minimal criteria for defining multipotent mesenchymal stromal cells. The International Society for Cellular Therapy position statement.* Cytotherapy, 2006. **8**(4): p. 315-7.
178. Kidd, S., et al., *The (in) auspicious role of mesenchymal stromal cells in cancer: be it friend or foe.* Cytotherapy, 2008. **10**(7): p. 657-67.
179. Fox, J.M., et al., *Recent advances into the understanding of mesenchymal stem cell trafficking.* Br J Haematol, 2007. **137**(6): p. 491-502.
180. Studeny, M., et al., *Bone marrow-derived mesenchymal stem cells as vehicles for interferon-beta delivery into tumors.* Cancer Res, 2002. **62**(13): p. 3603-8.
181. Mishra, P.J., J.W. Glod, and D. Banerjee, *Mesenchymal stem cells: flip side of the coin.* Cancer Res, 2009. **69**(4): p. 1255-8.
182. Chamberlain, G., et al., *Concise review: mesenchymal stem cells: their phenotype, differentiation capacity, immunological features, and potential for homing.* Stem Cells, 2007. **25**(11): p. 2739-49.
183. Masters, J.R. and G.N. Stacey, *Changing medium and passaging cell lines.* Nat Protoc, 2007. **2**(9): p. 2276-84.
184. Freshney, R.I., *Defined Media and Supplements*, in *Culture of Animal Cells*. 2010, John Wiley & Sons, Inc. p. 99-114.
185. Freshney, R.I., *Aseptic Technique*, in *Culture of Animal Cells*. 2010, John Wiley & Sons, Inc. p. 57-70.
186. Speirs, V., et al., *Short-term primary culture of epithelial cells derived from human breast tumours.* Br J Cancer, 1998. **78**(11): p. 1421-9.
187. Thermo Fisher Scientific, *Thermo Scientific SMARTchoice shMIMIC Lentiviral microRNA*. 2013, Thermo Fisher Scientific Inc. p. 47.
188. Barry, F.P. and J.M. Murphy, *Mesenchymal stem cells: clinical applications and biological characterization.* Int J Biochem Cell Biol, 2004. **36**(4): p. 568-84.
189. Gerstenfeld, L.C., et al., *Expression of differentiated function by mineralizing cultures of chicken osteoblasts.* Dev Biol, 1987. **122**(1): p. 49-60.
190. Abcam Ltd. *Abcam*. 2010; Available from: http://www.abcam.com/index.html?pageconfig=resource&rid=11446.
191. Givan, A.L., *Principles of flow cytometry: an overview.* Methods Cell Biol, 2001. **63**: p. 19-50.

192. Flow Book. *Flow Cytometry basic Introduction*. 2011; Available from: http://flowbook.denovosoftware.com/Flow_Book/Chapter_5%3A_Immunofluorescence_and_Colour_Compensation.
193. Baek, D., et al., *The impact of microRNAs on protein output.* Nature, 2008. **455**(7209): p. 64-71.
194. Hendrickson, D.G., et al., *Systematic identification of mRNAs recruited to argonaute 2 by specific microRNAs and corresponding changes in transcript abundance.* PLoS One, 2008. **3**(5): p. e2126.
195. Friedman, R.C., et al., *Most mammalian mRNAs are conserved targets of microRNAs.* Genome Res, 2009. **19**(1): p. 92-105.
196. Lall, S., et al., *A genome-wide map of conserved microRNA targets in C. elegans.* Curr Biol, 2006. **16**(5): p. 460-71.
197. SwitchGear Genomics. *Luciferase Reporter Construct*. 2010; Available from: http://sgg.worldzoo.net/lightswitch-integrated-mirna-target-validation-system.
198. ThermoScientific Ltd. *Optimal DharmaFECT Concentration*. 2010; Available from: http://www.thermoscientificbio.com/uploadedFiles/Resources/DharmaFECT-cell-type-guide.pdf?redirect=true.
199. McNeill, R.E., N. Miller, and M.J. Kerin, *Evaluation and validation of candidate endogenous control genes for real-time quantitative PCR studies of breast cancer.* BMC Mol Biol, 2007. **8**: p. 107.
200. Davoren, P.A., et al., *Identification of suitable endogenous control genes for microRNA gene expression analysis in human breast cancer.* BMC Mol Biol, 2008. **9**: p. 76.
201. Davis, H.E., J.R. Morgan, and M.L. Yarmush, *Polybrene increases retrovirus gene transfer efficiency by enhancing receptor-independent virus adsorption on target cell membranes.* Biophys Chem, 2002. **97**(2-3): p. 159-72.
202. Ross, D.S., *Radioiodine therapy for hyperthyroidism.* N Engl J Med, 2011. **364**(6): p. 542-50.
203. Schlumberger, M.J., *Papillary and follicular thyroid carcinoma.* N Engl J Med, 1998. **338**(5): p. 297-306.
204. Spitzweg, C. and J.C. Morris, *The sodium iodide symporter: its pathophysiological and therapeutic implications.* Clin Endocrinol (Oxf), 2002. **57**(5): p. 559-74.
205. Nicola, J.P., et al., *The Na+/I- symporter mediates active iodide uptake in the intestine.* Am J Physiol Cell Physiol, 2009. **296**(4): p. C654-62.
206. Cancroft, E.T. and S.J. Goldsmith, *99m Tc-pertechnetate scintigraphy as an aid in the diagnosis of breast masses.* Radiology, 1973. **106**(2): p. 441-4.
207. Eskin, B.A., et al., *Human breast uptake of radioactive iodine.* Obstet Gynecol, 1974. **44**(3): p. 398-402.
208. Lyttle, C.R., et al., *Peroxidase activity and iodide uptake in hormone-responsive and hormone-independent GR mouse mammary tumors.* J Natl Cancer Inst, 1979. **62**(4): p. 1031-4.
209. Venkataraman, G.M., et al., *Restoration of iodide uptake in dedifferentiated thyroid carcinoma: relationship to human Na+/I-symporter gene methylation status.* J Clin Endocrinol Metab, 1999. **84**(7): p. 2449-57.
210. Kogai, T., et al., *Regulation of sodium iodide symporter gene expression by Rac1/p38beta mitogen-activated protein kinase signaling pathway in MCF-7 breast cancer cells.* J Biol Chem, 2012. **287**(5): p. 3292-300.
211. Kogai, T., K. Taki, and G.A. Brent, *Enhancement of sodium/iodide symporter expression in thyroid and breast cancer.* Endocr Relat Cancer, 2006. **13**(3): p. 797-826.

212. Lund, A.H., *miR-10 in development and cancer.* Cell Death Differ, 2010. **17**(2): p. 209-14.
213. Manavalan, T.T., et al., *Differential expression of microRNA expression in tamoxifen-sensitive MCF-7 versus tamoxifen-resistant LY2 human breast cancer cells.* Cancer Lett, 2011. **313**(1): p. 26-43.
214. Pogribny, I.P., et al., *Alterations of microRNAs and their targets are associated with acquired resistance of MCF-7 breast cancer cells to cisplatin.* Int J Cancer, 2010. **127**(8): p. 1785-94.
215. Widschwendter, M., et al., *Loss of retinoic acid receptor beta expression in breast cancer and morphologically normal adjacent tissue but not in the normal breast tissue distant from the cancer.* Cancer Res, 1997. **57**(19): p. 4158-61.
216. Weiss, F.U., et al., *Retinoic acid receptor antagonists inhibit miR-10a expression and block metastatic behavior of pancreatic cancer.* Gastroenterology, 2009. **137**(6): p. 2136-45 e1-7.
217. Yerushalmi, R., et al., *Ki67 in breast cancer: prognostic and predictive potential.* Lancet Oncol, 2010. **11**(2): p. 174-83.
218. TargetScan. *Target Prediction Software microRNA.org*. 2012; Available from: http://www.microrna.org/microrna/getMrna.do?gene=6528&utr=10685&organism=9606&matureName=hsa-miR-339-5p#.
219. Berger, F., et al., *Mammary radioiodine accumulation due to functional sodium iodide symporter expression in a benign fibroadenoma.* Biochem Biophys Res Commun, 2006. **349**(4): p. 1258-63.
220. Willhauck, M., et al., *Functional sodium iodide symporter expression in breast cancer xenografts in vivo after systemic treatment with retinoic acid and dexamethasone.* Breast Cancer Res Treat, 2008. **109**(2): p. 263-72.
221. Kogai, T., et al., *Differential regulation of sodium/iodide symporter gene expression by nuclear receptor ligands in MCF-7 breast cancer cells.* Endocrinology, 2005. **146**(7): p. 3059-69.
222. Kogai, T., et al., *Retinoic acid stimulation of the sodium/iodide symporter in MCF-7 breast cancer cells is mediated by the insulin growth factor-I/phosphatidylinositol 3-kinase and p38 mitogen-activated protein kinase signaling pathways.* J Clin Endocrinol Metab, 2008. **93**(5): p. 1884-92.
223. Castillo, L., et al., *Analysis of retinoic acid receptor beta expression in normal and malignant laryngeal mucosa by a sensitive and routine applicable reverse transcription-polymerase chain reaction enzyme-linked immunosorbent assay method.* Clin Cancer Res, 1997. **3**(11): p. 2137-42.
224. Picard, E., et al., *Expression of retinoid receptor genes and proteins in non-small-cell lung cancer.* J Natl Cancer Inst, 1999. **91**(12): p. 1059-66.
225. Xu, X.C., et al., *Suppression of retinoic acid receptor beta in non-small-cell lung cancer in vivo: implications for lung cancer development.* J Natl Cancer Inst, 1997. **89**(9): p. 624-9.
226. Silva, J., et al., *Expression of thyroid hormone receptor/erbA genes is altered in human breast cancer.* Oncogene, 2002. **21**(27): p. 4307-16.
227. Kawamoto, H., H. Koizumi, and T. Uchikoshi, *Expression of the G2-M checkpoint regulators cyclin B1 and cdc2 in nonmalignant and malignant human breast lesions: immunocytochemical and quantitative image analyses.* Am J Pathol, 1997. **150**(1): p. 15-23.
228. Rudolph, P., et al., *Differential prognostic impact of the cyclins E and B in premenopausal and postmenopausal women with lymph node-negative breast cancer.* Int J Cancer, 2003. **105**(5): p. 674-80.

229. Kuhling, H., et al., *Expression of cyclins E, A, and B, and prognosis in lymph node-negative breast cancer.* J Pathol, 2003. **199**(4): p. 424-31.
230. Aaltonen, K., et al., *Cyclin D1 expression is associated with poor prognostic features in estrogen receptor positive breast cancer.* Breast Cancer Res Treat, 2009. **113**(1): p. 75-82.
231. John, B., et al., *Human MicroRNA targets.* PLoS Biol, 2004. **2**(11): p. e363.
232. Pines, J. and T. Hunter, *Human cyclin A is adenovirus E1A-associated protein p60 and behaves differently from cyclin B.* Nature, 1990. **346**(6286): p. 760-3.
233. Agarwal, R., et al., *Integrative analysis of cyclin protein levels identifies cyclin b1 as a classifier and predictor of outcomes in breast cancer.* Clin Cancer Res, 2009. **15**(11): p. 3654-62.
234. Murakami, H., et al., *Determination of the prognostic significance of cyclin B1 overexpression in patients with esophageal squamous cell carcinoma.* Virchows Arch, 1999. **434**(2): p. 153-8.
235. Nozoe, T., et al., *Significance of cyclin B1 expression as an independent prognostic indicator of patients with squamous cell carcinoma of the esophagus.* Clin Cancer Res, 2002. **8**(3): p. 817-22.
236. Soria, J.C., et al., *Overexpression of cyclin B1 in early-stage non-small cell lung cancer and its clinical implication.* Cancer Res, 2000. **60**(15): p. 4000-4.
237. Yoshida, T., et al., *The clinical significance of Cyclin B1 and Wee1 expression in non-small-cell lung cancer.* Ann Oncol, 2004. **15**(2): p. 252-6.
238. Ikuerowo, S.O., et al., *Alteration of subcellular and cellular expression patterns of cyclin B1 in renal cell carcinoma is significantly related to clinical progression and survival of patients.* Int J Cancer, 2006. **119**(4): p. 867-74.
239. Hassan, K.A., et al., *Cyclin B1 overexpression and resistance to radiotherapy in head and neck squamous cell carcinoma.* Cancer Res, 2002. **62**(22): p. 6414-7.
240. Takeno, S., et al., *Prognostic value of cyclin B1 in patients with esophageal squamous cell carcinoma.* Cancer, 2002. **94**(11): p. 2874-81.
241. Yuan, J., et al., *Cyclin B1 depletion inhibits proliferation and induces apoptosis in human tumor cells.* Oncogene, 2004. **23**(34): p. 5843-52.
242. Androic, I., et al., *Targeting cyclin B1 inhibits proliferation and sensitizes breast cancer cells to taxol.* BMC Cancer, 2008. **8**: p. 391.
243. Gattolliat, C.H., et al., *Expression of miR-487b and miR-410 encoded by 14q32.31 locus is a prognostic marker in neuroblastoma.* Br J Cancer, 2011. **105**(9): p. 1352-61.
244. Schwarzenbach, H., D.S. Hoon, and K. Pantel, *Cell-free nucleic acids as biomarkers in cancer patients.* Nat Rev Cancer, 2011. **11**(6): p. 426-37.
245. Bissell, M.J. and D. Radisky, *Putting tumours in context.* Nat Rev Cancer, 2001. **1**(1): p. 46-54.
246. Hu, M. and K. Polyak, *Molecular characterisation of the tumour microenvironment in breast cancer.* Eur J Cancer, 2008. **44**(18): p. 2760-5.
247. Reddig, P.J. and R.L. Juliano, *Clinging to life: cell to matrix adhesion and cell survival.* Cancer Metastasis Rev, 2005. **24**(3): p. 425-39.
248. Bidard, F.C., et al., *A "class action" against the microenvironment: do cancer cells cooperate in metastasis?* Cancer Metastasis Rev, 2008. **27**(1): p. 5-10.
249. Kopfstein, L. and G. Christofori, *Metastasis: cell-autonomous mechanisms versus contributions by the tumor microenvironment.* Cell Mol Life Sci, 2006. **63**(4): p. 449-68.
250. Weinberg, R.A., *Coevolution in the tumor microenvironment.* Nat Genet, 2008. **40**(5): p. 494-5.

251. Tlsty, T.D. and P.W. Hein, *Know thy neighbor: stromal cells can contribute oncogenic signals.* Curr Opin Genet Dev, 2001. **11**(1): p. 54-9.
252. Sappino, A.P., et al., *Smooth-muscle differentiation in stromal cells of malignant and non-malignant breast tissues.* Int J Cancer, 1988. **41**(5): p. 707-12.
253. Ronnov-Jessen, L., et al., *A fibroblast-associated antigen: characterization in fibroblasts and immunoreactivity in smooth muscle differentiated stromal cells.* J Histochem Cytochem, 1992. **40**(4): p. 475-86.
254. Tsukada, T., et al., *HHF35, a muscle actin-specific monoclonal antibody. II. Reactivity in normal, reactive, and neoplastic human tissues.* Am J Pathol, 1987. **127**(2): p. 389-402.
255. Kojima, Y., et al., *Autocrine TGF-beta and stromal cell-derived factor-1 (SDF-1) signaling drives the evolution of tumor-promoting mammary stromal myofibroblasts.* Proc Natl Acad Sci U S A, 2010. **107**(46): p. 20009-14.
256. Zeisberg, E.M., et al., *Discovery of endothelial to mesenchymal transition as a source for carcinoma-associated fibroblasts.* Cancer Res, 2007. **67**(21): p. 10123-8.
257. Kidd, S., et al., *Origins of the tumor microenvironment: quantitative assessment of adipose-derived and bone marrow-derived stroma.* PLoS One, 2012. **7**(2): p. e30563.
258. Ishii, G., et al., *Bone-marrow-derived myofibroblasts contribute to the cancer-induced stromal reaction.* Biochem Biophys Res Commun, 2003. **309**(1): p. 232-40.
259. Wu, Y., et al., *Mesenchymal stem cells enhance wound healing through differentiation and angiogenesis.* Stem Cells, 2007. **25**(10): p. 2648-59.
260. Yan, X.L., et al., *Mesenchymal stem cells from primary breast cancer tissue promote cancer proliferation and enhance mammosphere formation partially via EGF/EGFR/Akt pathway.* Breast Cancer Res Treat, 2012. **132**(1): p. 153-64.
261. Radisky, D.C., P.A. Kenny, and M.J. Bissell, *Fibrosis and cancer: do myofibroblasts come also from epithelial cells via EMT?* J Cell Biochem, 2007. **101**(4): p. 830-9.
262. Henniker, A.J., *Cd90.* J Biol Regul Homeost Agents, 2001. **15**(4): p. 392-3.
263. True, L.D., et al., *CD90/THY1 is overexpressed in prostate cancer-associated fibroblasts and could serve as a cancer biomarker.* Mod Pathol, 2010. **23**(10): p. 1346-56.
264. Quante, M., et al., *Bone marrow-derived myofibroblasts contribute to the mesenchymal stem cell niche and promote tumor growth.* Cancer Cell, 2011. **19**(2): p. 257-72.
265. Nimeus-Malmstrom, E., et al., *Cyclin B1 is a prognostic proliferation marker with a high reproducibility in a population-based lymph node negative breast cancer cohort.* Int J Cancer, 2010. **127**(4): p. 961-7.
266. Gaur, A., et al., *Characterization of microRNA expression levels and their biological correlates in human cancer cell lines.* Cancer Res, 2007. **67**(6): p. 2456-68.
267. Lu, J., et al., *MicroRNA expression profiles classify human cancers.* Nature, 2005. **435**(7043): p. 834-8.
268. Kota, J., et al., *Therapeutic microRNA delivery suppresses tumorigenesis in a murine liver cancer model.* Cell, 2009. **137**(6): p. 1005-17.
269. Esquela-Kerscher, A., et al., *The let-7 microRNA reduces tumor growth in mouse models of lung cancer.* Cell Cycle, 2008. **7**(6): p. 759-64.

Chapter 8

Appendices

Galway University Hospitals
Ospidéil na h-Ollscoile Gaillimh
UNIVERSITY HOSPITAL GALWAY
MERLIN PARK UNIVERSITY HOSPITAL

NUI Galway
OÉ Gaillimh

Feidhmeannacht na Seirbhíse Sláinte
Health Service Executive

GALWAY UNIVERSITY HOSPITALS - BIOBANK INFORMED CONSENT

Patient Information

Introduction

We would like to invite you to participate in a clinical research initiative at Galway University Hospitals to establish a BioBank. The purpose of the BioBank is to set up a resource that can support a diverse range of research programmes intended to improve the prevention, diagnosis and treatment of cancer. You are under no obligation to take part and if, having read the information below, you would prefer not to participate, we will accept your decision without question.

Although major advances have been made in the management of cancer, many aspects of the disease are not fully understood. It is hoped that our understanding of the disease will be improved through research. Galway University Hospitals are actively involved in research that aims to identify markers that will predict how a cancer develops, progresses and responds to a variety of treatments. This type of work requires the use of tissue and blood samples. It is hoped that it will eventually lead to improvements in the diagnosis, treatment and outcome for those who have cancer. Although this study may have no direct benefit to you, it is hoped that the results may benefit patients like you in the future.

Your Involvement

If you volunteer to participate in our BioBank, there will be no additional risks to you outside those of your standard investigation and treatment. Your identity will remain confidential. Your name will not be published or disclosed to anyone outside the study group. All research is covered by standard institutional indemnity insurance and is approved by a Research Ethics Committee that ensures the ethical nature of the research. Nothing in this document restricts or curtails your rights. You may withdraw your consent at any time. If you decide not to participate, or if you withdraw your consent, your standard of treatment will not be affected in any way.

Procedure

We invite all patients who are undergoing treatment and/or investigation to participate. All samples for research will be taken at the time you are attending the hospital for routine diagnostic tests.

(i) **Tissue Samples**

By participating, you give us consent to retain small pieces of your tissue obtained at the time of surgery. These samples will be stored and used in the future for research. They may be analysed in the surgical laboratory at GUH, or may be transferred to another laboratory for additional analysis using specialised equipment which is not yet available in Ireland. This will not affect your diagnosis in any way.

(ii) **Blood Samples**

By participating, you give us consent to take an extra blood sample (equivalent of 4 teaspoonfuls) at the same time that your blood is being taken for routine tests. These samples will be stored and used in the future for research. They may be analysed in the surgical laboratory at GUH, or may be transferred to another laboratory for additional analysis using specialised equipment which is not yet available in Ireland.

(iii) **Clinical Information**

By participating, you give us consent to store information relating to your diagnosis and treatment on a database. This information is only accessed by personnel directly involved in research within the Surgical Research Unit.

Further Information

If you would like further information about our BioBank, your participation and your rights, please contact the Surgical Research Unit (Tel: 091 524390).

If you would like further information about research projects that may be conducted, please contact your Consultant.

Thank you in anticipation of your assistance. Please read and sign the Consent section.

I have read the attached information sheet on the above project, dated _____

Please Initial Box ☐

GALWAY UNIVERSITY HOSPITALS - BIOBANK INFORMED CONSENT

PARTICIPANT DECLARATION

I have read, or had read to me, this consent form. I have had the opportunity to ask questions and all my questions have been answered to my satisfaction. I freely and voluntarily agree to be part of this research study, though without prejudice to my legal and ethical rights. I have received a copy of this agreement and I understand that, if there is a sponsoring company, a signed copy will be sent to that sponsor. I understand that I may withdraw from the study at any time.

(Name of sponsor): ……

PARTICIPANT'S NAME: ……

CONTACT DETAILS: ……

PARTICIPANT'S SIGNATURE: ……

DATE: ……

Where the participant is incapable of comprehending the nature, significance and scope of the consent required, the form must be signed by a person competent to give consent to his or her participation in the research study (other than a person who applied to undertake or conduct the study). If the participant is a minor (under 18 years old) the signature of parent or guardian must be obtained:

NAME OF CONSENTER, PARENT, OR GUARDIAN: ……

SIGNATURE: ……

RELATION TO PARTICIPANT: ……

DECLARATION OF INVESTIGATOR'S RESPONSIBILITY

I have explained the nature and purpose of this research study, the procedures to be undertaken and any risks that may be involved. I have offered to answer any questions and fully answered such questions. I believe that the participant understands my explanation and has freely given informed consent.

NAME OF RESEARCH NURSE OR INVESTIGATOR: ……

SIGNATURE: ……

DATE: ……

CONSULTANT: ……

Keep the original of this form in the investigators file, give one copy to the participant, and send one copy to the sponsor (if there is a sponsor).

BioBank Specimen Form Nov 2010

Complete form and send with specimens to Surgery Research Lab, CSI (Bleep 835, Ext. 4202)

Surname:	**First Name:**	**Referral Reason (Please Circle):** Breast - Colorectal - Prostate - Skin - Lung – Other _____	
Board No:	**RH No:**	**Consultant:**	**Cancer** ☐ **Noncancer** ☐ **Awaiting Dx** ☐
DOB:	**Sex:**	**Date:**	**Blood** ☐ **Tissue** ☐

Blood Specimen

		No. of Tubes
Tube	Yellow 5ml SST	1
	Purple 4ml EDTA	1
	Purple 10ml EDTA	1

Time Point (Tick Box)

- Pre Neoadjuvant ☐
- Peri Neoadjuvant ☐
- Pre Tumour Resection ☐
- Post Surgery (1 day) ☐
- Review / Follow Up ☐

Laboratory use only

Written Informed Consent (Tick Box)
Consent Form with specimen ☐
Consent Form in Patient Chart ☐

Shire Pt No.: _____
Date: _____
Signature:

Tissue Specimen

Type (Tick Box)	Liquid Nitrogen	RNA Later	Fresh (Media)
Tumour	☐	☐	☐
Tumour Assoc. Normal (TAN)	☐	☐	☐
Benign	☐	☐	☐
Normal	☐	☐	☐
Lymph Node	☐	☐	☐
Other_____	☐	☐	☐

General Information

Liquid Nitrogen
Empty tubes. Immerse in Liquid Nitrogen (LN2)

RNA later
Tubes labelled 'RNA later'. Place in biohazard bag

Fresh (Breast only)
Tubes containing pink media.Place in biohazard bag

Time Point (Tick Box)
Diagnostic Core Biopsy ☐
Tumour Resection ☐
Local Recurrence ☐

Breast Side: Right ☐ Left ☐

Surgical Procedure:

Form completed by (Sig/Date):

BioBank Specimen Form Nov 2010

Complete form and send with specimens to Surgery Research Lab, CSI (Bleep 835, Ext. 4202)

Surname:	**First Name:**	**Referral Reason (Please Circle):** Breast - Colorectal - Prostate - Skin - Lung – Other _____	
Board No:	**RH No:**	**Consultant:**	**Cancer** ☐ **Noncancer** ☐ **Awaiting Dx** ☐
DOB:	**Sex:**	**Date:**	**Blood** ☐ **Tissue** ☐

Blood Specimen

		No. of Tubes
Tube	Yellow 5ml SST	1
	Purple 4ml EDTA	1
	Purple 10ml EDTA	1

Time Point (Tick Box)

- Pre Neoadjuvant ☐
- Peri Neoadjuvant ☐
- Pre Tumour Resection ☐
- Post Surgery (1 day) ☐
- Review / Follow Up ☐

Laboratory use only

Written Informed Consent (Tick Box)
Consent Form with specimen ☐
Consent Form in Patient Chart ☐

Shire Pt No.: _____
Date: _____
Signature:

Tissue Specimen

Type (Tick Box)	Liquid Nitrogen	RNA Later	Fresh (Media)
Tumour	☐	☐	☐
Tumour Assoc. Normal (TAN)	☐	☐	☐
Benign	☐	☐	☐
Normal	☐	☐	☐
Lymph Node	☐	☐	☐
Other_____	☐	☐	☐

General Information

Liquid Nitrogen
Empty tubes. Immerse in Liquid Nitrogen (LN2)

RNA later
Tubes labelled 'RNA later'. Place in biohazard bag

Fresh (Breast only)
Tubes containing pink media.Place in biohazard bag

Time Point (Tick Box)
Diagnostic Core Biopsy ☐
Tumour Resection ☐
Local Recurrence ☐

Breast Side: Right ☐ Left ☐

Surgical Procedure:

Form completed by (Sig/Date):

Complete this section for Cancer Genetics Research Blood only

Age at Diagnosis: _____

Family History (Please tick)**:** Yes ☐ No ☐

Describe Family History (Include blood relatives, maternal/paternal and cancer type)**:**

_____

_____

_____

_____

Complete this section for Cancer Genetics Research Blood only

Age at Diagnosis: _____

Family History (Please tick)**:** Yes ☐ No ☐

Describe Family History (Include blood relatives, maternal/paternal and cancer type)**:**

_____

_____

_____

_____

LAST – Ireland
www.Last-Ireland.org
8th and 9th March, 2010

This is to certify that

Sonja Khan

Passed an assessment of the course based on the FELASA recommendations for Category B & C
Which implement the European Union Directive 86/609 Article 14.
A skills attainment record is presented with this certificate.

(Course Content on the back of certificate)

LAST-Ireland
26 JUN 2010
sec@last-ireland.org
www.last-ireland.org

Signed

Peter F. Nowlan
Course Organiser

Course Content Includes

- *An introduction to the history and ethics of animal experimentation*
- *Animal health - its impact on research*
- *The use of animals in scientific research - legal controls and applying for a licence*
- *Animal handling / Day-to-day animal care / Procedures videos*
- *Characteristics of laboratory animals; research implications.*
- *Experimental design / Statistical implications*
- *Case studies and critique /*
- *Working safely with animals*
- *Anaesthesia, analgesia and post-operative care*
- *Euthanasia*
- *Laboratory animals – working in Europe*
- *Alternatives to animals; the options*

Contact information:
Bio Resources Unit, Biochemistry Building, Trinity College Dublin, Dublin 2
Phone number: (01) 896 1008
E-Mail: sec@last-ireland.org

Communications arising from this work

OPEN ACCESS Freely available online

PLOS ONE

miR-379 Regulates Cyclin B1 Expression and Is Decreased in Breast Cancer

Sonja Khan[1], Cathy L. Brougham[1], James Ryan[1], Arisha Sahrudin[1], Gregory O'Neill[1], Deirdre Wall[2], Catherine Curran[1], John Newell[2], Michael J. Kerin[1], Roisin M. Dwyer[1*]

1 Discipline of Surgery, School of Medicine, National University of Ireland, Galway, Galway, Ireland, **2** HRB Clinical Research Facility and School of Mathematics, Statistics and Applied Mathematics, National University of Ireland, Galway, Galway, Ireland

Abstract

MicroRNAs are small non-coding RNA molecules that control gene expression post-transcriptionally, and are known to be altered in many diseases including breast cancer. The aim of this study was to determine the relevance of miR-379 in breast cancer. miR-379 expression was quantified in clinical samples including tissues from breast cancer patients (n=103), healthy controls (n=30) and patients with benign breast disease (n=35). The level of miR-379 and its putative target Cyclin B1 were investigated on all breast tissue specimens by RQ-PCR. Potential relationships with gene expression and patient clinicopathological details were also determined. The effect of miR-379 on Cyclin B1 protein expression and function was investigated using western blot, immunohistochemistry and proliferation assays respectively. Finally, the levels of circulating miR-379 were determined in whole blood from patients with breast cancer (n=40) and healthy controls (n=34). The level of miR-379 expression was significantly decreased in breast cancer (Mean(SEM) 1.9 (0.09) Log_{10} Relative Quantity (RQ)) compared to normal breast tissues (2.6 (0.16) Log_{10} RQ, $p<0.01$). miR-379 was also found to decrease significantly with increasing tumour stage. A significant negative correlation was determined between miR-379 and Cyclin B1 ($r=-0.31$, $p<0.001$). Functional assays revealed reduced proliferation ($p<0.05$) and decreased Cyclin B1 protein levels following transfection of breast cancer cells with miR-379. Circulating miR-379 was not significantly dysregulated in patients with breast cancer compared to healthy controls ($p=0.42$). This data presents miR-379 as a novel regulator of Cyclin B1 expression, with significant loss of the miRNA observed in breast tumours.

Citation: Khan S, Brougham CL, Ryan J, Sahrudin A, O'Neill G, et al. (2013) miR-379 Regulates Cyclin B1 Expression and Is Decreased in Breast Cancer. PLoS ONE 8(7): e68753. doi:10.1371/journal.pone.0068753

Editor: Anna Alisi, Bambino Gesu' Children Hospital, Italy

Received January 30, 2013; **Accepted** June 2, 2013; **Published** July 10, 2013

Funding: This study was supported by funding from the National Breast Cancer Research Institute (NBCRI) (www.nbcri.ie) and the Health Research Board of Ireland (HRB) (www.hrb.ie). The funders had no role in the study design, data collection and analysis, decision to publish, or preparation of this manuscript.

Competing interests: The authors have declared that no competing interests exist.

* E-mail: roisin.dwyer@nuigalway.ie

Introduction

MicoRNAs (miRNAs) are a class of small (19-25 nucleotides), non-coding RNA molecules which can be found in all eukaryotic cells, and repeatedly act to inhibit gene expression post-transcriptionally. They play key roles in regulation of gene expression by complementarily binding to the 3'-untranslated regions (UTRs) of target messengerRNAs (mRNAs) [1,2]. This results in repression of translation or directing the sequence-specific degradation of their target mRNAs [3]. miRNAs play a significant role in a wide range of physiological and pathological processes, including breast cancer. Furthermore they have been shown to be dysreguated in both tissue and circulation of cancer patients [4,5]. Increasing evidence implicates miRNAs in cancer progression, including tumour growth, differentiation, invasion and metastasis [6]. The miRNA of interest in this study, miR-379, is located on chromosome 14q32, 31 and to date, very little is known about its role in normal physiology. In the context of breast cancer, there is currently one report implicating miR-379 in the regulation of interleukin-11 (IL-11) production in breast cancer cell lines [7]. miR-379 has a predicted binding site on a key gene associated with breast cancer, Cyclin B1, which is known to be up-regulated and associated with poor patient outcome [8–11]. The Cyclin B1 3' untranslated region is 612bp in length, with computational algorithms (TargetScan, miRanda) predicting a binding site for miR379 starting at position 404 [12–14].

Cyclin B1 is a key initiator of mitosis. It has a crucial role in regulating Cyclin-dependent kinase 1 (Cdk1), which initiates the progression from G2 phase to mitosis [15]. Over-expression of Cyclin B1 is associated with a number of different

cancers including breast [8,11,16], oesophageal squamous cell [17,18], non-small cell lung [19,20] and renal cancer [21]. Further, over-expression of Cyclin B1 is associated with poor patient survival and increased resistance to radiotherapy in head and neck squamous cell carcinoma [22,23]. Researchers are investigating the potential of depleting Cyclin B1 expression in tumours as a therapeutic strategy, by initiating anti-proliferative and apoptosis-inducing properties [24,25]. Understanding miRNA mediated regulation of Cyclin B1 is therefore an exciting avenue of investigation. Currently two groups have shown the potential for miRNA-mediated regulation of Cyclin B1 in cancer cell lines [26,27]. The first study reported knock-down of endogenous miR-744 in a murine prostate cancer cell line which exhibited reduced Cyclin B1 expression suggesting positive regulation of the gene [26]. The second study investigated the effect of miR-494 on cell cycle progression through the G2/M phase of human cholangiocarcinoma cell lines, and found it to regulate a number of key genes involved in G2/M phase including Cyclin B1 [27].

In the present study, miR-379 expression was quantified in clinical samples which included tissues from breast cancer patients (n=103), healthy controls (n=30) and patients with benign breast disease (n=35). Any relationship with clinicopathological details was investigated. Cyclin B1 gene expression was also quantified and any association with miR-379 expression examined. The effect of miR-379 mimic on Cyclin B1 protein expression and function was investigated. Finally, the levels of circulating miR-379 were determined in patients with breast cancer (n=40) and healthy controls (n=34).

Results

MiR-379 expression in human breast tissues

MicroRNA extracted from malignant (n=103), normal (n=30) and fibroadenoma (n=35) breast tissue biopsies was analysed using RQ-PCR. miR-379 was detected in 100 out of 103 breast tumours samples, and was detectable in both normal and fibroadenoma tissue. Results were expressed as Log_{10} Relative Quantity (RQ). RQ-PCR of mature miR-379 in these samples revealed a significant decrease in expression in breast tumour samples (Mean(SEM) 1.9 (0.09) Log_{10} Relative Quantity) compared to normal tissue n=30 (2.6 (0.16) Log_{10} RQ, $p<0.01$, Figure 1). Samples were then stratified based on patient clinicopathological details. miR-379 expression was found to show a relationship with tumour stage. With increasing tumour stage (from stage 1 to stage 3), the level of miR-379 decreased significantly ($p<0.05$, Figure 2A). A similar trend was observed for tumour grade however this did not reach significance (Figure 2B). There was no association of miR-379 with other clinicopathological parameters, including histological subtype ($p=0.329$), tumour size ($p=0.243$), menstrual status ($p=0.486$) or epithelial subtype ($p=0.965$, results not shown).

Cyclin B1 expression in human breast tissues

Cyclin B1 expression was also quantified across a subset of 84 breast tissue specimens. Expression levels of Cyclin B1 were significantly elevated in breast cancer (n=40, 2.52 (0.10) Log_{10} RQ) compared to fibroadenoma (n=23, 2.15 (0.11) Log_{10} RQ, $p<0.05$) and normal breast tissue (n=21, 1.78 (0.10) Log_{10} RQ, $p<0.001$, Figure 3A). Any potential relationship between Cyclin B1 and miR-379 was then investigated. A significant negative correlation was observed between Cyclin B1 and miR-379 ($r= -0.31$, $p<0.002$, Figure 3B).

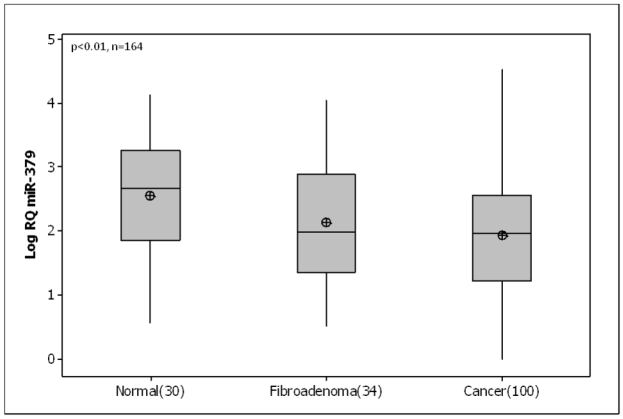

Figure 1. MicroRNA-379 (miR-379) expression in normal, fibroadenoma and malignant breast tissues. RQ-PCR of miR-379 revealed significantly decreased levels of expression in breast cancer n=100 (Mean(SEM) 1.9 (0.09) Log_{10} Relative Quantity) compared to normal tissue n=30 (2.6 (0.16) Log_{10} RQ, $p<0.01$).

doi: 10.1371/journal.pone.0068753.g001

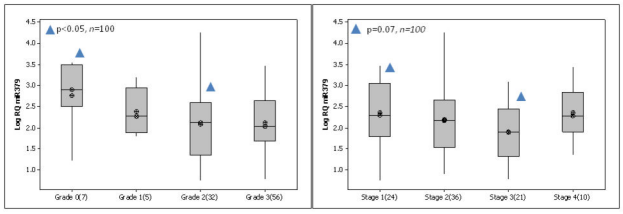

Figure 2. miR-379 expression across tumour stage and grade. (A) miR-379 expression across tumour stage. With increasing tumour stage, the level of miR-379 decreased significantly ($p<0.05$) (B) Level of miR-379 across tumour grade. A similar trend was observed for tumour grade, however it did not reach significance ($p=0.128$).

doi: 10.1371/journal.pone.0068753.g002

miR-379 Effect on Cell Proliferation

T47D cells were transfected with miR-379 and NTC-mimic as described, and the change in miR-379 expression quantified by RQ-PCR (Figure 4A). A significant elevation in miR-379 (5.76 log_{10} RQ relative to T47D cells transfected with NTC mimic) was confirmed (Figure 4A) prior to analysis of cell proliferation or Cyclin B1 protein expression.

The CellTiter 96® AQ_{ueous} Non-Radioactive Cell proliferation Assay (Promega) was used to determine cell proliferation 48

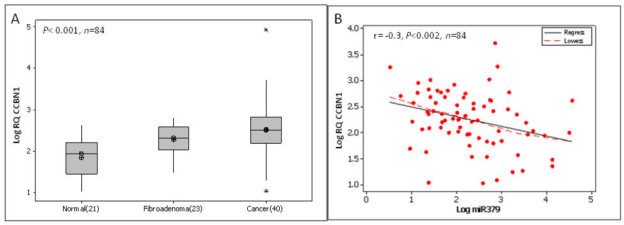

Figure 3. Cyclin B1 expression in normal, fibroadenoma and malignant breast tissues. (A) Cyclin B1 gene expression across all tissue types. Cyclin B1 gene expression was significantly elevated in breast cancer (Mean(SEM) 2.52 (0.10) Log_{10} RQ) compared to benign (2.15 (0.11) Log_{10} RQ, p<0.05) and normal breast tissue (1.78 (0.10) p<0.001). (B) Pearson Correlation of miR-379 and Cyclin B1. A significant negative correlation was observed between Cyclin B1 and miR-379 (r=-0.31, p<0.001).

doi: 10.1371/journal.pone.0068753.g003

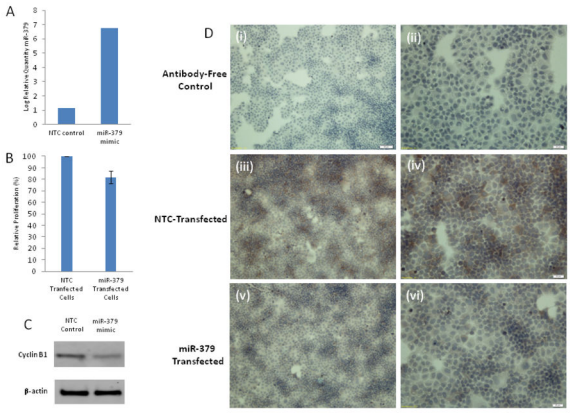

Figure 4. Transfection of T47D cells with miR-379 or a non-targeting control (NTC) mimic. (A) Confirmation of elevated miR-379 expression 48 hours following transfection with miR-379 mimic. (B) Cell proliferation following transfection, resulting in a decrease in proliferation (range 7-24%) in the presence of a miR-379 mimic (p<0.05). (C) The effect of miR-379 transfection on Cyclin B1 protein expression was also determined at 48 hours through western blot (C) and immunohistochemistry (D) (i, ii) antibody-free, (iii, iv) Cells transfected with NTC mimic, (v, vi) Cells transfected with miR-379 mimic for 48h, observed significantly reduced Cyclin B1 expression. Magnification (i, iii, v) 10X (50μm scale bar) and (ii, iv, vi) 20X (20μm scale bar).

doi: 10.1371/journal.pone.0068753.g004

hours following transfection with miR-379 in T47D cells. An inhibition of cell proliferation was observed (7-24% inhibition, p<0.05 Figure 4(B)) in cells transfected with miR-379 compared to those transfected with NTC-mimic.

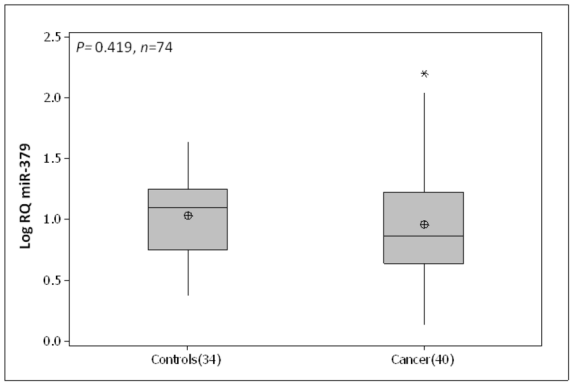

Figure 5. Circulating miR-379 expression across breast cancer patients and controls. No significant difference was observed between circulating miR-379 in breast cancer patients (Mean(SEM) 0.95 (0.07) Log_{10} RQ) and healthy controls (1.03 (0.05) Log_{10} RQ, p=0.42).

doi: 10.1371/journal.pone.0068753.g005

Cyclin B1 protein expression in cells transfected with miR-379

To confirm the effect of miR-379 on Cyclin B1 expression in T47D cells, cells were transfected with miR-379 or a NTC mimic, and protein extracted or cells fixed followed by western blot (Figure 4C) or immunohistochemistry (Figure 4D) respectively. Cyclin B1 protein was detected at the expected size of ~58kDa, with β-actin (loading control) detected at ~47kDa (Figure 4C). The level of immunoreactivity detected in miR-379 transfected cells was weaker than that observed when cells were transfected with the NTC mimic, with relative densitometry analysis revealing a >40% decrease in Cyclin B1 protein. This change in Cyclin B1protein expression was confirmed by immunohistochemical analysis of T47D cells fixed following transfection with miR-379 (Figure 4D). The negative control wells which did not receive an antibody, showed no staining (Figure 4D(i),(ii)). Robust native Cyclin B1 expression was detected in cells that had been transfected with NTC-mimic (Figure 4D(iii),(iv)). A significant reduction in Cyclin B1 staining was observed in cells transfected with a miR-379 mimic (Figure 4D(v),(vi)).

Circulating miR-379

The circulating level of miR-379 was quantified in whole blood of 40 breast cancer patients and 34 healthy controls. No significant difference was observed between circulating miR-379 in breast cancer patients (0.95 (0.07) Log_{10} RQ) and healthy controls (1.03 (0.05) Log_{10} RQ, p=0.42, Figure 5).

Discussion

There is no doubt that miRNAs play an important role in breast cancer, but the mode of action of many microRNAs has yet to be elucidated. Located on chromosome 14q32, 31, miR-379-410 is defined as a large cluster of brain-specific

miRNAs and has been implicated in neuroblastoma as a potential biomarker [28]. While miR-379 has been shown to regulate IL-11 production in breast cancer cell lines, there have been no previous reports regarding expression levels in breast tissues. In the present study, expression of miR-379 was examined in breast tissue specimens, and was detectable in 100 out of 103 samples, and all control tissues. The level of miR-379 was significantly decreased in breast cancer compared to normal breast tissue. Due to the decreased levels of miR-379, its expression was also investigated in the breast cancer cohort for any potential relationships with patient clinicopathological details. miR-379 expression showed a significant relationship with tumour stage, with increasing tumour stage the level of miR-379 decreased significantly. A similar trend was observed with tumour grade (p=0.077). It would be worth noting that increased numbers in the Grade 1 and 2 groups may have given more significance to this aspect of the study.

miR-379 has a putative binding site on Cyclin B1 which is a key initiator of mitosis and has previously shown a relationship with tumour stage and grade in breast cancer [11]. An immunohistochemistry-based analysis of specimens from over 1,300 invasive breast cancer patients also revealed a significant association with advanced tumour stage, grade, size, oestrogen and progesterone receptor status [11]. High Cyclin B1 expression is associated with poor patient prognosis [11]. Cyclin B1 expression was investigated in a subset of breast tissue specimens (n=84), with expression levels found to be up-regulated in breast cancer compared to normal and benign breast tissue. This is in agreement with previously published work [8,11,16]. Kawamoto et al. [8] showed Cyclin B1 expression increases from benign into malignant stages of breast disease. The present study also showed a significant increase from benign to malignant breast tissues. Further, a significant increase in expression of Cyclin B1 was detected in benign compared to normal tissues. Following this investigation, a scatterplot with linear regression lines was used to assess the relationship between miR-379 and Cyclin B1, with a strong negative correlation observed, indicating a potential negative regulation of Cyclin B1. Previous studies showed knock-down of Cyclin B1 in cancer cell lines resulted in reduced cell proliferation [24,25]. Therefore potential introduction of miR-379 could be used as a therapeutic intervention to regulate the expression of Cyclin B1 and further control tumour cell proliferation. Transfection of a breast cancer cell line with a miR-379 mimic resulted in reduced Cyclin B1 protein expression and inhibition of proliferation, supporting a role for miR-379 in direct regulation of Cyclin B1.

Circulating miRNAs have the potential as biomarkers for many diseases [29]. Circulating levels of miR-379 were investigated in cancer patients compared to healthy controls. While detectable in all samples, no significant difference was observed between breast cancer patients and controls. Based on this data, it would appear that miR-379 is not a useful systemic marker of disease, but highlights a potentially important role in the primary tumour microenvironment.

The data presented identifies a role for miR-379 as a regulator of Cyclin B1 expression, with a significant loss of the miRNA observed in breast tumours.

Materials and Methods

Ethics Statement

All experimental procedures involving tissue samples from human participants were approved by the Clinical Research Ethics Committee (University College Hospital, Galway). Written informed consent was obtained from each patient and all clinical investigation was performed according to the principles expressed in the Declaration of Helsinki.

Clinical Samples

Breast tissue specimens (n=168) were obtained at University College Hospital, Galway. The clinical patient samples comprised of 103 malignant tissue biopsies, 30 normal mammary tissue biopsies obtained at reduction mammoplasty, and 35 fibroadenoma tissues which are benign breast disease tissues. Full patient demographics and clinicopathological details were collected and maintained prospectively (Table 1). Samples were immersed in RNAlater® (Qiagen) for 24 hours, then the RNAlater was removed and the tissue stored at -80°C. Whole blood samples (n=74) were also collected from 40 breast cancer patients pre-operatively and 34 healthy controls with no family history of the disease. The bloods were stored at 4°C until required.

Cell Lines and Culture Conditions

T47D breast cancer cells were previously purchased from the American Type Culture Collection (Manassas, VA). Cells were cultured in RPMI-1640 media supplemented with 10% fetal bovine serum (FBS) and 100U/ml penicillin/ 100 µg streptomycin (P/S). Cells were incubated at 37°C and 5% CO_2 with a media change performed twice weekly.

Total and microRNA extraction

Breast tissue specimens or cell pellets were homogenised in 1 ml TRIzol® lysis reagent (Invitrogen) as previously described [30]. Total (large and micro) RNA was extracted from malignant (n=103), normal (n=30) and fibroadenoma (n=35) mammary tissue using the RNeasy Mini Kit (QIAGEN) as per manufacturer's instructions. MicroRNA was extracted from 1 ml of whole blood using an amended version of the TRI Reagent® BD technique (Molecular Research Center, Inc., Cincinnati, OH), as previously described [31]. Collected RNA was stored at -80°C.

Gene and microRNA Analysis

1µg of large RNA was reverse transcribed using SuperScript III reverse transcriptase enzyme (200U/µl), 0.1 M DTT, RT-5x Buffer, RNaseOUT Ribonuclease Inhibitor (40U/µl), Random primers (3µg/µl) and dNTP's (100mM)-Promega (Invitrogen, Carlsbad, CA, USA). TaqMan® Gene Expression Assays targeting Cyclin B1 were used in TaqMan® Universal Mastermix (Applied Biosystems). 100ng of mature microRNA

Table 1. Patient cohort and clinicopathological characteristics.

Breast Clinicopathological details	Cancer	Fibroadenoma	Normal
Number of patients	103	35	30
Median Patient Age yrs	56 (35-90)	44 (17-62)	46.5 (24-58)
Menopausal Status			
Post	72		
Pre	32		
Histological Subtype			
Invasive Ductal	78		
Invasive Lobular	11		
Other	*14*		
Intrinsic Subtype			
Luminal A (ER/PR +, HER2/neu-)	42		
Luminal B (ER/PR +, HER2/neu+)	18		
HER2 Over expressing (ER-, PR-, HER2/neu+)	16		
Triple-Negative (ER-, PR-, HER2/ neu-)	16		
Unknown	*11*		
Tumour Grade			
1	5		
2	32		
3	55		
Tumour size			
1	19		
2	39		
3	10		
UICC Stage			
Stage 1	23		
Stage 2	36		
Stage 3	21		
Stage 4	10		

was reverse transcribed using the MultiScribe™-based High-Capacity cDNA Archive Kit (dNTP 100mM, RT Buffer 10x, RNase Inhibitor 20U/µl, Stem loop primer 50nM, MultiScribe RT 50U/µl) (Appied Biosystems). The resulting cDNA for both mRNA and microRNA was analysed by ABI 79000 Fast real-time PCR system (Applied Biosystems). These reactions were carried out in a final volume of 10 µl comprising of 0.7 µl cDNA, 5 µl TaqMan® Universal PCR fast Master Mix (2x), 0.5 µl TaqMan® primer-probe mix (0.2µM), Forward primer (1.5µM), and Reverse Primer (0.7µM) (Applied Biosystems). The RQ-PCR cycle comprised of, 10-minute incubation at 95 °C followed by a 40 cycles at 95°C for 15 seconds and 60°C for 60 seconds. The use of an Inter-assay control derived from a breast cancer cell line (T47D) on each reaction allowed comparison of data across plates, and all reactions were carried out in triplicate with a standard deviation of < 0.3 considered acceptable. The relative quantity of mRNA and miRNA expression was calculated using the comparative cycle threshold (ΔΔCt). The endogenous controls used for gene expression were Mitochondrial Ribosomal Protein L19 (MRPL19) and Peptidyl-Prolyl Isomerase A (PPIA) [32]. For miRNA analysis, let-7a was the endogenous control [33], and for the blood protocol U6 was used as an endogenous control [34]. The geometric mean of the Ct value was used to normalise the data and the sample with the lowest expression level was applied as a calibrator.

Cell Transfection

T47D cells were transfected with miR-379-5p mimic (mature sequence: UGGUAGACUAUGGAACGUAGG; 50nM) or a non-specific control miRNA (non-target control (NTC)) mimic (50nM; Switchgear Genomics, USA). Transfections were performed using Lipofectamine™ 2000 (Invitrogen, California, USA) according to manufacturer's instructions.

Effect of miR-379 on cell proliferation

Cells were seeded into a 96-well plate at a density of 6 x 10^4 cells per well in antibiotic-free growth medium supplemented with 10% FBS to ensure 90-95% confluence at the time of transfection. miR-379 mimic or NTC mimic were transfected into T47D cells as described. The cells were incubated at 37°C in 5% CO_2 and medium was changed 24 hours after transfection. Cell proliferation was measured 48 hours following transfection using CellTiter 96® AQ_{ueous} Non-Radioactive Cell proliferation Assay (Promega). As per manufacturer's instruction, a mixture of tetrazolium compound (MTS) and phenazine methosulphate (PMS) were added to each well containing cells. The plate was incubated at 37°C and 5% CO_2 for 3 hours before reading absorbance on plate reader (Multiskan RC, Thermo, Fisher Scientific) at 490nm.

Effect of miR-379 on Cyclin B1 protein levels

For western blot analysis of protein expression, protein was extracted from T47D cells following transfection with the NTC mimic or miR-379 as described. Briefly, cells were washed and resuspended in Triton-X lysis buffer [150mM NaCl, 20 mM HEPES, 2 mM EDTA, 1% Triton-X100, 2mM Sodium Orthovanadate, 10mM Sodium Fluoride, 10ul/mL Protease inhibitor cocktail (Fisher Scientific)], frozen at -20°C and then centrifuged at 500 x g for 15 minutes at 4°C to remove cellular debris. The protein content was determined using the Micro BCA™ Protein Assay Kit (Thermo Scientific). Protein (100 µg) was reduced in DTT (0.5 M) for 10 minutes at 70°C and samples run on a 4-15% gradient pre-cast Mini-PROTEAN® TGX™ Gels (Bio-Rad) for 30 minutes at 200V. Protein molecular weight standards (20-220 kDa) were run simultaneously on each gel. Electroblotting was performed for 30 minutes at 100V to transfer protein samples to a nitrocellulose membrane. Blots were blocked in 5% milk in TBS-T [20 mM Tris, 137 mM NaCl, 0.1% Tween-20] for 1 hour,

and probed with an antibody targeting Cyclin B1 (1:5,000; Abcam), overnight and washed in TBS-T. β-actin (1:1,000, Abcam) was used to confirm equal loading in wells. Horseradish peroxidase labelled goat anti-rabbit (1:3,000; Abcam) antibody was then added to the membranes for 1.5 hours. Following washing steps, SuperSignal West Dura Chemiluminescent substrate (Thermo Scientific) was applied to the membranes for 5 minutes. Images were captured using a Syngene G-Box and GeneSnap software. For immunohistochemical analysis of Cyclin B1 expression, cells were plated into 4-well slides (Millicell® EZ slide, Millipore) at a density of 1.75 x 10^5 cells per well and transfected with NTC mimic or miR-379 as described. In brief, slides were put on ice for 15 minutes and then were fixed in ice-cold methanol at -20°C for 15 minutes. After methanol removal cells were incubated in 10% normal goat serum diluted in 10% PBS/ 0.05% Tween-20 for 30 minutes to block non-specific binding. A rabbit polyclonal antibody directed against human Cyclin B1 (1:100, ab48574, Abcam) was then applied for 90 minutes followed by washing in PBS/0.05% Tween-20. Cells were then washed and a secondary antibody tagged with HRP (1:1000, ab6721-1, Abcam) was applied for 30 minutes. After washing, detection was carried out using a peroxidise substrate kit containing the chromogen diaminobenzidine (Vector Laboratories, Burlingame, CA). Cells were then counterstained with haematoxylin for 3 minutes and the slides were dehydrated through serial alcohol immersions before mounting using Glycergel mounting medium (DAKO, Carpintera, CA).

Statistical Analysis

All data are presented as Mean (SEM), and graphically represented using boxplots and linear scatter plots. A two sample Student's t-test and a general model ANOVA were used to compare mean responses. Scatter plots were displayed using Linear Regression and Lowess smoother to determine the relationships between different populations. The level of relationship was determined using Pearson correlation coefficients.

Author Contributions

Conceived and designed the experiments: RMD. Performed the experiments: SK CB JR AS GO . Analyzed the data: SK RMD DW JN MJK. Contributed reagents/materials/analysis tools: MJK. Wrote the manuscript: SK RMD. Other: Technical expertise: CC .

References

1. Bartel DP (2004) MicroRNAs: genomics, biogenesis, mechanism, and function. Cell 116: 281-297. doi:10.1016/S0092-8674(04)00045-5. PubMed: 14744438.
2. Lim LP, Lau NC, Garrett-Engele P, Grimson A, Schelter JM et al. (2005) Microarray analysis shows that some microRNAs downregulate large numbers of target mRNAs. Nature 433: 769-773. doi:10.1038/nature03315. PubMed: 15685193.
3. Zeng Y, Yi R, Cullen BR (2003) MicroRNAs and small interfering RNAs can inhibit mRNA expression by similar mechanisms. Proc Natl Acad Sci U S A 100: 9779-9784. doi:10.1073/pnas.1630797100. PubMed: 12902540.
4. Sassen S, Miska EA, Caldas C (2008) MicroRNA: implications for cancer. Virchows Arch 452: 1-10. doi:10.1007/s00428-007-0532-2. PubMed: 18040713.
5. Heneghan HM, Miller N, Kelly R, Newell J, Kerin MJ (2010) Systemic miRNA-195 differentiates breast cancer from other malignancies and is a potential biomarker for detecting noninvasive and early stage disease. Oncologist 15: 673-682. doi:10.1634/theoncologist.2010-0103. PubMed: 20576643.
6. Calin GA, Croce CM (2006) MicroRNA signatures in human cancers. Nat Rev Cancer 6: 857-866. doi:10.1038/nrc1997. PubMed: 17060945.
7. Pollari S, Leivonen SK, Perälä M, Fey V, Käkönen SM et al. (2012) Identification of microRNAs inhibiting TGF-beta-induced IL-11 production in bone metastatic breast cancer cells. PLOS ONE 7: e37361. doi:10.1371/journal.pone.0037361. PubMed: 22629385.
8. Kawamoto H, Koizumi H, Uchikoshi T (1997) Expression of the G2-M checkpoint regulators cyclin B1 and cdc2 in nonmalignant and malignant human breast lesions: immunocytochemical and quantitative image analyses. Am J Pathol 150: 15-23. PubMed: 9006317.
9. Rudolph P, Kühling H, Alm P, Fernö M, Baldetorp B et al. (2003) Differential prognostic impact of the cyclins E and B in premenopausal and postmenopausal women with lymph node-negative breast cancer. Int J Cancer 105: 674-680. doi:10.1002/ijc.11132. PubMed: 12740917.
10. Kühling H, Alm P, Olsson H, Fernö M, Baldetorp B et al. (2003) Expression of cyclins E, A, and B, and prognosis in lymph node-negative breast cancer. J Pathol 199: 424-431. doi:10.1002/path.1322. PubMed: 12635132.
11. Aaltonen K, Amini RM, Landberg G, Eerola H, Aittomäki K et al. (2009) Cyclin D1 expression is associated with poor prognostic features in estrogen receptor positive breast cancer. Breast Cancer Res Treat 113: 75-82. doi:10.1007/s10549-008-9908-5. PubMed: 18240019.
12. Friedman RC, Farh KK, Burge CB, Bartel DP (2009) Most mammalian mRNAs are conserved targets of microRNAs. Genome Res 19: 92-105. PubMed: 18955434.
13. John B, Enright AJ, Aravin A, Tuschl T, Sander C et al. (2004) Human MicroRNA targets. PLOS Biol 2: e363. doi:10.1371/journal.pbio.0020363. PubMed: 15502875.
14. Lewis BP, Burge CB, Bartel DP (2005) Conserved seed pairing, often flanked by adenosines, indicates that thousands of human genes are microRNA targets. Cell 120: 15-20. doi:10.1016/j.cell.2004.12.035. PubMed: 15652477.
15. Pines J, Hunter T (1990) Human cyclin A is adenovirus E1A-associated protein p60 and behaves differently from cyclin B. Nature 346: 760-763. doi:10.1038/346760a0. PubMed: 2143810.
16. Agarwal R, Gonzalez-Angulo AM, Myhre S, Carey M, Lee JS et al. (2009) Integrative analysis of cyclin protein levels identifies cyclin b1 as a classifier and predictor of outcomes in breast cancer. Clin Cancer Res 15: 3654-3662. doi:10.1158/1078-0432.CCR-08-3293. PubMed: 19470724.
17. Murakami H, Furihata M, Ohtsuki Y, Ogoshi S (1999) Determination of the prognostic significance of cyclin B1 overexpression in patients with esophageal squamous cell carcinoma. Virchows Arch 434: 153-158. doi:10.1007/s004280050319. PubMed: 10071250.
18. Nozoe T, Korenaga D, Kabashima A, Ohga T, Saeki H et al. (2002) Significance of cyclin B1 expression as an independent prognostic indicator of patients with squamous cell carcinoma of the esophagus. Clin Cancer Res 8: 817-822. PubMed: 11895914.
19. Soria JC, Jang SJ, Khuri FR, Hassan K, Liu D et al. (2000) Overexpression of cyclin B1 in early-stage non-small cell lung cancer and its clinical implication. Cancer Res 60: 4000-4004. PubMed: 10945597.
20. Yoshida T, Tanaka S, Mogi A, Shitara Y, Kuwano H (2004) The clinical significance of Cyclin B1 and Wee1 expression in non-small-cell lung cancer. Ann Oncol 15: 252-256. doi:10.1093/annonc/mdh073. PubMed: 14760118.
21. Ikuerowo SO, Kuczyk MA, Mengel M, van der Heyde E, Shittu OB et al. (2006) Alteration of subcellular and cellular expression patterns of cyclin B1 in renal cell carcinoma is significantly related to clinical progression and survival of patients. Int J Cancer 119: 867-874. doi:10.1002/ijc.21869. PubMed: 16557593.
22. Hassan KA, Ang KK, El-Naggar AK, Story MD, Lee JI et al. (2002) Cyclin B1 overexpression and resistance to radiotherapy in head and neck squamous cell carcinoma. Cancer Res 62: 6414-6417. PubMed: 12438226.
23. Takeno S, Noguchi T, Kikuchi R, Uchida Y, Yokoyama S et al. (2002) Prognostic value of cyclin B1 in patients with esophageal squamous cell carcinoma. Cancer 94: 2874-2881. doi:10.1002/cncr.10542. PubMed: 12115375.

24. Yuan J, Yan R, Krämer A, Eckerdt F, Roller M et al. (2004) Cyclin B1 depletion inhibits proliferation and induces apoptosis in human tumor cells. Oncogene 23: 5843-5852. doi:10.1038/sj.onc.1207757. PubMed: 15208674.
25. Androic I, Krämer A, Yan R, Rödel F, Gätje R et al. (2008) Targeting cyclin B1 inhibits proliferation and sensitizes breast cancer cells to taxol. BMC Cancer 8: 391. doi:10.1186/1471-2407-8-391. PubMed: 19113992.
26. Huang V, Place RF, Portnoy V, Wang J, Qi Z et al. (2012) Upregulation of Cyclin B1 by miRNA and its implications in cancer. Nucleic Acids Res 40: 1695-1707. doi:10.1093/nar/gkr934. PubMed: 22053081.
27. Yamanaka S, Campbell NR, An F, Kuo SC, Potter JJ et al. (2012) Coordinated effects of microRNA-494 induce G(2)/M arrest in human cholangiocarcinoma. Cell Cycle 11: 2729-2738. doi:10.4161/cc.21105. PubMed: 22785131.
28. Gattolliat CH, Thomas L, Ciafrè SA, Meurice G, Le Teuff G et al. (2011) Expression of miR-487b and miR-410 encoded by 14q32.31 locus is a prognostic marker in neuroblastoma. Br J Cancer 105: 1352-1361. doi: 10.1038/bjc.2011.388. PubMed: 21970883.
29. Schwarzenbach H, Hoon DS, Pantel K (2011) Cell-free nucleic acids as biomarkers in cancer patients. Nat Rev Cancer 11: 426-437. doi: 10.1038/nrc3066. PubMed: 21562580.
30. Ryan J, Curran CE, Hennessy E, Newell J, Morris JC et al. (2011) The sodium iodide symporter (NIS) and potential regulators in normal, benign and malignant human breast tissue. PLOS ONE 6: e16023. doi: 10.1371/journal.pone.0016023. PubMed: 21283523.
31. Heneghan HM, Miller N, Kerin MJ (2010) Systemic microRNAs: novel biomarkers for colorectal and other cancers? Gut 59: 1002-1004; author reply 1004. doi:10.1136/gut.2009.200121. PubMed: 20581247
32. McNeill RE, Miller N, Kerin MJ (2007) Evaluation and validation of candidate endogenous control genes for real-time quantitative PCR studies of breast cancer. BMC Mol Biol 8: 107. doi: 10.1186/1471-2199-8-107. PubMed: 18042273.
33. Davoren PA, McNeill RE, Lowery AJ, Kerin MJ, Miller N (2008) Identification of suitable endogenous control genes for microRNA gene expression analysis in human breast cancer. BMC Mol Biol 9: 76. doi: 10.1186/1471-2199-9-76. PubMed: 18718003.
34. Roa W, Brunet B, Guo L, Amanie J, Fairchild A et al. (2010) Identification of a new microRNA expression profile as a potential cancer screening tool. Clin Invest Med 33: E124. PubMed: 20370992.

Send Orders of Reprints at reprints@benthamscience.net

14 *MicroRNA* 2013, *2,* 14-19

Isolation of Secreted microRNAs (miRNAs) from Cell-conditioned Media

Claire L. Glynn, Sonja Khan, Michael J. Kerin and Roisin M. Dwyer*

Discipline of Surgery, School of Medicine, National University of Ireland Galway, Galway, Ireland

Abstract: MicroRNAs (miRNAs) have been found to be stable in the circulation of cancer patients raising their potential as circulating biomarkers of disease. The specific source and role, however, of miRNAs in the circulation is unknown and requires elucidation to determine their true potential. In this study, along with primary tissue explants and primary stromal cells, three breast cancer cell lines were employed, including T47D, MDA-MB-231 and SK-BR-3. Tissue explants were harvested in theatre, with informed patient consent, and included tumour, tumour associated normal, and diseased lymph node samples. Cell-conditioned media containing all factors secreted by the cells were harvested. MiRNAs were extracted from samples using 5 different extraction techniques including the blood protocol, RNeasy® (Qiagen), miRNeasy® mini kit (Qiagen), mirVana™ isolation kit (Ambion) and RNAqueous® kit (Ambion). MiRNAs were successfully isolated from all media samples collected from cell lines, primary cells and fresh tissue explants. However, there was remarkable variation in yield depending on the extraction method used. Aliquots of the same samples were extracted, revealing the two column extraction protocol of the mirVana® miRNA isolation kit to be the most suitable approach. A range of miRNAs, including miR-16, miR-195, miR-497 and miR-10b, were successfully amplified. While miR-16 and miR-195 were detected in media from both cell lines and tissue explants, miR-497 and miR-10b were only detected in secretions from whole tissue explants. The ability to achieve reliable and reproducible miRNA yields from cell-conditioned media is vital for the successful amplification of miRNAs by RQ-PCR.

Keywords: Biomarker, breast cancer, cell culture media, circulation, extraction, microRNA, secretion.

INTRODUCTION

MicroRNAs (miRNAs) are a class of small (18-22 nucleotides), non-coding RNA molecules found in plants, animals, and DNA viruses which often act to inhibit gene expression post-transcriptionally. This is achieved by binding to specific messenger RNA (mRNA) targets and promoting their degradation and/or translational inhibition [1]. Hundreds of mRNAs may be regulated by only one miRNA and therefore they can exert their influences on a wide variety of gene expression networks [2]. MiRNAs play a vital role in the regulation of crucial biological and pathological processes, most notably in development, aging, cancer and neurological disease development and progression [3]. Indeed, it may prove difficult to find a fundamental biological process which miRNAs do not play a role in, with over half of mammalian messages under selective pressure to maintain pairing to miRNAs [4, 5]. As a result, miRNAs are being investigated as potential biomarkers which could be utilized in a wide variety of molecular applications, including the diagnosis of cancer, cardiovascular and auto-immune diseases [2, 6, 7]. The discovery that miRNAs are frequently up-regulated or down-regulated in tumours when compared to normal tissue supports their role as either oncomirs or tumour suppressors [6, 8, 9]. Initially, the majority of research focused on the role of miRNAs in tissue, however, more recently it has been discovered that miRNAs are in fact detectable in the circulation [10-15].

The use of circulating microRNAs as potential biomarkers of disease is a rapidly evolving field of study. This hot topic has initiated widespread study of the abundance, half-life and stability of miRNAs in the circulation, which require careful consideration if they are to be implemented in the clinical setting [12]. Numerous studies have been performed assessing the effect of specimen type, the presence of cellular contaminants and stability [10, 16-18]. Mitchell *et al.* [15] first reported the presence of miRNAs in the circulation in a remarkably stable form, while subsequent studies have also found circulating miRNAs to be significantly more stable than their protein counterparts during long term storage [18, 19]. It has been suggested that dysregulation of some miRNAs may be disease specific, for example, in the context of breast cancer, Heneghan *et al.* [20] reported that circulating miR-195 was significantly elevated only in breast cancer patients and not those with other tumour types.

In recent years, there has been an explosion of interest in miRNAs as potential biomarkers of disease, particularly with regards to their presence in the circulation [10, 13, 21]. Novel circulating biomarkers could improve the early detection, diagnosis and ultimately the clinical management of cancer [22]. However, the true source of miRNAs in the circulation and their exact secretory mechanism is relatively unknown [23]. A number of hypotheses have been put forward. Chin and Slack [11] suggested two possible pathways: 1. tumour miRNAs are present as a result of cell death and lysis, and 2. miRNAs are present as a result of being actively

*Address corresponding to this author at the Discipline of Surgery, School of Medicine, Clinical Science Institute, National University of Ireland Galway, Costello Road, Galway, Ireland; Tel: +353-91-544637;
Fax: +353-91-494509; E-mail: roisin.dwyer@nuigalway.ie

2211-5374/13 $58.00+.00

secreted by cells [11]. In terms of active secretion, more recent studies have suggested that this may involve encapsulation of miRNAs into microvessicles, including exosomes and shedding vesicles [24-26]. Alternatively, active secretion could be achieved using a microvesicle-free, RNA binding, protein-dependent pathway [27]. Microvesicles, and indeed exosomes, have been heralded as novel regulators of cell to cell communication, and thus could also provide a mechanism of miRNA transfer between cells [28-30]. An accumulating body of evidence suggests that extracellular vesicles such as exosomes have the ability to be secreted by donor cells and are taken up by acceptor cells [26, 31, 32]. This potential exchange of miRNAs is an exciting and novel dimension to the regulation of a cells phenotype, and is particularly important in cancer [33]. MiRNAs offer immense potential as circulating biomarkers of disease, however, it is essential that we firstly understand their true source and role in disease.

There have been relatively few published reports on the isolation of miRNAs from cell-conditioned media [34, 35]. In addition, there is currently no commercially available extraction kit/technique designed specifically for miRNA isolation from cell-conditioned media. Two research groups have reported successful isolation of miRNAs from the media of four cell lines [36, 37]. Kosaka *et al.* [36] reported miRNA isolation from the cell-conditioned media of HEK293T cells and COS-7 cells using the mirVana™ miRNA isolation kit (Ambion). Turchinovich *et al.* [37] reported use of the miRNeasy® micro Kit (Qiagen) with cell-conditioned media from HEK293T cells and two breast cancer lines, MCF7 and MDA-MB-231. However, it is worth noting the latter group drew attention to the very low yields which they were obtaining [37]. There are no published reports describing analysis of miRNA secretion from tumour tissue explants. Successful RNA analysis relies heavily on the yield, purity and integrity of the extracted RNA. Therefore, an optimum extraction protocol is essential.

The aim of this study was to identify the most reliable and reproducible method for the isolation of miRNAs from cell-conditioned media, utilizing both commercially available cell lines and tumour tissue harvested during surgery. The reproducibility and efficiency of 5 methods/kits were tested and compared. A prerequisite for successful amplification using RQ-PCR is an optimal microRNA yield, therefore an efficient method for RNA extraction is critical. A panel of four candidate microRNAs (miR-16, miR-195, miR-497 and miR-10b) were chosen for amplification by RQ-PCR in cell-conditioned media samples as these miRNAs have previously been implicated in the circulation of breast cancer patients [20, 38].

MATERIALS AND METHODS

Cell Culture

The following breast cancer cell lines had previously been purchased from the American Type Culture Collection (ATCC): T47D, MDA-MB-231 and SK-BR-3. Cells were cultured at 37°C, 5% CO_2, with a media change twice weekly and passage every 7 days. The media for each cell line was as follows: RPMI-1640 (T47D), Leibovitz-15 (MDA-MB-231) and McCoys 5A (SK-BR-3), each supplemented with 10% Foetal Bovine Serum (FBS), and 100IU/ml penicillin G/100 mg/ml streptomycin sulfate (Pen/Strep).

Tissue Explants

Following ethical approval from Galway University Hospitals (GUH) and written informed patient consent, tumour tissue harvested in theatre was weighed and placed into 2mls of culture media. The culture media employed consisted of DMEM +Glutamax supplemented with 10% FBS, and 100IU/ml Pen/Strep. These primary tissue samples included Tumour, Tumour Associated Normal (TAN), and diseased lymph node tissue. TAN refers to tissue at least 2cm from the site of the primary tumour.

Collection of Cell-conditioned Media

Tissues and cells were incubated in the appropriate media for a period of 24 hours at 37°C, 5% CO_2. The conditioned media (CM), containing all factors secreted by the cell lines and tissues, were then harvested from the cultures, centrifuged for 4 minutes at 201 x g RCFMax (1,000rpm Eppendorf 5810R, A-4-62) at 4°C, and stored at -20°C until required for extraction.

miRNA Isolation

This study investigated the use of five available and widely used miRNA isolation techniques, namely the blood protocol [21], RNeasy® (Qiagen), miRNeasy® mini kit (Qiagen), mirVana™ isolation kit (Ambion) and RNAqueous® kit (Ambion), Table **1**.

The blood protocol was developed in-house in the Discipline of Surgery, NUI Galway, and is a modified Trizol™ co-purification technique [20]. Previous studies have found this method to provide reliable miRNA yields from whole blood, plasma and serum [20, 40]. For each 1 ml of cell-conditioned media, phase separation was performed by the addition of 3 ml of Trizol®. 200 µl of 1-bromo-4 methoxybenzene was then added to augment the RNA phase separation process. Samples were then centrifuged at 4°C, 15,300 x g RCFMax (14,000rpm Eppendorf 5417R, F45-30-11) for 15 minutes. Total RNA was precipitated using isopropanol and washed with 75% ethanol prior to solubilisation with 60 µl of nuclease free water. Thus, each 1 ml of sample yielded 60 µl of total RNA solution, which was stored at -80°C.

The remaining four miRNA isolation techniques included in this study (Table **1**.) all employed commercially available kits which are broadly based on a column/filter isolation method.

Prior to extraction using the RNeasy®, miRNeasy®, mirVana™ and RNAqueous® isolation kits, the following steps were carried out to permit isolation of miRNA from cell-conditioned media:

1. Extractions were performed on 1ml of cell-conditioned media. 700µl of Trizol™ reagent was added to the sample and vortexed. The sample was then left to stand for 5 minutes at room temperature.
2. 140µl of chloroform was added and the sample shaken vigorously for 15 seconds.

Table 1. Methods of extraction used for isolation of miRNAs from cell-conditioned media.

Method	Source	Design Specification
Blood Protocol [20]	Discipline of Surgery adaption of the TRI Reagent® technique (Molecular Research Center, Inc., Cincinnati, OH) [20]	Utilizes Trizol® reagent and Bromoanisole.
RNeasy®	Qiagen	On-column method designed to isolate total RNA (i.e. small and large)
miRNeasy®	Qiagen	On-column method designed to specifically isolate microRNA
mirVana™	Ambion	Double column method designed to isolate both small and large RNA
RNAqueous®	Ambion	Phenol free method designed for total RNA isolation

3. Samples were centrifuged at 15,300 x g RCFMax (14,000rpm Eppendorf 5417R, F45-30-11), at 4°C, for 15 minutes.
4. The upper aqueous phase was transferred to a new tube, carefully avoiding the interphase.
5. The manufacturer's protocol for each kit was then followed from the separation step.

The RNeasy and miRNeasy Mini Kit (Qiagen®) both combine phenol/guanidine-based lysis of samples and a silica membrane column based purification. Following the steps described previously, the upper, aqueous phase was extracted, and ethanol was added to provide appropriate binding conditions for all RNA molecules from 18 nucleotides (nt) upwards. The sample was then applied to the RNeasy/miRNeasy Mini spin column, where the total RNA binds to the silica membrane and phenol and other contaminants are efficiently washed away. High quality RNA is then eluted in RNase-free water.

The RNAqueous® Kit (Ambion®) is designed for phenol-free total RNA isolation using a guanidinium-based lysis⁄denaturant and Glass Fiber Filter (GFF) separation technology. The RNAqueous method is based on the ability of glass fibers to bind nucleic acids in concentrated chaotropic salt solutions. Following the steps described previously, the lysate was diluted with an ethanol solution to make the RNA competent for binding to the GFF in the filter cartridge. This solution was passed through the filter pad where RNA binds and most other cellular contents flow through. The filter cartridge was washed 3 times to remove contaminants, and the RNA was eluted in RNase-free water.

The mirVana™ miRNA Isolation Kit (Ambion®) employs organic extraction, as described previously followed by purification on two sequential Glass Fibre Filters (GFF) under specialized binding and wash conditions. Unlike other methods, the mirVana™ kit utilizes two sequential GFFs, as it has been suggested that the small RNAs are essentially lost in the first filtration through the column and therefore a second filtration is required to capture the tiny microRNAs.

The concentration and purity of miRNA was assessed using NanoDrop™ 1000 spectrophotometer (Nanodrop Technologies, Willmington, DE, USA). The wavelength dependent extinction coefficient ''33'' was taken to represent the microcomponent of all RNA in solution.

Amplification of miRNAs

For each sample, 100ng of miRNA was reverse transcribed into cDNA using MultiScribe™ reverse transcriptase (Applied Biosystems, Foster City, CA, USA) and sequence-specific stem-loop primers (Applied Biosystems) which target the mature miRNA sequence. RQ-PCR was performed using TaqMan® probes (Applied Biosystems) specific for the miRNAs of interest, miR-16, miR-195, miR-497 and miR-10b. RQ-PCR was performed on a 7900 HT Fast Real-Time PCR System (Applied Biosystems). An Inter Assay Control (IAC), Reverse Transcription (RT) blank and a No Template Control (NTC) were included on each plate. All reactions were performed in triplicate. The threshold standard deviation accepted for intra- and inter-assay replicates was <0.3.

RESULTS AND DISCUSSION

A wide variety of sample types were extracted using the different extraction techniques. This included breast cancer cell lines (T47D, SK-BR-3, MDA-MB-231), tissue explants (tumour, tumour associated normal (TAN) and diseased lymph node) and primary cell populations *e.g.* stromal cells. A total of n=90 samples were extracted using each technique. A yield of >20ng/µl was required for RQ-PCR amplification and therefore anything obtained less than this was not considered sufficient. Only 20 out of the 90 samples yielded sufficient miRNA for progression. Examples of yields obtained from individual samples can be seen in Table **2**. The results were widely variable with typically the highest yields obtained from tissue explants, which is to be expected due to cellularity, with the highest yield obtained from diseased tumour lymph node tissue. It is worth noting, however, that miRNAs were also detected in the cell-conditioned media of breast cancer cell lines and primary stromal cells. Of the top 10 yields obtained from all samples, 8 of these were obtained using the mirVana™ miRNA isolation kit. The blood protocol and RNeasy® miRNA isolation

Table 2. MiRNA yield from conditioned media harvested from breast cancer cell lines and tissue explants.

Sample Identifier	Yield ng/µl
Lymph node Explant A	232.43
SK-BR-3	65.7
Tumour Explant A	64.9
T47D	63.2
Primary stromal cells	42.85
Tumour Explant B	37.12
Lymph node Explant A	32.7
MDA-MB-231	31.52
Tumour Explant	27.86
TAN Explant	24.24
SK-BR-3	21.87

techniques were found to be the least successful for the isolation of miRNA from cell-conditioned media.

This suggested that the mirVana™ isolation kit may be optimal for miRNA extraction from cell-conditioned media. A direct comparison of methods was then performed using the mirVana™, miRNeasy® and RNAqueous® isolation techniques on aliquots of the same samples. Here, 3 aliquots of the same samples were extracted using each of the 3 extraction techniques. There was significant variability of results obtained using the different extraction techniques, even from within the same sample, which can be seen in Table **3**.

The results showed that consistent reproducible results were not obtained using the miRNeasy® or RNAqueous® techniques. In all cases, the mirVana™ miRNA isolation kit provided consistently high and reproducible yields for the successful isolation of miRNAs from cell-conditioned media (*e.g.* 2-4 fold increase in yield with mirVana™ kit). A range of miRNAs, including miR-16, miR-195, miR-497 and miR-10b, were successfully amplified from each of these samples using RQ-PCR (Table **4**), confirming the presence of intact miRNAs.

While miR-16 and miR-195 were detectable in all cell-conditioned media samples collected from both fresh tissue explants and breast cancer cell lines, miR-497 and miR-10b were only detectable in media exposed to the fresh tissue explants. This suggests that other cellular components of the tumour may be the source of the miRNAs and not just the epithelial cells alone. This is a very interesting area and does require further investigation. The stability, and indeed the persistence of action, of miRNAs is a biophysical parameter which warrants careful consideration. Generally, miRNAs

Table 3. MiRNA yields obtained from aliquots of the same samples using the mirVana™, miRNeasy® and RNAqueous® techniques.

Sample Identifier	Method of Extraction	Yield ng/µl
T47D	mirVana™	63.2
	miRNeasy®	4.59
	RNAqueous®	12.92
MDA-MB-231	mirVana™	31.52
	miRNeasy®	4.17
	RNAqueous®	18.68
SK-BR-3	mirVana™	65.7
	miRNeasy®	4.61
	RNAqueous®	12.68

Table 4. Amplification of miR-16, miR-195, miR-497 and miR-10b in cell-conditioned media samples from breast cancer cell lines and tissue explants ('+' Denotes Detected, '-' Denotes Not Detected).

Sample	miR-16	miR-195	miR-497	miR-10b
T47D	+	+	-	-
MDA-MB-231	+	+	-	-
SK-BR-3	+	+	-	-
Tumour Explant	+	+	+	+
TAN Explant	+	+	+	+

are considered to be relatively stable with long half lives of approximately 2 weeks [15]. However, some studies have shown selected miRNAs to have relatively short half lives (~1-3.5hrs), with several brain abundant miRNAs shown to be surprisingly restricted [40]. In this current study, all of the cell-conditioned media samples were collected in the same way and were frozen at -20°C within 20 minutes of harvest. One would expect that if half life were the issue, then the miRNAs of interest would not be detectable in any of the samples collected.

CONCLUSION

The successful isolation of intact miRNAs from cell conditioned media in an *in vitro* setting is a prerequisite for expression analyses of secreted miRNAs. This study found the mirVana™ miRNA isolation kit to obtain the most reproducible and consistently high yields when compared to other methods available. The molecular mechanisms which drive this secretion have yet to be elucidated. The use of an optimal method for isolating these secreted miRNAs will support elucidation of the mechanism of secretion, the true cellular source and role of these molecules in the circulation.

ACKNOWLEDGEMENTS

This work was supported by funding received from Hardiman Research Scholarship award (C.L.G) and the National Breast Cancer Research Institute (NBCRI), Ireland.

REFERENCES

[1] Ambros V. The functions of animal microRNAs. Nature 2004; 431(7006): 350-5.

[2] Pritchard CC, Cheng HH, Tewari M. MicroRNA profiling: approaches and considerations. Nat Rev Genet 2012; 13(5): 358-69.

[3] Alvarez-Garcia I, Miska EA. MicroRNA functions in animal development and human disease. Development 2005; 132(21): 4653-62.

[4] Pasquinelli AE. MicroRNAs and their targets: recognition, regulation and an emerging reciprocal relationship. Nat Rev Genet 2012; 13(4): 271-82.

[5] Bartel DP. MicroRNAs: target recognition and regulatory functions. Cell 2009; 136(2): 215-33.

[6] Lu J, Getz G, Miska EA, *et al*. MicroRNA expression profiles classify human cancers. Nature 2005; 435(7043): 834-8.

[7] Tili E, Michaille JJ, Costinean S, Croce CM. MicroRNAs, the immune system and rheumatic disease. Nat Clin Pract Rheumatol 2008; 4(10): 534-41.

[8] Almeida MI, Reis RM, Calin GA. MicroRNA history: discovery, recent applications, and next frontiers. Mutat Res 2011; 717(1-2): 1-8.

[9] Calin GA, Dumitru CD, Shimizu M, *et al*. Frequent deletions and down-regulation of micro- RNA genes miR15 and miR16 at 13q14 in chronic lymphocytic leukemia. Proc Natl Acad Sci USA 2002; 99(24): 15524-9.

[10] Chen X, Ba Y, Ma L, *et al*. Characterization of microRNAs in serum: a novel class of biomarkers for diagnosis of cancer and other diseases. Cell Res 2008; 18(10): 997-1006.

[11] Chin LJ, Slack FJ. A truth serum for cancer--microRNAs have major potential as cancer biomarkers. Cell Res 2008; 18(10): 983-4.

[12] Cho WC. Circulating micrornas as minimally invasive biomarkers for cancer theragnosis and prognosis. Front Genet 2011; 2: 7.

[13] Gilad S, Meiri E, Yogev Y, *et al*. Serum microRNAs are promising novel biomarkers. PLoS One 2008; 3(9): e3148.

[14] Heneghan HM, Miller N, Lowery AJ, Sweeney KJ, Newell J, Kerin MJ. Circulating microRNAs as novel minimally invasive biomarkers for breast cancer. Ann Surg 2010; 251(3): 499-505.

[15] Mitchell PS, Parkin RK, Kroh EM, *et al*. Circulating microRNAs as stable blood-based markers for cancer detection. Proc Natl Acad Sci USA 2008; 105(30): 10513-8.

[16] McDonald JS, Milosevic D, Reddi HV, Grebe SK, Algeciras-Schimnich A. Analysis of circulating microRNA: preanalytical and analytical challenges. Clin Chem 2011; 57(6): 833-40.

[17] Tsui NB, Ng EK, Lo YM. Stability of endogenous and added RNA in blood specimens, serum, and plasma. Clin Chem 2002; 48(10): 1647-53.

[18] Wang K, Zhang S, Marzolf B, *et al*. Circulating microRNAs, potential biomarkers for drug-induced liver injury. Proc Natl Acad Sci USA 2009; 106(11): 4402-7.

[19] Li Y, Jiang Z, Xu L, Yao H, Guo J, Ding X. Stability analysis of liver cancer-related microRNAs. Acta Biochim Biophys Sin (Shanghai) 2011; 43(1): 69-78.

[20] Heneghan HM, Miller N, Kelly R, Newell J, Kerin MJ. Systemic miRNA-195 differentiates breast cancer from other malignancies and is a potential biomarker for detecting noninvasive and early stage disease. Oncologist 15(7): 673-82.

[21] Heneghan HM, Miller N, Kerin MJ. Circulating miRNA signatures: promising prognostic tools for cancer. J Clin Oncol 2010; 28(29): e573-4; author reply e5-6.

[22] Albulescu R, Neagu M, Albulescu L, Tanase C. Tissular and soluble miRNAs for diagnostic and therapy improvement in digestive tract cancers. Expert Rev Mol Diagn 2011; 11(1); 101-20.

[23] Chen X, Liang H, Zhang J, Zen K, Zhang CY. Secreted microRNAs: a new form of intercellular communication. Trends Cell Biol 22(3): 125-32.

[24] Mathivanan S, Ji H, Simpson RJ. Exosomes: extracellular organelles important in intercellular communication. J Proteomics 2010; 73(10): 1907-20.

[25] Ratajczak J, Wysoczynski M, Hayek F, Janowska-Wieczorek A, Ratajczak MZ. Membrane-derived microvesicles: important and underappreciated mediators of cell-to-cell communication. Leukemia 2006; 20(9): 1487-95.

[26] Valadi H, Ekstrom K, Bossios A, Sjostrand M, Lee JJ, Lotvall JO. Exosome-mediated transfer of mRNAs and microRNAs is a novel mechanism of genetic exchange between cells. Nat Cell Biol 2007; 9(6): 654-9.

[27] Vickers KC, Palmisano BT, Shoucri BM, Shamburek RD, Remaley AT. MicroRNAs are transported in plasma and delivered to recipient cells by high-density lipoproteins. Nat Cell Biol 2011; 13(4): 423-33.

[28] Rader DJ, Parmacek MS. Secreted miRNAs suppress atherogenesis. Nat Cell Biol 2012; 14(3): 233-5.

[29] Bang C, Thum T. Exosomes: New players in cell-cell communication. Int J Biochem Cell Biol 2012; 44(11): 2060-4.

[30] Chiba M, Kimura M, Asari S. Exosomes secreted from human colorectal cancer cell lines contain mRNAs, microRNAs and natural antisense RNAs, that can transfer into the human hepatoma HepG2 and lung cancer A549 cell lines. Oncol Rep 2012; 28(5): 1551-8.

[31] Montecalvo A, Larregina AT, Shufesky WJ, *et al*. Mechanism of transfer of functional microRNAs between mouse dendritic cells *via* exosomes. Blood 2012; 119(3): 756-66.

[32] Wang K, Zhang S, Weber J, Baxter D, Galas DJ. Export of microRNAs and microRNA-protective protein by mammalian cells. Nucleic Acids Res 2010; 38(20): 7248-59.

[33] Mittelbrunn M, Sanchez-Madrid F. Intercellular communication: diverse structures for exchange of genetic information. Nat Rev Mol Cell Biol 2012; 13(5): 328-35.

[34] Weber JA, Baxter DH, Zhang S, *et al*. The microRNA spectrum in 12 body fluids. Clin Chem 2010; 56(11): 1733-41.

[35] Lukiw WJ, Alexandrov PN, Zhao Y, Hill JM, Bhattacharjee S. Spreading of Alzheimer's disease inflammatory signaling through soluble micro-RNA. Neuroreport 2012; 23(10): 621-6.

[36] Kosaka N, Iguchi H, Yoshioka Y, Takeshita F, Matsuki Y, Ochiya T. Secretory mechanisms and intercellular transfer of microRNAs in living cells. J Biol Chem 2010; 285(23): 17442-52.

[37] Turchinovich A, Weiz L, Langheinz A, Burwinkel B. Characterization of extracellular circulating microRNA. Nucleic Acids Res 2011; 39(16): 7223-33.

[38] Roth C, Rack B, Muller V, Janni W, Pantel K, Schwarzenbach H. Circulating microRNAs as blood-based markers for patients with primary and metastatic breast cancer. Breast Cancer Res 2010; 12(6): R90.

[39] Nugent M, Miller N, Kerin MJ. Circulating miR-34a levels are reduced in colorectal cancer. J Surg Oncol 2012. [Epub 2012/06/01]

[40] Sethi P, Lukiw WJ. Micro-RNA abundance and stability in human brain: specific alterations in Alzheimer's disease temporal lobe neocortex. Neurosci Lett 2009; 459(2): 100-4.

Received: August 08, 2012 **Revised: October 12, 2012** **Accepted: November 07, 2012**

Breast Cancer Res Treat
DOI 10.1007/s10549-011-1410-9

PRECLINICAL STUDY

Influence of stromal–epithelial interactions on breast cancer in vitro and in vivo

Shirley M. Potter · Roisin M. Dwyer · Marion C. Hartmann · Sonja Khan · Marie P. Boyle · Catherine E. Curran · Michael J. Kerin

Received: 24 November 2010 / Accepted: 12 February 2011

Abstract Stromal cell-secreted chemokines including CCL2 have been implicated in the primary tumor microenvironment, as mediators of tumor cell migration, proliferation, and angiogenesis. Expression of CCL2 and its principal receptor CCR2 was analyzed by RQ-PCR in primary tumor cells and breast cancer cell lines. Breast cancer cell lines (MDA-MB-231, T47D) were co-cultured directly on a monolayer of primary breast tumor and normal stromal cells, retrieved using EpCAM+ magnetic beads, and changes in expression of *CCL2, CCR2*, *MMP11*, *ELK1*, *VIL2*, and *Ki67* detected by RQ-PCR. Epithelial cell migration and proliferation in response to stromal cell-secreted factors was also analyzed. In vivo, tumor xenografts were formed by co-injecting T47D cells with primary tumor stromal cells. Following establishment, tumors were harvested and digested, epithelial cells retrieved and analyzed by RQ-PCR. Whole tumor tissue was also analyzed by immunohistochemistry for CD31 and the *VIL2* encoded protein Ezrin. Tumor stromal cells expressed significantly higher levels of *CCL2* than normal cells, with no *CCR2* expression detected. Primary epithelial cells and breast cancer cell lines expressed elevated *CCL2*, with relative expression of *CCR2* found to be higher than the ligand. Interaction of breast cancer epithelial cells with primary tumor, but not normal stromal cells, stimulated increased expression of *CCL2* (8-fold), *ELK1* (6-fold), *VIL2* (6-fold), and *MMP11* (17-fold). Factors secreted by stromal cells, including CCL2, stimulated a significant increase in epithelial cell migration, with no effect on cell proliferation in vitro observed. In vivo, the presence of stromal cells resulted in tumors of increased volume, mediated at least in part through neoangiogenesis demonstrated by immunohistochemistry (CD31). Admixed tumor xenografts exhibited increased expression of *Ki67*, *MMP11*, *VIL2*, and *ELK1*. Elevated Ezrin protein was also detected, with increased cytoplasmic localization. The results presented highlight mechanisms through which breast cancer epithelial cells can harness stromal cell biology to support tumor progression.

Keywords Breast cancer · Stromal · Epithelial · Xenograft · Angiogenesis · Proliferation · Metastasis

Introduction

The primary breast tumor microenvironment plays a pivotal role in cancer initiation and progression [1]. Stromal cells are the predominant cell type in this microenvironment and evidence of their active participation in tumor progression is growing rapidly [2]. Tumor stromal cells are fundamentally different from the stroma of corresponding normal breast tissue [3], and have gene expression signatures that correlate with tumor grade and poor prognosis [4–6]. These properties appear to be retained following separation from malignant epithelial cells [7], suggesting tumor stroma is comprised of an independent fibroblastic subpopulation which supports malignant behavior [6, 8]. In invasive breast cancer, stromal cells are found in much higher proportion than in situ carcinomas, and predominantly at the invasive front [9]. Allinen et al. [10] showed that breast tumor stromal cells undergo extensive gene expression changes in progression from normal breast tissue to ductal carcinoma in situ (DCIS) to invasive ductal carcinoma.

S. M. Potter · R. M. Dwyer (✉) · M. C. Hartmann · S. Khan · M. P. Boyle · C. E. Curran · M. J. Kerin
Division of Surgery, School of Medicine,
National University of Ireland, Galway, Ireland
e-mail: roisin.dwyer@nuigalway.ie

Published online: 23 February 2011

In view of these central roles in the biology of breast cancer, understanding the mechanisms by which stromal cells mediate such effects is essential. Within the tumor microenvironment, stromal cells are the most active secretory cells [2, 11], and various paracrine mediators of their growth-promoting signals have been proposed, including cytokines, growth factors, and proteases [7, 12]. Studies implicate altered chemokine expression levels as an indicator of progression to tumorigenicity and metastatic capacity [13]. Orimo et al. [7] reported that tumor stromal cell derived CXCL12 promotes tumor growth and angiogenesis via its cognate receptor (CXCR4) expressed by carcinoma cells.

Indeed previous work by this group showed that whole breast tumor explants secreted high levels of CCL2 (MCP-1, monocyte chemotactic protein-1) and that stromal cells were responsible for the bulk of its secretion [14]. CCL2 is a 76-amino acid protein with a primary role in the immune context, regulating recruitment of monocytes/macrophages and other inflammatory cells to damaged or infected sites [15, 16]. CCL2 is minimally expressed by normal breast epithelial ducts [16]. In contrast, extensive CCL2 protein expression has been noted in breast tumor tissue [17, 18]. CCL2 functions through its main receptor CCR2, of which there are two isoforms, CCR2A and CCR2B [19, 20]. Recent research has implicated CCL2 as an active participant in the tumor microenvironment, influencing factors such as tumor-associated macrophages, growth, angiogenesis, and metastasis [17, 21, 22]. Expression of CCL2 protein in primary breast tumors was shown to have a significant prognostic value for relapse free survival, and correlated with high tumor grade [18, 23].

Although the mechanisms by which stromal cells promote tumorigenesis are not yet fully understood, their potential as novel therapeutic targets in breast cancer is apparent [24, 25]. However, in order for stromal–epithelial interactions, or stromal cells themselves, to emerge as appropriate targets for novel breast cancer therapies, further characterization of the molecular crosstalk between these two cell populations is required.

The results presented show that isolation of breast cancer epithelial cells following interaction with primary tumor stromal cells in vitro and in vivo, stimulates increased expression of genes associated with invasion, angiogenesis, and tumor progression. While stromal cells secreted high levels of CCL2, they were devoid of the CCR2 receptor expressed by epithelial cells, suggesting paracrine action of the chemokine, potentially mediating cell migration. Another novel finding of this study was that in vivo interaction with primary tumor stromal cells induced increased expression of *VIL2*/Ezrin, a protein that plays a key regulatory role in breast cancer metastasis. The results presented provide a valuable insight into intracellular crosstalk between stromal and epithelial cells in the breast tumor microenvironment, highlighting how epithelial cells can harness stromal cell biology to facilitate their invasion and progression.

Methods

Primary culture

Following ethical committee approval and written informed consent, fresh specimens of human breast cancer were harvested at surgery and primary cell cultures prepared, as described previously [14]. Normal controls were obtained from reduction mammaplasties. The digested cell suspension was separated into organoid, epithelial, and stromal fractions by differential centrifugation and cultured in selective media, as described [26]. Primary stromal cells were characterized by flow cytometry using the Guava® EasyCyte™ 8HT and analyzed using Incyte software. Cell type specific antibodies were used including Thy1/CD90, CD105, CD73, α-SMA, CD31, MUC1/CD221, CD34, and Cytokeratin (BD Pharmingen™). Appropriate isotype control antibodies were used and the results reflect the percent of positive cells compared with isotype controls. The level of expression of fibroblast activation protein (FAP) in tumor compared to normal stromal cells was also determined by real-time quantitative PCR (RQ-PCR) as described below.

Primary tumor epithelial cells ($n = 6$) were isolated from organoid and epithelial cell fractions. Epithelial cell adhesion molecule (EpCAM) positive cell-enriched populations were retrieved from these single cell suspensions by positive selection using EasySep magnetic beads (StemCell Technologies Inc.), according to manufacturers' protocol.

Culture of cell lines

The following breast cancer cell lines were included in this study: T47-D, ZR-75-1, MCF-7, BT-474 (estrogen and progesterone receptor positive, ER+, PR+), MDA-MB-231, SK-BR-3 (ER−, PR−), and MCF-10-2A (non-tumorigenic). These were purchased from the ATCC and cultured in Leibovitz-15 (MDA-MB-231), RPMI-1640 medium (T47-D, ZR-75-1, BT-474), McCoys 5A (SK-BR-3), and Eagles minimum essential medium (MCF-7) media, each supplemented with 10% FBS, and 100 IU/ml penicillin G/100 mg/ml streptomycin sulfate. MCF-10-2A cells were cultured in Dulbecco's modified Eagle medium (DMEM)-F12 medium supplemented with 5% horse serum, 20 ng/ml epidermal growth factor, 100 ng/ml cholera toxin, 0.01 mg/mL insulin, and 500 ng/ml hydrocortisone.

Collection of conditioned medium and CCL2 quantification

Conditioned media (CM), containing factors secreted by cells, was obtained from cultures. All cell populations were seeded in 6-well plates at a density of 2×10^5 cells per well in 2 ml DMEM containing 2% FBS (required for chemokine stability). DMEM was used to prepare media for all cell types to ensure that differences observed were not as a result of culture conditions. CM from co-culture experiments was harvested after 72 h, centrifuged (1 min, 1000 rpm, 4°C), and stored at −20°C until required. CM from individual stromal cell populations was harvested after 24 h in culture and used neat/undiluted, as a chemoattractant in migration assays or as a growth medium in proliferation assays. CM from stromal cells was analyzed for CCL2 content using Quantikine® Enzyme Linked Immunosorbent Assays (R&D Systems), following manufacturers' protocol.

In vitro cell migration assay

Transwell® Permeable Supports (Corning Inc, Sigma-Aldrich) were used to track migration of MDA-MB-231 cells in response to factors secreted by stromal cells, as described [14]. Briefly, MDA-MB-231 cells were inoculated into the insert, and their migration in response to stromal cell CM, serum free basal medium (negative control) basal medium with 2% FBS (baseline control), or basal medium with 10% FBS (positive control) in the well below was quantified. MDA-MB-231 migration in response to stromal cells in the presence of a CCL2 monoclonal antibody (40 ng/mL) was also quantified. Migrated cells were counted in five fields of view per membrane using an Olympus BX60 microscope and image analysis® software. Each experiment was repeated in triplicate, with results expressed as mean ± SEM.

In vitro cell proliferation assay

Cell proliferation was assessed using the ViaLight™ Plus Kit (Cambrex), and based on bioluminescent measurement of ATP. Breast cancer epithelial cell lines (MDA-MB-231 and T47D) were seeded into 96-well plates (6×10^3 cells per well) and allowed to adhere overnight. Medium was removed and substrates added. Test substrates included tumor or normal stromal cell CM, and increasing concentrations of hCCL2 (50–300 pg/mL) standards. Basal and complete medium were used as negative and positive controls, respectively. Plates were incubated for 48 h and ATP levels measured on a LuminoSkan Ascent Luminometer (Thermo). Data represent the mean reading of 8 wells and are expressed as mean ± SEM.

Real-time quantitative PCR

Cells were homogenized in 1 ml of QIAzol Lysis reagent and total RNA isolated using the RNeasy® Mini Kit (QIAGEN Ltd.) as per manufacturer's instructions. cDNA was generated using SuperScript III reverse transcriptase enzyme (Invitrogen) and amplified by real-time quantitative PCR (RQ-PCR) using the ABI Prism 7000 (Applied Biosystems). Taqman® Universal Master Mix and Gene Expression Assays (Applied Biosystems) designed for the target genes (*FAP*, *CCL2, CCR2A, CCR2B, MMP11, Ki67, VIL 2, ELK 1*), and control genes *Mitochondrial Ribosomal Protein L19* (*MRPL19*), and *Peptidylprolyl Isomerase A* (*PPIA*) were used.

Due to the low yields from primary epithelial cell cultures the TaqMan® PreAmp Cells-to-Ct™ Kit (Applied Biosystems) was used for gene expression analysis on these cells. Briefly, this protocol involves an intermediate amplification step between reverse transcription and RQ-PCR in which the cDNA is enriched for target genes.

The comparative C_T method for relative quantification was used, allowing determination of the quantity of the target gene in each sample population normalized to endogenous control genes (*MRPL19* and *PPIA*) and compared to a calibrator, and was expressed in a linear form using the formula $2^{-\Delta\Delta C_T}$ [27]. Gene expression levels in primary tumor epithelial and stromal cells were determined relative to the levels in epithelial and stromal cells from normal breast tissue harvested at reduction mammaplasty. In the case of epithelial cell lines, levels were expressed relative to those of non-tumorigenic MCF-10-2A cells. In co-culture experiments, expression levels in the epithelial cell population post co-culture were expressed relative to expression levels in these cells cultured alone.

Co-culture of tumor stromal and epithelial cells

Primary tumor stromal cells ($n = 6$ individual donors A–F, luminal A $n = 4$, luminal B $n = 2$), or normal stromal cells ($n = 4$ individual donors) suspended in stromal medium were plated into T75 cm^2 flasks (1×10^6 cells per flask) and allowed to adhere overnight. Breast cancer epithelial cell lines (MDA-MB-231 or T47D) were seeded onto the monolayers of stromal cells at the same density. The individual cell populations were also cultured alone in parallel. Co-cultures were all established in stromal medium, so any changes observed could not be attributed to differences in culture conditions. Following direct co-culture adherent cells were washed twice with PBS and trypsinized into a single cell suspension and the epithelial fraction retrieved using EasySep EpCAM+ magnetic beads (Stem Cell Technologies Inc.). RNA was extracted from

retrieved epithelial cells and changes in gene expression resulting from their interaction with tumor and normal stromal cells identified by RQ-PCR, as described.

Growth of breast cancer xenografts in mice

Animal studies were carried out in accordance with experimental guidelines set out by the institutional ethics committee. Female athymic nude mice (Harlan Laboratories UK Ltd.) were implanted with 17-β-estradiol 60-day slow release pellets (Innovative Research of America), to support growth of estrogen receptor positive T47D cells. Mice were divided into three groups and given a subcutaneous injection of T47D cells alone (5.6×10^5 cells), or T47D cells admixed with tumor stromal cells (1×10^6) derived from two individual donors ($n = 6$ in each group). Tumors were measured weekly using callipers and volume estimated (volume (mm^3) = length $\times$ width $\times$ height $\times$ 0.52). Following 10 weeks of tumor growth, animals were killed by CO_2 inhalation and tumors harvested. Tissue for immunostaining was immediately immersed in 4% paraformaldehyde for 24 h, transferred to 30% sucrose for 24 h, snap frozen in an isopentane/liquid nitrogen bath and stored at −80°C until required for cryosectioning. Tumor tissue harvested for retrieval of epithelial cells was immediately immersed in basal culture media, minced using crossed blade scalpels and digested overnight using collagenase as described [14]. Epithelial cells were then retrieved from the mixed population using $EpCAM^+$ magnetic beads. Cells were pelleted and stored at −80°C until required for RNA isolation.

Immunohistochemistry

Frozen tissue samples from xenografts were cryosectioned (5 µm sections) and allowed to air dry at RT followed by rehydration in PBS–0.05% Tween-20. Following blocking of endogenous peroxidases, antigen retrieval was performed using citrate buffer. Sections were then analyzed using the Ventana Discovery™ machine with antibodies specific to CD31 (AbCAM), and Ezrin (AbCAM). Once staining was complete sections were washed in warm soapy water, dehydrated in serial alcohol immersions, mounted using DPX mounting medium and examined using a Leica DFC 300 FX light microscope, with Leica Software, V 2.3.4.

Statistical analysis

Data were analyzed using the software package SPSS 15.0 and are presented as mean ± SEM of triplicate experiments. Results with a $P < 0.05$ were considered statistically significant. All tests were two-tailed. Levene's test confirmed equal variance of observations in each group and permitted parametric data to be compared using a student's unpaired t test. Normality was confirmed using the Kolmogorov–Smirnov test.

Results

Epithelial and stromal cell isolation and characterization

Primary breast stromal cells displayed a typical fibroblastic morphology and when characterized by flow cytometry (Fig. 1) were shown to be positive for CD90 (>95% positive, Fig. 1a), CD105 (>95% positive, Fig. 1b), CD73 (>95% positive, Fig. 1c), and alpha-smooth muscle actin (α-SMA), and negative for CD31 (<2% positive, Fig. 1d), CD34 (<5% positive), MUC1/CD221 (<5% positive), and cytokeratin (<2% positive, Fig. 1e). Tumor stromal cells were found to have higher expression of α-SMA (range 60–87% positive), a marker of activated fibrobalsts (myofibroblasts), than normal stromal cells (range 2–68% positive). In agreement with previous reports [28, 29], RQ-PCR analysis also revealed significantly higher expression of fibroblast activation protein (FAP) in tumor compared to normal stromal cells (Fig. 1f, $P < 0.001$). Epithelial cells were selected using magnetic beads, based on EpCAM positivity and were confirmed to be cytokeratin positive (>95% positive). Levels of expression of *CCL2*, and its receptor *CCR2*, were determined in each cell population relative to the geometric mean expression of endogenous control genes, and values expressed relative to normal counterparts ($2^{-\Delta\Delta C_T}$, Fig. 2). In the case of stromal cells, expression of *CCL2* was significantly higher in each population of tumor stromal cells ($n = 6$, A–F) compared to mean *CCL2* expression from $n = 4$ normal stromal cells isolated from reduction mammaplasties (mean 1.05 log fold increase $P < 0.05$, Fig. 2a). In contrast both tumor and normal stromal cells failed to express either isoform of the CCL2 receptor, *CCR2A* or *CCR2B*. Expression of CCL2 and CCR2 was also analyzed in primary breast cancer epithelial cells ($n = 6$, Fig. 2b). Relative expression of *CCR2* was higher than the ligand (*CCR2*; mean 1.45 log RQ, *CCL2*; mean 0.78 log RQ) (Fig. 2b). *CCL2*/*CCR2* expression analysis was also performed on five breast cancer epithelial cell lines and mean values expressed relative to non-tumorigenic MCF-10-2A cells (Fig. 2c).

Effect of direct co-culture on CCL2 secretion and expression

In vitro secretion of CCL2 was quantified when the cells were cultured individually and in direct co-culture (Fig. 3a). The baseline of the graph represents the sum of what each

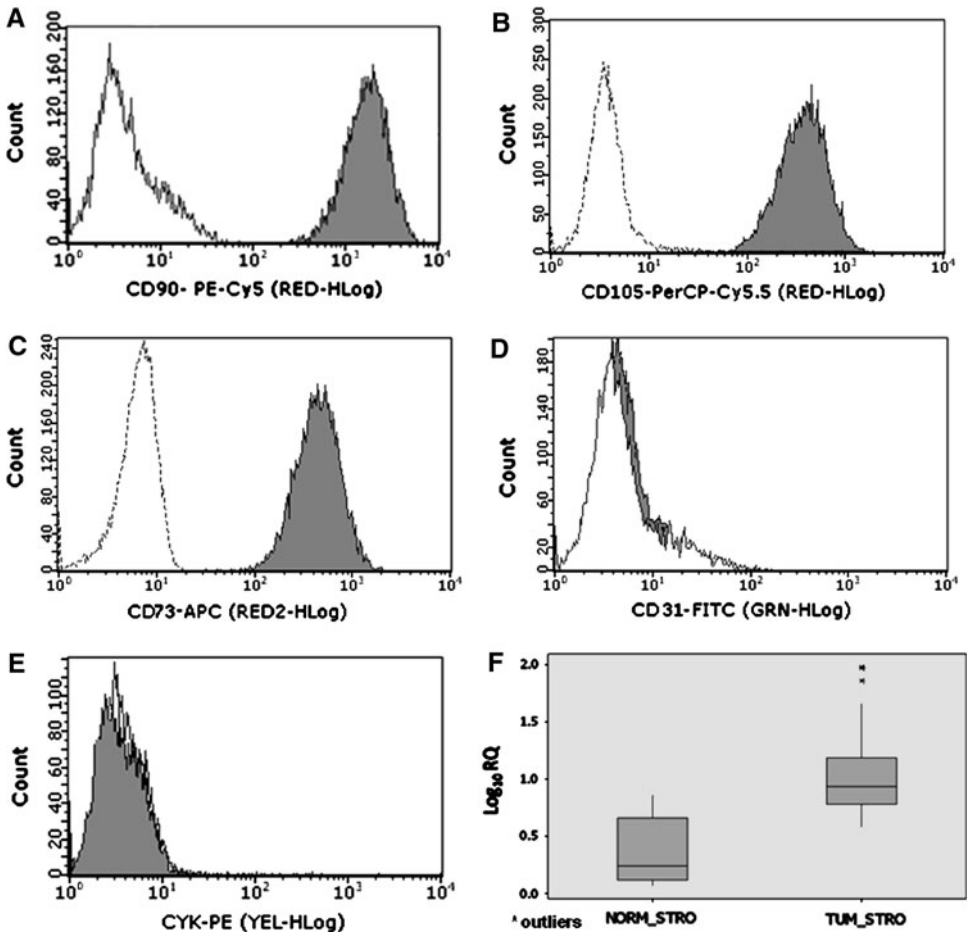

Fig. 1 Primary stromal cell characterization. Example of mammary stromal cell characterization by flow cytometry (**a**–**e**). Isotype controls are shown in *white*, with analytical samples shown in *gray*. Stromal cells were shown to be positive for CD90 (**a**), CD105 (**b**), CD73 (**c**), and negative for CD31 (**d**), and cytokeratin (**e**). RQ-PCR analysis also revealed significantly higher expression of fibroblast activation protein (FAP) in tumor ($n = 22$) compared to normal ($n = 8$) stromal cells (**f**, $P < 0.001$)

cell population secreted when cultured individually, with each bar representing the amount by which the co-culture population differed from this. Following 72-h co-culture of breast cancer cell lines on a monolayer of stromal cells, CCL2 levels were significantly higher than that seen from the individual populations (mean increase for T47D+ tumor stromal cells: 4901 ± 1953 pg/ml, MDA-MB-231 + tumor stromal cells: 5035 ± 1294 pg/ml, $P < 0.05$, Fig. 3a). This effect was significantly higher than that seen when these cells were co-cultured with normal stromal cells ($P < 0.05$). Following in vitro co-culture with primary tumor/normal stromal cells, epithelial tumor cells were retrieved using $EpCAM^+$ magnetic beads, and expression of *CCL2* analyzed. Levels of gene expression are expressed relative to levels detected in breast cancer cells cultured alone ($2^{-\Delta\Delta C_T}$). *CCL2* gene expression levels reflected protein secretion trends, with expression increased in both breast cancer populations following co-culture with stromal cells (Fig. 3b). This upregulation was significantly higher when co-cultured with tumor (mean fold increase: T47D 9.07 ± 2.85, MDA-MB-231 8.41 ± 4.36) compared to normal stromal cells (T47D 4.03 ± 2.37 MDA-MB-231 2.47 ± 0.77, $P < 0.05$). In contrast to *CCL2* expression, *CCR2* expression levels were decreased following co-culture compared to the cells cultured alone.

Cell migration and proliferation

MDA-MB-231 showed significantly greater chemotaxis in response to tumor compared to normal stromal cells (Fig. 4a). This effect was subsequently blocked by the addition of a monoclonal antibody to *CCL2* (range 27–64% blockade). Breast cancer cells also displayed a dose dependent increase in chemotaxis towards commercial standards of *CCL2*, with similar results observed in SK-Br-3 and MCF-7 cells (results not shown).

There was no significant change in proliferation of breast cancer epithelial cells in response to factors secreted by tumor or normal stromal cells (Fig. 4b). Recombinant standards of CCL2 were also found to have no effect on cell proliferation (results not shown).

Expression of invasion/proliferation associated genes

In both breast cancer cell lines, expression levels of the invasion associated gene *MMP11*, was significantly

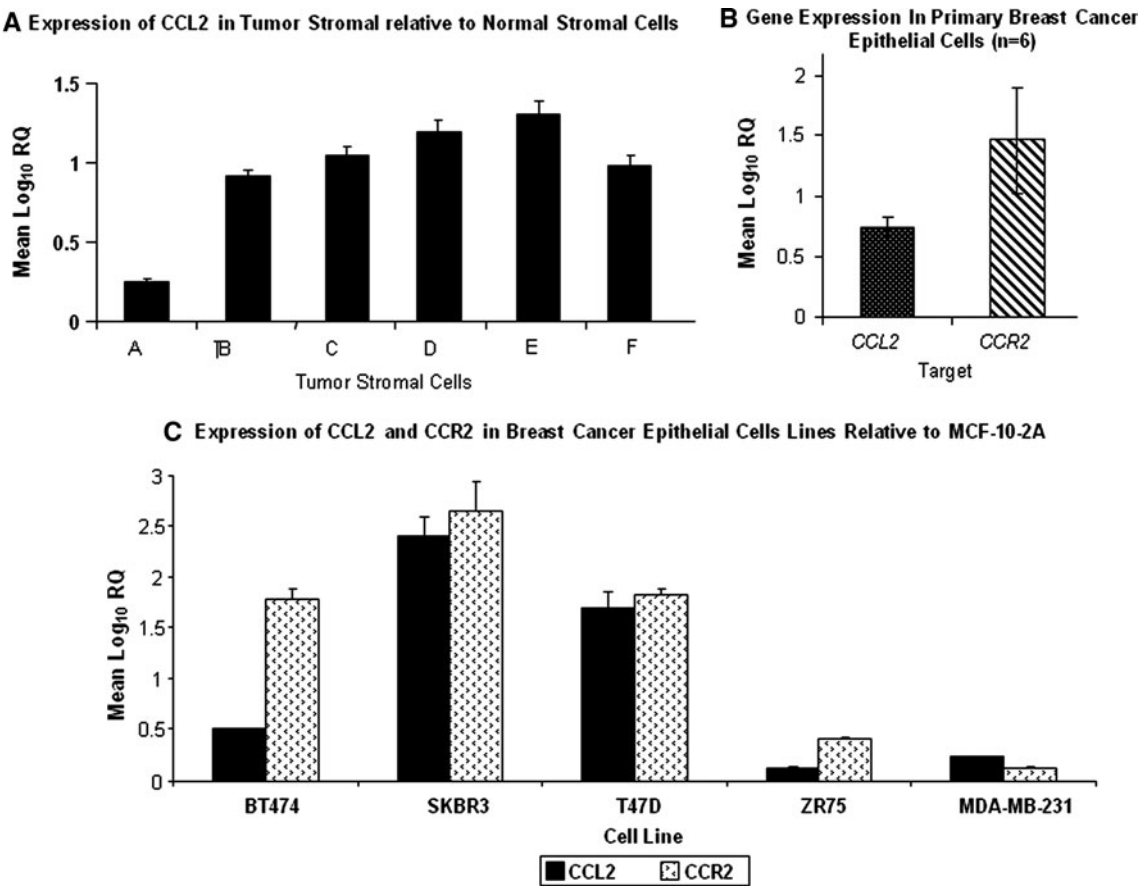

Fig. 2 CCL2 and CCR2 expression in breast cancer cells. **a** Expression of CCL2 in tumor stromal ($n = 6$ individual donors) compared to normal stromal cells ($n = 4$ individual donors), represented by the baseline. CCR2 expression was not detected in any stromal cell population examined. **b** CCL2 and CCR2 gene expression in primary breast cancer epithelial cells isolated from fresh breast tumors ($n = 6$ individual donors). Results are expressed as $\log_{10}$ RQ values, relative to normal counterparts ($n = 2$) ($2^{-\Delta\Delta C_T}$). **c** Breast cancer epithelial cell lines express *CCL2*, and its principal receptor *CCR2*. Results are expressed as $\log_{10}$ RQ values, and relative to non-tumorigenic MCF-10-2A cells

increased following co-culture with tumor compared to normal stromal cells (Fig. 5a, b; $P < 0.05$). While expression levels of the proliferative marker, *Ki67*, increased following co-culture with normal stromal cells, it decreased when the co-cultures involved tumor stromal cells. Expression levels of the invasion associated gene *VIL2*, and the oncogene, *ELK1*, were significantly upregulated in T47D cells following co-culture in a tumor specific fashion (Fig. 5a; $P < 0.05$).

In vivo co-culture

T47D cells were injected alone or coinjected with tumor stromal cells subcutaneously into nude mice. These tumor stromal cells were derived from two separate human invasive ductal breast carcinomas, Tum A Stro (Luminal A, Grade 3, T1, N0) and Tum B Stro (Luminal A, Grade 2, T1, N0). T47D cells co-mixed with tumor stromal cells exhibited a faster rate of growth and generated tumors of greater volume at the endpoint of 10 weeks than T47D injected alone (mean tumor volume ± SEM: T47D 33 ± 5 mm^3, T47D + Tum A Stro 118 ± 15 mm^3, T47D + Tum B Stro 63 ± 9 mm^3; Fig. 6a). Xenografts that developed in the presence of tumor stromal cells also displayed neovascularisation, confirmed by positive staining for the endothelial marker, CD31 (Fig. 6b; b [10×], c [20×], d [40×]), while tumors formed from T47D cells alone were negative for CD31 (Fig. 6b; a [40×]). Mixed stromal–epithelial xenografts displayed greater intensity of Ezrin staining throughout the tumors and increased cytoplasmic localization of the protein (Fig. 6c; b, arrows) compared to epithelial xenografts which predominantly displayed membranous staining (Fig. 6c; a, arrows).

Upon tumor harvesting at necropsy, mixed tumor xenografts were digested and the T47D cells retrieved with epithelial specific beads. Subsequent analysis allowed identification of gene expression changes in these isolated epithelial cells resulting from their in vivo interaction with

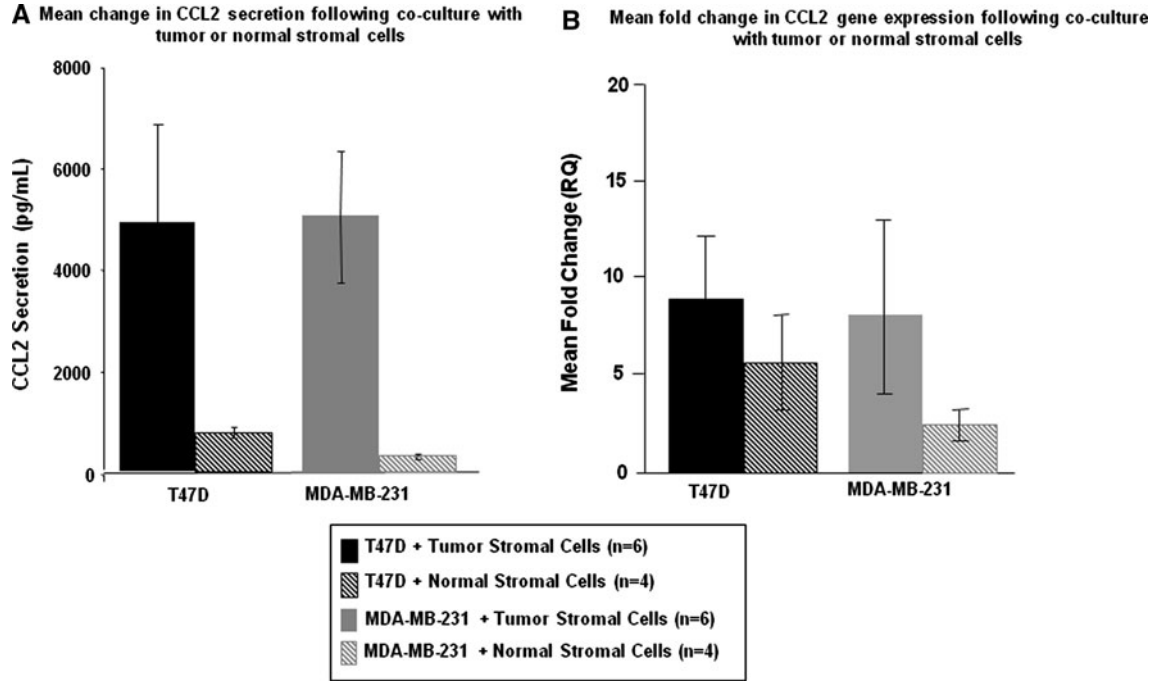

Fig. 3 Interaction of tumor stromal and epithelial cells results in increased CCL2 protein secretion and gene expression. **a** CCL2 secretion: the baseline of the graph represents the sum of what each cell population secreted when cultured individually, with each *bar* representing the amount by which the co-culture population differed from this. Data presented represent mean ± SEM of triplicate experiments, using six individual tumor stromal populations and four individual normal stromal populations. **b** Following in vitro co-culture of primary stromal cells with breast cancer cell lines, epithelial cells were retrieved using EpCAM+ magnetic beads, and expression of *CCL2* analyzed. Data presented represent mean fold change values ±SEM of triplicate experiments, and are expressed relative to levels detected in the breast cancer cells cultured alone ($2^{-\Delta\Delta C_T}$)

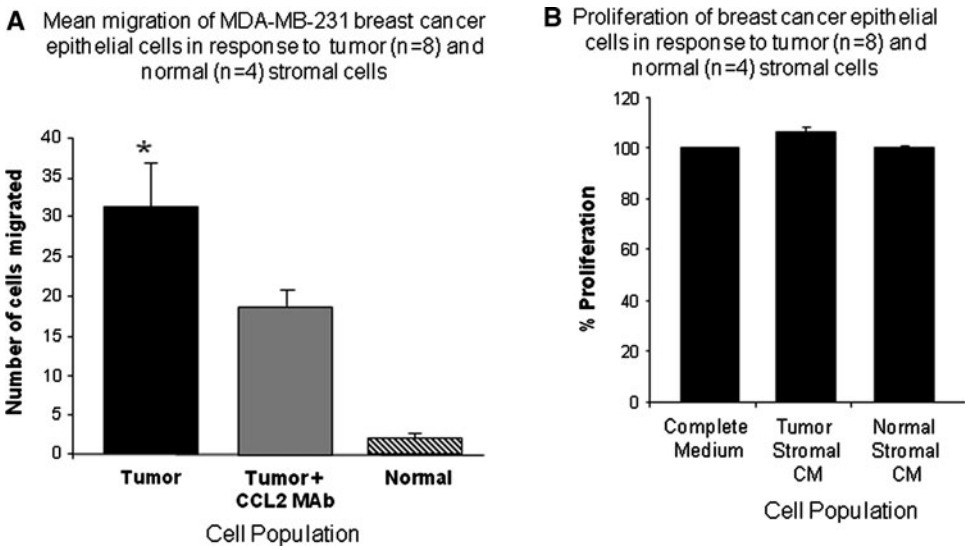

Fig. 4 Interaction of tumor stromal and epithelial cells in vitro: effect on migration and proliferation. **a** Factors secreted by primary tumor stromal cells induce increased migration of breast cancer epithelial cells. This effect was subsequently blocked by the addition of a monoclonal antibody to CCL2. **b** A Vialight™ assay was used to assess relative proliferation of breast cancer cells (MDA-MB-231 and T47D), in response to stromal cell CM (tumor stromal cells and normal stromal cells). Proliferation induced by complete medium was taken as 100%. Results are displayed as mean % proliferation of the 2 cell lines ±SEM, from triplicate experiments

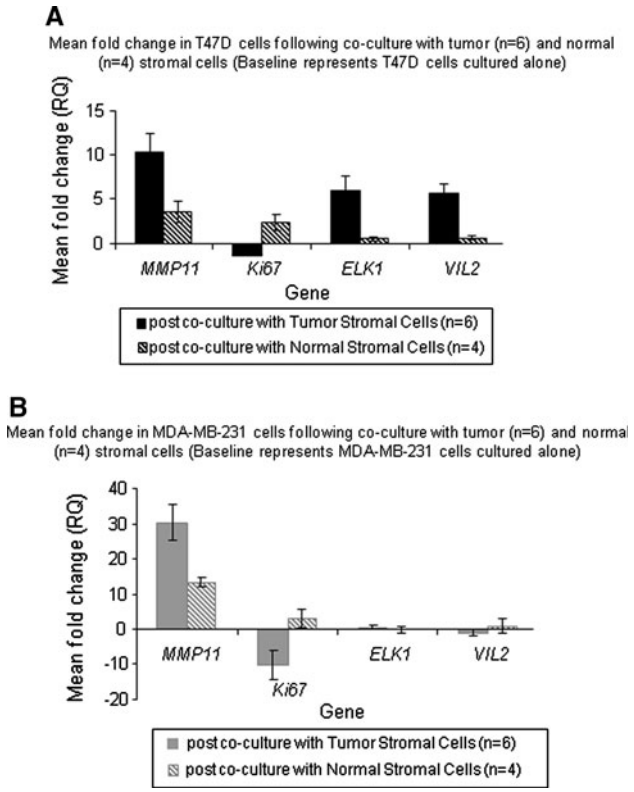

Fig. 5 Interaction of tumor stromal and epithelial cells in vitro: effect on gene expression. Interaction with tumor stromal cells induces increased expression of invasion associated genes and decreased expression of proliferative markers in breast cancer epithelial cells T47D (**a**) and MDA-MB-231 (**b**). Data presented represent mean fold change values ±SEM of triplicate experiments, and are expressed relative to levels detected in the breast cancer cells cultured alone ($2^{-\Delta\Delta C_T}$)

tumor stromal cells (Fig. 6d). The epithelial cells displayed increased expression of the invasion and migration associated genes *MMP11*, *VIL2*, and *ELK1* following in vivo co-culture with tumor stromal cells (range 0.2–3.6 log fold increase, Fig. 6d). Interestingly these cells also displayed increased expression of the proliferative marker *Ki67*, which was downregulated in the in vitro co-culture set-up.

Discussion

The current study highlights potential mechanisms through which malignant epithelial cells can harness stromal cell biology to facilitate their invasion into the tumor microenvironment.

There is accumulating evidence pointing to a pivotal role for chemokines in controlling migration, growth, and differentiation of tumor cells [30]. The current study shows that isolated primary tumor epithelial cells displayed elevated expression of *CCL2*, as well as its principal receptor, *CCR2*. In terms of breast cancer, the potential tumorigenic role of CCL2 and CCR2 is poorly defined to date. In the current study, primary tumor stromal cells had significantly higher expression of the CCL2 gene than normal stromal cells. CCL2 exerts its effects through a principal receptor, CCR2 [31], of which two isoforms (A and B) have been identified. *CCR2* receptor expression has previously been shown in two cell lines, MDA-MB-231 and T47D [32]. The current study reports that along with these and other breast cancer cell lines, breast cancer epithelial cells isolated from fresh breast tumors express *CCR2A*, while both isoforms were undetectable in tumor stromal cells, suggesting a paracrine role for the chemokine. CCL2 was detected in the CM of all tumor stromal cells examined and in significantly higher quantities than normal stromal cells. Directional cell migration is an integral part of cancer cell invasion during metastasis, involving changes in cell cytoskeleton and adhesion [33]. In the current study factors secreted by tumor stromal cells induced migration of breast cancer epithelial cells, shown to be mediated at least in part by CCL2. Furthermore direct contact between tumor stromal and epithelial cells induced a synergistic increase in CCL2 secretion and gene expression. The disparity between protein secretion and gene expression levels may be accounted for by post-translational modifications, which would not be detected at the gene expression level.

It is worth noting that in vitro and in vivo interaction with tumor stromal cells induced increased expression of *VIL2* in epithelial cells. Ezrin, the coded product of the *VIL2* gene, is a membrane-cytoskeleton crosslinker known to regulate cell adhesion and motility, as well as overall metastatic potential [34]. Moreover, mixed tumor xenografts not only achieved increased tumor volume, but also displayed increased cytoplasmic localization of Ezrin protein, compared to tumors formed from T47D cells alone. The switch from apical to cytoplasmic Ezrin localization has previously been shown to correlate with high tumor grade, high *Ki67* expression (also shown in this study) and metastasis [35].

The presence of stromal cells in vivo resulted in positive staining for CD31, indicating active neoangiogenesis within tumors xenografts [36], a known effect of CCL2 [17, 21]. Emphasis must be placed on the fact that in this study baseline gene expression levels were analyzed in primary breast cancer epithelial cells isolated from fresh tumors; however, to support triplicate repeats of all experiments performed, breast cancer cell lines were employed in functional experiments.

The results presented also show that interaction with tumor stromal cells induced *MMP11* upregulation in breast cancer epithelial cells, with a similar degree of upregulation in vitro and in vivo. MMP11 has been shown to promote tumor progression [37], and is upregulated in invasive

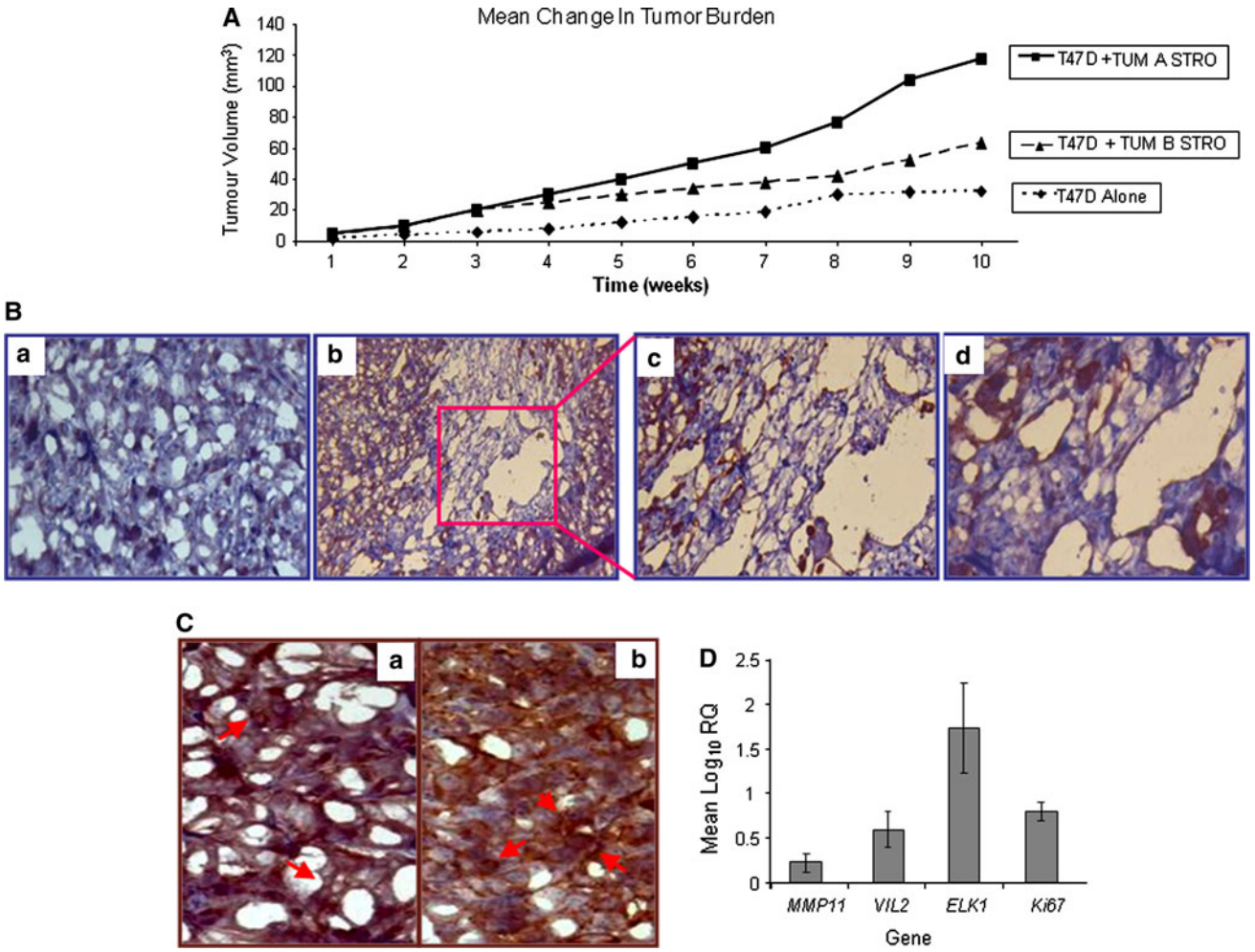

Fig. 6 Interaction of tumor stromal and epithelial cells in vivo. T47D cells were injected alone or coinjected with tumor stromal cells subcutaneously into nude mice. **a** Mixed stromal–epithelial xenografts exhibited increased tumor volume. Data represent mean ± SEM for $n = 6$ in each group. **b** Xenografts that developed in the presence of tumor stromal cells (*b* [×10], *c* [×20], *d* [×40]) stained positive for CD31, indicating neovascularization, while those composed of epithelial cells alone did not (*a* [×40]). **c** Mixed stromal–epithelial xenografts displayed greater intensity Ezrin staining and increased cytoplasmic localization of the protein (**b**), compared to those composed of epithelial cells alone where more membrane targeted staining was visible (**a**). **d** Upon harvesting, tumors were digested and T47D cells were retrieved from mixed xenografts with epithelial specific beads, RNA extracted and RQ-PCR performed. Results are expressed relative to expression levels in epithelial cells isolated from tumors formed from T47D cells alone. Each *bar* represents mean $\log_{10}$ RQ ± SEM for both groups (Tum A Stro and Tum B Stro, $n = 6$ in each group)

relative to in situ ductal carcinoma [4]. Furthermore tumor stromal cells also induced increased expression of *ELK1* in T47D cells in vitro and in vivo. *ELK1*, a member of the ets oncogene family, promotes tumor progression, and is critical to regulation of cell proliferation and apoptosis [38]. While ELK1 expression was increased in vitro (six-fold increase), the level of increase was markedly higher in vivo (54-fold).

A challenge in breast cancer research is the availability of models that faithfully reflect the complexity of the disease. The majority of in vivo xenograft models are homotypic, involving the introduction of breast cancer cell lines alone into the mouse microenvironment [39]. In this and other recent studies [7, 40], breast cancer epithelial cells were admixed with tumor stromal cells isolated from human breast tumors and introduced into mice, forming heterotypic 3-dimensional xenografts which more accurately simulate stromal–epithelial interactions in the tumor microenvironment. This is the first study to retrieve and analyze epithelial cells following in vivo co-culture. While the majority of targets showed similar trends in both in vitro and in vivo models, the disparity in some results can be explained by the fact that cultures grown on a non-physiological 2-dimensional substratum lack exposure to components of the extracellular matrix that are present in the 3-dimensional in vivo microenvironment [40]. Given the heterogeneity of breast cancer, no individual model reflects all aspects of the disease, however, every attempt

should be made to reflect in vivo events and models that focus on epithelial cells alone fall short on this.

Understanding the dynamic and reciprocal crosstalk between stromal and epithelial cells will deepen our knowledge of the tumorigenic process, and may also facilitate exploitation of stromal–epithelial interactions as valid targets for novel therapies.

Acknowledgments Shirley Potter and Roisin Dwyer were funded by the Health Research Board of Ireland, a Clinical Research Training Fellowship and Research Project Grant, respectively. Marion Hartmann was funded by Breast Cancer Ireland. Funding was also received from the National Breast Cancer Research Institute.

Conflict of interest The authors declare that they have no competing interests.

References

1. Lorusso G, Ruegg C (2008) The tumor microenvironment and its contribution to tumor evolution toward metastasis. Histochem Cell Biol 130:1091–1103
2. Kalluri R, Zeisberg M (2006) Fibroblasts in cancer. Nat Rev Cancer 6:392–401
3. Mueller MM, Fusenig NE (2004) Friends or foes—bipolar effects of the tumour stroma in cancer. Nat Rev Cancer 4:839–849
4. Ma XJ, Dahiya S, Richardson E, Erlander M, Sgroi DC (2009) Gene expression profiling of the tumor microenvironment during breast cancer progression. Breast Cancer Res 11:R7
5. Finak G, Bertos N, Pepin F, Sadekova S, Souleimanova M et al (2008) Stromal gene expression predicts clinical outcome in breast cancer. Nat Med 14:518–527
6. Singer CF, Gschwantler-Kaulich D, Fink-Retter A, Haas C, Hudelist G et al (2008) Differential gene expression profile in breast cancer-derived stromal fibroblasts. Breast Cancer Res Treat 110:273–281
7. Orimo A, Gupta PB, Sgroi DC, Arenzana-Seisdedos F, Delaunay T et al (2005) Stromal fibroblasts present in invasive human breast carcinomas promote tumor growth and angiogenesis through elevated SDF-1/CXCL12 secretion. Cell 121:335–348
8. Kim JB, Stein R, O'Hare MJ (2005) Tumour–stromal interactions in breast cancer: the role of stroma in tumourigenesis. Tumour Biol 26:173–185
9. Elenbaas B, Weinberg RA (2001) Heterotypic signaling between epithelial tumor cells and fibroblasts in carcinoma formation. Exp Cell Res 264:169–184
10. Allinen M, Beroukhim R, Cai L, Brennan C, Lahti-Domenici J et al (2004) Molecular characterization of the tumor microenvironment in breast cancer. Cancer Cell 6:17–32
11. Bhowmick NA, Neilson EG, Moses HL (2004) Stromal fibroblasts in cancer initiation and progression. Nature 432:332–337
12. Tlsty TD, Coussens LM (2006) Tumor stroma and regulation of cancer development. Annu Rev Pathol 1:119–150
13. Muller A, Homey B, Soto H, Ge N, Catron D et al (2001) Involvement of chemokine receptors in breast cancer metastasis. Nature 410:50–56
14. Dwyer RM, Potter-Beirne SM, Harrington KA, Lowery AJ, Hennessy E et al (2007) Monocyte chemotactic protein-1 secreted by primary breast tumors stimulates migration of mesenchymal stem cells. Clin Cancer Res 13:5020–5027
15. Zlotnik A, Yoshie O, Nomiyama H (2006) The chemokine and chemokine receptor superfamilies and their molecular evolution. Genome Biol 7:243
16. Christopherson K 2nd, Hromas R (2001) Chemokine regulation of normal and pathologic immune responses. Stem Cells 19:388–396
17. Saji H, Koike M, Yamori T, Saji S, Seiki M et al (2001) Significant correlation of monocyte chemoattractant protein-1 expression with neovascularization and progression of breast carcinoma. Cancer 92:1085–1091
18. Ueno T, Toi M, Saji H, Muta M, Bando H et al (2000) Significance of macrophage chemoattractant protein-1 in macrophage recruitment, angiogenesis, and survival in human breast cancer. Clin Cancer Res 6:3282–3289
19. Charo IF, Myers SJ, Herman A, Franci C, Connolly AJ et al (1994) Molecular cloning and functional expression of two monocyte chemoattractant protein 1 receptors reveals alternative splicing of the carboxyl-terminal tails. Proc Natl Acad Sci USA 91:2752–2756
20. Wong LM, Myers SJ, Tsou CL, Gosling J, Arai H et al (1997) Organization and differential expression of the human monocyte chemoattractant protein 1 receptor gene. Evidence for the role of the carboxyl-terminal tail in receptor trafficking. J Biol Chem 272:1038–1045
21. Salcedo R, Ponce ML, Young HA, Wasserman K, Ward JM et al (2000) Human endothelial cells express CCR2 and respond to MCP-1: direct role of MCP-1 in angiogenesis and tumor progression. Blood 96:34–40
22. Neumark E, Sagi-Assif O, Shalmon B, Ben-Baruch A, Witz IP (2003) Progression of mouse mammary tumors: MCP-1-TNFalpha cross-regulatory pathway and clonal expression of promalignancy and antimalignancy factors. Int J Cancer 106:879–886
23. Chavey C, Bibeau F, Gourgou-Bourgade S, Burlinchon S, Boissiere F et al (2007) Oestrogen receptor negative breast cancers exhibit high cytokine content. Breast Cancer Res 9:R15
24. Albini A, Sporn MB (2007) The tumour microenvironment as a target for chemoprevention. Nat Rev Cancer 7:139–147
25. Joyce JA (2005) Therapeutic targeting of the tumor microenvironment. Cancer Cell 7:513–520
26. Speirs V, Green AR, Walton DS, Kerin MJ, Fox JN, Carelton PJ, Desai SB, Atkin SL (1998) Short-term primary culture of epithelial cells derived from human breast tumours. Br J Cancer 78:1421–1429
27. Livak KJ, Schmittgen TD (2001) Analysis of relative gene expression data using real-time quantitative PCR and the 2(-Delta Delta C(T)) method. Methods 25:402–408
28. Santos AM, Jung J, Aziz N, Kissil JL, Pure E (2009) Targeting fibroblast activation protein inhibits tumor stromagenesis and growth in mice. J Clin Invest 119:3613–3625
29. Scanlan MJ, Raj BK, Calvo B, Garin-Chesa P, Sanz-Moncasi MP et al (1994) Molecular cloning of fibroblast activation protein alpha, a member of the serine protease family selectively expressed in stromal fibroblasts of epithelial cancers. Proc Natl Acad Sci USA 91:5657–5661
30. Balkwill F (2004) Cancer and the chemokine network. Nat Rev Cancer 4:540–550
31. Charo IF (1999) CCR2: from cloning to the creation of knockout mice. Chem Immunol 72:30–41
32. Nam JS, Kang MJ, Suchar AM, Shimamura T, Kohn EA et al (2006) Chemokine (C–C motif) ligand 2 mediates the prometastatic effect of dysadherin in human breast cancer cells. Cancer Res 66:7176–7184
33. Jiang P, Enomoto A, Takahashi M (2009) Cell biology of the movement of breast cancer cells: intracellular signalling and the actin cytoskeleton. Cancer Lett 284:122–130

34. Li Q, Wu M, Wang H, Xu G, Zhu T et al (2008) Ezrin silencing by small hairpin RNA reverses metastatic behaviors of human breast cancer cells. Cancer Lett 261:55–63
35. Sarrio D, Rodriguez-Pinilla SM, Dotor A, Calero F, Hardisson D et al (2006) Abnormal ezrin localization is associated with clinicopathological features in invasive breast carcinomas. Breast Cancer Res Treat 98:71–79
36. Bingle L, Lewis CE, Corke KP, Reed MW, Brown NJ (2006) Macrophages promote angiogenesis in human breast tumour spheroids in vivo. Br J Cancer 94:101–107
37. Motrescu ER, Blaise S, Etique N, Messaddeq N, Chenard MP et al (2008) Matrix metalloproteinase-11/stromelysin-3 exhibits collagenolytic function against collagen VI under normal and malignant conditions. Oncogene 27:6347–6355
38. Hsieh YH, Wu TT, Tsai JH, Huang CY, Hsieh YS et al (2006) PKCalpha expression regulated by Elk-1 and MZF-1 in human HCC cells. Biochem Biophys Res Commun 339:217–225
39. Vargo-Gogola T, Rosen JM (2007) Modelling breast cancer: one size does not fit all. Nat Rev Cancer 7:659–672
40. Olsen CJ, Moreira J, Lukanidin EM, Ambartsumian NS (2010) Human mammary fibroblasts stimulate invasion of breast cancer cells in a three-dimensional culture and increase stroma development in mouse xenografts. BMC Cancer 10:444

Dwyer *et al. Stem Cell Research & Therapy* 2010, **1**:25
http://stemcellres.com/content/1/3/25

stem cell research&therapy

REVIEW

Advances in mesenchymal stem cell-mediated gene therapy for cancer

Roisin M Dwyer[1,2]*, Sonja Khan[1], Frank P Barry[2], Timothy O'Brien[1,2] and Michael J Kerin[1]

Abstract

Mesenchymal stem cells have a natural tropism for tumours and their metastases, and are also considered immunoprivileged. This remarkable combination of properties has formed the basis for many studies investigating their potential as tumour-specific delivery vehicles for suicide genes, oncolytic viruses and secreted therapeutic proteins. The aim of the present review is to discuss the range of approaches that have been used to exploit the tumour-homing capacity of mesenchymal stem cells for gene delivery, and to highlight advances required to realize the full potential of this promising approach.

Introduction

Despite significant advances in the field of gene therapy for cancer, two major obstacles remain that continue to limit the clinical potential of this approach: lack of tumour tropism of vectors, and stimulation of an immune response. These barriers preclude systemic administration of current vectors to efficiently target metastatic disease. The combination of cellular therapy and gene delivery is an attractive option as it will potentially protect the vector from immune surveillance, and will support targeted delivery of a gene or therapeutic protein to the tumour site.

Mesenchymal stem cells

Mesenchymal stem cells (MSCs) are nonhaematopoietic stem cells that have generated a significant amount of interest as a result of their apparent ability to home to the tumour site following systemic delivery. MSCs have an inherent ability both to self-renew and to differentiate into multiple lineages including osteoblasts, chondrocytes and adipocytes [1]. The cells are readily isolated from the stromal compartment of bone marrow, along with a number of other sources including adipose tissue, trabecular bone and skeletal muscle [2]. Although a single marker for MSCs has not been isolated, a panel of specific antigens has been identified, including expression of CD105, CD73 and CD90 in >95% of the culture, and an absence of CD14, CD34, CD19, HLA-DR and CD45 [3]. When introduced systemically to healthy animals, MSCs have been shown to home preferentially to the lung, liver and bone, and were found to a lesser extent in other tissues. Upon injury, however, the migratory pathway changes to preferentially target sites of injury [4].

Although MSCs have potential uses in regenerative medicine and a number of different disease models, the present review will specifically focus on their potential for targeted gene delivery in the context of cancer. This is an exciting area of research that has gained considerable momentum in recent years, with studies reporting engineered MSCs specifically targeting multiple tumour types followed by local secretion of therapeutic proteins (IFNβ [5-7], IL-2 [8,9], IL-12 [10-12], pigment epithelium-derived factor [13], NK4 [14], TNF-related apoptosis inducing ligand (TRAIL) [15-18]), expression of prodrug activating suicide genes (herpes simplex virus-thymidine kinase [19-21], cytosine deaminase [22]), and delivery of replicating oncolytic viruses [16,19,23-25]. A major advantage of MSCs in this setting is that they are considered immunoprivileged, possibly due to low expression of Ag(HLA) MHC class 1, and no expression of CD40, CD80 and CD86 [4]. The cells are also known to secrete prostaglandin, transforming growth factor beta and hepatocyte growth factor, which regulate the T-cell immune response, thereby decreasing the probability of a cytotoxic T-cell response to transduced cells [17].

Resident MSCs suppress both transient and continuous immune surveillance, which aims at facilitating the healing process [26]. This immune privilege in the context of cancer, however, has the potential to support tumour progression. Djouad and colleagues reported growth of B16 melanoma cells in allogenic animals only in the presence of MSCs, suggesting that protection from the host immune response supported tumour establishment

*Correspondence: roisin.dwyer@nuigalway.ie
[1]Division of Surgery, School of Medicine, Clinical Science Institute, National University of Ireland Galway, Galway, Ireland
Full list of author information is available at the end of the article

[27]. Further studies by the same group revealed that MSCs administered in low numbers with Renca adenocarcinoma cells actually induced tumour rejection [28]. MSCs were also shown to inhibit outgrowth of colon carcinoma in rats, with complete inhibition seen when the number of MSCs were at least equal to the number of tumour cells. Tumour establishment using the mixed cell population was found to induce more infiltration of monocytes and granulocytes than the individual populations alone [29].

This observation may be explained by the fact that high numbers of MSCs have been shown to suppress alloreactive T cells, with very low numbers found to stimulate lymphocyte proliferation [30]. Indeed, additional evidence suggests that the context with which MSCs are introduced *in vivo* may influence their immune phenotype [26].

Tumour tropism

Tumour-specific migration of MSCs is not completely understood, but appears to be dependent upon the biological properties of the tumour microenvironment, as well as the native tropism of selected cells. Integration of MSCs into the tumour stroma is thought to be mediated by high local concentrations of inflammatory chemokines and growth factors. The tumour microenvironment is considered a site of chronic inflammation [31]. This environment may mediate MSC migration through secretion of soluble factors such as epidermal growth factor, vascular endothelial growth factor-A, fibroblast growth factor, platelet-derived growth factor, stromal-derived growth factor-1α (SDF-1α/CXCL12), IL-8, IL-6, granulocyte–macrophage colony-stimulating factor, granulocyte colony-stimulating factor, Ang1, monocyte chemoattractant protein-1 (CCL2), haematopoietic growth factor, transforming growth factor beta-1 and urokinase-type plasminogen activator [32-37].

The process of MSC mobilization to the tumour is thought to be regulated similarly to leukocyte migration through integrins and adhesion molecules [38]. Molecules involved in leukocyte trafficking – such as tethering, rolling, adhesion and transmigration from the bloodstream to the tissue – are expressed on MSCs. These include integrins, selectins and chemokine receptors. Both P-selectin and vascular cell adhesion molecule-1 have been found to influence the adhesion of MSCs in endothelium [39].

MSCs express a wide range of molecules, including growth factors, chemokines, adhesion molecules and toll-like receptors, on their surface [38-44]. MSCs are known to functionally express chemokine receptors CCR1, CCR4, CCR7, CCR9, CCR10, CXCR4, CXCR5, CXCR6, CX3CR1 and c-met, which has been increasingly linked to tumour tropism [40-43]. The mechanism of MSC migration, however, is still not fully elucidated.

The most documented chemokine receptor implicated in targeted homing of MSCs is CXCR4, which has potential in cell mobilization and homing [45]. A study by Wynn and colleagues reported that CXCR4 is highly expressed on MSCs, but mainly intracellularly (83 to 98%) rather than on the surface [46]. Another study reported no detectable CXCR4 expression on MSCs [42]. Variable expression of CXCR4 detected in different studies has been suggested to be related to sensitivity of the trypsin digestion procedure used [44], differences in culture conditions, and heterogeneity of MSC populations. *In vitro* three-dimensional culture of MSCs as spheroids was shown to increase SDF-1α signalling, which restored functional expression of its receptor CXCR4 and homing potential that is crucial for therapeutic applications [47].

Although the tumour tropism of MSCs is generally accepted, it is certainly dependent on the tumour model. Variation in levels of MSC engraftment reported in different studies may be explained by differences in MSC isolation, culture conditions and experimental protocols used. Within individual studies, however, variable levels of MSC engraftment have been reported in different tumour types, most probably due to differences in the microenvironment created by the tumour in question [48]. The proportion of MSCs engrafted was not found to be related to tumour size [48].

A recent study further highlighted the role that the degree of inflammation in a tumour microenvironment plays in the level of MSC recruitment [7]. In a study of MSC-IFNβ-mediated therapy of pancreatic cancer, treatment with an anti-inflammatory agent resulted in reduction of MSC engraftment in the tumour, and reversed the tumour inhibitory effects observed [7].

Enhancing tumour tropism of mesenchymal stem cells

Modification of the tumour microenvironment

The apparent role of inflammation in MSC tumour tropism has also been harnessed to increase engraftment through tumour irradiation, which is associated with release of several cytokines from exposed tissue [48,49]. Klopp and colleagues found that low-dose irradiation of the tumour microenvironment enhanced MSC tropism and engraftment at the tumour site [49]. Irradiation resulted in apoptosis and increased release of inflammatory signals at the site of radiation, including TNFα, platelet-derived growth factor, as well as chemokines CCL2 and CCR8 [49]. The effect of tumour radiotherapy on localization of lentivirus-transduced MSCs in a variety of tumour types has also been reported [48]. Irradiation increased MSC localization in LoVo, HT-29 (colon) and MDA-231 (breast), but not UMSCC1 (head and neck) xenografts. This study also reported a

modest elevation in CCL2 expression in irradiated tumours, although it was not found to correlate with MSC infiltration [48]. Inflammation plays a critical role in tumour progression [50], and therefore stimulation to support MSC homing to tumours would not be a viable option. Radiotherapy is frequently a component of cancer therapy, however, and therefore could work in combination with MSC-based gene delivery to support improved targeting of MSCs to tumours.

Modification of the mesenchymal stem cell surface

While variations in MSC engraftment have been observed in different tumour models, attempts are being made to improve tumour tropism and infiltration through modification of the MSC surface. Cell rolling is a critical step of the adhesion cascade supporting rapid deceleration of cells from the bloodstream, and is mediated by selectins expressed on the endothelium of the target organ. Immobilized sialyl Lewis X on MSCs was shown to induce cell rolling on the P-selectin surface under dynamic shear flow conditions *in vitro*, and may have potential applications in improving MSC engraftment *in vivo* [51]. In one study where native MSC tropism for the tumour of interest was not detected, MSCs were engineered to overexpress the epidermal growth factor receptor – which binds transforming growth factor alpha and epidermal growth factor. Transduced MSCs had enhanced migratory properties towards GL261 gliomas or B16 melanoma *in vivo* [52]. Following establishment of improved engraftment, the cells were further engineered to secrete IFNγ, resulting in increased animal survival [52].

Mesenchymal stem cell-mediated virus delivery

A significant advantage of MSCs as cellular vehicles is their accessibility for genetic manipulation *in vitro*. Recent studies have incorporated the use of lentivirus-mediated transduction [13,16,48,53], retrovirus-mediated transduction [10,19,20,22] or plasmid-mediated transduction [21]; however, the majority remain adenovirus based [5-8,11,14,15,17,18,23-25,54,55]. MSCs have a low coxsackie and adenovirus receptor, high-integrin phenotype, which results in low transfection efficiency using wildtype adenoviruses. Modification of the adenovirus fibre or knob domain has been used to improve adenovirus-mediated transgene expression. Incorporation of an arginine–glysine–aspartate motif into the adenovirus fibre or the 5/3 knob domain of human adenovirus serotype 3 supports coxsackie and adenovirus receptor-independent transfer and improves MSC transduction efficiency [14,23-25,55].

This approach has evolved to include the use of conditionally replicating adenoviruses, which support delivery of an increased viral load specifically to the tumour site [23-25]. Clearly the timing is important here to avoid toxicity to MSCs prior to engraftment at the target site. The cycle of MSC adenovirus replication has been reported to have relatively slow kinetics, which may allow time for MSCs to reach the target site before replication causes cell death [56]. The delivery of oncolytic viruses does not rely on long-term survival and proliferation of cellular vehicles, as they are destroyed by viral replication. Capsid-modified oncolytic adenoviruses have been coupled with the use of transcription-specific promoters to limit ectopic viral amplification in non-target cells [55]. MSCs have also been engineered to express the herpes simplex virus-thymidine kinase followed by administration of the prodrug ganciclovir for targeted cancer suicide gene therapy [19-21]. Based on similar principles, retrovirus transduction of adipose-derived MSCs to express cytosine deaminase, followed by systemic administration of the prodrug 5-fluorocysteine, mediated a strong anti-tumour effect *in vivo* [22].

Localized delivery of therapeutic proteins

Along with their tumour tropism, MSCs have been shown to integrate into and persist in the tumour stroma [5]. This integration has supported their use as delivery vehicles for various biological agents, whose systemic administration is precluded due to their short half-life and toxicity at the doses required for therapy. MSCs can efficiently produce biological products at tumour sites and so have the potential to improve pharmacokinetics of secreted agents [5].

In a number of tumour models, MSCs expressing IFNβ have been shown to result in decreased tumour burden and increased animal survival [5-7]. Increased systemic levels of IFNβ or secretion at sites distant from the tumour were not effective, indicating that regional secretion was required [5-7]. MSCs engineered to secrete IL-12 and embedded in a matrix adjacent to tumours were also reported to have a significant therapeutic effect [10]. Similar to findings in the case of IFNβ, regional secretion was required, with no reduction in growth observed when the implant was placed in the opposite flank to the tumour [10].

MSCs expressing the hepatocyte growth factor antagonist NK4 *in vivo* were also found to prolong animal survival by inhibiting tumour-associated angiogenesis, lymphoangiogenesis and induction of cancer cell apoptosis [14]. Local secretion of pigment epithelium-derived factor in a model of hepatocellular carcinoma through lentivirus transduction of MSCs similarly resulted in lower tumour volume, reduced lung metastases and improved survival through inhibition of tumour angiogenesis [13].

Further, MSCs secreting IL-2 [8,9] or IL-12 [10,11] were shown to elicit an immunological reaction, and to

stimulate inflammatory cell infiltration of the tumour tissue. The observed anticancer effect was shown to be immune mediated and absent in immunodeficient animals [10]. Delivery of MSC-IL-12 did not cause systemic toxicity, and resulted in increased serum and tumour levels of IL-12. In contrast, administration of Ad-IL-12 only increased serum IL-12 levels and induced systemic toxicity [11]. Therefore it appears that MSC-mediated local delivery of a therapeutic agent may be better tolerated by the host without inducing an unacceptable immune response [11].

TRAIL induces caspase-mediated apoptosis in tumour cells that overexpress the receptor. Like most healthy tissues, MSCs are resistant to TRAIL-induced apoptosis due to their very low levels of active receptors [17]. As a result of this, MSCs secreting TRAIL have been used in models of lung cancer, breast cancer, cervical cancer and brain cancer *in vivo*, resulting in significant anti-tumour effects [15-18,53]. In one study using a lentiviral vector, TRAIL expression was placed under the control of a *tet* promoter, supporting conditional activation using doxycycline [16]. In an animal model of lung metastases of breast cancer, this controlled, local delivery of TRAIL completely cleared metastatic disease in a selection of animals [16]. Interestingly, when MSC-TRAIL cells were co-injected with tumour cells for subcutaneous tumour formation, only doxycycline-mediated activation on the day of tumour cell inoculation (day 0) caused a significant decrease in tumour weight. Activation following tumour establishment (day 25) did not result in a change in tumour burden [16].

Potential role in tumourigenesis

Although beyond the scope of the current review, the potential role of MSCs in tumour initiation or promotion is a significant concern that must be addressed fully to allow MSC-mediated therapy for cancer to realize its full potential. This role remains a topic of continued debate. Expansion of MSCs *in vitro* will be required for therapeutic application and so their stability in culture is paramount. Spontaneous transformation of human MSCs has been reported following long-term passage *in vitro* [57,58], while Bernardo and colleagues found no evidence of human MSC transformation [59]. Indeed the majority of studies have shown that human MSCs are stable, while murine MSCs are more prone to genetic transformation during *in vitro* culture, and may be capable of forming sarcomas *in vivo* [59-63]. Although transformation of human MSCs appears unlikely, and very rare, these studies certainly emphasize the importance of stringent monitoring of MSCs, including karyotyping, before application in the clinical setting.

MSCs have also been implicated as tumour supportive when co-injected in the presence of a variety of tumour cell types, including breast [64-67], ovarian [68], melanoma [27], glioma [69,70] and colon [71,72] tumour cells. The majority of these studies, however, used an equal or even excess number of MSCs over tumour cells. The data generated provide important information on interactions between MSCs and tumour cells, although the models are unlikely to reflect the *in vivo* situation. MSCs were shown to integrate into the tumour stroma and were demonstrated to exert their effects at least partly through secretion of paracrine factors including CCL5, IL-6 and SDF-1α [64,65,68]. There is also evidence that MSCs may serve as precursors for carcinoma-associated fibroblasts and/or pericytes, playing a potentially important role in tumour angiogenesis through differentiation and the release of proangiogenic factors [67-69,71-76]. Additionally, as previously mentioned, the immunosuppressive qualities of MSCs may support tumour development and progression through protection of cancer cells from immune surveillance [27].

Conversely, co-injection of MSCs has also been shown to result in tumour suppression in a model of colon cancer [29], hepatoma [77] and melanoma [78].

In terms of MSC-mediated gene delivery, understanding the role of MSCs following engraftment at the site of a pre-established tumour is required. The majority of studies outlined here, using MSCs engineered to deliver therapeutic agents, have resulted in significant anti-tumour effects *in vivo*. Unmodified MSCs were also shown to result in tumour suppression in some cases [7,8,79], with the majority showing no effect on tumour progression following engraftment at the site of an established tumour [13,18,23,53,55,69,75]. Repeat intravenous administration of MSCs over 3 weeks, however, was shown to stimulate increased tumour growth in a model of pancreatic cancer [21]. Similar to the level of MSC engraftment in tumours, it seems that the effect of MSCs following engraftment will be tumour specific – probably dependent on a range of factors including the method of MSC isolation and culture, the experimental model, the number of cells engrafted in the tumour, and the milieu of growth factors and inflammatory cytokines present within the tumour microenvironment.

Conclusion

The studies outlined highlight very promising potential for MSC-mediated delivery of therapeutic agents directly to tumour tissue, with remarkable progress made in the past decade. Clearly MSCs have a number of advantages as cellular vehicles – they are relatively easy to isolate and expand, specifically target tumours and their metastases following systemic delivery, can be transduced efficiently with a range of vectors, have immunosuppressive properties, have the ability to express therapeutic proteins in secretory form and can support amplification

of oncolytic viruses. The potential for MSC-mediated tumour promotion, however, must be addressed. Further understanding the biology of MSCs, and the specific combination of factors controlling their tumour-specific migration and persistence, will support translation to the clinical setting.

Abbreviations

Ad, adenovirus; IFN, interferon; IL, interleukin; MHC, major histocompatibility complex; MSC, mesenchymal stem cell; SDF-1α, stromal-derived growth factor-1α (CXCL12); TNF, tumour necrosis factor; TRAIL, TNF-related apoptosis inducing ligand.

Competing interests

The authors declare that they have no competing interests.

Acknowledgements

Funding was received from the National Breast Cancer Research Institute, the Health Research Board of Ireland and Science Foundation Ireland.

Author details

[1]Division of Surgery, School of Medicine, Clinical Science Institute, National University of Ireland Galway, Galway, Ireland. [2]Regenerative Medicine Institute, Orbsen building, National University of Ireland Galway (NUIG), Galway, Ireland.

Published: 9 August 2010

References

1. Pittenger MF, Mackay AM, Beck SC, Jaiswal RK, Douglas R, Mosca JD, Moorman MA, Simonetti DW, Craig S, Marshak DR: **Multilineage potential of adult human mesenchymal stem cells.** *Science* 1999, **284:**143-147.
2. Barry FP, Murphy JM: **Mesenchymal stem cells: clinical applications and biological characterization.** *Int J Biochem Cell Biol* 2004, **36:**568-584.
3. Dominici M, Le Blanc K, Mueller I, Slaper-Cortenbach I, Marini F, Krause D, Deans R, Keating A, Prockop D, Horwitz E: **Minimal criteria for defining multipotent mesenchymal stromal cells. The International Society for Cellular Therapy position statement.** *Cytotherapy* 2006, **8:**315-317.
4. Kidd S, Spaeth E, Klopp A, Andreeff M, Hall B, Marini FC: **The (in) auspicious role of mesenchymal stromal cells in cancer: be it friend or foe.** *Cytotherapy* 2008, **10:**657-667.
5. Studeny M, Marini FC, Champlin RE, Zompetta C, Fidler IJ, Andreeff M: **Bone marrow-derived mesenchymal stem cells as vehicles for interferon-beta delivery into tumors.** *Cancer Res* 2002, **62:**3603-3608.
6. Nakamizo A, Marini F, Amano T, Khan A, Studeny M, Gumin J, Chen J, Hentschel S, Vecil G, Dembinski J, Andreeff M, Lang FF: **Human bone marrow-derived mesenchymal stem cells in the treatment of gliomas.** *Cancer Res* 2005, **65:**3307-3318.
7. Kidd S, Caldwell L, Dietrich M, Samudio I, Spaeth EL, Watson K, Shi Y, Abbruzzese J, Konopleva M, Andreeff M, Marini FC: **Mesenchymal stromal cells alone or expressing interferon-beta suppress pancreatic tumors in vivo, an effect countered by anti-inflammatory treatment.** *Cytotherapy* 2010. [Epub ahead of print]
8. Nakamura K, Ito Y, Kawano Y, Kurozumi K, Kobune M, Tsuda H, Bizen A, Honmou O, Niitsu Y, Hamada H: **Antitumor effect of genetically engineered mesenchymal stem cells in a rat glioma model.** *Gene Therapy* 2004, **11:**1155-1164.
9. Stagg J, Lejeune L, Paquin A, Galipeau J: **Marrow stromal cells for interleukin-2 delivery in cancer immunotherapy.** *Hum Gene Ther* 2004, **15:**597-608.
10. Eliopoulos N, Francois M, Boivin MN, Martineau D, Galipeau J: **Neo-organoid of marrow mesenchymal stromal cells secreting interleukin-12 for breast cancer therapy.** *Cancer Res* 2008, **68:**4810-4818.
11. Chen X, Lin X, Zhao J, Shi W, Zhang H, Wang Y, Kan B, Du L, Wang B, Wei Y, Liu Y, Zhao X: **A tumor-selective biotherapy with prolonged impact on established metastases based on cytokine gene-engineered MSCs.** *Mol Ther* 2008, **16:**749-756.
12. Duan X, Guan H, Cao Y, Kleinerman ES: **Murine bone marrow-derived mesenchymal stem cells as vehicles for interleukin-12 gene delivery into Ewing sarcoma tumors.** *Cancer* 2009, **115:**13-22.
13. Gao Y, Yao A, Zhang W, Lu S, Yu Y, Deng L, Yin A, Xia Y, Sun B, Wang X: **Human mesenchymal stem cells overexpressing pigment epithelium-derived factor inhibit hepatocellular carcinoma in nude mice.** *Oncogene* 2010, **29:**2784-2794.
14. Kanehira M, Xin H, Hoshino K, Maemondo M, Mizuguchi H, Hayakawa T, Matsumoto K, Nakamura T, Nukiwa T, Saijo Y: **Targeted delivery of NK4 to multiple lung tumors by bone marrow-derived mesenchymal stem cells.** *Cancer Gene Ther* 2007, **14:**894-903.
15. Grisendi G, Bussolari R, Cafarelli L, Petak I, Rasini V, Veronesi E, De Santis G, Spano C, Tagliazzucchi M, Barti-Juhasz H, Scarabelli L, Bambi F, Frassoldati A, Rossi G, Casali C, Morandi U, Horwitz EM, Paolucci P, Conte P, Dominici M: **Adipose-derived mesenchymal stem cells as stable source of tumor necrosis factor-related apoptosis-inducing ligand delivery for cancer therapy.** *Cancer Res* 2010, **70:**3718-3729.
16. Loebinger MR, Eddaoudi A, Davies D, Janes SM: **Mesenchymal stem cell delivery of TRAIL can eliminate metastatic cancer.** *Cancer Res* 2009, **69:**4134-4142.
17. Mohr A, Lyons M, Deedigan L, Harte T, Shaw G, Howard L, Barry F, O'Brien T, Zwacka R: **Mesenchymal stem cells expressing TRAIL lead to tumour growth inhibition in an experimental lung cancer model.** *J Cell Mol Med* 2008, **12:**2628-2643.
18. Kim SM, Lim JY, Park SI, Jeong CH, Oh JH, Jeong M, Oh W, Park SH, Sung YC, Jeun SS: **Gene therapy using TRAIL-secreting human umbilical cord blood-derived mesenchymal stem cells against intracranial glioma.** *Cancer Res* 2008, **68:**9614-9623.
19. Uchibori R, Okada T, Ito T, Urabe M, Mizukami H, Kume A, Ozawa K: **Retroviral vector-producing mesenchymal stem cells for targeted suicide cancer gene therapy.** *J Gene Med* 2009, **11:**373-381.
20. Matuskova M, Hlubinova K, Pastorakova A, Hunakova L, Altanerova V, Altaner C, Kucerova L: **HSV-tk expressing mesenchymal stem cells exert bystander effect on human glioblastoma cells.** *Cancer Lett* 2010, **290:**58-67.
21. Zischek C, Niess H, Ischenko I, Conrad C, Huss R, Jauch KW, Nelson PJ, Bruns C: **Targeting tumor stroma using engineered mesenchymal stem cells reduces the growth of pancreatic carcinoma.** *Ann Surg* 2009, **250:**747-753.
22. Kucerova L, Altanerova V, Matuskova M, Tyciakova S, Altaner C: **Adipose tissue-derived human mesenchymal stem cells mediated prodrug cancer gene therapy.** *Cancer Res* 2007, **67:**6304-6313.
23. Dembinski JL, Spaeth EL, Fueyo J, Gomez-Manzano C, Studeny M, Andreeff M, Marini FC: **Reduction of nontarget infection and systemic toxicity by targeted delivery of conditionally replicating viruses transported in mesenchymal stem cells.** *Cancer Gene Ther* 2010, **17:**289-297.
24. Hakkarainen T, Sarkioja M, Lehenkari P, Miettinen S, Ylikomi T, Suuronen R, Desmond RA, Kanerva A, Hemminki A: **Human mesenchymal stem cells lack tumor tropism but enhance the antitumor activity of oncolytic adenoviruses in orthotopic lung and breast tumors.** *Hum Gene Ther* 2007, **18:**627-641.
25. Komarova S, Kawakami Y, Stoff-Khalili MA, Curiel DT, Pereboeva L: **Mesenchymal progenitor cells as cellular vehicles for delivery of oncolytic adenoviruses.** *Mol Cancer Ther* 2006, **5:**755-766.
26. Petrie Aronin CE, Tuan RS: **Therapeutic potential of the immunomodulatory activities of adult mesenchymal stem cells.** *Birth Defects Res C Embryo Today* 2010, **90:**67-74.
27. Djouad F, Plence P, Bony C, Tropel P, Apparailly F, Sany J, Noel D, Jorgensen C: **Immunosuppressive effect of mesenchymal stem cells favors tumor growth in allogeneic animals.** *Blood* 2003, **102:**3837-3844.
28. Djouad F, Bony C, Apparailly F, Louis-Plence P, Jorgensen C, Noel D: **Earlier onset of syngeneic tumors in the presence of mesenchymal stem cells.** *Transplantation* 2006, **82:**1060-1066.
29. Ohlsson LB, Varas L, Kjellman C, Edvardsen K, Lindvall M: **Mesenchymal progenitor cell-mediated inhibition of tumor growth in vivo and in vitro in gelatin matrix.** *Exp Mol Pathol* 2003, **75:**248-255.
30. Le Blanc K, Tammik L, Sundberg B, Haynesworth SE, Ringden O: **Mesenchymal stem cells inhibit and stimulate mixed lymphocyte cultures and mitogenic responses independently of the major histocompatibility complex.** *Scand J Immunol* 2003, **57:**11-20.
31. Dvorak HF: **Tumors: wounds that do not heal. Similarities between tumor stroma generation and wound healing.** *N Engl J Med* 1986, **315:**1650-1659.
32. Feng B, Chen L: **Review of mesenchymal stem cells and tumors: executioner or coconspirator?** *Cancer Biother Radiopharm* 2009, **24:**717-721.
33. Nakamizo A, Marini F, Amano T, Khan A, Studeny M, Gumin J, Chen J, Hentschel S, Vecil G, Dembinski J, Andreeff M, Lang FF: **Human bone**

marrow-derived mesenchymal stem cells in the treatment of gliomas. *Cancer Res* 2005, **65:**3307-3318.
34. Nakamura K, Ito Y, Kawano Y, Kurozumi K, Kobune M, Tsuda H, Bizen A, Honmou O, Niitsu Y, Hamada H: **Antitumor effect of genetically engineered mesenchymal stem cells in a rat glioma model.** *Gene Ther* 2004, **11:**1155-1164.
35. Studeny M, Marini FC, Dembinski JL, Zompetta C, Cabreira-Hansen M, Bekele BN, Champlin RE, Andreeff M: **Mesenchymal stem cells: potential precursors for tumor stroma and targeted-delivery vehicles for anticancer agents.** *J Natl Cancer Inst* 2004, **96:**1593-1603.
36. Wels J, Kaplan RN, Rafii S, Lyden D: **Migratory neighbors and distant invaders: tumor-associated niche cells.** *Genes Dev* 2008, **22:**559-574.
37. Dwyer RM, Potter-Beirne SM, Harrington KA, Lowery AJ, Hennessy E, Murphy JM, Barry FP, O'Brien T, Kerin MJ: **Monocyte chemotactic protein-1 (MCP-1) secreted by primary breast tumors stimulates migration of mesenchymal stem cells (MSCs).** *Clin Cancer Res* 2007, **13:**5020-5027.
38. Chamberlain G, Fox J, Ashton B, Middleton J: **Concise review: mesenchymal stem cells: their phenotype, differentiation capacity, immunological features, and potential for homing.** *Stem Cells* 2007, **25:**2739-2749.
39. Ruster B, Gottig S, Ludwig RJ, Bistrian R, Muller S, Seifried E, Gille J, Henschler R: **Mesenchymal stem cells display coordinated rolling and adhesion behavior on endothelial cells.** *Blood* 2006, **108:**3938-3944.
40. Ringe J, Strassburg S, Neumann K, Endres M, Notter M, Burmester GR, Kaps C, Sittinger M: **Towards in situ tissue repair: human mesenchymal stem cells express chemokine receptors CXCR1, CXCR2 and CCR2, and migrate upon stimulation with CXCL8 but not CCL2.** *J Cell Biochem* 2007, **101:**135-146.
41. Honczarenko M, Le Y, Swierkowski M, Ghiran I, Glodek AM, Silberstein LE: **Human bone marrow stromal cells express a distinct set of biologically functional chemokine receptors.** *Stem Cells* 2006, **24:**1030-1041.
42. Von Luttichau I, Notohamiprodjo M, Wechselberger A, Peters C, Henger A, Seliger C, Djafarzadeh R, Huss R, Nelson PJ: **Human adult CD34-progenitor cells functionally express the chemokine receptors CCR1, CCR4, CCR7, CXCR5, and CCR10 but not CXCR4.** *Stem Cells Dev* 2005, **14:**329-336.
43. Sordi V, Malosio ML, Marchesi F, Mercalli A, Melzi R, Giordano T, Belmonte N, Ferrari G, Leone BE, Bertuzzi F, Zerbini G, Allavena P, Bonifacio E, Piemonti L: **Bone marrow mesenchymal stem cells express a restricted set of functionally active chemokine receptors capable of promoting migration to pancreatic islets.** *Blood* 2005, **106:**419-427.
44. Chamberlain G, Wright K, Rot A, Ashton B, Middleton J: **Murine mesenchymal stem cells exhibit a restricted repertoire of functional chemokine receptors: comparison with human.** *PLoS One* 2008, **3:**e2934.
45. Shi M, Li J, Liao L, Chen B, Li B, Chen L, Jia H, Zhao RC: **Regulation of CXCR4 expression in human mesenchymal stem cells by cytokine treatment: role in homing efficiency in NOD/SCID mice.** *Haematologica* 2007, **92:**897-904.
46. Wynn RF, Hart CA, Corradi-Perini C, O'Neill L, Evans CA, Wraith JE, Fairbairn LJ, Bellantuono I: **A small proportion of mesenchymal stem cells strongly expresses functionally active CXCR4 receptor capable of promoting migration to bone marrow.** *Blood* 2004, **104:**2643-2645.
47. Potapova IA, Brink PR, Cohen IS, Doronin SV: **Culturing of human mesenchymal stem cells as three-dimensional aggregates induces functional expression of CXCR4 that regulates adhesion to endothelial cells.** *J Biol Chem* 2008, **283:**13100-13107.
48. Zielske SP, Livant DL, Lawrence TS: **Radiation increases invasion of gene-modified mesenchymal stem cells into tumors.** *Int J Radiat Oncol Biol Phys* 2009, **75:**843-853.
49. Klopp AH, Spaeth EL, Dembinski JL, Woodward WA, Munshi A, Meyn RE, Cox JD, Andreeff M, Marini FC: **Tumor irradiation increases the recruitment of circulating mesenchymal stem cells into the tumor microenvironment.** *Cancer Res* 2007, **67:**11687-11695.
50. Coussens LM, Werb Z: **Inflammation and cancer.** *Nature* 2002, **420:**860-867.
51. Sarkar D, Vemula PK, Zhao W, Gupta A, Karnik R, Karp JM: **Engineered mesenchymal stem cells with self-assembled vesicles for systemic cell targeting.** *Biomaterials* 2010, **31:**5266-5274.
52. Sato H, Kuwashima N, Sakaida T, Hatano M, Dusak JE, Fellows-Mayle WK, Papworth GD, Watkins SC, Gambotto A, Pollack IF, Okada H: **Epidermal growth factor receptor-transfected bone marrow stromal cells exhibit enhanced migratory response and therapeutic potential against murine brain tumors.** *Cancer Gene Ther* 2005, **12:**757-768.
53. Sasportas LS, Kasmieh R, Wakimoto H, Hingtgen S, van de Water JA, Mohapatra G, Figueiredo JL, Martuza RL, Weissleder R, Shah K: **Assessment of therapeutic efficacy and fate of engineered human mesenchymal stem cells for cancer therapy.** *Proc Natl Acad Sci U S A* 2009, **106:**4822-4827.
54. Sonabend AM, Ulasov IV, Tyler MA, Rivera AA, Mathis JM, Lesniak MS: **Mesenchymal stem cells effectively deliver an oncolytic adenovirus to intracranial glioma.** *Stem Cells* 2008, **26:**831-841.
55. Stoff-Khalili MA, Rivera AA, Mathis JM, Banerjee NS, Moon AS, Hess A, Rocconi RP, Numnum TM, Everts M, Chow LT, Douglas JT, Siegal GP, Zhu ZB, Bender HG, Dall P, Stoff A, Pereboeva L, Curiel DT: **Mesenchymal stem cells as a vehicle for targeted delivery of CRAds to lung metastases of breast carcinoma.** *Breast Cancer Res Treat* 2007, **105:**157-167.
56. Pereboeva L, Komarova S, Mikheeva G, Krasnykh V, Curiel DT: **Approaches to utilize mesenchymal progenitor cells as cellular vehicles.** *Stem Cells* 2003, **21:**389-404.
57. Rubio D, Garcia-Castro J, Martin MC, de la Fuente R, Cigudosa JC, Lloyd AC, Bernad A: **Spontaneous human adult stem cell transformation.** *Cancer Res* 2005, **65:**3035-3039.
58. Wang Y, Huso DL, Harrington J, Kellner J, Jeong DK, Turney J, McNiece IK: **Outgrowth of a transformed cell population derived from normal human BM mesenchymal stem cell culture.** *Cytotherapy* 2005, **7:**509-519.
59. Bernardo ME, Zaffaroni N, Novara F, Cometa AM, Avanzini MA, Moretta A, Montagna D, Maccario R, Villa R, Daidone MG, Zuffardi O, Locatelli F: **Human bone marrow derived mesenchymal stem cells do not undergo transformation after long-term in vitro culture and do not exhibit telomere maintenance mechanisms.** *Cancer Res* 2007, **67:**9142-9149.
60. Zhou YF, Bosch-Marce M, Okuyama H, Krishnamachary B, Kimura H, Zhang L, Huso DL, Semenza GL: **Spontaneous transformation of cultured mouse bone marrow-derived stromal cells.** *Cancer Res* 2006, **66:**10849-10854.
61. Miura M, Miura Y, Padilla-Nash HM, Molinolo AA, Fu B, Patel V, Seo BM, Sonoyama W, Zheng JJ, Baker CC, Chen W, Ried T, Shi S: **Accumulated chromosomal instability in murine bone marrow mesenchymal stem cells leads to malignant transformation.** *Stem Cells* 2006, **24:**1095-1103.
62. Tolar J, Nauta AJ, Osborn MJ, Panoskaltsis Mortari A, McElmurry RT, Bell S, Xia L, Zhou N, Riddle M, Schroeder TM, Westendorf JJ, McIvor RS, Hogendoorn PC, Szuhai K, Oseth L, Hirsch B, Yant SR, Kay MA, Peister A, Prockop DJ, Fibbe WE, Blazar BR: **Sarcoma derived from cultured mesenchymal stem cells.** *Stem Cells* 2007, **25:**371-379.
63. Li H, Fan X, Kovi RC, Jo Y, Moquin B, Konz R, Stoicov C, Kurt-Jones E, Grossman SR, Lyle S, Rogers AB, Montrose M, Houghton J: **Spontaneous expression of embryonic factors and p53 point mutations in aged mesenchymal stem cells: a model of age-related tumorigenesis in mice.** *Cancer Res* 2007, **67:**10889-10898.
64. Karnoub AE, Dash AB, Vo AP, Sullivan A, Brooks MW, Bell GW, Richardson AL, Polyak K, Tubo R, Weinberg RA: **Mesenchymal stem cells within tumour stroma promote breast cancer metastasis.** *Nature* 2007, **449:**557-563.
65. Muehlberg FL, Song YH, Krohn A, Pinilla SP, Droll LH, Leng X, Seidensticker M, Ricke J, Altman AM, Devarajan E, Liu W, Arlinghaus RB, Alt EU: **Tissue-resident stem cells promote breast cancer growth and metastasis.** *Carcinogenesis* 2009, **30:**589-597.
66. Rhodes LV, Muir SE, Elliott S, Guillot LM, Antoon JW, Penfornis P, Tilghman SL, Salvo VA, Fonseca JP, Lacey MR, Beckman BS, McLachlan JA, Rowan BG, Pochampally R, Burow ME: **Adult human mesenchymal stem cells enhance breast tumorigenesis and promote hormone independence.** *Breast Cancer Res Treat* 2010, **121:**293-300.
67. Galie M, Konstantinidou G, Peroni D, Scambi I, Marchini C, Lisi V, Krampera M, Magnani P, Merigo F, Montani M, Boschi F, Marzola P, Orru R, Farace P, Sbarbati A, Amici A: **Mesenchymal stem cells share molecular signature with mesenchymal tumor cells and favor early tumor growth in syngeneic mice.** *Oncogene* 2008, **27:**2542-2551.
68. Spaeth EL, Dembinski JL, Sasser AK, Watson K, Klopp A, Hall B, Andreeff M, Marini F: **Mesenchymal stem cell transition to tumor-associated fibroblasts contributes to fibrovascular network expansion and tumor progression.** *PloS one* 2009, **4:**e4992.
69. Bexell D, Gunnarsson S, Tormin A, Darabi A, Gisselsson D, Roybon L, Scheding S, Bengzon J: **Bone marrow multipotent mesenchymal stroma cells act as pericyte-like migratory vehicles in experimental gliomas.** *Mol Ther* 2009, **17:**183-190.
70. Yu JM, Jun ES, Bae YC, Jung JS: **Mesenchymal stem cells derived from human adipose tissues favor tumor cell growth in vivo.** *Stem Cells Dev* 2008, **17:**463-473.
71. Shinagawa K, Kitadai Y, Tanaka M, Sumida T, Kodama M, Higashi Y, Tanaka S, Yasui W, Chayama K: **Mesenchymal stem cells enhance growth and metastasis of colon cancer.** *Int J Cancer* 2010. [Epub ahead of print]

72. Zhu W, Xu W, Jiang R, Qian H, Chen M, Hu J, Cao W, Han C, Chen Y: **Mesenchymal stem cells derived from bone marrow favor tumor cell growth in vivo.** *Exp Mol Pathol* 2006, **80:**267-274.
73. Wu Y, Wang J, Scott PG, Tredget EE: **Bone marrow-derived stem cells in wound healing: a review.** *Wound Repair Regen* 2007, **15(Suppl 1):**S18-S26.
74. Wu Y, Chen L, Scott PG, Tredget EE: **Mesenchymal stem cells enhance wound healing through differentiation and angiogenesis.** *Stem Cells* 2007, **25:**2648-2659.
75. Mishra PJ, Mishra PJ, Humeniuk R, Medina DJ, Alexe G, Mesirov JP, Ganesan S, Glod JW, Banerjee D: **Carcinoma-associated fibroblast-like differentiation of human mesenchymal stem cells.** *Cancer Res* 2008, **68:**4331-4339.
76. Bagley RG, Weber W, Rouleau C, Yao M, Honma N, Kataoka S, Ishida I, Roberts BL, Teicher BA: **Human mesenchymal stem cells from bone marrow express tumor endothelial and stromal markers.** *Int J Oncol* 2009, **34:**619-627.
77. Qiao L, Xu Z, Zhao T, Zhao Z, Shi M, Zhao RC, Ye L, Zhang X: **Suppression of tumorigenesis by human mesenchymal stem cells in a hepatoma model.** *Cell Res* 2008, **18:**500-507.
78. Maestroni GJ, Hertens E, Galli P: **Factor(s) from nonmacrophage bone marrow stromal cells inhibit Lewis lung carcinoma and B16 melanoma growth in mice.** *Cell Mol Life Sci* 1999, **55:**663-667.
79. Khakoo AY, Pati S, Anderson SA, Reid W, Elshal MF, Rovira, II, Nguyen AT, Malide D, Combs CA, Hall G, Zhang J, Raffeld M, Rogers TB, Stetler-Stevenson W, Frank JA, Reitz M, Finkel T: **Human mesenchymal stem cells exert potent antitumorigenic effects in a model of Kaposi's sarcoma.** *J Exp Med* 2006, **203:**1235-1247.

doi:10.1186/scrt25
Cite this article as: Dwyer RM, *et al.*: **Advances in mesenchymal stem cell-mediated gene therapy for cancer.** *Stem Cell Research & Therapy* 2010, **1:**25.

Breast Cancer Res Treat
DOI 10.1007/s10549-010-0734-1

PRECLINICAL STUDY

Potential role of mesenchymal stem cells (MSCs) in the breast tumour microenvironment: stimulation of epithelial to mesenchymal transition (EMT)

F. T. Martin · R. M. Dwyer · J. Kelly · S. Khan · J. M. Murphy · C. Curran · N. Miller · E. Hennessy · P. Dockery · F. P. Barry · T. O'Brien · M. J. Kerin

Received: 5 August 2009 / Accepted: 6 January 2010

Abstract Bone marrow-derived mesenchymal stem cells (MSCs) are known to specifically migrate to and engraft at tumour sites. Understanding interactions between cancer cells and MSCs has become fundamental to determining whether MSC-tumour interactions should be harnessed for delivery of therapeutic agents or considered a target for intervention. Breast Cancer Cell lines (MDA-MB-231, T47D & SK-Br3) were cultured alone or on a monolayer of MSCs, and retrieved using epithelial specific magnetic beads. Alterations in expression of 90 genes associated with breast tumourigenicity were analysed using low-density array. Expression of markers of epithelial–mesenchymal transition (EMT) and array results were validated using RQ-PCR. Co-cultured cells were analysed for changes in protein expression, growth pattern and morphology. Gene expression and proliferation assays were also performed on indirect co-cultures. Following direct co-culture with MSCs, breast cancer cells expressed elevated levels of oncogenes (NCOA4, FOS), proto-oncogenes (FYN, JUN), genes associated with invasion (MMP11), angiogenesis (VEGF) and anti-apoptosis (IGF1R, BCL2). However, universal downregulation of genes associated with proliferation was observed (Ki67, MYBL2), and reflected in reduced ATP production in response to MSC-secreted factors. Significant upregulation of EMT specific markers (N-cadherin, Vimentin, Twist and Snail) was also observed following co-culture with MSCs, with a reciprocal downregulation in E-cadherin protein expression. These changes were predominantly cell contact mediated and appeared to be MSC specific. Breast cancer cell morphology and growth pattern also altered in response to MSCs. MSCs may promote breast cancer metastasis through facilitation of EMT.

Keywords Mesenchymal stem cells (MSCs) · Breast cancer · Epithelial–mesenchymal transition (EMT) · Invasion · Co-culture

F. T. Martin · R. M. Dwyer (✉) · J. Kelly · S. Khan · C. Curran · N. Miller · E. Hennessy · M. J. Kerin
Department of Surgery, National University of Ireland Galway, Galway, Ireland
e-mail: roisin.dwyer@nuigalway.ie

J. M. Murphy · F. P. Barry · T. O'Brien
Regenerative Medicine Institute, National University of Ireland Galway, Galway, Ireland

P. Dockery
Department of Anatomy, National University of Ireland Galway, Galway, Ireland

Introduction

Breast cancer remains the most common malignancy in women, accounting for one quarter of all female cancers [1]. The preferential spread of tumour cells to bone and subsequent development of osteolytic metastatic deposits remains a devastating event in the course of the disease [2, 3]. It is now understood that tumour epithelial cells develop in a symbiotic rather than an independent manner with surrounding stroma. This stromal environment consists of a dynamic network of immune cells, fibroblasts, tumour vasculature and extracellular matrix [4]. Tumours actively recruit cells, including bone marrow-derived mesenchymal stem cells (MSCs), into the tumour microenvironment and these cells may play a role in facilitating cancer progression [5]. MSCs are a subset of non-haematopoietic cells found within the bone marrow stroma that have an innate ability both to self renew and to differentiate into cells of multiple lineages, including osteoblasts,

Published online: 20 January 2010

chondrocytes and adipocytes [6]. They have also been seen to influence the morphology and proliferation of cells within their vicinity through both cell to cell interactions and the secretion of chemoattractant cytokines and paracrine factors [7–10]. Studies assessing systemically delivered MSCs have confirmed that these circulating cells engraft and facilitate healing at sites of inflammation and injury including head trauma, stroke and myocardial infarction [10, 11]. Malignancy may also be considered as a nidus of chronic inflammation or "wound that never heals" [12] and reports have shown a similar pattern of MSC engraftment at these sites [11]. This tumour homing ability has prompted researchers to analyse MSCs as possible vectors for the targeted delivery of anti-cancer agents to tumour microenvironments [13]. However, evidence suggests that interactions between MSCs and breast cancer cells may impact upon the phenotype of the cancer cell and promote their metastatic potential [7–9, 14–16]. Understanding these interactions has become fundamental to determining whether the homing ability of MSCs should be harnessed for delivery of therapeutic agents or whether the MSC-tumour interactions should be considered a target for intervention.

Studies that have analysed direct interactions between breast cancer cells and MSCs report distinct proliferative and morphological changes in the cancer cells [7, 8]. Growth patterns of cancer cells in co-culture change from a clustered to a single cell distribution, and these morphological alterations have been related to a significant downregulation of cell adhesion molecules E-cadherin and epithelial specific antigen (ESA) [7, 8]. Conflicting reports exist with relation to the effect of MSCs on proliferation of breast cancer cells, with some studies reporting no change [7] and others suggesting proliferative changes occurring in an oestrogen-dependant manner [8, 9].

More recently, a pivotal study by Karnoub et al. [14] reported that, when mixed with breast cancer cells prior to implantation, MSCs enhance breast cancer cell motility, invasion and metastatic potential in vivo. Knockdown of the CCL5–CCR5 loop led to an abrogated metastatic response confirming that these paracrine interactions play an important role in MSC-mediated metastatic spread [14]. These studies highlight the distinct effect that MSCs have on breast cancer cells, and thus understanding the pathways governing these effects remains imperative.

Epithelial to mesenchymal transition (EMT) is a process essential to organogenesis during embryonic development [17], however its reactivation during adult life has been ascribed to certain pathological processes including the facilitation of carcinogenesis [18]. EMT has been shown to promote the detachment of cancer cells from the primary tumour and facilitate their subsequent migration through the acquisition of stem like properties, including a loss of cellular polarity, adhesion and proliferation [18, 19]. Studies have demonstrated evidence of EMT in primary human breast carcinomas showing a proclivity towards the more invasive basal breast cancer phenotype [20, 21]. Despite recognition of the role EMT plays in the metastatic cascade, stimuli inducing EMT at the primary tumour site remain largely unknown.

Further understanding of MSC/tumour cell interactions is required to determine their role in breast cancer progression or therapy. This study aimed to further elucidate the effect MSCs have on breast cancer cells and to potentially identify pathways mediating these effects.

Materials and methods

Cell culture

Breast cancer cell lines included MDA-MB-231 cells cultured in Liebowitz-15 medium (L-15); T47D cells cultured in RPMI 1640 medium; and SK-Br-3 cells cultured in McCoys-5a medium. Normal human embryonic lung fibroblasts (WI-38 cells) were cultured in Eagle's minimal essential medium (EMEM). All media were supplemented with 10% foetal bovine serum (FBS), 100 IU/ml penicillin/100 µg/ml streptomycin (P/S) and 1% L-glutamine.

Mesenchymal stem cells (MSCs) were supplied by the Regenerative Medicine Institute (REMEDI) at NUI Galway. With ethical approval and informed consent, bone marrow was aspirated from the iliac crests of healthy donors following a defined clinical protocol [22]. MSCs were isolated from the marrow aspirates by direct plating and subsequently cultured for 12–15 days to deplete the non-adherent haematopoietic cell fraction. Cells were maintained in Dulbecco's modified Eagle's medium (DMEM) supplemented with pre-selected FBS (10%) and P/S. The ability of MSCs to differentiate into chondrocytes, adipocytes and osteoblasts was confirmed prior to use. Characterisation of surface receptors was performed targeting the markers CD105, CD73, CD90 (positive) and CD34, CD45 (negative). MSCs derived from three separate donors were utilised for experiments. All cells were maintained at 37°C and 5% CO_2.

Direct co-culture

Primary MSCs or normal fibroblasts (WI-38 cells) were seeded at a density of 2×10^4 cells/cm^2 and allowed to adhere overnight. Breast cancer cell lines were then seeded at a density of 1.3×10^4 cells/cm^2 onto the monolayers of MSCs or normal fibroblasts. All cell types were cultured individually in parallel as controls. Cells were maintained in MSC specific medium and following a 3- or 7-day

incubation, media was harvested and epithelial cells retrieved as described below.

Retrieval of epithelial cells

Following direct co-culture epithelial cells were separated from MSCs in co-culture using an EasySep® positive selection kit (Stem Cell Technologies). As per manufacturer's instructions, co-culture populations were trypsinised and dispersed into a single cell suspension, and EasySep® positive selection cocktail and magnetic nanoparticles were added during serial incubations on ice. The magnetic nanoparticles bind selectively to viable epithelial cells which are positively selected by placing the tube in a magnet. Retrieved cells were centrifuged and stored at −80°C until required for RNA extraction.

Gene expression

RNA was extracted from both cells cultured alone and epithelial cells retrieved following co-culture with MSCs or WI-38 cells using the RNeasy® Mini Kit (QIAGEN Ltd.) following manufacturer's protocol. cDNA was generated using SuperScript III reverse transcription enzyme and analysed by both Taqman® low-density array (TLDA) and relative quantitative-PCR (RQ-PCR). The array plate was designed to simultaneously measure expression of 90 genes specifically associated with breast cancer tumourigenicity and six endogenous controls. Following identification of target genes of interest, co-culture experiments were repeated in triplicate and results validated by RQ-PCR using the ABI Prism 7000 sequence detector system (Applied Biosystems). Predeveloped Taqman® assay reagents (PDARS) specific to genes associated with EMT, including N-cadherin, Vimentin, Twist and Snail, were also used to quantify changes in expression by RQ-PCR. The comparative C_T method was used to quantify expression of genes and this was normalised to the endogenous control, peptidyl-prolyl isomerase A (PPIA). Results from cells retrieved from co-culture were expressed relative to the same cells cultured alone. Changes in gene expression were expressed using the $2^{-\Delta\Delta CT}$ method [23] and the fold change in triplicate experiments was recorded and presented as Mean ± SEM.

Collection of conditioned media (CM) for indirect co-culture

MSCs were seeded at a density of 2×10^4 cells/cm^2 in DMEM supplemented with pre-selected FBS (10%) and P/S. Media was aspirated at 24 h intervals and transferred to breast cancer cell lines to determine the effect of MSC secreted factors on cell proliferation and gene expression (indirect co-culture) as described below. Breast cancer cells grown in MSC medium that had not been exposed to MSCs served as a control.

Proliferation assay

Breast cancer cell lines were seeded onto 96-well white-walled plates at a density of 8×10^3 cells/well in 100 µl media and allowed to adhere overnight. Media was aspirated and replaced with MSC-conditioned medium (CM) as described above at 24 h intervals for 72 h. An Apoglow® assay was performed to assess changes in proliferation based on the level of ATP production as quantified by a luminometer. Results presented represent triplicate experiments and are expressed as Mean ± SEM.

Indirect co-culture

Breast cancer cells were cultured in media that had been exposed to MSCs as described above. Following culture in MSC CM, cells were lysed and RNA extracted. Changes in expression of genes associated with EMT were quantified by RQ-PCR as described for the direct co-culture experiments.

Western blot analysis

Protein was extracted from cells cultured individually and those retrieved following co-culture. Briefly, cells were washed and resuspended in Triton-X lysis buffer [150 mM NaCl, 20 mM HEPES, 2 mM EDTA, 1% Triton-X100, 2 mM sodium orthovanadate, 10 mM sodium fluoride, 10ul/ml protease inhibitor cocktail (Fisher Scientific)], frozen at –20°C and then centrifuged at 500×g for 15 min at 4°C to remove cellular debris. The protein content was determined using the Micro BCA™ protein assay kit (Thermo Scientific). Protein (40 µg) was reduced in DTT (0.5 M) for 10 min at 70°C and samples run on a 4–12% gradient pre-cast NuPAGE Bis–Tris polyacrylamide gel for 1 h at 200 V. Protein molecular weight standards (20–220 kDa) were run simultaneously on each gel. Electroblotting was performed for 1 h at 25 V to transfer protein samples to a nitrocellulose membrane. Blots were blocked in 5% milk in TBS-T [20 mM Tris, 137 mM NaCl, 0.1% Tween-20] for 1 h, and probed with antibodies targeting E-cadherin (1 µg/ml, R & D Systems), Vimentin (1:100, Abcam) or Snail (1 µg/ml, Abcam) for 1.5 h and washed in TBS-T. β-actin was used to confirm equal loading in wells. Horseradish peroxidase-labelled goat anti-rabbit (1:3,000; Abcam) or rabbit anti-mouse antibody (1:2,000; Abcam) was then added to the membranes for 1.5 h. Following washing steps, SuperSignal West Pico chemiluminescent substrate (Thermo Scientific) was applied to the

membranes for 5 min. Images were captured using a Syngene G-Box and GeneSnap software.

Immunohistochemistry and fluorescent microscopy

After 72 h co-culture in chamber slides, cells were fixed in methanol. Immunohistochemical analysis was performed using monoclonal antibodies targeting E-cadherin (R&D Systems), MNF116 pancytokeratin (Dako, Denmark) and CD90 (Dako, Denmark). E-cadherin and CD90 were visualised using the chromagen 3,3′-diaminobenzidine (DAB), with acid fast red (RED) used for detection of pancytokeratin in dual staining experiments.

In order to assess changes in breast cancer cell morphology in response to MSCs, cells were dual labelled and examined by fluorescence microscopy. Prior to mixing the cell populations, epithelial breast cancer cells were labelled with PKH26 (red fluorescent label, excitation 551 nm, emission 567 nm, Sigma). Following 72 h co-culture, cells were fixed in 4% paraformaldehyde and the cytoskeleton of the mixed populations was labelled with Alexafluor® 488 phalloidin (green fluorescent label, excitation 495 nm, emission 518 nm, Invitrogen, Eugene, OR). Cells were examined using an Olympus IX81-ZDC® microscope and Confocal Andor Revolution spinning disc system®.

Results

Cell separation

Cell separation using the EasySep® positive selection kit (Stem Cell Technologies) was assessed. Following two washes, a positive retrieval rate of 94.4 ± 1.1% was achieved (range 92–97.5% retrieval). It has previously been shown in an extensive study by Woelfle et al. [24], that the immunoselection procedure does not alter breast cancer cell gene expression. In order to further confirm this, expression of Vimentin, E-cadherin, CXCL12 and CXCR4 in breast cancer cells selected with beads, was compared to unselected cells with a <1-fold change in gene expression detected.

Analysis of gene expression

Low-density array analysis of 90 genes associated with breast cancer tumourigenicity was performed on all breast cancer cell lines retrieved following 72 h co-culture with MSCs, relative to the same cells cultured alone. Any change >2.5-fold is presented (Table 1). Upregulation of oncogenes, proto-oncogenes and genes associated with angiogenesis, anti-apoptosis and invasion was observed. A

Table 1 Results from low-density array analysis of breast cancer cells retrieved following co-culture with MSCs

Gene function	Gene symbol	Gene name	Fold change		
			Sk-Br3	T47D	MDA-MB-231
Oncogene and proto-oncogenes	NCOA4	Nuclear receptor co-activator 4	3.7	3.7	N/A
	FOS	Osteosarcoma oncogene	6.1	38.9	5.5
	MUC1	Mucin 1	6.1	1.6	N/A
	FYN	FYN oncogene	11	17.6	1.9
	JUN	JUN oncogene	3.2	3.4	2.7
	MET	MET proto-oncogene	3.3	15.4	N/A
	EPHA2	Ephrin receptor A2	2.3	5.5	1.5
Macrophage marker	CD68[a]	CD68 macrophage antigen/microsialin	8.1	35	3.7
Angiogenesis	VEGF	Vascular endothelial growth factor A	7.3	12	N/A
Anti-apoptosis	IGF1R	Insulin-like growth factor 1 receptor	3.5	1.2	2
	BCL2[a]	B-cell CLL/lymphoma 2	9.4	6.3	N/A
	CAV-1[a]	Caveolin 1	8.5	3994	1.2
EMT induction	TGFBR2[a]	Transforming growth factor-beta receptor type II	8.7	2142	1.8
	ACVR1[a]	Activin A receptor type 1/TGF beta superfamily receptor 1	6.7	3.3	3.3
Proliferation	CCNE1	Cyclin E1	−2.8	−2.1	N/A
	MKi67[a]	Antigen identified by monoclonal antibody Ki-67	−3.3	−4.9	−2.4
	MYBL2	Myeoblastosis oncogene	−5.5	−4.4	−2
Invasion and migration	MMP11[a]	Matrix metallopeptidase 11 (Stromelysin 3)	15.2	2.9	20
	CXCL12[a]	Stromal cell-derived factor 1	9,949	−1.2	17,066

Results presented show genes where at least one cell line had ≥2.5-fold increase or decrease in expression following co-culture with MSCs

[a] Genes which were then validated in triplicate experiments by RQ-PCR

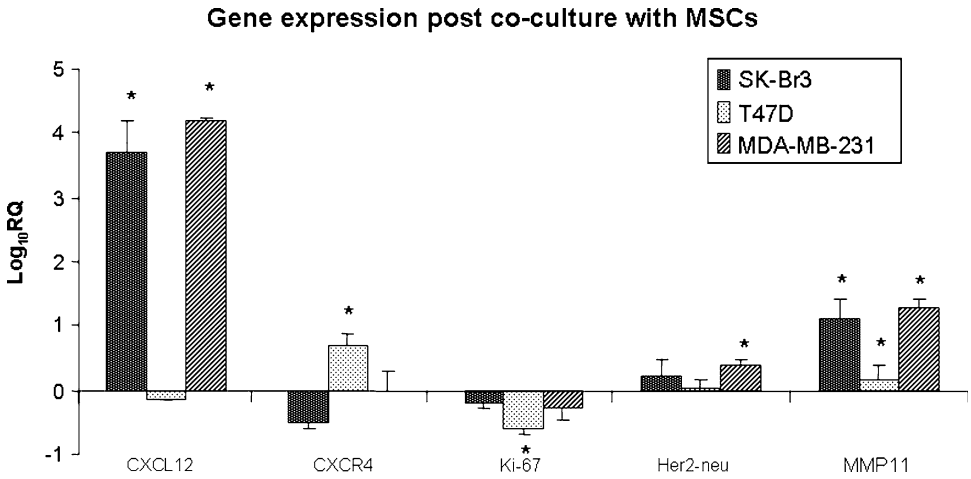

Fig. 1 Change in breast cancer cell gene expression following co-culture with MSCs. Results presented as Mean ± SEM Log_{10} relative quantity in triplicate experiments. The baseline represents the level of expression in breast cancer cell lines cultured individually. * Denotes $P < 0.05$

range of genes exhibited greater than 10-fold upregulation (FOS, FYN, MET, VEGF, CD68 and MMP11) whilst others were upregulated over 1,000-fold (CAV-1, TGFßR2 and CXCL12). However, down-regulation of genes associated with proliferation (Ki67, CCNE1 and MYBL2) was recorded across all breast cancer cells following co-culture with MSCs.

Observed changes in specific genes of interest were validated in triplicate experiments using RQ-PCR (Fig. 1). Significant upregulation of the chemokine, CXCL12, was observed in SK-Br3 cells (9,949 ± 4,787-fold, $P < 0.05$) following co-culture with a reciprocal downregulation in its cognate receptor CXCR4 (3 ± 1-fold). In MDA-MB-231 cells, CXCL12 expression was significantly increased (17,066 ± 1,109-fold), whereas T47D cells exhibited upregulation of its receptor, CXCR4 (6 ± 2-fold, $P < 0.05$). The proliferation marker, Ki-67, was down-regulated in all breast cancer cells (range: 2–4-fold decrease, T47D $P < 0.05$), whilst the invasive marker, MMP11, was significantly upregulated.

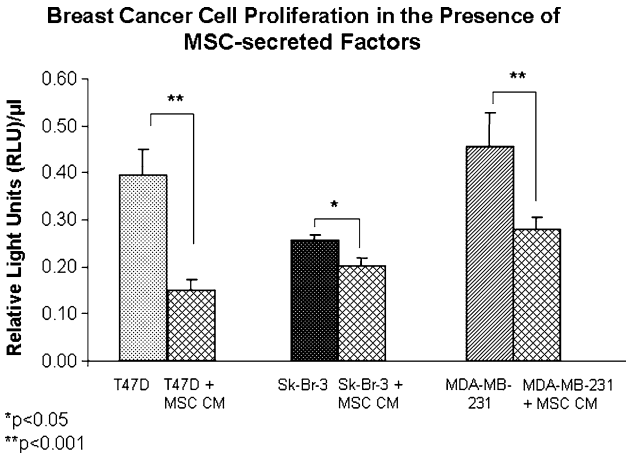

Fig. 2 Changes in proliferation of breast cancer cells exposed to factors secreted by MSCs for 72 h. Cell proliferation was measured using an Apoglow® assay in T47D, SK-Br3 & MDA-MB-231 cells cultured alone and in MSC-conditioned media. Results presented represent mean of triplicate experiments ± SEM. *RLU* Relative light units detected on luminometer. * $P < 0.05$; ** $P < 0.001$

Cell proliferation in response to MSC secreted factors

Breast cancer cells were cultured in the presence of MSC CM for 72 h after which ATP levels were quantified using a luminometer-based Apoglow® assay (Fig. 2). There was a significant reduction in proliferation observed in all three breast cancer cell lines cultured in the presence of factors secreted by MSCs (SK-Br-3 $P < 0.05$; T47D and MDA-MB-231 $P < 0.001$).

Expression of markers associated with EMT

Significant upregulation in defined markers of EMT were observed in both SK-Br3 and T47D cells retrieved following 72 h co-culture with MSCs (Fig. 3a). Due to the magnitude of the increases seen, results are expressed as Log_{10} values. Upregulation of most EMT markers in the MDA-MB-231 cell line occurred to a lesser degree: Vimentin (3-fold), Snail (5-fold) and N-cadherin (50-fold), whilst Twist expression increased >10,000-fold. In order to determine whether the effects seen were transient, T47D and Sk-Br3 cells were also retrieved following 7 days direct co-culture with MSCs. In the case of the T47D cells, a significant increase in Vimentin (244-fold) and Snail (5-fold) was still detected, whilst Twist and N-cadherin had returned to baseline. At Day 7, the SK-Br3 cells retained increased expression of N-cadherin (28-fold), Vimentin (153-fold) and Snail (10-fold).

In order to determine whether the changes in gene expression were detected at the protein level, protein was extracted from cells cultured individually and those retrieved following co-culture. Lysates were then subjected

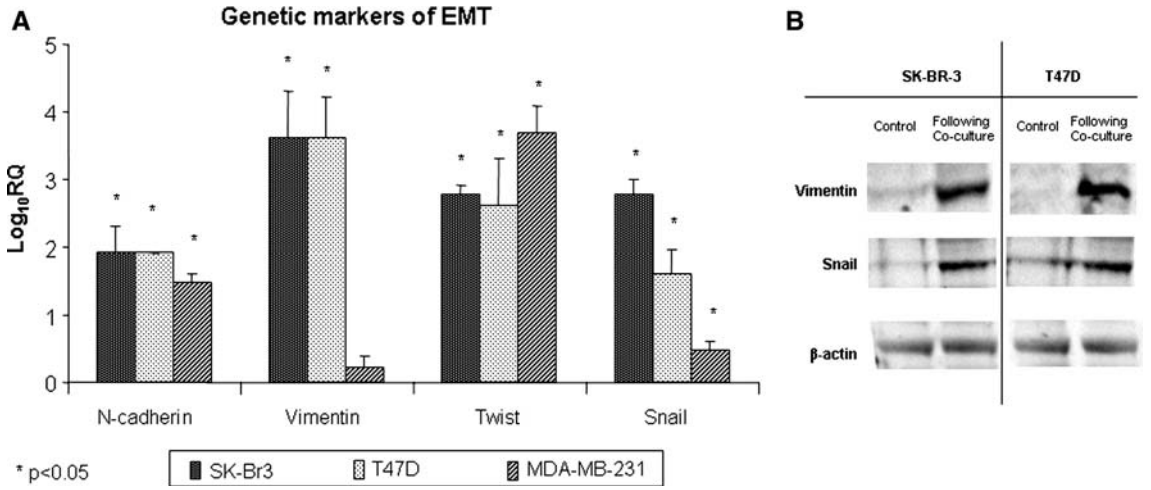

Fig. 3 **a** Changes in breast cancer cell expression of specific EMT genes following co-culture with MSCs. The baseline represents the level of expression in breast cancer cell lines cultured individually. Results presented represent mean of triplicate experiments ± SEM. * Denotes $P < 0.05$. **b** Protein analysis: Western blot of Sk-Br3 and T47D cells alone and following direct co-culture with MSCs, targeting Vimentin and Snail. β-actin was used to confirm uniform sample loading

to western blot using antibodies directed against Vimentin, Snail (Fig. 3b) and E-cadherin (Fig. 5c). In order to confirm that differences seen were not as a result of variation in protein sample, β-actin was also targeted and found to be at similar levels in all samples. Increased expression of Vimentin and Snail protein was detected in both Sk-Br3 and T47D protein lysates harvested from cells retrieved following direct co-culture with MSCs (Fig. 3b).

Overall, the greatest increase in all EMT markers examined was seen in Sk-Br3 cells. In order to determine whether this was an MSC specific effect, SK-Br3 cells were cultured directly on a confluent monolayer of normal fibroblasts (WI-38 cells). No significant change in expression of genes associated with EMT was observed following co-culture with WI-38 cells. Mesenchymal markers N-cadherin and Vimentin were downregulated 1.5- and 2.1–fold, respectively, with expression of the transcription factors Twist and Snail both decreased by 1.5- and 1.4-fold, respectively (results not shown).

Expression of EMT markers following indirect co-culture

In order to determine whether results observed were due to cell contact-mediated effects, breast cancer cells were exposed to MSC-conditioned medium and changes in expression of the same EMT markers were analysed (Fig. 4). In T47D and SK-Br3 cells, a small increase in

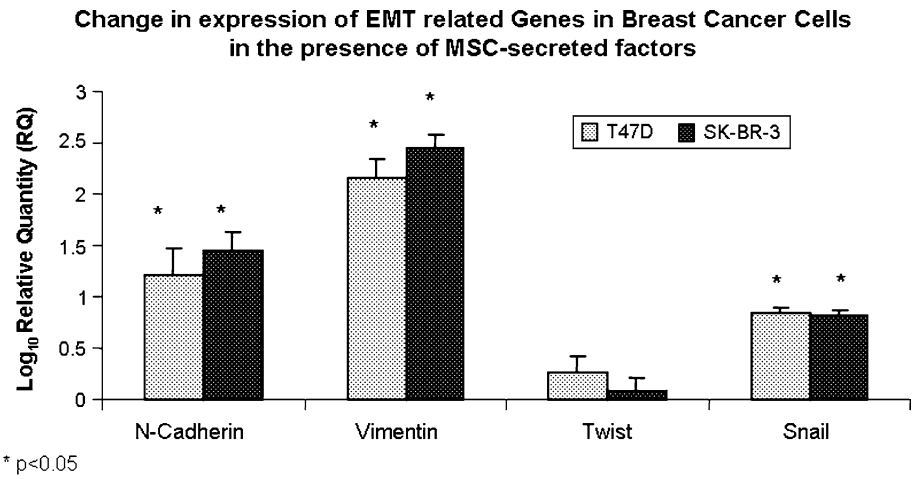

Fig. 4 Changes in expression of EMT genes in breast cancer cells following culture in MSC-conditioned medium (indirect co-culture). The baseline represents the level of expression in breast cancer cell lines cultured in the same medium that had not been exposed to MSCs. Results presented represent mean of triplicate experiments ± SEM. No change in expression of EMT markers was observed in MDA-MB-231 cells following indirect co-culture (results not shown)

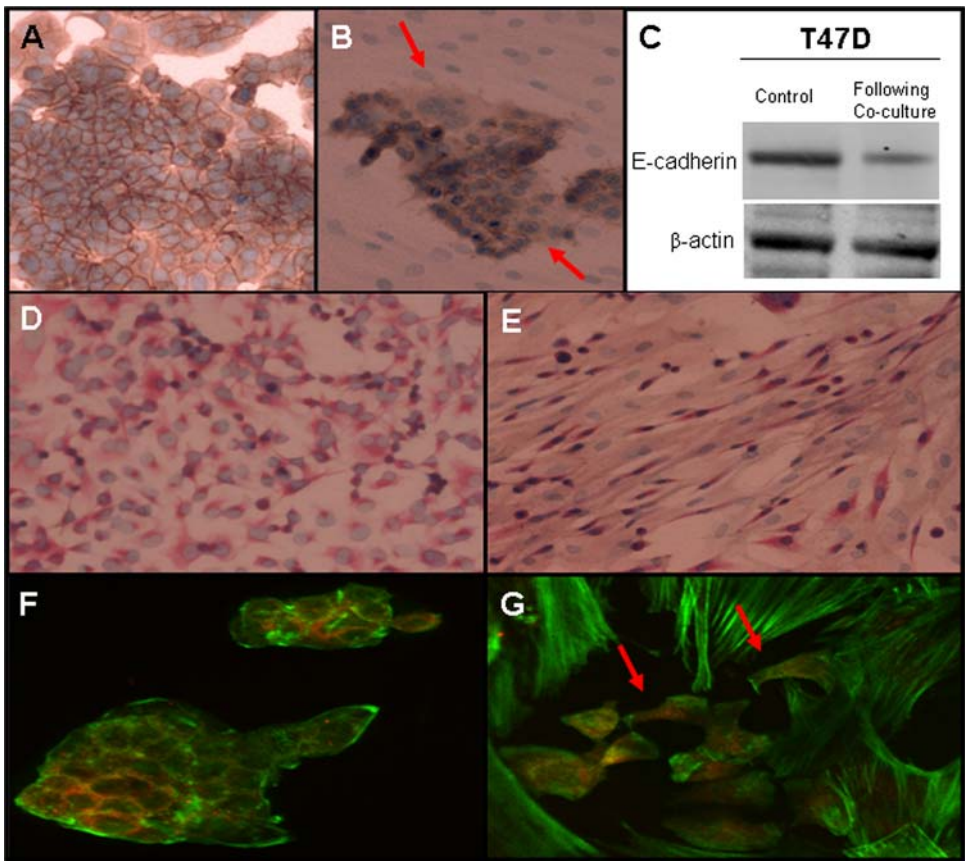

Fig. 5 **a**–**g** Immunostaining of breast cancer cells and MSCs cultured individually and in direct co-culture on chamber slides for 72 h. E-cadherin staining: **a** T47D cells, **b** T47D + MSCs, **c** confirmation of reduced E-cadherin by western blot of protein lysates from T47D cells cultured individually and those retrieved following direct co-culture with MSCs. β-actin was used to confirm uniform sample loading. Dual staining with cell type specific antibodies; *red*—epithelial specific pancytokeratin, *blue*—haemotoxylin stained nuclei. **c** MDA-MB-231 cells, **d** MDA-MB-231 + MSCs. Confocal fluorescent images of cell cytoskeletons stained with Alexafluor (*green*). Epithelial cells were also labelled with PKH26 (*red*) prior to mixing: **e** T47D cells **f** T47D + MSCs. All images presented are at 200× magnification

expression of Twist and Snail was observed (range 1–2-fold and 4–7-fold, respectively). A greater upregulation was seen in N-cadherin (range 9–32-fold) with the most marked increase observed in vimentin expression (range 158–276-fold). Although the changes in expression were significant ($P < 0.05$) for Snail, Twist and Vimentin, the increase was considerably lower than that seen in the same cells following direct co-culture with MSCs (Fig. 3). When the length of exposure to MSC-secreted factors was increased to 7 days, levels of target expression had returned to baseline (<2-fold change in gene expression compared to cells cultured in standard medium). No change in expression of EMT markers was observed in MDA-MB-231 cells following indirect co-culture (results not shown).

Immunohistochemistry

Breast cancer cells and MSCs cultured individually and in co-culture were stained with cell type specific antibodies to distinguish populations and analyse changes in morphology and growth pattern. Changes in E-cadherin protein expression were also examined. E-cadherin has strong membrane-targeted expression in T47D cells (Fig. 5a), whilst MSCs have no detectable expression. When T47D cells were cultured on a monolayer of MSCs, a marked decrease was observed in the intensity of E-cadherin staining (Fig. 5b). E-cadherin expression was particularly reduced at junctions where T47D cells were in direct contact with the MSCs (indicated by *arrows*) compared with cells located within a cluster of breast cancer cells. This change in E-cadherin protein expression was confirmed by western blot of T47D protein lysates harvested from cells cultured individually, and those retrieved following co-culture (Fig. 5c).

Dual staining

Breast cancer cells (MDA-MB-231) cultured alone stained positive for the epithelial specific cytokeratin, MNF116 (*red*), with nuclei counterstained with haematoxylin (*blue*), and grew in a typical random asymmetric pattern (Fig. 5d). Stromal cells (MSCs) staining positive for CD90 grew in a symmetrical pattern with a typical parallel alignment of spindle-shaped cells when cultured alone. When cultured on a monolayer of MSCs, MDA-MB-231 cells altered their growth pattern from the random cellular distribution observed to align in parallel with adjacent MSCs (Fig. 5e) reflecting a change in cellular polarity.

Confocal fluorescent microscopy

PKH26-labelled (*red*) T47D cells when cultured alone were seen to grow in a typical clustered growth pattern, with the Alexafluor-labelled cell cytoskeleton (*green*) seen to be non-branching and closely adherent to the nuclei (Fig. 5f). These same cells, when co-cultured directly on a monolayer of MSCs, appeared to lose cellular adhesion leading to a more dispersed single cell distribution. Furthermore, the breast cancer cell cytoskeleton was more branching and elongated (indicated by *arrows*), and appeared to polarise in the direction of adjacent Mesenchymal Stem cells (Fig. 5g).

Discussion

Mesenchymal Stem Cells have been reported to interact with breast cancer cells that have metastasised to bone marrow [25] as well as being actively recruited to the primary tumour stromal interface [15]. This tumour homing quality has prompted investigators to assess MSCs as possible delivery vectors for anti-cancer therapies [13]. In order to realise their therapeutic potential, interactions between MSCs and breast cancer cells must be fully elucidated.

Studies have previously analysed breast cancer cells and MSCs in direct co-culture noting specific morphological and phenotypical alterations in the breast cancer cells [7–9, 14]. However, isolation of the cells following co-culture and analysis of changes in gene expression has not previously been assessed. Immunomagnetic selection targeting antigens such as EpCAM is used to capture circulating tumour cells or enrich tumour cells from mixed cell samples. The immunomagnetic enrichment technique itself has previously been shown to have no significant effect on the gene expression profile of breast cancer cells [24].

Reports from this laboratory and others have shown a significant increase in migration of breast cancer cells in response to factors secreted by MSCs [25, 26], and this was reflected by increased expression of migratory genes seen here including MMP11 and CXCL12 [27]. Oncogenes and proto-oncogenes were upregulated both in a cell specific manner and, in the case of FOS and JUN, across all breast cancer cells retrieved following co-culture with MSCs. FOS and JUN are both major components of the activator protein-1 (AP-1) transcription factor complex which has been shown to positively regulate cellular motility and migration [28].

CAV-1 is now considered a marker of poor prognosis with up-regulation correlated to increased cellular dissemination and cell survival [29]. CAV-1 has been shown to mediate its anti-apoptotic properties through upregulation of IGF-1R which was also elevated in the cells following co-culture with MSCs. Interestingly, a universal downregulation of genes associated with proliferation (Ki-67, MYBL2 and CCNE1) was observed in all breast cancer cells retrieved from co-culture. Subsequent analysis of ATP production by breast cancer cells in the presence of MSC-secreted factors (indirect co-culture), revealed a significant reduction in proliferation of all cancer cells. These results concur with those of Hombauer and Minguell [7] who noted no increase in proliferative activity when MCF-7 cells were grown alone or on a monolayer of MSCs.

The apparent promotion of oncogenes and genes associated with invasion and migration with an inhibition of proliferation fits a profile seen in EMT [18, 19]. In order to further investigate whether MSCs were exerting their effects through induction of EMT, a number of specific genetic markers of EMT were examined in breast cancer cells following co-culture. Anti-apoptotic transcription factors, Twist and Snail, and mesenchymal protein markers, Vimentin and N-cadherin have been consistently associated with mesenchymal transition in epithelial cells [21, 30]. Vimentin upregulation is commonly observed in more invasive basal cancer subtypes and has been positively correlated with poor prognosis in breast cancer patients [31]. Interestingly, Vimentin was upregulated in both T47D and SK-Br-3 cells with no significant upregulation in the MDA-MB-231 breast cancer population. This may be due to the relatively high expression of Vimentin already present in the more invasive MDA-MB-231 cells [32]. This upregulation in Vimentin was confirmed at the protein level, and also detected following 7 days of in vitro co-culture. Significant upregulation of N-cadherin, Twist and Snail was recorded across all breast cancer cells retrieved from co-culture with MSCs although to a lesser extent in the MDA-MB-231 cells. This proportional difference in EMT changes recorded between MDA-MB-231 cells and other less invasive breast cancer subtypes coincides with findings recorded by Karnoub et al. [14] who noted that MDA-MB-231 cells exist in a state of "partial EMT" and that, within their study, CCL5 secreted by MSCs did not lead to advancement of this EMT phenotype.

Further analysis of array data confirmed upregulation of a number of genes associated with EMT induction including TGFßR2 [33] and ACVR1 [34], both receptors for TGFß, which is known to stimulate mesenchymal transition in epithelial cells [35]. Research suggests that upregulated expression of TGFßR2 is an absolute requirement for TGFß-mediated EMT [36]. Vascular endothelial growth factor (VEGF), typically associated with angiogenesis, was also upregulated. Non-Angiogenic functions of VEGF include anti-apoptotic and pro-migratory properties [37] as well as an important role in the

initiation of EMT through upregulation of Snail expression [38]. EMT appears to be at least partly dependant on VEGF signalling as studies that have blocked VEGF noted a proportional decrease in EMT [39].

In order to investigate whether changes seen were specific to MSCs, breast cancer cells were directly cultured with normal fibroblasts (WI-38 cells), resulting in no significant change in EMT-related gene expression. This suggests that the effects observed were MSC specific. In order to assess whether changes in gene expression were mediated solely through cell to cell contact, breast cancer cells were also cultured in MSC-conditioned medium. No change in expression of EMT markers was seen in MDA-MB-231 cells exposed to MSC-conditioned medium. Both T47D ad SK-Br3 cells exhibited a relatively mild upregulation in expression of Twist, Snail and N-cadherin, with the most marked increase seen in Vimentin expression. Although significant, these changes following indirect co-culture occurred to a much lesser degree than those seen in cells directly cultured with MSCs. Also, the effects were found to be transient in the indirect co-culture model used, with gene expression returning to baseline following 7 days of indirect co-culture. This may be due to cell contact-mediated inhibition of MSC proliferation, and resultant reduction in secretion of mediating factors. Overall the data suggest that changes in gene expression observed were predominantly mediated through direct cell to cell contact.

Decreased expression of the cell adhesion protein E-cadherin and the resultant cellular dissociation is another marker consistent with the process of EMT [18]. Previous studies investigating breast cancer cells directly co-cultured with MSCs have shown a significant downregulation in E-cadherin protein expression in breast cancer cells [7, 8] an observation also noted in the current study. Dual staining to distinguish between cell populations in co-culture also highlighted alterations in morphology and growth patterns of breast cancer cells. T47D cells appeared to lose adhesiveness and separate from their normal clustered growth pattern, with cells adjacent to MSCs branching and polarising towards the mesenchymal cells. These changes coincide with the loss of apico-basal polarity seen in cells that undergo EMT [18].

Recent literature has significantly advanced our understanding of the pivotal role EMT plays in the metastatic cascade. Initially regarded with a degree of scepticism, mesenchymal transition has been observed at the primary tumour site in a cohort of 479 human breast cancer samples and a positive correlation with basal breast cancer phenotype confirmed [20]. Despite these developments, the stimulus inducing EMT at the primary tumour site remains unknown. The current study suggests that MSCs that are actively recruited to tumour stromal microenvironments may act as a stimulus to induce EMT in breast cancer cells and actively increase breast cancer metastatic potential.

Acknowledgements This study was supported by funding from the National Breast Cancer Research Institute (NBCRI), a Royal College of Surgeons in Ireland (RCSI) Surgical Research Grant (F.T. Martin), a Health Research Board Project Grant (R.M. Dwyer), and a Science Foundation Ireland CSET award (J.M. Murphy, F.P. Barry and T. O'Brien).

References

1. Jemal A, Siegel R, Ward E et al (2008) Cancer statistics, 2008. CA Cancer J Clin 58:71–96
2. Coleman RE, Rubens RD (1987) The clinical course of bone metastases from breast cancer. Br J Cancer 55:61–66
3. Espey DK, Wu XC, Swan J et al (2007) Annual report to the nation on the status of cancer, 1975–2004, featuring cancer in American Indians and Alaska Natives. Cancer 110:2119–2152
4. Bhowmick NA, Moses HL (2005) Tumor-stroma interactions. Curr Opin Genet Dev 15:97–101
5. Hu M, Polyak K (2008) Molecular characterisation of the tumour microenvironment in breast cancer. Eur J Cancer 44:2760–2765
6. Pittenger MF, Mackay AM, Beck SC et al (1999) Multilineage potential of adult human mesenchymal stem cells. Science 284:143–147
7. Hombauer H, Minguell JJ (2000) Selective interactions between epithelial tumour cells and bone marrow mesenchymal stem cells. Br J Cancer 82:1290–1296
8. Fierro FA, Sierralta WD, Epunan MJ et al (2004) Marrow-derived mesenchymal stem cells: role in epithelial tumor cell determination. Clin Exp Metastasis 21:313–319
9. Sasser AK, Mundy BL, Smith KM et al (2007) Human bone marrow stromal cells enhance breast cancer cell growth rates in a cell line-dependent manner when evaluated in 3D tumor environments. Cancer Lett 254:255–264
10. Chen J, Zhang ZG, Li Y et al (2003) Intravenous administration of human bone marrow stromal cells induces angiogenesis in the ischemic boundary zone after stroke in rats. Circ Res 92:692–699
11. Spaeth E, Klopp A, Dembinski J et al (2008) Inflammation and tumor microenvironments: defining the migratory itinerary of mesenchymal stem cells. Gene Ther 15:730–738
12. Dvorak HF (1986) Tumors: wounds that do not heal. Similarities between tumor stroma generation and wound healing. N Engl J Med 315:1650–1659
13. Kumar S, Chanda D, Ponnazhagan S (2008) Therapeutic potential of genetically modified mesenchymal stem cells. Gene Ther 15:711–715
14. Karnoub AE, Dash AB, Vo AP et al (2007) Mesenchymal stem cells within tumour stroma promote breast cancer metastasis. Nature 449:557–563
15. Dwyer RM, Potter-Beirne SM, Harrington KA et al (2007) Monocyte chemotactic protein-1 (MCP-1) secreted by primary breast tumors stimulates migration of mesenchymal stem cells (MSCs). Clin Cancer Res 13:5020–5027
16. Molloy AP, Martin FT, Dwyer RM et al (2009) Mesenchymal stem cell secretion of chemokines during differentiation into osteoblasts, and their potential role in mediating interactions with breast cancer cells. Int J Cancer 124:326–332
17. Nakaya Y, Sheng G (2008) Epithelial to mesenchymal transition during gastrulation: an embryological view. Dev Growth Differ 50:755–766

18. Thiery JP, Sleeman JP (2006) Complex networks orchestrate epithelial-mesenchymal transitions. Nat Rev Mol Cell Biol 7:131–142
19. Brabletz T, Jung A, Spaderna S et al (2005) Opinion: migrating cancer stem cells—an integrated concept of malignant tumour progression. Nat Rev Cancer 5:744–749
20. Sarrio D, Rodriguez-Pinilla SM, Hardisson D et al (2008) Epithelial-mesenchymal transition in breast cancer relates to the basal-like phenotype. Cancer Res 68:989–997
21. Mani SA, Guo W, Liao MJ et al (2008) The epithelial-mesenchymal transition generates cells with properties of stem cells. Cell 133:704–715
22. Barry FP, Murphy JM (2004) Mesenchymal stem cells: clinical applications and biological characterization. Int J Biochem Cell Biol 36:568–584
23. Livak KJ, Schmittgen TD (2001) Analysis of relative gene expression data using real-time quantitative PCR and the 2(-delta delta C(T)) method. Methods 25:402–408
24. Woelfle U, Breit E, Pantel K (2005) Influence of immunomagnetic enrichment on gene expression of tumor cells. J Transl Med 3:12
25. Corcoran KE, Trzaska KA, Fernandes H et al (2008) Mesenchymal stem cells in early entry of breast cancer into bone marrow. PLoS ONE 3:e2563
26. Molloy AP, Martin FT, Dwyer RM et al (2008) Mesenchymal stem cell secretion of chemokines during differentiation into osteoblasts, and their potential role in mediating interactions with breast cancer cells. Int J Cancer 124:326
27. Gelmini S, Mangoni M, Serio M et al (2008) The critical role of SDF-1/CXCR4 axis in cancer and cancer stem cells metastasis. J Endocrinol Invest 31:809–819
28. Eferl R, Wagner EF (2003) AP-1: a double-edged sword in tumorigenesis. Nat Rev Cancer 3:859–868
29. Pinilla SM, Honrado E, Hardisson D et al (2006) Caveolin-1 expression is associated with a basal-like phenotype in sporadic and hereditary breast cancer. Breast Cancer Res Treat 99:85–90
30. De Wever O, Pauwels P, De Craene B et al (2008) Molecular and pathological signatures of epithelial-mesenchymal transitions at the cancer invasion front. Histochem Cell Biol 130:481–494
31. Thomas PA, Kirschmann DA, Cerhan JR et al (1999) Association between keratin and vimentin expression, malignant phenotype, and survival in postmenopausal breast cancer patients. Clin Cancer Res 5:2698–2703
32. McInroy L, Maatta A (2007) Down-regulation of vimentin expression inhibits carcinoma cell migration and adhesion. Biochem Biophys Res Commun 360:109–114
33. Galliher AJ, Schiemann WP (2006) Beta3 integrin and Src facilitate transforming growth factor-beta mediated induction of epithelial-mesenchymal transition in mammary epithelial cells. Breast Cancer Res 8:R42
34. Mercado-Pimentel ME, Runyan RB (2007) Multiple transforming growth factor-beta isoforms and receptors function during epithelial-mesenchymal cell transformation in the embryonic heart. Cells Tissues Organs 185:146–156
35. Derynck R, Akhurst RJ, Balmain A (2001) TGF-beta signaling in tumor suppression and cancer progression. Nat Genet 29:117–129
36. Han G, Lu SL, Li AG et al (2005) Distinct mechanisms of TGF-beta1-mediated epithelial-to-mesenchymal transition and metastasis during skin carcinogenesis. J Clin Invest 115:1714–1723
37. Mercurio AM, Lipscomb EA, Bachelder RE (2005) Non-angiogenic functions of VEGF in breast cancer. J Mammary Gland Biol Neoplasia 10:283–290
38. Wanami LS, Chen HY, Peiro S et al (2008) Vascular endothelial growth factor-A stimulates Snail expression in breast tumor cells: implications for tumor progression. Exp Cell Res 314:2448–2453
39. Enciso JM, Gratzinger D, Camenisch TD et al (2003) Elevated glucose inhibits VEGF-A-mediated endocardial cushion formation: modulation by PECAM-1 and MMP-2. J Cell Biol 160:605–615